SPIS TREŚCI - CONTENTS

NEW MEMBERS OF THE SCIENTIFIC BOARD

Prof. Hong-Zhong Huang, Prof. David Valis, Prof. Olgierd Hryniewicz, and Prof. Krzysztof Kołowrocki have joined the Scientific Board of Maintenance and Reliability. Below, we present their profiles.

Prof. Hong-Zhong Huang is a professor and Dean of the School of Mechanical, Electronic, and Industrial Engineering, University of Electronic Science and Technology of China. He has held visiting appointments at several universities in the USA, Canada, and Asia. He received a Ph.D. degree in Reliability Engineering from Shanghai Jiaotong University, China, and has published 150 journal papers and 5 books in the fields of reliability engineering, optimization design, fuzzy sets theory, and product development. He is a Fellow of ISEAM (International Society of Engineering Asset Management), a member of ESRA (European Safety and Reliability Association) Technical Committee on System Reliability, a Regional Editor of International Journal of Reliability and Applications, and an Editorial Board Member of International Journal of Reliability, Quality and Safety Engineering, International Journal of Quality, Statistics, and Reliability, International Journal of Reliability and Quality Performance, International Journal of Performability Engineering, Advances in Fuzzy Sets and Systems, and The Open Mechanical Engineering Journal. He received the William A. J. Golomski Award from the Institute of Industrial Engineers in 2006, the Best Paper Award of the 8th International Conference on Frontiers of Design and Manufacturing in 2008, and the Best Paper Award of the International Conference on Materials and Reliability in 2011. His current research interests include system reliability analysis, warranty, maintenance planning and optimization, and computational intelligence in product design.

Prof. David Vališ works at the University of Defence, Brno, the Czech Republic. His scientific work and technical activities are related to the development of dependability theory and safety and risk analysis of complex technical (military) systems and transport equipment. He conducts applied research in these fields. He is currently involved in a research team investigating the problems of event description, defining the causes and consequences of events, specifications and measures in the description of events, consequences of event verification, mission profile description, mission success assessment, and implementation of the obtained results in analyses. Over the last 5 years, he has authored or co-authored 6 books and more than 100 technical papers, published mainly abroad. He has also participated in several research projects. As an active member of the IEC TC 56, he has participated in the development of several standards in the fields of reliability and risk/safety. His fields of experience include dependability theory – fundamentals and applications, applied techniques of reliability assessment, risk assessment methods, risk assessment of technical systems, and operation of systems.

Prof. Olgierd Hryniewicz is Full Professor at the Systems Research Institute of the Polish Academy of Sciences and the Warsaw School of Information Technology and Management. He specializes in the theory of reliability and statistical quality control of technological objects. He is author of over 200 scientific publications including 43 books. He is a member of the Committee on Evaluation of Scientific Institutions at the Ministry of Science and Higher Education, a member of the Information Technology Committee of the Polish Academy of Sciences, and Vice Chair of the National Committee on Cooperation with the International Institute for Applied Systems Analysis (IIASA).

Prof. Krzysztof Kołowrocki is a Professor and Head of Mathematics Department at the Faculty of Navigation of Gdynia Maritime University. His field of interest is mathematical modeling of safety and reliability of complex systems and processes. He has published over 300 scientific works. He is Chair of the Polish Safety and Reliability Association. His homepage can be found at http://www.am.gdynia.pl/~katmatkk/.

LINGAITIS L P, MJAMLIN S, BARANOVSKY D, JASTREMSKAS V. **Experimental Investigations on operational reliability of diesel locomotives engines.** Eksploatacja i Niezawodnosc - Maintenance and Reliability 2012; 14 (1): 6-11.

In work experimental researches of longevity and technical and operating parameters of diesel engine diesels are presented 10D100 with modified tribosystems. The last are instrumental in the rapid starting and decline of wear depending on time of starting, thus, such diesel practically on any speed and loading modes can be exploited without the promoted wear. At the modified shells of cylinders the wear of compression rings does not affect the size of breach of gases in carter. Thus, the modified tribosystems provide maximal longevity and providing of high technical and operating parameters of diesel engine.exploitation risk was assessed and the lifespan of the pipelines, after which the pipelines shall be replaced by new structures, were determined.

KUCHARCZYK W. **Ablative and abrasive wear of phenolic-formaldehyde glass laminates with powder fillers.** Eksploatacja i Niezawodnosc - Maintenance and Reliability 2012; 14 (1): 12-18.

This paper reports the results of wearing out polymer composites: the ablative wear, after 30 s of treating with hot combustion gases, as well as the abrasive wear, after 1000 s of friction using the loose abradant in the T-07 tester. The specimens were made of phenolic-formaldehyde matrix, glass fabrics-reinforcement and powder fillers: the corundum Al_2O_3 and the carbon powder C. It was qualified the qualitative and the quantitative effect of components on the average linear rate of ablation v_a and the average mass intensity of abrasive wear I_z. It was proved, that composites with the smaller intensity of abrasive wear I_z are characterized by bigger rate of ablative using up.

ŻUROWSKI W. **Structural factors contributing to increased wear resistance of steel friction couples.** Eksploatacja i Niezawodnosc - Maintenance and Reliability 2012; 14 (1): 19-24.

Research into abrasive wear resistance in conditions of dry friction and oxidative wear have been carried out. It has been found that the increase of wear resistance of solid bodies appears where the temperature of a friction area is equal to the characteristic temperature and frictional resistance is stabilized. Increasing wear resistance of a system of bodies is effected by systems transfer of material between surfaces of rubbing bodies and presence of ferrum oxides: *FeO* and Fe_3O_4 and with decreasing share of Fe_2O_3 up to its disappearance. Resistance to abrasive wear in conditions of dry friction and oxidative wear was tested in two frictional systems. Specimens were made from steels C45 in two condition of heat treatment. Counter-specimens were made from 145Cr6. In order to identify composition and structure of the friction products and the types of ferrous compounds arising from friction, especially secondary oxide structures, present on the surface of rubbing components, Mössbauer spectral analysis was applied. The wear testing required construction of an original test device to measure wear in conditions of formation and regulation of the isothermic limit of temperature variation at a precisely determined distance from a contact of rubbing bodies by means of release (by cooling) of heat energy.

ZHANG T, BAI G, GUO B. **Success probability model of phased mission systems with limited spares.** Eksploatacja i Niezawodnosc – Maintenance and Reliability 2012; 14 (1): 24–32.

This paper builds a model to analyze the success probability of phased mission systems (PMS) with given limited spares. The configuration and success criteria of phased mission may vary from phase to phase. Most reliability analysis techniques and tools of phased mission systems assume that there is no spare replacement during the phased mission or the component repair times are neglected. However, for some phased missions, failed components can be replaced by spares during the mission or in the interval of the phases and the spare replacement times are generally not negligible. By considering minimal spare replacement policy (MSRP) which is often used in military exercise, this paper presents a mathematical model for success probability analysis of phased mission which is based on minimal path set and system state analysis methods. Then, the model was demonstrated and validated by an example of military exercise.

LINGAITIS L P, MJAMLIN S, BARANOVSKY D, JASTREMSKAS V. **Badania eksperymentalne operacyjnej niezawodności eksploatacyjnej silników diesel dla spalinowozów.** Eksploatacja i Niezawodnosc - Maintenance and Reliability 2012; 14 (1): 6-11.

W artykule przedstawiono rezultaty badań eksperymentalnych trwałości i parametrów techniczno-eksploatacyjnych silnika diesla spalinowozu 10D100 ze zmodyfikowanymi systemami ciernymi. Zmodyfikowane systemy cierne gwarantują szybsze uruchomienie silnika, tym samym zmniejszając zużycie związane z uruchamianiem. Ponadto taki diesel może być praktycznie eksploatowany we wszystkich trybach prędkości i obciążenia bez podwyższonego zużycia. W wyniku modyfikacji tulei cylindrów ścieranie pierścieni kompresyjnych nie powoduje zwiększonego przedostawania się gazu do skrzyni korbowej. W ten sposób zmodyfikowane systemy cierne gwarantują maksymalną niezawodność parametrów eksploatacyjnych spalinowozów z silnikiem diesla.

KUCHARCZYK W. **Zużywanie ablacyjne i ścierne laminatów fenolowo-formaldehydowych – szklanych z napełniaczami proszkowymi.** Eksploatacja i Niezawodnosc - Maintenance and Reliability 2012; 14 (1): 12-18.

Przedstawiono wyniki badań zużywania kompozytów polimerowych: ablacyjnego, po 30 s oddziaływania wysokotemperaturowego strumienia gazów palnych oraz ściernego, po 1000 s tarcia próbki luźnym ścierniwem w testerze T-07. Doświadczeniom poddano szklane laminaty fenolowo-formaldehydowe z napełniaczami proszkowymi: korundem Al_2O_3 oraz pyłem węglowym C. Określono jakościowy i ilościowy wpływ komponentów na wartości zużywania: średnią liniową szybkość ablacji v_a oraz średnią masową intensywności zużywania I_z. Stwierdzono, że kompozyty o składach fazowych zapewniających mniejszą intensywność zużywania ściernego charakteryzują się większą szybkością zużywania ablacyjnego.

ŻUROWSKI W. **Czynniki strukturalne umożliwiające uzyskanie zwiększonej odporności na zużywanie stalowych par trących.** Eksploatacja i Niezawodnosc - Maintenance and Reliability 2012; 14 (1): 19-24.

Przeprowadzono badania odporności na zużycie w warunkach tarcia suchego i zużywania utleniającego. Stwierdzono, że zwiększona odporność na zużycie występuje, gdy temperatura strefy tarcia osiąga wartość równą temperaturze charakterystycznej dla danego układu a opory tarcia są stabilizowane. Towarzyszy temu przenoszenie materiału pomiędzy współpracującymi powierzchniami i obecność w strefie tarcia tlenków żelaza: *FeO* i Fe_3O_4, przy zmniejszeniu (do zaniku) ilości Fe_2O_3. W artykule przedstawiono badania odporności na zużycie dla dwóch par trących. Próbki wykonano ze stali C45 w dwóch stanach technologicznych. Przeciwpróbki wykonano ze stali 145Cr6. W celu identyfikacji składu i struktury powstałych podczas tarcia związków żelaza, a szczególnie tlenkowych struktur wtórnych występujących na powierzchni trących się ślizgaczy, wykorzystano analizę spektralną Mössbauera. Badania zużyciowe wymagały skonstruowania oryginalnego urządzenia badawczego, pozwalającego na pomiar zużycia w warunkach utworzenia i regulowania granicy izotermicznej, w ściśle określonej odległości od styku trących się ciał poprzez odbieranie (w wyniku chłodzenia) ciepła.

ZHANG T, BAI G, GUO B. **Model prawdopodobieństwa sukcesu systemów o zadaniach okresowych z ograniczoną liczbą części zamiennych.** Eksploatacja i Niezawodnosc – Maintenance and Reliability 2012; 14 (1): 24–32.

W niniejszej pracy skonstruowano model do analizy prawdopodobieństwa sukcesu systemów o zadaniach (misjach) okresowych (ang. phased mission systems, PMS) z daną, ograniczoną liczbą części zamiennych. Konfiguracja systemu oraz kryteria sukcesu zadania okresowego mogą być różne dla różnych faz zadania. Większość technik i narzędzi służących do analizy systemów o zadaniach okresowych nie zakłada wymiany części podczas zadania okresowego lub nie bierze pod uwagę czasu wykonania napraw elementów składowych. Tymczasem, w niektórych zadaniach okresowych istnieje możliwość wymiany elementów składowych na zapasowe bądź to w trakcie trwania zadania bądź też w przerwach pomiędzy fazami, a czas takiej wymiany zazwyczaj nie jest bez znaczenia. Biorąc pod uwagę politykę minimalnej wymiany części (ang. minimal spare replacement policy, MSRP), często stosowaną podczas ćwiczeń wojskowych, w niniejszym artykule przedstawiono matematyczny model do analizy prawdopodobieństwa sukcesu zadania okresowego, oparty na dwóch metodach: minimalnych ścieżek zdatności oraz analizy stanu systemu. Możliwość wykorzystania modelu zilustrowano i zweryfikowano na podstawie przykładowych ćwiczeń wojskowych.

VALIŠ D, KOUCKY M, ZAK L. **On approaches for non-direct determination of system deterioration.** Eksploatacja i Niezawodnosc – Maintenance and Reliability 2012; 14 (1): 33–41.

Nowadays the system requirements are set up and evaluated in various manners. We have plenty of excellent options available taking about an item technical state. We can also consider other states by many diagnostic options. The paper deals with the mathematical processing, monitoring and analysis of the oil field data got as a result from the laser spectrography in frame of the tribodiagnostic oil tests. The mathematical methods based on time series and their analysis and calculation processed by suitable method are used in the paper for oil data analysis. Due to the fact that the data sample is classified as fuzzy and uncertain from many reasons the FIS (Fuzzy Inference System) is used.

VALIŠ D, KOUCKY M, ZAK L. **Metody pośredniego badania starzenia się systemu.** Eksploatacja i Niezawodnosc – Maintenance and Reliability 2012; 14 (1): 33–41.

Obecnie wymagania systemu mogą być ustalane i oceniane w różny sposób. Mamy do dyspozycji wiele doskonałych opcji oceny stanu technicznego obiektów. Istnieje również wiele możliwości diagnozowania innych stanów. W artykule przedstawiono proces matematycznego przetwarzania, monitorowania i analizy danych eksploatacyjnych dotyczących oleju uzyskanych na podstawie spektrografii laserowej przeprowadzonej w ramach diagnostyki tribologicznej. Do analizy danych wykorzystano metody matematyczne oparte na szeregach czasowych oraz odpowiednie metody analizy i obliczania szeregów czasowych. Ponieważ dostępne dane sklasyfikowano jako rozmyte i niepewne, zastosowano System Wnioskowania Rozmytego FIS.

KNEFEL T. **Technical assessment of Common Rail injectors on the ground of overflow bench tests.** Eksploatacja i Niezawodnosc – Maintenance and Reliability 2012; 14 (1): 42–53.

The majority of actually produced Diesel engines operated as power units in passenger cars are equipped with injection systems of Common Rail type. Injectors with solenoid valve are implemented to a large extent of these engines. In the paper is discussed an assessment of differences in fuel dosing accomplished by injectors of various generations and are estimated quantities of fuel needed to actuate operation of the injectors. It has been specified a share of overflow volume in dose of injected fuel. One introduced also an index of efficiency, as a quantity to evaluate amount of decompressed fuel. Elementary overflows and differences in the elementary overflows are presented, both in case of efficient and inefficient injectors. There are evaluated leaks for elements from the 1st generation. It has been proposed a methodology of proceeding to assess technical conditions of the injectors after some time of operation.

KNEFEL T. **Ocena techniczna wtryskiwaczy Common Rail na podstawie doświadczalnych badań przelewów.** Eksploatacja i Niezawodnosc – Maintenance and Reliability 2012; 14 (1): 42–53.

Większość aktualnie produkowanych silników o zapłonie samoczynnym do napędu samochodów osobowych jest wyposażona w układy zasilania typu Common Rail. W dużej liczbie stosowane są wtryskiwacze z elektromagnetycznym zaworem. W artykule przedstawiono ocenę różnic w dawkowaniu realizowanym przez wtryskiwacze różnych generacji oraz oszacowano ilości paliwa niezbędne do uruchomienia wtryskiwaczy. Określono udział przelewu w dawce wtryskiwanego paliwa. Wprowadzono pojęcie wskaźnika sprawności, jako wielkości umożliwiającej ocenę ilości rozprężanego paliwa. Przedstawiono jednostkowe przelewy i różnice w jednostkowych przelewach zarówno dla sprawnych wtryskiwaczy, jak i niesprawnego. Wyznaczono przecieki dla elementów I generacji. Zaproponowano metodykę postępowania przy ocenie stanu technicznego wtryskiwaczy po pewnym okresie eksploatacji.

RUSIŃSKI E, CZMOCHOWSKI J, PIETRUSIAK D. **Problems of steel construction modal models identification.** Eksploatacja i Niezawodnosc – Maintenance and Reliability 2012; 14 (1): 54–61.

Complex identification of steel construction modal models requires simultaneous numerical and experimental analysis of the object. Such an approach allows to obtain more accurate results while the methods complement each other. Results presented, concern stacker feeding bridge which operates in open pit mine. Operational modal analysis was made. Application of this method enables to assess influence of working condition on the modal characteristic. Experimental results were validated with use of numerical method.

RUSIŃSKI E, CZMOCHOWSKI J, PIETRUSIAK D. **Problemy identyfikacji modeli modalnych stalowych ustrojów nośnych.** Eksploatacja i Niezawodnosc – Maintenance and Reliability 2012; 14 (1): 54–61.

Kompleksowa identyfikacja modeli modalnych stalowych ustrojów nośnych, wymaga ujęcia zarówno eksperymentalnego jak i numerycznego. Obie metody stanowią wzajemne uzupełnienie i umożliwiają dokładniejszą identyfikację. Przedstawione wyniki badań dotyczą mostu podającego zwałowarki działającej w kopalni węgla brunatnego. Przeprowadzono eksploatacyjną analizę modalną. Zastosowanie tej właśnie metody badawczej, uwzględnia wpływ warunków działania i obciążenia obiektu. Wyniki uzyskane w ten sposób zestawiono z eksperymentem numerycznym.

SUN R, PENG WW, HUANG HZ, LING D, YANG J. **Improved reliability data curve fitting method by considering samples distinction**. Eksploatacja i Niezawodnosc – Maintenance and Reliability 2012; 14 (1): 62–71.

In engineering practice, we face a problem of using some collected data to evaluate a kind of machine or equipment. Curve fitting is a common method to solve this problem. Least square method is wildly applied in this procedure. If the source data of curve fitting can be grouped in samples and the distinction of samples obviously express some character in source data collecting which cannot be ignored. Conventional curve fitting method cannot handle these source data. To deal with this disadvantage, we introduce an improved curve fitting method. Through source data analysis, we can find out the relationship between sample location and weight factor in curve fitting, and use these weight factors for curve fitting. To approach the true curve, we introduce an iterative procedure to modify the weight factors. An engineering example is given to illustrate this proposed method.

SUN R, PENG WW, HUANG HZ, LING D, YANG J. **Udoskonalona metoda dopasowywania krzywych do danych niezawodnościowych uwzględniająca różnice między próbkami**. Eksploatacja i Niezawodnosc – Maintenance and Reliability 2012; 14 (1): 62–71.

W praktyce inżynieryjnej stykamy się z problemem wykorzystania zgromadzonych danych do oceny maszyn lub sprzętu. Dopasowywanie krzywych to metoda powszechnie używana do rozwiązywania tego typu problemów. W procedurze tej szeroko stosuje się metodę najmniejszych kwadratów. Jeżeli dane wejściowe dopasowywane krzywą można pogrupować tak by tworzyły oddzielne próbki, a różnice między próbkami w sposób oczywisty odzwierciedlają pewną właściwość dotyczącą gromadzenia danych, której nie można pominąć, to konwencjonalna metoda dopasowywania krzywych nie pozwala na analizę takich danych wejściowych. Aby przezwyciężyć to ograniczenie, przedstawiamy udoskonaloną metodę dopasowywania krzywych. Poprzez analizę danych wejściowych, możemy określić związek pomiędzy położeniem próbki a czynnikiem ważonym w dopasowaniu krzywej oraz wykorzystać czynniki ważone przy dopasowywaniu krzywej. Aby osiągnąć jak najdokładniejsze przybliżenie do krzywej rzeczywistej wprowadziliśmu procedurę iteratywną modyfikującą czynniki ważone. Zastosowanie zaproponowanej metody zilustrowano na przykładzie danych z badań niezawodnościowych.

RUSIN A, WOJACZEK A. **Optimization of power machines maintenance intervals taking the risk into consideration**. Eksploatacja i Niezawodnosc – Maintenance and Reliability 2012; 14 (1): 72–76.

The goal of preventive as well as corrective maintenances is to keep or to restore acceptable level of efficiency and safety of operation of given object. Optimization of maintenance processes allows obtaining these effects at possibly lowest costs. Mathematic model of optimization of maintenance intervals having regard to the risk are presented in the paper. Precise calculations were made for steam turbines that operate in power units.

RUSIN A, WOJACZEK A. **Optymalizacja okresów międzyremontowych maszyn energetycznych z uwzględnieniem ryzyka.** Eksploatacja i Niezawodnosc – Maintenance and Reliability 2012; 14 (1): 72–76.

Celem obsług prewencyjnych jak i korekcyjnych jest zachowanie lub przywrócenie akceptowalnego poziomu efektywności i bezpieczeństwa eksploatacji danego obiektu. Optymalizacja działań remontowych pozwala na uzyskanie tych efektów przy możliwie niskich kosztach. W artykule przedstawiono model matematyczny optymalizacji okresów międzyremontowych z uwzględnieniem ryzyka. Szczegółowe obliczenia przeprowadzono dla turbin pracujących w blokach energetycznych dużej mocy.

SAHARKHIZ E, BAGHERPOUR M, REZA FEYLIZADEH M R, AFSARI A. **Software performance evaluation of a computerized maintenance management system: a statistical based comparison.** Eksploatacja i Niezawodnosc – Maintenance and Reliability 2012; 14 (1): 77–83.

In today highly competitive markets, application of maintenance management systems is un-avoidable. However, in refinery environments due to huge investment amount of operating systems, applying advanced maintenance management systems (Such as Computerized Maintenance Management System which is called CMMS) is increasingly seems to be a crucial task. In order to implement high performance CMMS software, the existing ones should be analyzed. In this paper, performance of two CMMS related software entitled IFS™ and MAINTA™, are introduced, analyzed and compared using significant statistical analysis with a case study in a refinery. The results of both hypothesis testing and economical study finally proposed the MAINTA™ software.

RADKOWSKI S, SZCZUROWSKI K. **Use of vibroacoustic signals for diagnosis of prestressed structures.** Eksploatacja i Niezawodnosc – Maintenance and Reliability 2012; 14 (1): 84–91.

The paper presents the issue of assessment of the technical condition of a prestressed structure while particularly underscoring the possibilities offered by amplitude modulation effects which are found in the observed vibroacoustic signal. The basis for such an approach is the thesis that change of distribution of stress in the cross-section of a prestressed structure is accompanied by a measurable change of the parameters of a vibroacoustic signal. The thesis stems from the assumption that the condition of prestressing of a structure, as it is being bent, is accompanied by the phenomenon of dispersion and hence of the change of wave propagation parameters, especially the occurrence of a measurable difference between the values of phase and group velocities. Analysis of the relations between the state of stress and the values of phase and group velocities creates the possibilities of developing the reverse diagnostic models and determining the quantitative changes of such parameters of technical condition as compressive forces, Young's modul or the stress in the structure.

SAHARKHIZ E, BAGHERPOUR M, REZA FEYLIZADEH M R, AFSARI A. **Ocena działania oprogramowania komputerowego systemu zarządzania utrzymaniem ruchu. Badania statystyczno-porównawcze.** Eksploatacja i Niezawodnosc – Maintenance and Reliability 2012; 14 (1): 77–83.

Na dzisiejszych, niezwykle konkurencyjnych rynkach, zastosowanie systemów zarządzania utrzymaniem ruchu jest niezbędne. Przykładem są zakłady rafinerii, w których, ze względu na wysokie sumy inwestowane w systemy operacyjne, zastosowanie zaawansowanych systemów utrzymania ruchu (takich jak Komputerowy System Zarządzania Utrzymaniem Ruchu CMMS) wydaje się coraz bardziej istotnym zadaniem. Aby jednak wdrożyć wysokiej klasy oprogramowanie CMMS, należy najpierw przeanalizować istniejące programy. W niniejszym artykule, przedstawiono, przeanalizowano i porównano za pomocą analizy statystycznej działanie dwóch programów typu CMMS o nazwach IFS™ oraz MAINTA™. Analizy oparto na studium przypadku przeprowadzonym w rafinerii. Wyniki testowania hipotez oraz analizy ekonomicznej wyłoniły oprogramowanie MAINTA™ .

RADKOWSKI S, SZCZUROWSKI K. **Wykorzystanie sygnału wibroakustycznego w diagnostyce struktur sprężonych.** Eksploatacja i Niezawodnosc – Maintenance and Reliability 2012; 14 (1): 84–91.

W pracy przedstawiono zagadnienie oceny stanu technicznego struktury sprężonej ze szczególnym uwypukleniem możliwości wykorzystania efektów modulacji amplitudowej występujących w obserwowanym sygnale wibroakustycznym. Podstawą takiego podejścia jest teza że zmianie rozkładu naprężeń w przekroju poprzecznym struktury sprężonej towarzyszy mierzalna zmiana parametrów sygnału wibroakustycznego. Wynika ona z założenia, że wraz z wywołaniem stanu sprężenia wstępnego w zginanej konstrukcji zachodzi zjawisko dyspersji, a tym samym zmiana parametrów propagacji fali, w szczególności występowanie mierzalnej różnicy wartości prędkości fazowej i grupowej. Analiza relacji między stanem naprężeń a wartościami prędkości fazowej i grupowej stwarza możliwość budowania diagnostycznych modeli odwrotnych i wyznaczania ilościowych zmian takich parametrów stanu technicznego, jak siły sprężające, moduł Younga czy naprężenia panujące w konstrukcji.

SCIENCE AND TECHNOLOGY

LINGAITIS L P, MJAMLIN S, BARANOVSKY D, JASTREMSKAS V. Experimental investigations on operational reliability of diesel locomotives engines. Eksploatacja i Niezawodnosc – Maintenance and Reliability 2012; 14 (1): 6–11.

Leonas Povilas LINGAITIS
Sergey MJAMLIN
Denis BARANOVSKY
Virgilijus JASTREMSKAS

EXPERIMENTAL INVESTIGATIONS ON OPERATIONAL RELIABILITY OF DIESEL LOCOMOTIVES ENGINES

BADANIA EKSPERYMENTALNE OPERACYJNEJ NIEZAWODNOŚCI EKSPLOATACYJNEJ SILNIKÓW DIESEL DLA SPALINOWOZÓW

In work experimental researches of longevity and technical and operating parameters of diesel engine diesels are presented 10D100 with modified tribosystems. The last are instrumental in the rapid starting and decline of wear depending on time of starting, thus, such diesel practically on any speed and loading modes can be exploited without the promoted wear. At the modified shells of cylinders the wear of compression rings does not affect the size of breach of gases in carter. Thus, the modified tribosystems provide maximal longevity and providing of high technical and operating parameters of diesel engine.

Keywords: *longevity, technical and operating parameters, diesel engine, tribosystem, wear.*

W artykule przedstawiono rezultaty badań eksperymentalnych trwałości i parametrów techniczno-eksploatacyjnych silnika diesla spalinowozu 10D100 ze zmodyfikowanymi systemami ciernymi. Zmodyfikowane systemy cierne gwarantują szybsze uruchomienie silnika, tym samym zmniejszając zużycie związane z uruchamianiem. Ponadto taki diesel może być praktycznie eksploatowany we wszystkich trybach prędkości i obciążenia bez podwyższonego zużycia. W wyniku modyfikacji tulei cylindrów ścieranie pierścieni kompresyjnych nie powoduje zwiększonego przedostawania się gazu do skrzyni korbowej. W ten sposób zmodyfikowane systemy cierne gwarantują maksymalną niezawodność parametrów eksploatacyjnych spalinowozów z silnikiem diesla.

Słowa kluczowe: *trwałość, parametry techniczno-eksploatacyjne, silniki spalinowozów, system cierny, zużycie.*

1. Introduction

Operating railway's locomotives leads to natural obsolescence of the engines as well as other components and details that consequently increases the number of failures. In order to increase operating reliability and durability of locomotive's diesel engines it is purposeful to monitor their technical condition constantly as elimination of failures requires plenty of time and material resources during exploitation [10, 11, 13].

In this work, the subject of research has been chosen an engine 10D100 that is installed in locomotives and there is plenty of statistical data collected about it [1].

The main impact on the diesels durability is made by the resistance to wear [4, 9, 12, 14] of cylinder – piston group and crank – rocker tribosystem mechanisms (TS). Diesel locomotives durability can be increased by hardening (supporting) or modifying (TS) elements, accelerating friction as well as performing technical maintenance and repair qualitatively.

Plenty of wear resistance increasing methods are not applied for the improvement of cylinder – piston and crank – rocker tribosystems due to high cost and scale factor [3, 11]. While selecting surface hardening method for the above-mentioned details of the mechanisms it is necessary to estimate their production scale and technical – economic benefits of the hardening [7]. Accordingly, existing methods for the increasing wear resistance of the surfaces cannot be applied for the diesels throughout [5, 8].

It is possible to use several methods at once as applying complex of several technical methods with constructional solutions and proper attitude to diesels operating process can be achieved an ultimate effect. Using known parts surface hardening methods for the diesels it is possible to reduce wear from 1 to 10 times [9, 12], however objectionable phenomenon (faults) can occur [1, 2, 6].

Introduced diesels durability increase method [9] distinguishes for TS working surfaces being processed by laser suing carbonic acid gas or natural graphite with niobis all-together [4]. We will review and compare modified and unmodified tribosystems of the diesel locomotives by these methods hereinafter.

2. Results of the investigations

Under winter conditions starting-up diesel locomotives within the low temperatures of cooling fluid and oil leads to high increase of tribosystems wear particularly those as „casing-rim“ and „crankshaft-insert“. It can be shown graphically by wear rate dependency on start-up duration of tribosystem by the example of 10D100 diesel (Fig. 1)

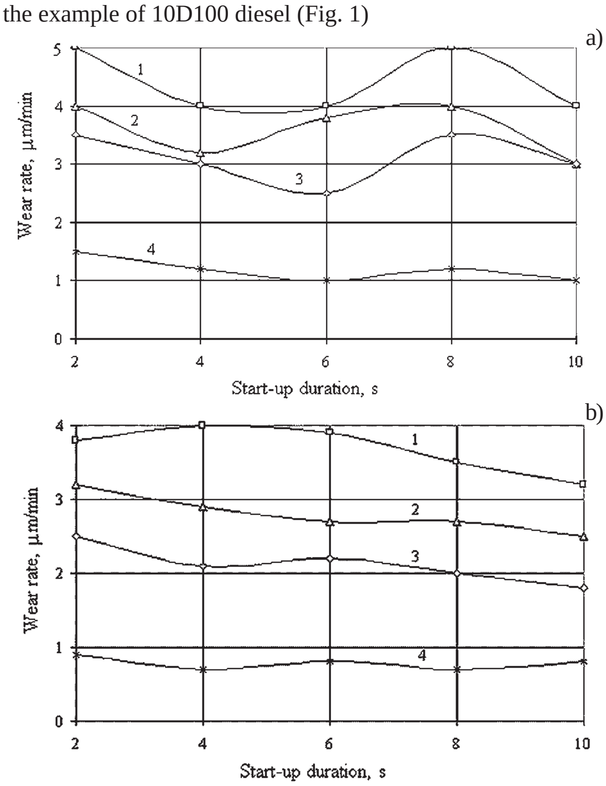

Fig. 1. Wear rate dependency on start-up duration of diesel 10D100 tribosystems „casing - rim“ (a) and „crankshaft – insert“ (b) within oil temperatures of the engine: 1 – 0ºC; 2 – 5ºC; 3 – 10ºC; 4 – 20ºC

We can see from the graphs that wear rate is 4 times greater comparing at temperatures 1ºC and 20ºC in both cases with cylinder casings and crankshaft inserts. This graph testifies that the more we want to reduce wear resistance of the diesel tribosystem the more we need to heat engine oil and reduce duration of the start-up. Here comes additional question – when it is expedient to stop diesel and when it is not? However, it is necessary to evaluate all economic fuel rates and engine wear indexes for that.

Under slight relative displacements of the surfaces of tribosystems during the start-up, wear rate of the diesel locomotives increases due to absence of oil film between the contact surfaces. Superficial layers of the TS are disrupted as they contact with each other without any gap, dominated by dry friction or boundary friction and resulting all negative outcomes.

There are given experimental wear results of bearing inserts of crankshaft and cylindrical casing when diesel locomotives are operating loaded in Fig. 2.

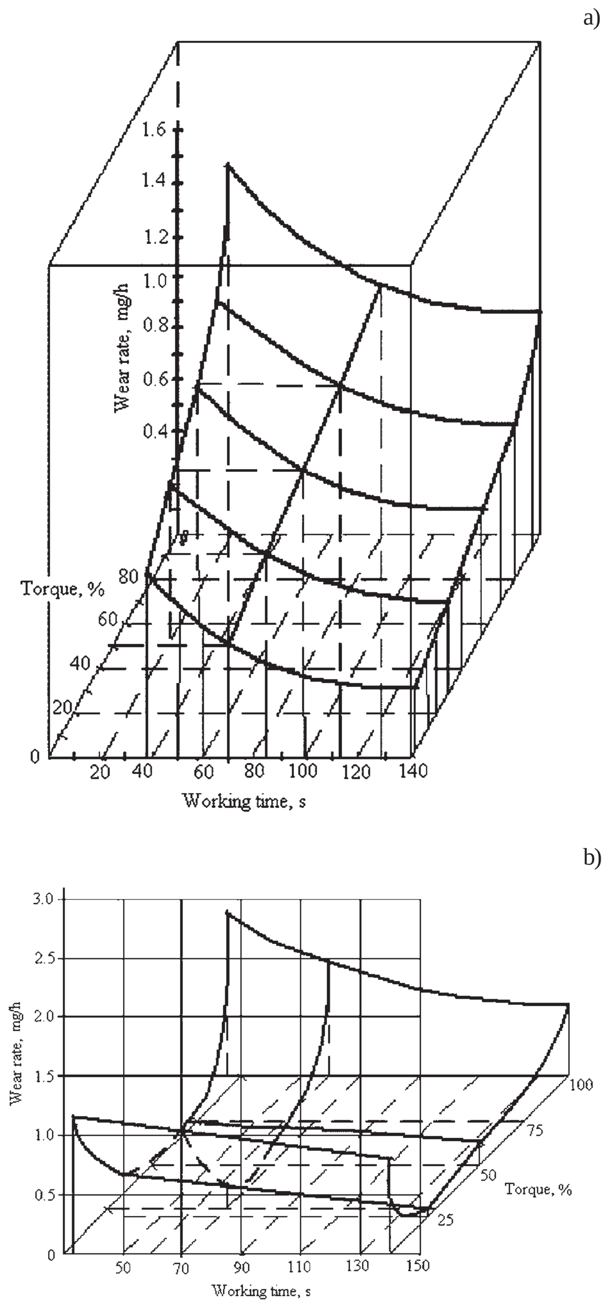

Fig. 2. Wear rate dependency on the workload duration of the cylindrical casings (a) and main inserts of the crankshaft (b) of the diesel locomotives 10D100

We can see here that load, i.e. torque of the crankshaft impacts wear of the diesel tribosystem at the beginning of engines' work. It is also explainable by the non-graded lubrication of the crankshaft bearing inserts and cylindrical casings.

Diesel locomotives are started-up 10–30 times per day. Moreover, technical – exploitation values (heating temperature, thickness of the oil film between contacting surfaces etc.) of the indexes varies at any case. Accordingly, in order to secure the highest durability possible, it is necessary to motivate diesels usage logarithm throughout all steps: start-up, heating, operating and braking.

Start-up of the engines is conditioned by the heated air at the end of compression stroke. Air temperature at the end of compression stroke depends on the reached pressure, temperature of the environment, revolution frequency of the crankshaft as well as wears degree of cylindrical piston parts. Pressure at the cylinder falls and frequency of revolutions of the crankshaft required for the start-up of the engine, i.e. minimal frequency of the crankshaft revolutions at which start-up of the engine is possible, increases regarding to the last reason.

Some of the air gets into the crankcase through the gaps when air is under pressure in the cylinder and parts of the cylinder-piston are too much affected by wear. Therefore falls the pressure in the cylinder herewith temperature at the end of compression stroke. Carburation proceeds worse, i.e. solution of small fuel drops, evaporation and mixing with air, that ignitable compound could flame up. In this case, frequency of the crankshaft revolutions must be high enough. Other significant amount of heat that diverges after pressing air is transferred to the cooling fluid through the walls of the cylinders resulting in the lowering pressure and temperature at the cylinder. Further increasing wear of cylinder – piston tribosystem leads to the moment when it is impossible diesel to set into action.

Huge impact in the start-up of the diesel has an oil film between the walls of the casings. Oil not only reduces wear of the cylinder walls but performs a cylinder presurizement function. Oil flow from the wall of cylinder has been decreased after performed laser modification on diesel tribosystem using natural graphite and carbonic acid gas that leads to the faster start-up of the diesel engine and reduce wear during the start-up by 7–10 times. Certainly, those diesels that are stopped and started-up more often experience more rapid wear. It is proven by the experimental results given in Fig. 3.

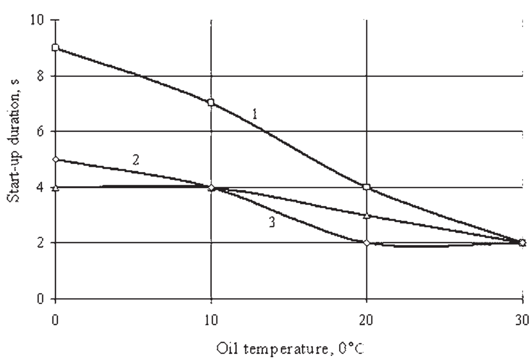

Fig. 3. Start-up duration dependency on the engine oil temperature of the diesel locomotives 10D100: 1 – basic version; 2 – modified by the TS carbonic acid gas; 3 – modified tribological system by natural graphite with niobis

Data of Fig. 3 testifies that start-up time shortens from 1.8 to 2.2 times when oil temperature is 0°C when diesel tribosystem is modified. At the beginning of the start-up wear of the tribosystems has been increased and exceeds constant operating regime's value of the resistance several times. That can be explained by poor lubricating conditions of the contact surfaces at the initial state of diesels operation.

Hereinafter TS wear data of diesel locomotives are specified according to their working hours after the start-up (Fig. 4).

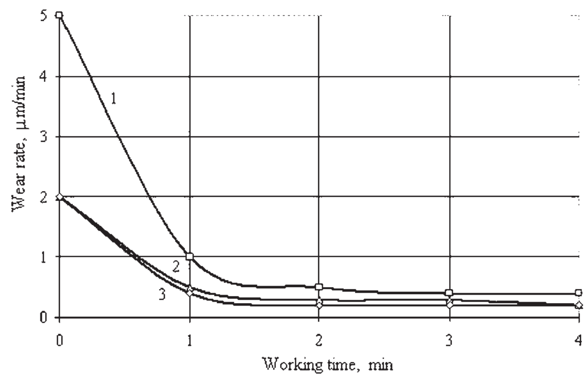

Fig. 4. Wear manner of the diesel locomotive 10D100 tribosystems after the start-up: 1 – basic version; 2 – modified by TS carbonic acid gas; 3 – modified by TS natural graphite with niobis

It is clearly observable that wear of the modified diesel tribosystems during first working minutes (during the start-up) is 2.0–2.5 times lower. Hereby, in order to assure minimal duration of the diesels start-up, minimal wear of tribosystem and hugest exploitation durability it is purposeful to apply la-

a)

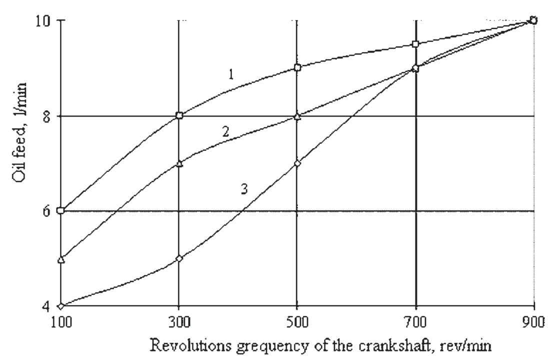

b)

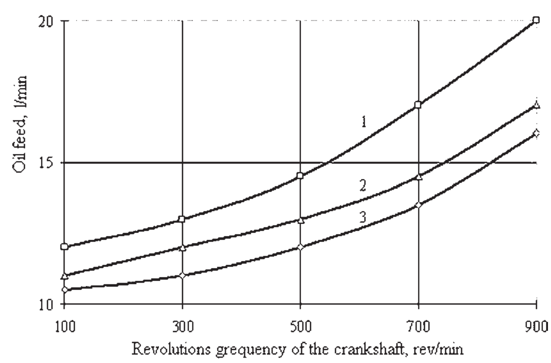

Fig. 5. Diesel 10D100 feed of the oil depending on the frequency of crankshaft revolutions at given oil temperature 20°C (a) and 40°C (b): 1 – basic version; 2 – modified by TS carbonic acid gas; 3 – modified by TS natural graphite with niobis

ser modification of TS by carbonic acid gas or natural graphite with niobis.

Usually, diesel locomotives are heated without load gradually whilst rising temperature of the engine's oil until exploitation values.

As it was above-mentioned, huge impact on the locomotive tribosystems wear is performed by the amount of oil that accesses contacting friction surfaces. Its amount depends on the efficiency of the oil pump (Fig. 5).

The graphs in Fig. 5 show that amount of oil in modified TS is noticeably smaller than comparing with basic variant at both temperatures 20°C and 40°C, implying that film of oil keeps a tight hold in modified tribosystems and thus guarantees the most beneficial liquid friction and hermetic condition in the casing pair. It was observed during investigations that oil feed remains almost steady after the locomotive has been driven more than 300 thousand km implying in uniform, slow-motioned manner of wear.

Amount of oil that is supplied between contact surfaces is insufficient at low temperatures and can lead to damage of the tribosystems friction surfaces (melting of bearings, chips of cylindrical casings). Modification of TS contacting surfaces by carbonic acid gas or natural graphite with niobis helps in preventing from the above-mentioned failures starting-up engines at low temperatures as modification maintains sufficient lubrication of contacting surfaces.

Characteristic value of wear degree for the main tribosystem of diesel locomotives is an amount of burnt-out oil depending on the grind-in (Fig. 6). Furthermore, increasing amount of burnt-out oil leads to conclusion that wear level of the main tribosystems is close or at critical state. Wear of the cylinder-piston group can be also described by the amount of the gas lead to the crankcase (Fig. 7).

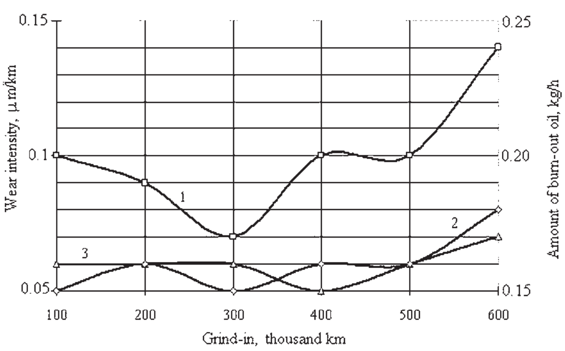

Fig. 6. Wear and amount of burnt-out oil dependency in cylinder-piston tribosystem of the diesel locomotive 10D100 depending on the grind-in: 1 – basic version; 2 – modified by TS carbonic acid gas; 3 – modified by TS natural graphite with niobis

As it is shown in the graphs, the amount of burnt-out oil during the exploitation period from 100 to 600 thousand km of locomotives is proportionate to the wear level of the cylinder-piston group at the tribosystem. When 600 thousand km are reached, i.e. when wear level is highest, burnt-out amount of oil is 1.4 times lower comparing to the basic engine in the diesels if using modified tribosystems.

As we can see from the graphs, gas leak to the crankcase is noticeably lower (2) when comparing to the basic variant (1) when modified cylinder casings of the diesel 10D100 are used,

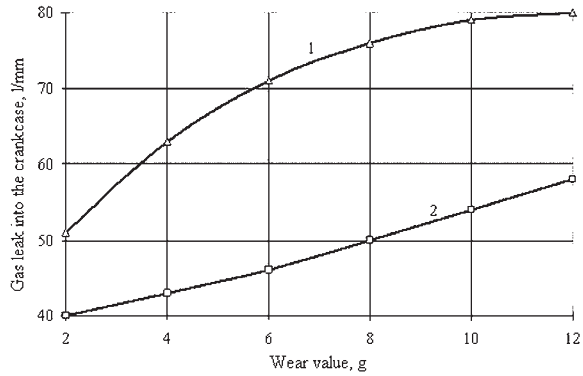

Fig. 7. Compression rims wear influence on the gas leak to the crankcase of the diesel locomotives 10D100: 1 – basic variant; 2 – cylinder casings modified by the natural graphite with niobis

the implication is that the gap of tribosystem „cylinder casing-compression rims" varies very slightly.

Wear resistance of diesel locomotive TS under the loaded regime can be evaluated according to their wearing rate when constant frequency of the crankshaft revolutions and variable oil supplies with the high pressure pump are applied: results are given in Fig. 8.

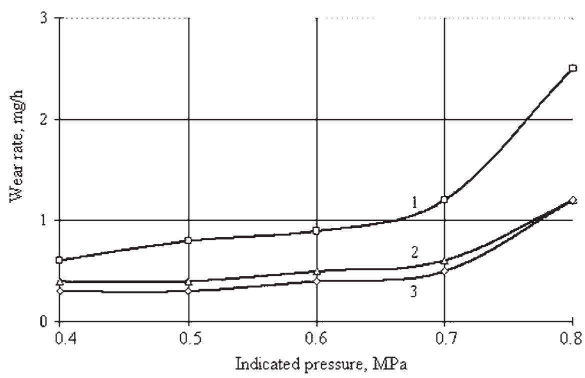

Fig. 8. Wear rate of the first piston rim of the diesel locomotives 10D100 depending on the indicated pressure: 1 – basic variant; 2 – TS modified by the carbonic acid gas; 3 – TS modified by the natural graphite with niobis

As we can see from the graphs, an absolute value of the TS wear that determine resource of the diesel increases due to the increase of load.

Resistance to wear at various velocity regimes of the diesel locomotive tribosystems can be evaluated while changing frequency of revolutions of the crankshaft at the same time feeding fuels to the cylinders by high pressure pump. Change of velocity regime has an impact on the formation of ignitable compound and its combustion as well as on the mechanical and thermal loads of diesel tribosystems. Increasing frequency of revolutions of the crankshaft increase wear rate of tribosystems because of the temperature increase and higher dynamical and friction forces in „cylinder-piston" and „crank - rocker" tribosystems.

Decreasing frequency of revolutions of the crankshaft below the recommended limit leads in increase of wear rate as hydrodynamic lubrication regime becomes worse. Comparative wear rate of the „crankshaft-insert" tribosystem of diesel locomotives depending on the frequency of revolutions of the

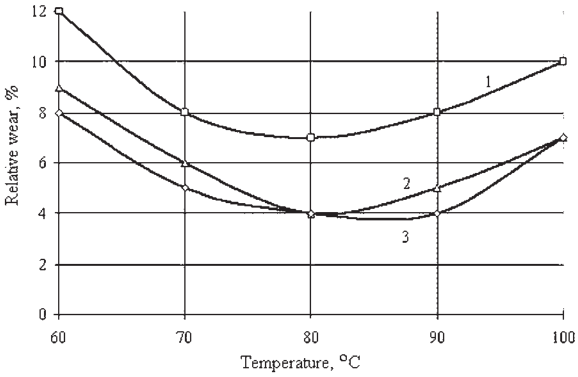

Fig. 9. Relative wear dependency on the temperature of cooling fluid of the diesel locomotives 10D100 tribosystems: 1 – basic variant; 2 – modified tribosystems by carbonic acid gas; 3 – modified tribosystems by natural graphite with niobis

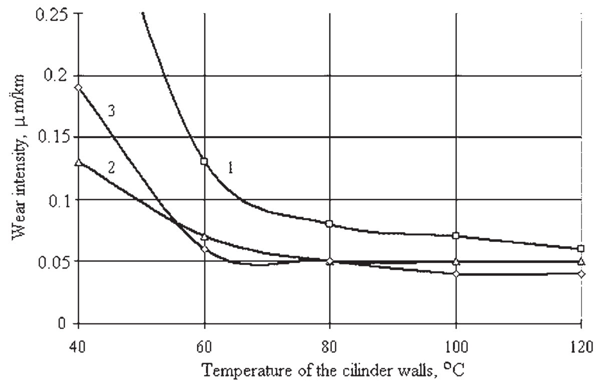

Fig. 10. Cylindrical casing wear dependency on the wall temperature of the diesel locomotive 10D100: 1 – basic variant; 2 – modified tribosystems by carbonic acid gas; 3 – modified tribosystems by natural graphite with niobis

crankshaft is the same as in cylinder-piston tribosystem. Minimal wear occurs in the revolutions to 500 rev/mm.

Increased wear of tribosystems in the range of high frequency revolutions of the crankshaft is explained by increased pressure and resistance, higher temperature of working surfaces and oils, whilst at low frequency revolutions of the crankshaft is explained by decreased effectiveness of the oil film on diesel tribosystems.

Hereby, the results of the investigation show that after modification of diesel locomotive tribosystems with carbonic acid gas or natural graphite there exist an optimal working regime which maintenance leads to guaranteed minimal wear and maximal durability of main diesel elements.

Temperature working regime of the locomotives can be graded according to temperatures of cooling fluid and engine oil during the exploitation. Superheat of the engine decreases viscosity of oil, cracks film of oil, deforms parts that results in increased wear rate of the latter.

It is known from the passport data that optimal thermal regime of cooling fluid is 70–90°C at which wear of tribosystems is minimal. There were performed investigations for the wear rate of tribosystems at the temperature range 60–100°C. The total results of wearing of the diesel depend on the temperature of cooling fluid and are shown in Fig. 9.

Results of the investigations indicates that certificate's data are confirmed for the basic variant of the diesels and the one modified by carbonic acid gas, i.e. the lowest wear is achieved when temperature of the cooling fluid is held approximately by 80°C. However, for the diesels modified by natural graphite with niobis an optimal temperature is nearly 90°C.

Besides that, considerable importance for the wear intensity of cylindrical casings of locomotives has corrosion processes. At low cooling fluid and oil temperatures some surfaces of the casings are irrigated by condensate which consists of diesel products containing combinations of sulphur and other gases active for corrosion. Resulting to that a chemical corrosion occur forming oxides that increase corrosion - mechanical wear in tribosystem „cylindrical casing- rim". Wear of cylindrical casing of diesels 10D100 depending on the wall temperature of the casing is shown in Fig. 10.

Results indicate that sufficiently intense wear of the cylinder casings occurs while diesel is heated after the launch. Wear intensity becomes practically steady after it reaches optimal temperature of 80–90°C. We can also see here that the most favorable kind of TS modification is the one with natural graphite with niobis.

While investigation of wear manner of diesels TS at non-stationary (non-steady) regimes it was observed that wear of the cylindrical casings, pistons, main and rocker crankshaft inserts increases by more than 20 %. That is associated with fact what at non-steady regimes, when comparing to steady ones, increases influence of the inertia forces on loads, operating conditions of oil become worse, normal steady combustion process at the cylinders breaks down. As it was above-mentioned, it is impossible to reject transitions from liquid friction to the critical as well as increased corrosive wear.

In such a way, it is necessary to maintain constant (stationary) regimes during exploitation of locomotives with unmodified diesel tribosystems. If it is impossible then transitions from one regime to another must be performed uniformly that can be hardly implemented on the railroad.

Diesels are not that sensitive to the change of regimes and fulfill operating conditions on the railroads much better at the same time as well as increase durability and their usage effectiveness when tribosystems of the diesel locomotives are modified.

3. Conclusions

The following conclusions can be made after performed investigations on engines of diesel locomotives 10D100:

1. Wear of the parts is 10 times higher comparing to established diesel working regimes during the diesels start-up.
2. Modified diesel tribosystems shorten start-up duration and depending on that decreases wear 7–10 times.
3. Diesels can be operated at all velocity and load regimes without increased wear with modified tribosystems.
4. Wear of compression rims does not have influence on the gas leak to the crankcase of the engine using modified casings of the cylinders i.e. gap of the tribosystem „cylinder casing – compression rims" does not vary practically as its slight increase is compensated by the hard film of oil.

Maximum durability of diesel locomotives can be achieved by modified tribosystems.

4. References

1. Benjumea P, Agudelo J, Agudelo A. Effect of the degree of unsaturation of biodiesel fuels on engine performance, combustion characteristics, and emissions. Energy fuels 2011; 25(1): 77–85.
2. Freitas S, Pratas M. J, Ceriani R, Lima A, Coutinho J. A. 2011. Evaluation of predictive models for the viscosity of biodiesel. Energy fuels 2011; 25(1): 352–358.
3. Goryacheva I, Zakharov S, Soshenkov S. et al. Tribodynamic simulation of wheel/rail profile evolution and contact-fatigue damage accumulation for some variable track and vehicle parameters. Railway Research Institute Bulletin "VNIIZht Bulletin" 2011. Moscow, 1: 13–19.
4. Józwik J, Pieśko P, Krajewski G. Evaluation of QC10 ballbar diagnostics method for CNC machine. Eksploatacja i Niezawodnosc – Maintenance and Reliability 2010; 3(47): 10–20.
5. Kmita T, Skoneczny W. Increase of operational durability of a plastic material-oxide coating couple as a result of the application of a pulsed anodizing process. Eksploatacja i Niezawodnosc – Maintenance and Reliability 2010; 1(45): 77–82.
6. Li R, Kang R, Huang N, Chen W, Chen Y. A practical approach for network application reliability assessment. Eksploatacja i Niezawodnosc – Maintenance and Reliability 2009; 4(44): 17–27.
7. Lingaitis L. P, Pukalskas S. The economic effect of using biological diesel oil on railway transport. Transport 2008; 23(4):287–290.
8. Wojciechowski L, Nosal S. Increase of operational durability of a plastic material-oxide coating couple as a result of the application of a pulsed anodizing process. Eksploatacja i Niezawodnosc – Maintenance and Reliability 2010; 1(45): 83–90.
9. Барановский Д. Експериментальні дослідження триботехнічних властивостей трибосистем дизелів у процесі їх модифікування [Baranovsky D. Experimental studies of the properties tribosystems diesels in the process of modification]. Вісник ДІАТ, 2010; № 2, 48–52 с. (in Ukrainian).
10. Бервинов В. Техническое диагностирование локомотивов [Bervinov V. Technical diagnostics locomotives]. Москва:УМК МПС России, 1999; 190 с. (in Russian).
11. Гурвич И. Износ и долговечность двигателей [Gurvich I. Wear and longer engine life]. Горький: Волговятское издательство, 1970; 176 с. (in Russian).
12. Иванов В, Антропов В, Савин Н. 1973. Повышение надежности и срока службы цилиндровых гильз тепловозных дизелей типа Д100 [Ivanov I; Antropov V.; Savin N. Increased reliability and lifetime of the cylinder liner diesel engines D100 type]. Москва: Транспорт, Выпуск 504б, 1973; 22–37 с.(in Russian).
13. Мямлин С. Моделирование динамики рельсовых экипажей: монография [Mjamlin S. Modelling the dynamics of railway vehicles]. Днепропетровск: Новая деология, 2002; 240 с. (in Russian).
14. Тартаковский Э. 1973. Качество ремонта и надежность тепловозов [Tartakovsky E. Quality of repair and reliability of locomotives]. Москва: Транспорт, 1973; 134 с. (in Russian).13–19 p.

Prof. dr. habil. Leonas Povilas Lingaitis
Department of Railway Transport
Vilnius Gediminas Technical University
J. Basanavičiaus str., 28-135, LT-03224 Vilnius, Lithuania
E-mail: Leonas.Lingaitis@vgtu.lt

Prof. dr. habil. Sergey Mjamlin
Dneprpetrovsk National University of Railway Transport
Ak. Lazaryana Str. 2, UA-49010 Dnepropetrovsk, Ukraine
E-mail: mjamlin@nzn.diit.edu.ua

Prof. dr. Denis Baranovsky
Department of Automation Control Systems and Electric Drive
Kremenchuk Mykhailo Ostrohradskyi National University
Pershotravneva Str. 20, UA-39600 Kremenchuk, Ukraine
E-mail: secr@kdu.edu.ua

Virgilijus Jastremskas, MSc. (Eng)
Department of Railway Transport
Vilnius Gediminas Technical University
J. Basanaivičiaus str., 28-135, LT-03224 Vilnius, Lithuania
E-mail: v.jastremskas@litrail.lt

Article citation info:
KUCHARCZYK W. Ablative and abrasive wear of phenolic-formaldehyde glass laminates with powder fillers. Eksploatacja i Niezawodnosc – Maintenance and Reliability 2012; 14 (1): 12–18.

Wojciech KUCHARCZYK

ABLATIVE AND ABRASIVE WEAR OF PHENOLIC-FORMALDEHYDE GLASS LAMINATES WITH POWDER FILLERS

ZUŻYWANIE ABLACYJNE I ŚCIERNE LAMINATÓW FENOLOWO-FORMALDEHYDOWYCH – SZKLANYCH Z NAPEŁNIACZAMI PROSZKOWYMI*

This paper reports the results of wearing out polymer composites: the ablative wear, after 30 s of treating with hot combustion gases, as well as the abrasive wear, after 1000 s of friction using the loose abradant in the T-07 tester. The specimens were made of phenolic-formaldehyde matrix, glass fabrics-reinforcement and powder fillers: the corundum Al_2O_3 and the carbon powder C. It was qualified the qualitative and the quantitative effect of components on the average linear rate of ablation v_a and the average mass intensity of abrasive wear I_z. It was proved, that composites with the smaller intensity of abrasive wear I_z are characterized by bigger rate of ablative using up.

Keywords: *ablation, abrasive wear, powder fillers, glass laminates.*

Przedstawiono wyniki badań zużywania kompozytów polimerowych: ablacyjnego, po 30 s oddziaływania wysokotemperaturowego strumienia gazów palnych oraz ściernego, po 1000 s tarcia próbki luźnym ścierniwem w testerze T-07. Doświadczeniom poddano szklane laminaty fenolowo-formaldehydowe z napełniaczami proszkowymi: korundem Al_2O_3 oraz pyłem węglowym C. Określono jakościowy i ilościowy wpływ komponentów na wartości zużywania: średnią liniową szybkość ablacji v_α oraz średnią masową intensywności zużywania I_z. Stwierdzono, że kompozyty o składach fazowych zapewniających mniejszą intensywność zużywania ściernego charakteryzują się większą szybkością zużywania ablacyjnego.

Słowa kluczowe: *ablacja, zużywanie ścierne, napełniacze proszkowe, laminaty szklane.*

1. Introduction

Modified polymer composites as ablative materials to prevent the excess rise in temperature has been mostly used in armament industry as well as aircraft, rocket and space technology [7, 6]. Such materials can also be used as passive fire protection of load-bearing structures in large-volume buildings [12, 19], tunnels [5, 13], as well as in electronic, optic and magnetic data protection systems, etc.

The development of compositions, manufacturing technologies and research into the characteristics of ablative materials has become of great importance due to the threat of terrorists attacks. It is in the USA that the analysis of the causes and consequences of such disastrous events as Oklahoma City or World Trade Center attacks [12, 19] has brought about a thorough scientific investigation into the behavior of such materials. Ablative materials are beginning to be used in protection of public facilities and structures [12, 19, 5, 13] which can be exposed to fire hazard or short-term, intensive erosive heat flux.

Thanks to autonomous shields and ablative shielding we can protect building structures and people's lives in heat load incidents with temperatures much exceeding permissible standards since the classical flameproof materials cannot prevent the increase in temperature at the rear side of protective shields as effectively as ablative materials whose high characteristics of substitute heat resistance r_{kp} [$m^2 \cdot K/W$] allows the reduction of temperatures by anything from several dozens degrees to ~ 2 000 °C with the use of relatively thin insulation shields.

The ITA (International Tunneling Association) guidelines, for example, recommend flameproof shielding in transport tunnels that should reduce the temperature of concrete down to 350 °C (exceeding this value results in the drop of its rigidity by 50% of the nominal value [20]) and prevent it from peeling and splitting off. The temperature of steel elements used in such constructions must not exceed 300 °C [5, 13] as this is the value beyond which the strength of steel decreases dramatically [2].

Despite the fact that ablative materials have been used for many years we still do not know the dependencies between the quality and contents of a given phase composition of and its ablative characteristics in relation to other operational features of the composites that are used in thermo-insulating shields. [8, 4 , 21].

This paper attempts to answer the question of the influence of the quantitative and qualitative phase composition of phenolic-formaldehyde glass laminates with powder fillers on ablative wear (average linear rate of ablation v_α [μm/s]) and whether the ablative wear of a composite is related to abrasive wear resistance of the basic material (mass intensity of abrasive wear I_z [mg/s]).

(*) Tekst artykułu w polskiej wersji językowej dostępny w elektronicznym wydaniu kwartalnika na stronie ***www.ein.org.pl***

2. Ablation of polymer composites

The ablation process is the process of exchanging of heat and mass which, due to physical changes and chemical reactions, results in chemical and structural changes of the material with simultaneous heat absorption, which reduces heating up of the material below the front of ablation (Fig. 1). The heat influx causes relocation of the ablation front deeper into the material and thickening of the porous ablative surface [8].

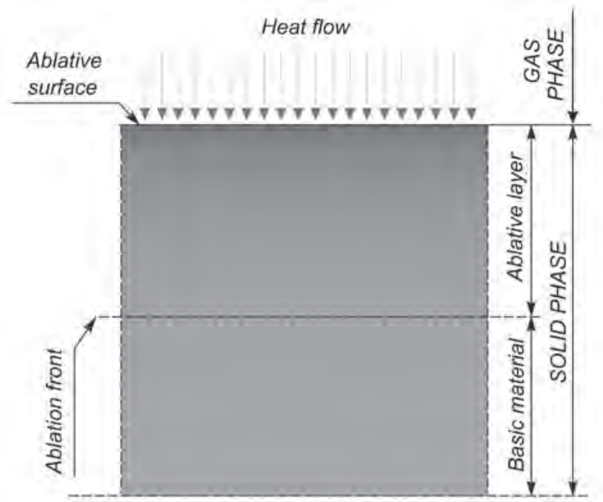

Fig. 1. Physical model of ablation [8]

In polymer composites, when the ablation temperature has been exceeded, there occur endothermic reactions involved in the thermal decomposition of the matrix material due to which the effective specific heat of c_p resins reach very high values. In their pure form such resins are a very good thermo-insulating ablative material [6, 4, 21]. However, due to their softening as well as the porosity and brittleness of the formed ablative surface they require an addition of high-melting fibre fillers [7, 6, 14] or powder fillers [17, 1].

In his paper [3] Yu. I. Dimitrienko proposed a classification of ablation processes in composites treated with heat fluxes (Fig. 2). The process of mass loss $m = \rho \cdot V$ (where ρ is density and V is volume) due to the heat and thermo-mechanical impact of gas fluxes may result in a change in either density or volume as well as in a simultaneous change of both values [3].

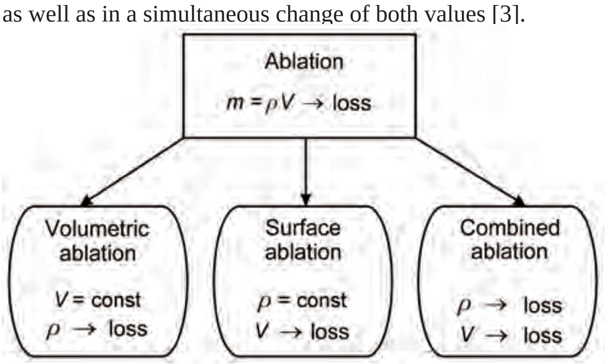

Fig. 2. Classification of main ablation processes of materials: m - mass ρ - density and V - volume [3]

The process of density loss where the volume remains unchanged is a pyrolysis which occurs in temperatures 500 ÷ 1000 °C and is characteristic for polymer composites. Such a process is called *volumetric ablation*. The process in which there occurs a volume loss with unchanged density is called *surface ablation*. It is typical for oxidization o graphite, metals and their alloys, glass as well as some types of fusible ceramic materials. A simultaneous occurrence of both processes of thermal degradation is referred to as *combined ablation*. Combined ablation usually takes place in high temperatures (1000 ÷ 1500 °C) and results from thermal and erosive gas impact. In all of the above-mentioned cases there occur ablative wear (which is sometimes purely erosive) of the basic material [3].

To be able to take the full advantage of ablative materials we need to be aware of their ablative wear characteristics, which have to be taken into consideration at the early stage of the technological design. This includes a loss in active volume of the material that is not subject to ablation. The effect is characterized by linear ablation rate ν_α [μm/s] defined as the average rate of dislocation of the ablation front i.e. the average rate of formation of ablative surface and so-called *vitreous slag*. If we determine the rate of ablation it is possible to determine the temporary location of the ablation front and, in consequence, to determine the thickness of active insulating layer [6, 1, 3, 11].

Processes of ablative wear of thermo-insulating shielding of structures and machinery, which can be exposed to fire hazard, or short-term, intensive erosive heat flux usually occur in failure situations which are incidental by assumption. Throughout the course of its normal operation in the usual operating temperatures, the ablative thermo-insulating shielding of the machinery is exposed to service and mechanical loads (including abrasive wear), which have a negative influence of the ablative characteristics of the materials [7, 21, 3].

3. Choice of materials

Based of bibliography [7, 14, 21], the following materials have been used to prepare the specimens of glass fibre laminate with powder fillers:

1. Thermosetting matrix: PF resins (*Modofen* 54S and *Nowolak MR* used in 1:1 weight ratio) manufactured by Organika-Sarzyna Chemical Works.

2. Fibre reinforcement: balanced glassfibre fabric STR-022 of 250 g/m² manufactured by Krosno Glassworks SA.

3. Powder fillers: *corundum* Al_2O_3 (ALO G5-4) with grains of 2 to 5 μm with the minimal contents of aluminum oxide of 99,5% (95% α Al_2O_3) manufactured by Ajka Amumina, Hungary; fine grain carbon powder C of 5 μm and purity of 98%.

4. Design of experiments

The number of experiments and the phase compositions of specimens have been determined on the basis of the experimental design, (Table 1) [10, 15] i.e. 2-level orthogonal full factorial design for replicated 2^3 factorial experiments. The composite materials constitute the three input parameters x_i with 2-level coding (–1 as low value and +1 as high value):

x_1 – mass contents of the matrix: 24% (– 1) and 30% (+1);
x_2 – number of fibreglass fabric layers: 8 (– 1) and 12 (+1);
x_3 – proportion of Al_2O_3 corundum to the total mass of both fillers $Al_2O_3/(Al_2O_3 + C)$: 20% (– 1) and 80% (+1).

The components of the response variable y (the output parameters) are the average linear rate of ablation ν_α [μm/s] and the average mass intensity of abrasive wear I_z [mg/s].

Table 2 shows the factual phase compositions of the tested phenolic- of formaldehyde laminates and their coding. The regression indexes b_1, b_2, b_3 and the interaction indexes b_{12}, b_{13}, b_{23}, b_{123} determine the influence of a given input value (or several input values i.e. interactions) on $\bar{y}$ which is the output value in the equation of the experiment objective (1) [10, 15]:

$$\bar{y} = b_0 + b_1x_1 + b_2x_2 + b_3x_3 + b_{12}x_1x_2 + b_{13}x_1x_3 + b_{23}x_2x_3 + b_{123}x_1x_2x_3 \quad (1)$$

The values of regression indexes are achieved from the equation (2):

$$\frac{\sum_{j=1}^{8} x_{ij} \cdot \bar{y}_j}{N} \qquad i = 0, 1, 2, 3 \qquad (2)$$

The statistical analysis of the results aims at determining the significance of regression indexes b_i and assessing their influence on the value of output parameter $\bar{y}$ with the following equations [10, 15]. Variance (3) and error in determination of regression indexes (4) are:

$$s(\bar{y}) = \sqrt{\frac{\Sigma d_j^2}{2N}} \quad (3) \qquad s(b_i) = \sqrt{\frac{s^2(\bar{y})}{N}} \quad (4)$$

where:

$d_j = \bar{y} - y_{jk}$ ($\bar{y}$ - the average of k number of measurements; y_{jk} - value of the k^{th} measurement in the j^{th} test; $k = 1, 2$; N - number of tests).

The significance of regression indexes b_i was value for the t-Student's distribution, where $t_{obl} >> t_{tabl}$ ($t_{tabl} = 2{,}306$ with probability $P = 0{,}95$). The equation (5) is thus fulfilled and following transformations we achieve equations (6) and (7):

$$\frac{b_i \cdot \sqrt{N}}{s(\bar{y})} = t_{obl.} \quad (5) \qquad b_i = \frac{2{,}306 \cdot s(\bar{y})}{\sqrt{N}} \quad (6)$$

$$b_{istot} \geq b_i = \frac{2{,}306}{\sqrt{8}} \cdot s(\bar{y}) = 0{,}8153 \cdot s(\bar{y}) \qquad (7)$$

5. Ablation and abrasive wear tests

5.1. The ablation testing conditions

The ablation tests of the composites were carried out with the following assumptions: thermophysical characteristics of the materials are solely the temperature function; the heat flux during the test is of constant value; the isothermal surface of the ablation front constitute the ablation surface (Fig. 1); the heat exchange of the outer surface with the environment is omitted [7, 8].

The specimens (10 x 25 x 35 mm cubes) were placed in a shielding of flameproof plaster-cardboard panel and exposed to gas heat flux for $\tau = 30$ seconds. Burning of acetylene and oxygen mixture (with the oxygen/acetylene ratio of 1:1,2) in a *PU-241A* blowpipe provided the source of heat. The blowpipe was equipped with Attachment 3 to ensure so-called neutral flame. The blowpipe was placed perpendicular to the surface of the laminate (in the middle of the 25 x 35 mm side). The ablation surface was situated at the end of the flame reducing zone i.e.

Table 1. Two-level full factorial design for replicated 2^3 factorial experiments [10, 15]

j^*	x_0	x_1	x_2	x_3	x_1x_2	x_1x_3	x_2x_3	$x_1x_2x_3$	y_j
1	+	−	−	−	+	+	+	−	
2	+	+	−	−	−	−	+	+	
3	+	−	+	−	−	+	−	+	
4	+	+	+	−	+	−	−	−	
5	+	−	−	+	+	−	−	+	
6	+	+	−	+	−	+	−	−	
7	+	−	+	+	−	−	+	−	
8	+	+	+	+	+	+	+	+	
	b_0	b_1	b_2	b_3	b_{12}	b_{13}	b_{23}	b_{123}	

* *j-value is a test number and also the number of the composite whose phase composition is determined by function of x_i*

Table 2. Coding of variables and the factual phase compositions of the composites

Test no.	Mass ratio of materials in a composite [%]						
	matrix (x_1)		fibreglass fabric (x_2)		powder fillers (x_3)		
						Al_2O_3	C
1	−	24	−	18	−	11,6	46,4
2	+	30	−		−	10,4	41,6
3	−	24	+	25	−	10,2	40,8
4	+	30	+		−	9,0	36,0
5	−	24	−	13	+	50,4	12,6
6	+	30	−		+	45,6	11,4
7	−	24	+	19	+	45,6	11,4
8	+	30	+		+	40,8	10,2

Table 3. Parameters and condition for tribological tests [18]

Load of specimen against counterspecimen: $P = 44$ N	Counterspecimen: a steel roll covered with rubber (hardness of 78 ÷ 85 Sh A)
Rate of rotation of counterspecimen: $n = 60$ r.p.m.	Abradant: electrocorundum no. 90 (PN-76/M-59115)
Duration of test (number of counterspecimen rotations): $\tau = 1000$ s ($N_b = 1000$ rotations)	Output value: Wear intensity I_z [mg/s]

10 mm from its cone. The flame temperature at the ablation surface was approx. 2 500°C [8, 17, 1, 16].

After the heat treatment tests the cross sections of the specimens were made and the measurements of the ablation front and the depth of its relocation were taken to determine the average linear ablation rate v_a.

5.2. Assessment of the intensity of abrasive wear

A modified *T-07* tester for assessment of the abrasion resistance of materials and metal coatings to friction against loose abradant was used do determine the mass intensity of abrasive wear I_z (the change in mass in relation to wearing period) complying with the testing condition and parameters recommended by the manufacturer (see Table 3) [18, 22].

The shape and dimensions of the specimens [9, 22] are shown in Figure 3a while Figure 3b depict a specimen after the abrasive test. The sliding surface and the direction of the friction force were set perpendicular to the glass layers of the laminate (see Fig. 3a) [9].

a)

b)

Fig. 3. A tested specimen [9, 22]: a) structural drawing, b) after the test

5.3. The results of ablation tests and tribological tests

The results of ablation tests (the average linear ablation rate v_a) and tribological tests (the average mass intensity of abrasive wear I_z) are presented in Table 4 while Figure 4 shows its graphic interpretation.

The aim of the experiment was to find such a composite whose values of the average linear ablation rate v_a the average mass intensity of abrasive wear I_z are the lowest. These conditions have been fairly met by specimen 4 whose phase composition consists of 30% matrix, 25% fibre glass fabric reinforcement, 9% corundum Al_2O_3, and 36% carbon powder C (fig. 4).

5.4. Statistical analysis of test results

The regression indexes and their significance, the variance, and the determination error were calculated based on the data provided in Table 4 and with formulas (2), (3), (4), and (7). The results are presented in Table 5. The **bold print** marks b_i values, which are lower than b_{istot} but burdened with the error $s(b_i)$ which allows to assess the b_i as statistically significant. The empty cells in the Table mean that the given index is not of any statistical significance and has been omitted. The analysis of the values of b_i - coefficients and the signs preceding them let us assess the influence of independent variables x_i on the output values (response variable). The graphic interpretations of the relation of both response variables (the output parameters) to the phase variables are presented in Figures 5 to 7.

Having analysed the values and preceding signs of the regression and interaction indexes, we can confirm that for the assumed range of independent variables, there exist the relation of the wear parameters to the coding variables that is to the phase composition of the composite.

The higher content of the matrix results in a significant decrease in abrasive wear I_z while the average rate of ablation v_a rises (negative and positive coefficient b_i for both components of the response variable respectively). The content of matrix influences the abrasive wear values in the most significant manner. Thus if its content is lower, the increase in the content of hard corundum must follow.

The change in the number of the fibreglass fabric layers (the change of the content of glass reinforcement) does not have any significant influence on any of the examined wear parameters (insignificant values of b_2). However, the increase in the content of glass reinforcement (x_2) together with the content of matrix (x_1) i.e. the decrease in the content of powder fillers results in a noticeable drop in the ablation rate and a slight increase in the wear resistance (negative b_{12}).

With the higher content of Al_2O_3 (i.e. the lower content of powder carbon C) the wear intensity I_z slightly drops (negative b_3 and b_{13}) but there is a considerable rise in the rate of ablation v_a (positive b_3). The higher number of fibreglass fabric layers (x_2) with simultaneous increase in the content of Al_2O_3

Table 4. The results of ablation tests and tribological tests

Parameter		Number of test 1	2	3	4	5	6	7	8
matrix [%]		24	30	24	30	24	30	24	30
fibreglass fabric [%]		18		25		13		19	
powder fillers [%]	Al_2O_3	11,6	10,4	10,2	9,0	50,4	45,6	45,6	40,8
	C	46,4	41,6	40,8	36,0	12,6	11,4	11,4	10,2
v_a [μm/s]		121	158	125	128	130	166	157	172
I_z [mg/s]		1,11	1,28	1,50	0,89	1,40	0,70	1,31	0,83

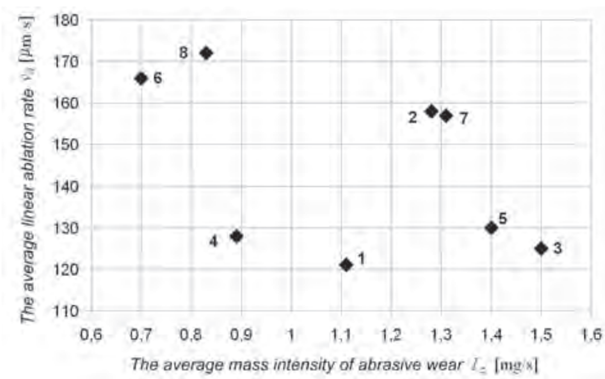

Fig. 4. The tests results: the average linear ablation rate v_a and the average mass intensity of abrasive wear I_z

Table 5. Statistics of coefficients the equations of the response variable

	b_0	b_1	b_2	b_3	b_{12}	b_{13}	b_{23}	b_{123}	$\bar{y}$	$s(b_i)$	b_{istot}
v_a [μm/s]	144,5	11,4		11,5	-6,9		7,5		6,9	2,4	5,6
I_z [mg/s]	1,13	-0,21		**-0,07**	**-0,07**	**-0,09**		0,13	0,11	0,04	0,1

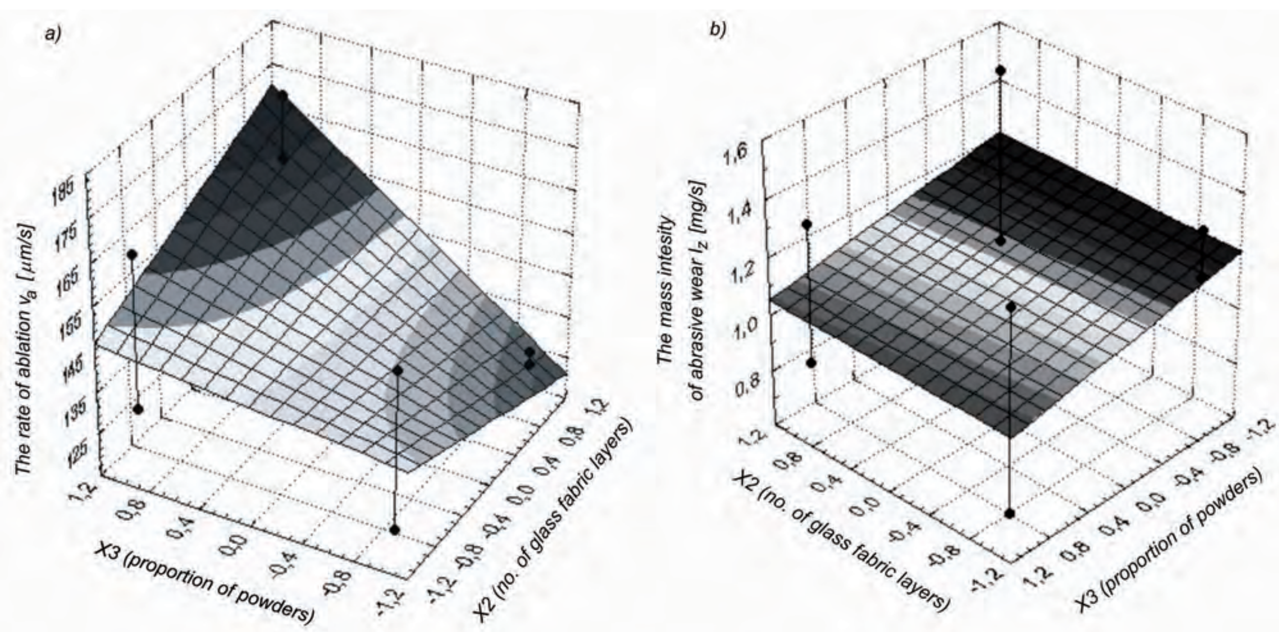

Fig. 5. Relation of abrasive wear to phase composition for variable $x_1 = 0$, (27% resin): a) the average linear rate of ablation v_a, b) the average mass intensity of abrasive wear I_z.

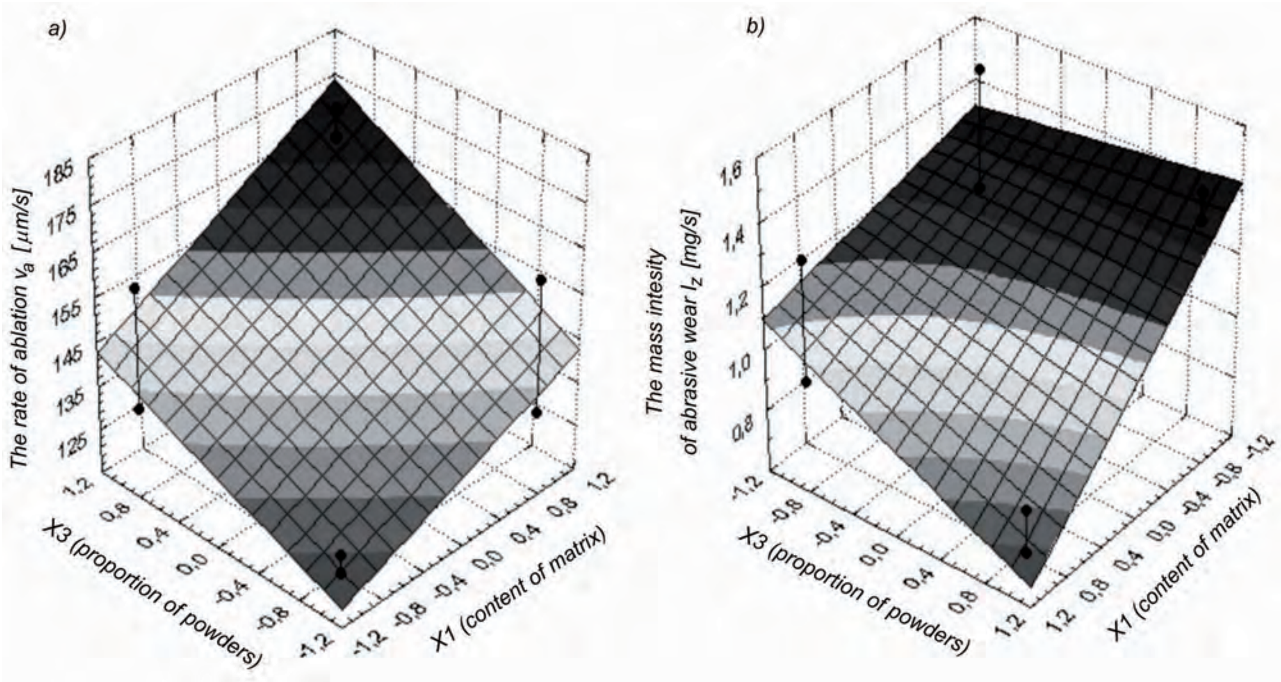

Fig. 6. Relation of abrasive wear to phase composition for variable $x_2 = 0$, (10 layers of glass fabric): a) the average linear rate of ablation v_a, b) the average mass intensity of abrasive wear I_z.

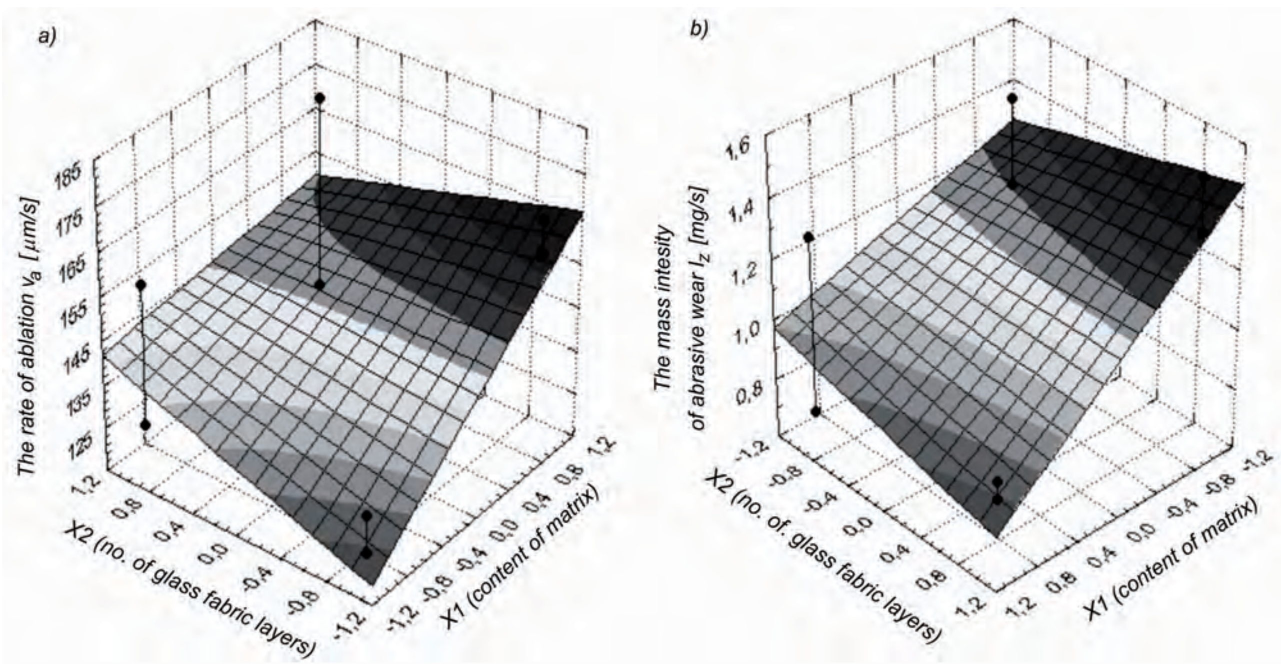

Fig. 7. Relation of abrasive wear to phase composition for variable $x_3 = 0$, (50% C and 50% Al_2O_3): a) the average linear rate of ablation v_a, b) the average mass intensity of abrasive wear I_z.

(a drop in the content of $C - x_3$) results in increasing ablation wear of the composite (b_{23}). The abrasive wear is more intense if both the content of matrix and of the fibreglass reinforcement is higher, despite the predominance of hard corundum in relation to powder carbon when the content of fillers has been decreased (b_{123}).

6. Conclusions

1. Composites whose phase composition provides lower wear intensity I_z have higher ablation rate v_α.

2. The wear intensity decreases when the content of matrix is higher or when corundum Al_2O_3 is predominant in the filler mixture. A high amount of resins, which guarantees the adequate solutioning and hardening of the composite, prob-

ably hinders the removal of filler grains in the abrasion process while a high content of corundum increases the resistance to abrasion.

3. An opposite dependence can be observed for the rate of ablation v_α which decreases due to either a lower content of matrix i.e. the constant content of fibreglass reinforcement and the higher content of a given powder filler, or due to predominant content of powder carbon *C*. A lower content of pyrolytic carbon (the main component of the thermoinsulating ablation layer), which is a product of the matrix decomposition process, is compensated by higher amounts of carbon dust due to the higher content of powders as well as its proportion to corundum.

4. The slow rate of ablation v_a can be also achieved by decreasing the content of powder fillers maintaining the minimum amount of corundum Al_2O_3 and maximum amount of powder carbon *C*, which involves more matrix and glass reinforcement.

5. Within the scope of the assumed independent variables, the composite, which is the most resistant to abrasion, contains the maximum amount of corundum Al_2O_3 (minimum amount of powder carbon *C*) with the highest possible solutioning of resins and 10 layers of glass fabric.

7. Bibliography

1. Bahramian A R, Kokabi M. Ablation mechanism of polymer layered silicate nanocomposite heat shield. Journal of Hazardous Materials 2009; 166: 445-454.
2. Bielajew N M. Wytrzymałość materiałów. Warszawa: Wydawnictwo MON, 1954.
3. Dimitrienko Yu I. Thermal stresses in ablative composite thin-walled structures under intensive heat flows. International Journal of Engineering Science 1997; 35/1: 15-31.
4. Feng-Er Yu. Study on the ablation materials of modified polyurethane/polysiloxane. Doctoral dissertation. Guangzhou: National Sun Yat-sen University. Materials Science and Engineering Department, 2004.
5. Haack A. Latest achievements and perspectives in tunnel safety. 30th ITA - World Tunnel Congress. Singapore: May 22th -27th 2004.
6. Jackowski A. Numeryczne rozwiązanie głównego problemu ablacji. Biuletyn WAT 1986; 6(460): 11-21.
7. Jackowski A. Ablacja ścianki płaskiej w warunkach erozyjnego unoszenia warstwy ablacyjnej. Biuletyn WAT 1986; 6(460): 23-33.
8. Kucharczyk W. Kształtowanie ablacyjnych właściwości termoochronnych kompozytów polimerowych napełniaczami proszkowymi. Rozprawa doktorska. Radom: Politechnika Radomska, 2007.
9. Kucharczyk W, Żurowski W. Odporność na zużycie ścierne hybrydowych laminatów termoutwardzalnych o właściwościach ablacyjnych. Tribologia 2003; 4(190): 277-286.
10. Leszek W. Badania empiryczne. Wybrane zagadnienia metodyczne. Radom: Wydawnictwo ITE w Radomiu, 1997.
11. Lin W-S. Steady ablation on the surface of a two-layer composite. International Journal of Heat and Mass Transfer 2005; 48: 5504-5519.
12. NIST NCSTAR 1, Federal Building and Fire Safety Investigation of The World Trade Center Disaster. Final report on the Collapse of the World Trade Center. U.S. Washington: Government Printing Office, September 2005.
13. Ono K, Otsuka T. Fire design requirement for various tunnels. 32nd ITA - World Tunnel Congress. Seoul: April 25th 2006.
14. Patton R D, Pittman Jr C U, Wang L, Hill J R, Day A. Ablation, mechanical and thermal conductivity properties of vapour grown carbon fiber-phenolic matrix composites. Composites Part A 2002; 33: 243-251.
15. Polański Z. Planowanie doświadczeń w technice. Warszawa: PWN, 1984.
16. Jurga J, Jurkowski B, Sterzyński T i inni. Nowe kierunki modyfikacji i zastosowań tworzyw sztucznych. Kucharczyk W. Termoochronne właściwości ablacyjne szklanych laminatów fenolowo-formaldehydowych. Poznań: Wydawnictwo Politechniki Poznańskiej, 2004; 45-49.
17. Song G M, Zhou Y, Wang Y-J. Effect of carbide particles on the ablation properties of tungsten composites. Materials Characterization 2003; 50: 293-303.
18. Tester do badania ścieralności T-07. Instrukcja obsługi. Radom: ITE w Radomiu, 1995.
19. Wilkinson T. The World Trade Center and 9/11. The discussion of some engineering design issues. National Conference "Safe Buildings for This Century". Sydney: Australian Institute of Building Surveyors, 2002.
20. Willam K, Rhee I, Shing B. Interface damage model for thermomechanical degradation of heterogeneous materials. Computer Methods in Applied Mechanics and Engineering 2004; 193: 3327-3350.
21. Wojtkun F, Sołncew Ju P. Materiały specjalnego przeznaczenia. Radom: Wydawnictwo Politechniki Radomskiej, 2001.
22. Żurowski W. Tribologiczne badania termoutwardzalnych kompozytów proszkowych do zastosowań ciernych. Przemysł Chemiczny 2010; 12(89): 1678-1681.

Wojciech KUCHARCZYK, Ph D
Department of Mechanical Engineering
Technical University of Radom
Krasickiego 54B Street, 26-600 Radom
E-mail: wojciech.kucharczyk@pr.radom.pl

Article citation info:
ŻUROWSKI W. Structural factors contributing to increased wear resistance of steel friction couples. Eksploatacja i Niezawodnosc – Maintenance and Reliability 2012; 14 (1): 19–23.

Wojciech ŻUROWSKI

STRUCTURAL FACTORS CONTRIBUTING TO INCREASED WEAR RESISTANCE OF STEEL FRICTION COUPLES

CZYNNIKI STRUKTURALNE UMOŻLIWIAJĄCE UZYSKANIE ZWIĘKSZONEJ ODPORNOŚCI NA ZUŻYWANIE STALOWYCH PAR TRĄCYCH

Research into abrasive wear resistance in conditions of dry friction and oxidative wear have been carried out. It has been found that the increase of wear resistance of solid bodies appears where the temperature of a friction area is equal to the characteristic temperature and frictional resistance is stabilized. Increasing wear resistance of a system of bodies is effected by systems transfer of material between surfaces of rubbing bodies and presence of ferrum oxides: FeO and Fe_3O_4 and with decreasing share of Fe_2O_3 up to its disappearance. Resistance to abrasive wear in conditions of dry friction and oxidative wear was tested in two frictional systems. Specimens were made from steels C45 in two condition of heat treatment. Counter-specimens were made from 145Cr6. In order to identify composition and structure of the friction products and the types of ferrous compounds arising from friction, especially secondary oxide structures, present on the surface of rubbing components, Mössbauer spectral analysis was applied. The wear testing required construction of an original test device to measure wear in conditions of formation and regulation of the isothermic limit of temperature variation at a precisely determined distance from a contact of rubbing bodies by means of release (by cooling) of heat energy.

Keywords: *Mössbauer spectral analysis, oxide structures, dry friction, tribological wear.*

Przeprowadzono badania odporności na zużycie w warunkach tarcia suchego i zużywania utleniającego. Stwierdzono, że zwiększona odporność na zużycie występuje, gdy temperatura strefy tarcia osiąga wartość równą temperaturze charakterystycznej dla danego układu a opory tarcia są stabilizowane. Towarzyszy temu przenoszenie materiału pomiędzy współpracującymi powierzchniami i obecność w strefie tarcia tlenków żelaza: FeO i Fe_3O_4, przy zmniejszeniu (do zaniku) ilości Fe_2O_3. W artykule przedstawiono badania odporności na zużycie dla dwóch par trących. Próbki wykonano ze stali C45 w dwóch stanach technologicznych. Przeciwpróbki wykonano ze stali 145Cr6. W celu identyfikacji składu i struktury powstałych podczas tarcia związków żelaza, a szczególnie tlenkowych struktur wtórnych występujących na powierzchni trących się ślizgaczy, wykorzystano analizę spektralną Mössbauera. Badania zużyciowe wymagały skonstruowania oryginalnego urządzenia badawczego, pozwalającego na pomiar zużycia w warunkach utworzenia i regulowania granicy izotermicznej, w ściśle określonej odległości od styku trących się ciał poprzez odbieranie (w wyniku chłodzenia) ciepła.

Słowa kluczowe: *analiza spektralna Mössbauera, struktury tlenkowe, tarcie suche, zużycie tribologiczne.*

1. Introduction

Presented research into wear resistance is based on analysis of thermodynamic transformations which occur in an open thermodynamic system. The equation of energy balance is adopted as the starting point for considering processes of friction and wear and the issue of wear resistance at the macroscopic level of matter organisation. The phenomenological approach leads to an analytical description of wear resistance where the structure and microscopic properties of matter are not taken into account. Load, friction coefficient, and temperature in the friction area are the set parameters in experiments conducted in accordance with this phenomenological approach.

Many tribological studies[14, 15, 17, 18], including by the most recent [16], suggest that ambient factors (humidity, type of surrounding medium, vacuum, and temperature) have substantial impact on friction and wear of elements. Such arguments fail to account for the possibility of stabilising temperature in the friction area, for instance, or the friction coefficient itself, which can be quite precisely controlled and stabilised.

Assuming a stabilised temperature in the friction area and a stabilised friction coefficient allows for determining the greatest resistance of a friction system, defined as wear's specific work for the given system. In this case, specific work of wear is the quotient of work of friction and mass wear of the system (i.e. both the elements). The remaining parameters of the friction process, that is, pressure, sliding velocity, and friction path can be set freely. In effect, optimum friction parameters can be determined so that resistance of the system is or approaches maximum.

The ambient temperature of a friction joint affects physical and resistance properties of rubbing materials and formation of secondary oxidational structures. Many authors have undertaken research in conditions of oxidational wear. Theories of the oxidational wear have been developed [7, 21, 22, 27]. Impact of temperature in the friction area on formation of oxidational

(*) Tekst artykułu w polskiej wersji językowej dostępny w elektronicznym wydaniu kwartalnika na stronie ***www.ein.org.pl***

structures has been assessed [1, 2, 23, 26]. The temperature in the friction area was not stabilised in all these cases. This article presents results of research that help to explain phenomena and processes in the friction joints under conditions of dry friction and oxidational wear with a stabilised temperature in the friction area. Wear mechanisms can be determined and cooperating materials can be properly selected only in this way.

2. Research into wear resistance

Tribological research at low temperatures require special apparatus. This type of equipment was designed and has been employed at the Institute of Machine Design, Technical University of Radom, since 1990s [29, 30, 31]. New rigs have been designed for such testing, including TT-3 tester used in presented researches.

A system of rubbing metallic bodies constituted the object of testing. A ring and slider system became the physical expression of the object (Fig. 1). The ring is the rotating element of the friction couple. Two fixed sliders have been applied in the form of a sample with a flat contact surface to the ring.

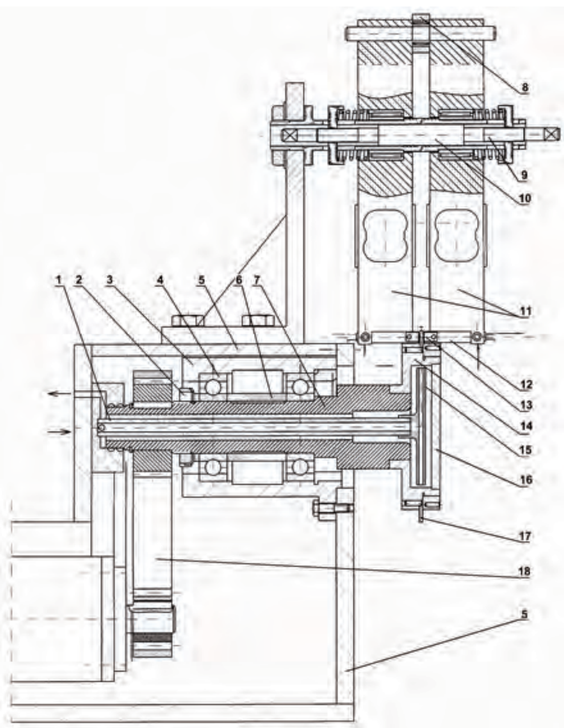

Fig. 1. Diagram of TT-3 tester: 1 – cooling pipe, 2 – lock nut, 3 – bearing sleeve, 4 – ball bearing, 5 – body, 6 – distancing sleeve, 7 – cylinder, 8 – mainstay of the moment of friction measurement, 9 – Roman screw, 10 – sliding sleeve of the clamp against the specimen, 11 – extensometer bridge of loading, 12 – clamp of the specimen, 13 – specimen, 14 – cooling disc, 15 – internal cooling disc, 16 – cover of the cooling disc, 17 – counter-specimen, 18 – driving cogbelt.

The sample material may be selected for each separate matching in order to determine impact of physical properties, chemical composition, hardness, and structure of a material on increasing resistance to wear. A sample made of both metallic and other materials can be used.

A system of two samples that are symmetrically pressed against a disc provides for even distribution of loading. The system guarantees equal loading of both the samples and facilitates measurement of the friction force and, if necessary, measurement of the total linear wear of the samples. The main and the most important feature of the device is that it enables the user to stabilize the temperature of the friction zone.

A series of experimental testing, some of which is discussed in the present paper, has been conducted using TT-3. The research was designed to determine if and what structural transformations in cooperating elements determine increased resistance to wear.

Resistance to wear was tested in conditions of oxidational wear and dry friction in order to determine at what temperature (referred to as the characteristic temperature) a given matching of materials exhibits greater resistance to tribological wear. The article presents testing of the following system: steel C45 in two conditions of heat treatment in association with hardened 145Cr6 steel (63HRC). Characteristics of the materials are provided in Tables 1 and 2.

Table 1. Characteristics of slider (items 1 and 2) and ring (item 3) materials)

No.	Material	Condition of heat treatment	Hardness	Chemical composition, %
1.	Steel C45	normalised	18 HRC	C – 0,5 Mn – 0,67 Si – 0,21 Ni – 0,08 Cr – 0,15
2.		hardened and tempered at 873 K	19HRC	
3.	Steel 145Cr6	hardened	63 HRC	C – 1,4 Mn – 0,59 Si – 0,28 Ni – 0,08 Cr – 1,6 V – 0,17

C45 is a constructional carbon steel, most commonly used heat-treated in medium-loaded machinery elements (axles, cranks, gears, discs). Structures of both normalised and heat-treated C45 steel were tested. 145Cr6 is a cold-work tool steel, oil-hardened and with stable dimensions once hardened, resistant to abrasion.

Testing of wear resistance of C45/145Cr6 matchings has demonstrated a significant (and expected) dependence of wear resistance on friction area temperature. The wear increased at a temperature of c. 268 K in the case of C45(norm)/145Cr6 matching. This value is in line with earlier publications [30]. With regard to the matching of C45(873)/145Cr6, the temperature of maximised resistance was different, and the maximum specific work of wear reached 70MJ/g. Values of characteristic temperatures and the corresponding wear resistance are listed in Table 3.

Wear measurements for matchings of heat-treated C45 showed a significant dependence between resistance obtained at a given friction area temperature and structure of a material. Matching of a heat-treated C45 tempered at 873 K with a structure characterised by fine divorced pearlite in a ferritic matrix proved the best, with a resistance approx. 160% greater than in the case of normalised C45 steel.

Table 2. Structures of C45 and 145Cr6 steels

Material	View of the structure	Description of the structure
normalised C45 steel	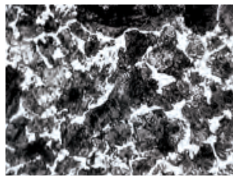	pearlite-ferritic: ferrite around equiaxial pearlite grains of high dispersion; pearlite grains are medium-sized
C45 tempered at 873 K/1h	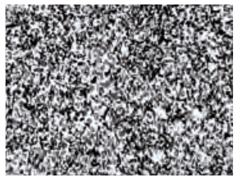	Fine divorced pearlite; cementite balls are evenly distributed in the ferrite matrix
145Cr6 hardened 63 HRC	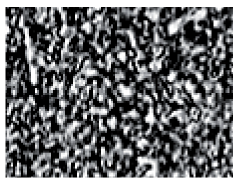	Structure of fine-acicular (cryptoacicular) martensite with low quantity of very fine carbides $(Fe,Cr)_3C$

A measurable accumulation of particles over the cooperating elements could be observed in a majority of cases under testing. The accumulation could (and most likely did) occur where no mass increments were recorded as well. In the circumstances, migration of material particles between the cooperating surfaces took place, as in the transfer model described in [31]. On the basis of Mössbauer spectral analysis, nanometric particles and native material (ferrite and martensite) particles could be detected in the wear products, which further confirms this scenario. Occurrence of austenite, on the other hand, points to presence of counterspecimen particles.

Presence of the nanoparticles, a result of abrasion in the system, can reinforce the material [19] and modify the degree of heterogeneity of mechanical properties. In effect, the refinement of structure can be expected to alter, to a lesser or greater extent, both the weight and operation of the individual component mechanisms of the reinforcement, i.e. dissolution, deformation, and dislocation mechanisms. Above all, scaling down the grain from micro to nanometric dimensions improves its resistance properties.

Mechanisms of the material's phase transitions at the time of friction must be clarified. Results of Mössbauer spectral analysis suggest diffusive supersaturation of ferrite with carbon as a result of elastic-plastic interactions at the contact of rough surfaces of cooperating elements. Thermal phenomena at the frictional contact play a certain role, too, although they are not decisive due to intense heat escaping from the frictional contact. Principles of self-organisation of tribological systems described by Kostecki [10] are important to explanation of this issue. Kostecki cites formation of secondary structures in effect of metals accumulation at the time of friction as an example of a practical application of the self-organisation.

Where values of wear's specific work are great, it is interesting to explain how the material of rubbing bodies behaves in their contact area and what properties their surface layer exhibits in this situation.

Surfaces of sliders made of normalised C45 steel, hardened and tempered at 873 K post friction in a regime of heightened resistance, were tested in a matching with a 145Cr6 steel ring (the so-called optimum conditions). Friction surfaces of each matching were tested prior to and after wear testing. The tests were carried out at the laboratory of the Department of Physics, Mechanical Faculty, Technical University of Radom.

Mössbauer testing employed spectroscopy using the isotope ^{57}Fe as the source of radiation and ^{57}Co in a rhodium matrix displaying activity of approximately 40 mCu.

Conversion Effect Mössbauer Spectroscopy (CEMS) was utilised to test steel surfaces. In order to identify phases in the specimens and to estimate their percentage contribution, Mössbauer spectra were analysed numerically by means of specialist software NORMOS, designed according to the minimisation procedure and the method of least squares with additional constraints [3, 6, 12, 13]. Phases occurring in the entire series specimens (though not necessarily in each specimen) were specified in this way. These were: ferrite (α-Fe), martensite, iron carbide Fe_3C, iron oxide $Fe_{1-x}O$ (wustite), magnetite Fe_3O_4, hematite Fe_2O_3, austenite (γ-Fe). Set hyperfine parameters defined in [11, 25], identical (or within a definite range) for a full series of measurements, were applied to these phases in the second stage.

An example of Mössbauer spectrum, generated by means of CEMS with regard to steel surfaces, is illustrated in Figure 2.

In Figure 2 the black thick line marks a theoretical curve that best matches experimental points. Other lines denote all the components representing ferrite, martensite, iron carbide components, austenite, iron oxide and magnetite components.

Shape of the spectra is characteristic of crystalline materials: they comprise sharp lines of a width slightly more than double the natural width. The number of components (i.e. single lines, doublets or sextets) as well as their hyperfine parameters depend on the number and type of phases in the specimen. For instance, the spectrum of pure iron of bcc (*body centred cu-*

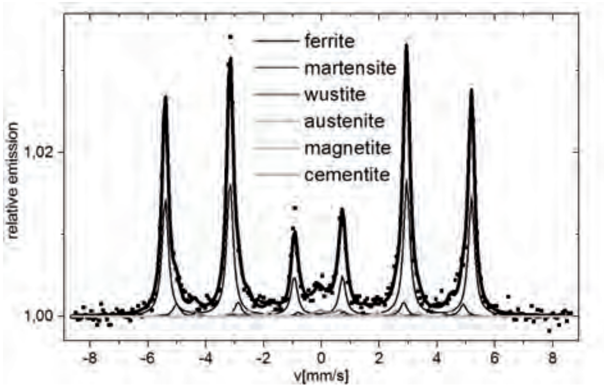

Fig. 2. Spectrum of C45 post friction in the regime of increased resistance to wear (p=0,588 MPa, v=0,4 m/s, μ=0,4, T=268 K, t=5400 s)

bic) structure has the shape of a single sextet with a hyperfine magnetic field (at room temperature) equal to 33.0 T (tesla), an isomeric shift equal zero, and quadrupole split equal to zero. Alloy materials normally exhibit a certain degree of chemical disorder related to varied chemical environment of ^{57}Fe atoms and possibly some topological disorder – in the case of interstitial alloys. This leads to appearance of additional components (sextets) in the spectrum that represent iron atoms which have one or more atoms of alloy additions in the nearest coordination zones, where hyperfine parameters of these components depend, among other factors, on types of additions, whereas the numbers and intensities of components are primarily connected to concentration of alloy additions. Fixed shares of structural components are placed in table 4.

3. Conclusions

The results of Mössbauer analysis presented here allow for some generalisation of the wear process. They indicate that martensite deposits on the sample surface while the share of magnetite is approximately 2÷3 times greater than of wustite at the time of friction in the regime of maximised resistance to wear. Share of cementite prior to and post friction varies irregularly. Martensite settling on the slider surface may originate (by way of migration) from the counterspecimen surface, though it may also be the frictional martensite discussed by other authors [4]. Processes of frictional hardening and/or tempering of rough peaks, producing the so-called secondary frictional structures, may occur in the case of steel. It is currently impossible to determine clearly what share of martensite is a product of friction. The wear mechanisms generally correspond to the classic

Table 3. Values of maximum specific work of wear for tested matchings

Matching	Characteristic temperature, K	Specific work of wear, MJ/g
C45(norm)/145Cr6	268	36
C45(873)/145Cr6	278	70

method of increasing resistance to wear: soft particles set in a hard matrix arise while oxides build an intermediary layer that relieves the friction.

Depositing of magnetite on the slider surface may be related to magnetic properties of the system. Since the friction couple under consideration consists of magnetic elements, it is easier for Fe_3O_4 particles to adhere to rubbing surfaces. Lack of significant (measurable) quantities of Fe_2O_3 is interesting. According to the recognised mechanism of oxidational wear, all the three types of iron oxides should occur on the specimen surface. Yet only trace amounts of hematite appear in the regime of friction at a temperature that assures enhanced resistance to wear. Similar mechanisms of oxide generation in various regimes of friction have been described in [5, 8 , 9, 20, 24, 28]. Appearance of relatively substantial quantities of the native material particles (originating from phase components of steel) may be a result of the oxide wear particles acting upon the material of both the slider and the counterspecimen. Ferrite is a rather soft phase (hardness of c. 90 HB). Iron oxides are relatively hard, on the other hand, and can therefore have an abrasive effect on ferrite. Presence of austenite points to transfers of the counterspecimen material particles to the slider, since austenite is not found in the structure of the specimen material.

Particles that leave a system and reduce its weight are treated as wear. Particles remaining within the system do not cause its weight to reduce. They migrate between cooperating surfaces, settle on their surfaces or in the frictional contact.

Foregoing considerations can lead to a conclusion that factors contributing to increased wear resistance in the above mentioned research are the following:

- the presence in the friction zone of iron oxides: the increase of the quantity of iron monoxide FeO and Fe3O4, and decrease (to the disappearance) of the quantity Fe2O3,
- the migration (transfer of material) between surfaces of rubbing bodies of wear particles coming from ferrite, martensite and oxides,
- the enrichment of specimen surface into martensite coming from the hard counterspecimen and martensite being a result of diffusive influences.

Table 4. Occurrence and shares of phase components on the surface of test specimens

Specimen (slider / ring)	Share of structural component [%]					
	bccFe + bctFe ferrite + martensite	fcc austenite	Fe_3C	Fe_3O_4	Fe_xO	Other
C45(norm) / 145Cr6 post friction	76,6 + 7,1 = 83,7	0,1	0,1	2,9	7,8	5,4 (i.a. nanoparticles)
C45(norm) before friction	90,0 (±1%)	0,0	5,5 (±15%)	0,6	0,7 (±15%)	3,2
C45(873) / 145Cr6 post friction	89,5 + 1,2 = 90,7	0,2	3,8	0,7	1,5	3,1 (i.a. nanoparticles)
C45(873) before friction	90,9 + 0,8 = 91,7	0,0	3,6	0,0	0,9	3,8

4. References

1. Allen C B, Quinn T F J, Sullivan J L: The oxidational wear of high-chromium ferritic steel on austenitic stainless steel. ASME Trans. J. Tribol. 1986; 108: 172-179.
2. Archard J F. The temperature of rubbing surfaces. Wear 1958/59; 2: 438-455.
3. Brand R A, Le Caër G. Improving the validity of Mössbauer hyperfine parameter distributions: the maximum entropy formalism and its applications. Nucl. Instr. Methods B 1988; 34: 272.
4. Dobrzański L A. Materiały inżynierskie. Warszawa: Wydawnictwo Naukowo-Techniczne, 2006.
5. Garbar I I. Gradation of oxidational wear of metals. Tribology International 2002; 35: 749-755.
6. Hesse J, Rűbartch A. Model independent evaluation of overlapped Mössbauer spectra. J. Phys. E.: Sci. Instrum. 1974; 7: 526.
7. Hong H, Hochman R F , Quinn T F J. A new approach to the oxidational theory of mild wear. STLE Trans. 1988; 31: 71-75.
8. Hu Z S, Dong J X, Chen G X. Study on antiwear and reducing friction additive of nanometer ferric oxide. Tribology International 1998; Vol. 31, No. 7: 355-360.
9. Jiaren Jiang, Stott F H, and Stack M M. The role of triboparticulates in dry sliding wear. Tribology International 1998; Vol. 31, No. 5: 245-256.
10. Kostecki B I. Basic conditions of tribological system self-organization. Tribologia 1988; 4: 4-14.
11. 11. Kurosawa K, Li H L, Ujihira Y, Nomura K, Mochizuki E, Hayashi H. Characterization by CEMS, XRD, and XPS of oxidized layers formed on the surface of carbonitrided low-carbon steel. Materials Characterization 1995; 34: 241-249.
12. La Caër G, Delacroix P. Characterization of nanostructured materials by Mössbauer spectrometry. Nanostruct. Mat. 1996; 7: 127-135.
13. Le Caër G, Dubois J M. Evaluation of hyperfine parameter distributions from overlapped Mossbauer spectra of amorphous alloys. J. Phys. E.: Sci. Instrum. 1979;12: 1083.
14. Maldonado D. The influence of dynamic properties of tribotesters on coefficient of friction. Zagadnienia Eksploatacji Maszyn 2008; 3(155): 7-18.
15. Maldonado D. The influence of test parameters on the coefficient of friction. Tribologia 2008; 6: 83-92.
16. Mańkowska A, Michalczewski R, Szczerek M, Wulczyński J. Niskotemperaturowe charakterystyki tribologiczne stalowych skojarzeń ciernych. Tribologia 2010; 1: 77-92.
17. Mańkowska A, Piekoszewski W, Szczerek M. Badania tarcia i zużycia powłok przeciwzużyciowych w próżni. Tribologia 2009; 3: 125-138.
18. Michalczewski R, Piekoszewski W, Szczerek M, Tuszyński W, Wiśniewski M. Effect of friction pair configuration and surroundings conditions on friction and wear. Zagadnienia Eksploatacji Maszyn 1998; 2(114): 301-308.
19. Muszka K. Wpływ rozdrobnienia struktury na mechanizmy umocnienia stali niskowęglowych umacnianych plastycznie. Rozprawa doktorska. Kraków: AGH, 2008.
20. Quinn T F J. Oxidational wear modeling. Part III. The effects of speed and elevated temperatures. Wear 1998; 216: 262-275.
21. Quinn T F J. Oxidational wear. Wear 1971; 18: 413-419.
22. Quinn T F J. Review of oxidational wear. Part I: The origins of oxidational wear. Tribol. Int. 1983; 16: 257-271.
23. So H, Yu D S, Chuang C Y. Formation and wear mechanism of tribooxides and the regime of oxidational wear of steel. Wear 2002; 253: 1004-1015.
24. So H. The mechanism of oxidational wear. Wear 1995; 184: 161-167.
25. Spikes H: Tribology research in the twenty-first century. Tribology International 2001; 34: 789-799.
26. Straffelini G, Trabucco D, Molinari A. Oxidative wear of heat-treated steels. Wear 2001; 250: 485-491.
27. Sullivan J., Quinn T F J, Rowson D M. Developments in the oxidational theory of mild wear. Tribol. Int. 1980; 12: 153-158.
28. Umeda A, Sugimura J, Yamamoto Y. Characterization of wear particles and their relations with sliding conditions. Wear 1998; 216: 220-228.
29. Żurowski W. Badania maksymalnej odporności układów metali na zużywanie tribologiczne na zmodyfikowanej maszynie T-01. Wrocław: Prace Naukowe Instytutu Konstrukcji i Eksploatacji Maszyn Politechniki Wrocławskiej, 2002.
30. Żurowski W. Energetyczny aspekt wzrostu odporności metali na zużywanie w procesie tarcia technicznie. Rozprawa doktorska. Kielce: Politechnika Świętokrzyska, 1996.
31. Żurowski W. Wear resistance maximization of frictional interface systems (in SAIT Tribology 2008 Proceedings ed. P. de Vaal). Pretoria: SAIT, 2008.

Wojciech Żurowski, Ph.D.
Technical University of Radom
Faculty of Mechanical Engineering
Malczewskiego 29 Str.
26-600 Radom, Poland
wojciech.zurowski@pr.radom.pl

Article citation info:
ZHANG T, BAI G, GUO B. Success probability model of phased mission systems with limited spares. Eksploatacja i Niezawodnosc – Maintenance and Reliability 2012; 14 (1): 24–32.

Tao ZHANG
Guanghan BAI
Bo GUO

SUCCESS PROBABILITY MODEL OF PHASED MISSION SYSTEMS WITH LIMITED SPARES

MODEL PRAWDOPODOBIEŃSTWA SUKCESU SYSTEMÓW O ZADANIACH OKRESOWYCH Z OGRANICZONĄ LICZBĄ CZĘŚCI ZAMIENNYCH

This paper builds a model to analyze the success probability of phased mission systems (PMS) with given limited spares. The configuration and success criteria of phased mission may vary from phase to phase. Most reliability analysis techniques and tools of phased mission systems assume that there is no spare replacement during the phased mission or the component repair times are neglected. However, for some phased missions, failed components can be replaced by spares during the mission or in the interval of the phases and the spare replacement times are generally not negligible. By considering minimal spare replacement policy (MSRP) which is often used in military exercise, this paper presents a mathematical model for success probability analysis of phased mission which is based on minimal path set and system state analysis methods. Then, the model was demonstrated and validated by an example of military exercise.

Keywords: *success probability; phased mission systems; spare replacement; minimal path set; state transition probability.*

W niniejszej pracy skonstruowano model do analizy prawdopodobieństwa sukcesu systemów o zadaniach (misjach) okresowych (ang. phased mission systems, PMS) z daną, ograniczoną liczbą części zamiennych. Konfiguracja systemu oraz kryteria sukcesu zadania okresowego mogą być różne dla różnych faz zadania. Większość technik i narzędzi służących do analizy systemów o zadaniach okresowych nie zakłada wymiany części podczas zadania okresowego lub nie bierze pod uwagę czasu wykonania napraw elementów składowych. Tymczasem, w niektórych zadaniach okresowych istnieje możliwość wymiany elementów składowych na zapasowe bądź to w trakcie trwania zadania bądź też w przerwach pomiędzy fazami, a czas takiej wymiany zazwyczaj nie jest bez znaczenia. Biorąc pod uwagę politykę minimalnej wymiany części (ang. minimal spare replacement policy, MSRP), często stosowaną podczas ćwiczeń wojskowych, w niniejszym artykule przedstawiono matematyczny model do analizy prawdopodobieństwa sukcesu zadania okresowego, oparty na dwóch metodach: minimalnych ścieżek zdatności oraz analizy stanu systemu. Możliwość wykorzystania modelu zilustrowano i zweryfikowano na podstawie przykładowych ćwiczeń wojskowych.

Słowa kluczowe: *prawdopodobieństwo sukcesu, systemy o zadaniach okresowych, wymiana części, minimalna ścieżka zdatności, prawdopodobieństwo przejść między stanami.*

1. Introduction

Military exercise is a very important way for increasing the operational skills of operators and commanders of weapon systems. It is also used to evaluate the battle or support effectiveness of a troop. Most of exercise missions consist of several phases that must be accomplished in sequence as phased mission systems (PMS). The system configuration, success criteria, and component behavior may vary from phase to phase. How to evaluate the success probability of an exercise mission with maintenance resources plan given is very important.

In many military exercises, the weapon systems will be transferred to a position which is far away from base camp and they will stay there for a period of time. Because of the limited capability of maintenance and requirement of rapid recovering in exercise, normally spare replacement is the main maintenance type in exercises. Fortunately most units of weapon systems are designed to be the line replacement units (LRU) which can be replaced easily on line. And in order to recover the failed system as quickly as possible, the minimal spare replacement policy (MSRP) will be used in practice mostly. Under MSRP, the last component whose failure causes the system failure directly will be replaced firstly. The modern automatic fault diagnosis system makes it possible and the failed components will not be repaired in the mission normally.

Here is a real example. There are two power subsystems in the surface-to-air missile system. Both of them have components of the same type. One called electric generator produces electricity for other subsystems and it has one component of this type. The other one is able to not only produce electricity but also provide power for moving and it has two components of this type in parallel. The typical exercise of this kind of systems can be divided into three phases: move only, still tracking&shooting and move with tracking&shooting. In the move only phase, the power subsystem for moving should be working and the other subsystem doesn't need to be working. In the still tracking&shooting phase, at least one power subsystem should be working. In the move with tracking&shooting phase, both two power subsystems should be working. The phase fault trees for this exercise mission are shown in Fig.1, which is the relationship between those three components of two subsystems. Under MSRP, the first failed component supposing C_1 will not be replaced in phase 1. But after the second one C_2 fails, it will be replaced if there are enough spares left. In phase 2, only the last failed one should be replaced. However, before the phase 3 begins, the component C_3 should be replaced firstly if it has failed in phase 2. It also should be replaced after its failure in phase 3. Most exercises have schedules of the exercise include the beginning time and deadline of every phase. Normally, phase mission can be finished before the deadline. So there is free time for these activities of spares replacement. The mission will fail if the total maintenance time goes beyond the maximal free time in any phase.

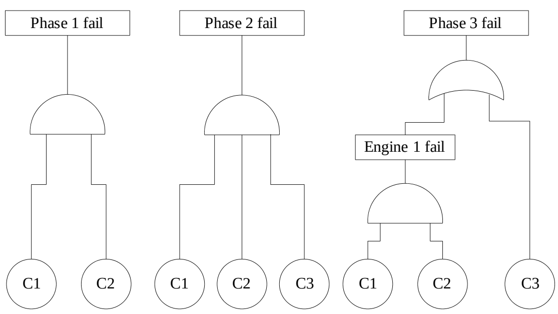

Fig.1. Phase fault trees for a mission of the surface-to-air missile system.

Such a weapon system in exercise can be considered as a PMS and some methods advanced in PMS can be used to evaluate the success probability. In recent years, many models and methods have been put forward to deal with the reliability analysis of PMS, such as Markov-chain[1], combinatorial models [2], fault tree methods [3-5] and Petri-nets [6,7] etc. BDD is more efficient for Boolean expression manipulation and the reliability analysis based on the BDD representation of the system structure function is fast, and straightforward. A BDD-based algorithm that greatly improves the computation efficiency of the PMS reliability solution was proposed in [8, 9, 10]. Considering the repair activities in the mission, a hierarchical modeling approach for the reliability analysis of phased-mission systems with repairable components was advanced in [11]. It didn't take into account spare replacements. S.P. Chew [7] describes the use of a Petri net (PN) to model the reliability of phased missions with maintenance-free operating periods (MFOP). There is no any maintenance in MFOP. Following each MFOP is a period, known as a maintenance recovery period (MRP), where the system is repaired to such a level that it is capable of completing the next MFOP. It is appropriate for some systems whose maintenance can't be done during the missions, such as the aircraft systems. But there are many exceptions, such as the move only phase of the surface-to-air missile system mentioned above. Some models of reliability analysis of PMS considering spare replacement are advanced in [12,13]. However, unfortunately the spare replacement times are neglected and these approaches have not taken into account MSRP.

In this paper, a mathematical model for success probability analysis of PMS is advanced. In this model, MSRP is considered and the spare replacement time is not neglected. The spares used in MSRP is cold standby. The rest of the paper is organized as follows. Section 2 describes the nomenclatures, problem and assumptions. In Section 3, the success probability model for phased mission systems with spares replacement is described. Section 4 gives the calculation of system state transition probability. In Section 5, a practical example of a military exercise and the experimental results are given. In Section 6, a conclusion is given.

2. Problem description

2.1 Nomenclatures

n number of phases of PMS.

T_i^{Work} work time of phase i, $i=1,2...,n$ . .

T_i^{Max} maximal duration time of phase i, $i=1,2...,n$ $T_i^{Max} \geq T_i^{Work}$

T_i^{Free} free time of phase i, $i=1,2,...,n$. $T_i^{Free}=T_i^{Max}-T_i^{Work}$

When $T_i^{Max}=T_i^{Work}$, any spare replacement activities are not permitted in the i^{th} phase. When $T_i^{Max}>T_i^{Work}$, spare replacement activities are permitted in the ith phase but the total replacement time should be less than the free time T_i^{Free}.

N number of components in PMS.

M number of component types in PMS.

Y_i i^{th} component type, .

N_i number of components of the i^{th} type, .

λ_i failure rate of components of the i^{th} type, .

T^R vector of the spare replacement times $T^R=(t_1^R, t_2^R,...,t_M^R)$, t_i^R, is the spare replacement time of the i^{th} component.

C_i state of the ith component, i. $i=1,2,...,N$, $C_i = \begin{cases} 1, & \textit{the ith component is up} \\ 0, & \textit{the ith component is down} \end{cases}$

F system success logic function, $F=f(C_1, C_2, ..., C_N)$.

S system state vector , $S = (s_1, s_2, \ldots, s_N)$, s_i is the *i*th component state.

S_B system state vector at the beginning of phase.

S_E system state vector at the end of phase.

$S_B^{(i)}$ system state vector at the beginning of operation phase i .

$S_E^{(i)}$ system state vector at the end of phase i , $S_E^{(i)} = S_B^{(i+1)}$.

θ system state vector when all components are down, so $\theta = (0, 0, \ldots, 0)$.

I system state vector when all components are up, so $\mathrm{I} = (1, 1, \ldots, 1)$.

$C(S)$ set of components whose states are up in system state S , $C(S) = \{C_i \mid s_i = 1\}$. For example, when $S = (1, 0, 1, 1)$, $C(S) = \{C_1, C_3, C_4\}$.

$|S|$ count of components whose states are up in system state S . For example, when $S = (1, 0, 1, 1)$, $|S| = 3$.

$|S|_{Y_i}$ count of components of the *i*th component type whose states are up in system state S . $|\mathrm{I}|_{Y_i} = N_i$.

The system state vector operations are defined as follows:

$$s_i + s_j = \begin{cases} 1, & s_i = 1,\ s_j = 1\ ;\ s_i = 0,\ s_j = 1\ ;\ s_i = 1,\ s_j = 0 \\ 0, & s_i = 0,\ s_j = 0 \end{cases}$$ is equivalent to the logical OR.

$$s_i - s_j = \begin{cases} 0, & s_i = 1,\ s_j = 1\ ;\ s_i = 0,\ s_j = 1\ ;\ s_i = 0,\ s_j = 0 \\ 1, & s_i = 1,\ s_j = 0 \end{cases}$$

$S^{(i)} + S^{(j)} = (s_1^{(i)} + s_1^{(j)}, s_2^{(i)} + s_2^{(j)}, \ldots, s_N^{(i)} + s_N^{(j)})$.

$S^{(i)} - S^{(j)} = (s_1^{(i)} - s_1^{(j)}, s_2^{(i)} - s_2^{(j)}, \ldots, s_N^{(i)} - s_N^{(j)})$.

$S^{(i)} \le S^{(j)} : S^{(i)} - S^{(j)} = \theta$.

$S^{(i)} < S^{(j)} : S^{(i)} - S^{(j)} = \theta$ and $\left|S^{(j)} - S^{(i)}\right| > 0$.

$S^{(i)} \ge S^{(j)} : S^{(j)} - S^{(i)} = \theta$.

$S^{(i)} > S^{(j)} : S^{(j)} - S^{(i)} = \theta$ and $\left|S^{(i)} - S^{(j)}\right| > 0$.

$L_f(F)$ set of the system state vectors whose system state is up and system success logic function is F . For example, when $F = C_1C_2 + C_1C_3$, $L_f(F) = \{(1, 1, 1), (1, 0, 1), (1, 1, 0)\}$. It can be obtained by the path sets.

$L_m(F)$ set of the system state vectors whose system state is up, but it will be down if any up component fails, and system success logic function is F . $L_m(F)$ is a subset of $L_f(F)$. For example, when $F = C_1C_2 + C_1C_3$, $L_m(F) = \{(1, 0, 1), (1, 1, 0)\}$. It can be obtained by the minimal path sets.

$\bar{X} = (x_1, x_2, \ldots, x_M)$ vector of the amount of spares. x_i stands for the amount of spares for the *i*th component type. The vector operations are defined as follows:

$\bar{X}^{(m)} \ge \bar{X}^{(n)}$ $\left(x_1^{(m)}, x_2^{(m)}, \ldots, x_M^{(m)}\right) \ge \left(x_1^{(n)}, x_2^{(n)}, \ldots, x_M^{(n)}\right) : x_i^{(m)} \ge x_i^{(n)}$ for $i = 1,2,\ldots,M$.

$\bar{X}^{(m)} > \bar{X}^{(n)}$ $\left(x_1^{(m)}, x_2^{(m)}, \ldots, x_M^{(m)}\right) > \left(x_1^{(n)}, x_2^{(n)}, \ldots, x_M^{(n)}\right) : \bar{X}^{(m)} \ge \bar{X}^{(n)}$ and $x_i^{(m)} > x_i^{(n)}$ for at least one i .

$\bar{X}^*$ vector of the amount of initial spares, $\bar{X}^* = \left(x^*_1, x^*_2, \ldots, x^*_M\right)$.

$\bar{X}_B^{(i)}$ vector of the amount of available spares in the beginning of phase i , $\bar{X}_B^{(1)} = \bar{X}^*$.

$\bar{X}_E^{(i)}$ vector of the amount of available spares in the end of phase i , $\bar{X}_E^{(i)} = \bar{X}_B^{(i+1)}$.

$P\left(S_B, S_E, \bar{X}, F, T^{Work}, T^{Max}\right)$ system state transition probability from S_B to S_E and the vector of the amount of consumed spares equal to $\bar{X}$ when the system success logic function is F , the total work time is T^{Work} and the maximal duration time is T^{Max} .

$\bar{X}_D(S, F)$ vector of the amount of spares which will be used to make the system functional when the current system state is S and the system success logic function is F . We know easily $\bar{X}_D(S, F) = \bar{0}$ if $S \in L_f(F)$ under MSRP. $\bar{X}_D(S, F) > \bar{0}$, where $S \notin L_f(F)$. For example, $F = C_1C_2 + C_1C_3$, C_1 is one type and C_2, C_3 are another type. $S = (1, 0, 0)$. We can get $\bar{X}_D(S, F) = (0, 1)$ under MSRP and $\bar{X}_D(S, F) = (0, 2)$ under perfect maintenance policy.

$S_D(S, F)$ vector of system state after the spare replacement when the current system state is S and the system success logic function is F . $S_D(S, F) \in L_f(F)$, $S_D(S, F) = S$, where $S \in L_f(F)$. As above example, we can get $S_D(S, F) = (1, 0, 1)$ under MSRP and $S_D(S, F) = (1, 1, 1)$ under perfect maintenance policy.

F_i system success logic function in phase i, i =1,2,...,n.

For example, in Fig. 1, F , $F_1 = F_3 = C_1C_2 + C_1C_3 + C_2C_3$, $F_2 = C_1 + C_2 + C_3$.

2.2 Problem description

The aim is to evaluate the mission success probability when the system initial state is $S_0 \in L_f(F_1)$, the amount of initial spares is $\bar{X}^*$ and the system success logic function and the work time of each phase are given.

The phased mission system discussed in this paper is required to satisfy the following assumptions:

1) The failures of different components are statistically independent.
2) All failed components are not repairable in the mission.
3) All components are characterized by a negative exponential distribution.
4) The spare replacement policy in phased mission is MSRP.

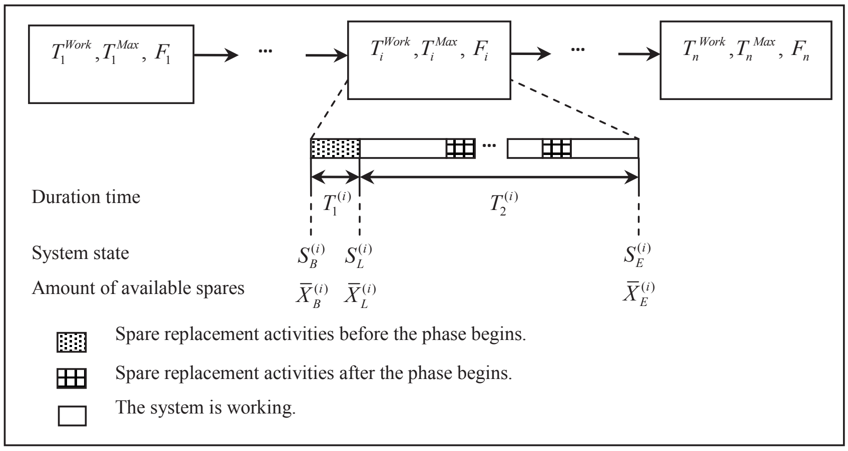

Figure 2 – Process analysis of phased mission system with spare replacement

3. Success probability model of phased mission systems with spares replacement

Fig. 2 shows the processes of the phased mission system and some nomenclatures which will be used in our model.

3.1 Spare replacement process analysis

Before the ith phase mission begins, the spare replacement may need to be done because the system success logic functions of different phases are different. This process is called as the check and spare replacement process. If there are enough spares for replacement, the system state transits from $S_B^{(i)}$ to $S_L^{(i)}$ after this process. Hence,

$$S_L^{(i)} = S_D\left(S_B^{(i)},\ F_i\right) \text{ and } S_L^{(i)} \in L_f(F_i) \tag{1}$$

It is known that $\bar{X}_D(S_B^{(i)},\ F_i)$ is the vector of the amount of spares which will be used when the current system state is $S_B^{(i)}$ and the system success logic function is F_i . So

$$\bar{X}_L^{(i)} = \bar{X}_B^{(i)} - \bar{X}_D(S_B^{(i)},\ F_i) \tag{2}$$

The duration time of spare replacement activities before the next phase begins is as below.

$$T_1^{(i)} = \bar{X}_D(S_B^{(i)},\ F_i)T^R \tag{3}$$

After the ith phase mission begins, the system state transits from $S_L^{(i)}$ to $S_E^{(i)}$. $S_E^{(i)} = S_B^{(i+1)}$. Let $\bar{X}^{(i)}$ be the vector of the amount of consumed spares in the ith phase. The duration time will be given as below.

$$T_2^{(i)} = T_i^{Work} + \bar{X}^{(i)}T^R \tag{4}$$

3.2 Calculation of success probability

If the whole mission can be completed successfully, the following conditions should be satisfied.

1) All phases have to be finished successfully, so the end system state of any phase should be in the set of system up states. Hence, $\forall$ $S_E^{(i)}, i = 1,2,...,n$, $S_E^{(i)} \in L_f(F_i)$.
2) Because of the fact that there exists space replacements only when the system fails under MSRP, the end system state will not be better than the state when the system has been just made to be functional. Hence, $S_E^{(i)} \le S_D\left(S_E^{(i-1)}, F_i\right)$.
3) In any phase, the total replacement time is not more than the free time. $T_1^{(i)} + T_2^{(i)} - T_i^{Work} \le T_i^{Free}$.
4) The total amount of spare usage $\bar{X}$ is not more than $\bar{X}^*$

$$\bar{X} = \sum_{i=1}^{n}\left(\bar{X}_D\left(S_E^{(i-1)},\ F_i\right) + \bar{X}^{(i)}\right) \le \bar{X}^*$$

,
.

Let $\left(S_E^{(1)},\ S_E^{(2)},\ ...,\ S_E^{(n)}, \bar{X}^{(1)}, \bar{X}^{(2)}, ...,, \bar{X}^{(n)}\right)$ be a system state sequences. Let SB be the set of all feasible system state combinations and spare usage scenarios. Because all phases have to be finished successfully, then

$$SB = \left\{ \left(S_E^{(1)},\ S_E^{(2)},\ ...,\ S_E^{(n)}, \bar{X}^{(1)}, \bar{X}^{(2)}, ...,, \bar{X}^{(n)}\right) \middle| \begin{array}{l} \forall S_E^{(i)}, i = 1,2,...,n, S_E^{(i)} \in L_f(F_i) \textit{ and} \\ S_E^{(i)} \le S_D\left(S_E^{(i-1)}, F_i\right) \textit{and} \\ \bar{X}_D(S_B^{(i)},\ F_i)T^R + \bar{X}^{(i)}T^R \le T_i^{Free} \textit{and} \\ \sum_{i=1}^{n}\left(\bar{X}_D\left(S_E^{(i-1)},\ F_i\right) + \bar{X}^{(i)}\right) \le \bar{X}^* \end{array} \right\} \tag{5}$$

Hence, to obtain the success probability, the probabilities are summed over all feasible system state combinations and spare usage scenarios. So

$$P_{mission} = \sum_{\left(S_0, S_E^{(1)},\ S_E^{(2)},\ ...,\ S_E^{(n)}\right) \in SB} P\left(S_E^{(1)},\ S_E^{(2)},\ ...,\ S_E^{(n)}, \bar{X}^{(1)}, \bar{X}^{(2)}, ..., \bar{X}^{(n)}\right) \tag{6}$$

Where $P\left(S_E^{(1)},\ S_E^{(2)},\ ...,\ S_E^{(n)}, \bar{X}^{(1)}, \bar{X}^{(2)}, ..., \bar{X}^{(n)}\right)$ is the probability of that the total amount sequences of consumed spares are $\bar{X}^{(1)}, \bar{X}^{(2)}, ...,, \bar{X}^{(n)}$ and the system state sequences are $S_0, S_E^{(1)},\ S_E^{(2)},\ ...,\ S_E^{(n)}$. It is calculated as shown below,

$$P\left(S_E^{(1)},\ S_E^{(2)},\ \ldots,\ S_E^{(n)}, \bar{X}^{(1)}, \bar{X}^{(2)}, \ldots, \bar{X}^{(n)}\right) = \\ = \prod_{i=1}^{n} P\left(S_D(S_E^{(i-1)}, F_i),\ S_E^{(i)},\ \bar{X}^{(i)},\ F_i,\ T_i^{Work},\ T_i^{Max}\right) \quad (7)$$

The calculation of $P\left(S_B,\ S_E,\ \bar{X},\ F,\ T^{Work},\ T^{Max}\right)$ will be described in section 4.

4. Calculation of system state transition probability

Some lemmas are given before discussing how to calculate the system state transition probability. All Lemmas as below satisfy the following conditions.

1) The system success logic function is F.
2) The system total work time is T^{Work}.
3) The maximal duration time is T^{Max}.
4) The system state is initially and it transits to S_E finally.
5) $S_B \in L_f\left(F\right)$, $S_E \in L_f\left(F\right)$.

Let $S_1 = S_B - S_E - \sum_{L_k \in L_m(F)} L_k$, $S_2 = S_E - \sum_{L_k \in L_m(F)} L_k$,

$$S_3 = \left(s_1^{(3)}, s_2^{(3)}, \ldots, s_N^{(3)}\right) \mid s_i^{(3)} = \begin{cases} 1 & s_i^{(E)} = 1 \text{ and } S_E\left(s_i^{(E)} \to 0\right) \notin L_f\left(F\right) \\ 0 & other \end{cases}, i = 1, 2, \ldots, N$$

$S_4 = S_E - S_2 - S_3$, $S_5 = S_B - S_1 - S_2 - S_3 - S_4$,

$$H_j = \left\{ i \middle| \ \left|S_j\right|_{Y_i} > 0,\ i = 1,\ 2,\ \ldots,\ M \right\}, j = 1, 2, \ldots, 5$$, .

Where $S_E\left(s_i^{(E)} \to 0\right)$ stands for the system state vector after setting the ith component state $s_i^{(E)}$ of S_E to zero.

$$S_E\left(s_i^{(E)} \to 0\right) = \left(s_1^{(E)}, s_2^{(E)}, \ldots, s_{i-1}^{(E)}, 0, s_{i+1}^{(E)}, \ldots, s_{N-1}^{(E)}, s_N^{(E)}\right).$$

Lemma 1. $C\left(S_1\right)$ is the set of all components which satisfy the following condition.

1) It does not belong to any minimal path sets.
2) It fails in the mission.
3) It has not been replaced by any spares in the mission.

Proof. Let $S_L = \sum_{L_k \in L_m(F)} L_k$, $\forall C_i \in C\left(S_1\right)$, so $s_i^{(1)} = 1$. It means and $s_i^{(B)} = 1$ and $s_i^{(E)} = 0$. So the ith component state changes from 1 to 0 and it failed in the mission. $s_i^{(L)} = 0$ is equivalent to that the ith component does not belong to any minimal path sets. So it does not have to be replaced if it fails under MSRP.

Lemma 2. $C\left(S_2\right)$ is the set of all components which satisfy the following condition.

1) It does not belong to any minimal path sets.
2) It is always up during the mission.
3) It has not been replaced by any spares in the mission.

Proof. Let $S_L = \sum_{L_k \in L_m(F)} L_k$, $\forall C_i \in C\left(S_2\right)$, so $s_i^{(2)} = 1$. It means $s_i^{(E)} = 1$ and $s_i^{(L)} = 0$. $s_i^{(L)} = 0$ is equivalent to that the ith component does not belong to any minimal path sets. So it does not have to be replaced if it fails under MSRP. $s_i^{(E)} = 1$ is equivalent to that the ith component is up when the mission is over. Hence, it is always up during the mission.

Lemma 3. $C\left(S_3\right)$ is the set of all components which satisfy the following condition.

1) It is up when the mission is over.
2) It has to be replaced if it fails after the system state is changed to be , otherwise the system will be down.

Proof. $\forall C_i \in C\left(S_3\right)$, so $s_i^{(3)} = 1$. It means $s_i^{(E)} = 1$ and $S_E\left(s_i^{(E)} = 0\right) \notin L_f\left(F\right)$. $s_i^{(E)} = 1$ is equivalent to that the ith component is up when the mission is over. $S_E\left(s_i^{(E)} = 0\right) \notin L_f\left(F\right)$ is equivalent to that the system will be down if it fails after the system state is changed to be S_E. So the ith component should be replaced if it fails after the system state is changed to be S_E, otherwise the system will be down.

Lemma 4. $C\left(S_4\right)$ is the set of all components which satisfy the following condition.

1) It is up when the mission is over.
2) It does not need to be replaced if it fails in the phase.

Proof. $\forall C_i \in C\left(S_4\right)$, so $s_i^{(4)} = 1$. It means $s_i^{(E)} = 1$ and $s_i^{(2)} = 0$ and $s_i^{(3)} = 0$. $s_i^{(E)} = 1$ is equivalent to that the *i*th component is up when the mission is over. $S_4 = S_E - S_2 - S_3$ means $C\left(S_4\right) \cap C\left(S_2\right) \neq \varnothing$ and $C\left(S_4\right) \cap C\left(S_3\right) \neq \varnothing$. Because $C\left(S_3\right)$ is the set of all components which should be replaced after its failure by Lemma 3. So $C\left(S_4\right)$ is the set of all components which do not need to be replaced if they fail.

Lemma 5. $C\left(S_5\right)$ is the set of all components which satisfies the following condition.

1) It does not belong to all minimal path sets but it belongs to at least one minimal path set.
2) It fails in the mission without spare replacement.

Proof. $\forall C_i \in C\left(S_5\right)$, so $s_i^{(5)} = 1$. It means $s_i^{(B)} = 1$ and $s_i^{(1)} = 0$ and $s_i^{(2)} = 0$ and $s_i^{(3)} = 0$ and $s_i^{(4)} = 0$. So the ith component is down when the mission is over. $s_i^{(E)} = 0$. Let $S_L = \sum_{L_k \in L_m(F)} L_k$, $s_i^{(1)} = 0$ and $s_i^{(E)} = 0$ means $s_i^{(L)} = 1$. So ith the component belongs to at least one minimal path set but it does not belong to all minimal path sets because of $s_i^{(E)} = 0$ and $S_E \in L_f\left(F\right)$.

Lemma 6. $C(S_B)=C(S_1+S_2+S_3+S_4+S_5)$ and $C(S_1),\ C(S_2),\ C(S_3),\ C(S_4),\ C(S_5)$ are disjoint.

Proof

$S_1+S_2+S_3+S_4+S_5=S_1+S_2+S_3+S_4+S_B-S_1-S_2-S_3-S_4=S_B$, it means that $C(S_B)=C(S_1+S_2+S_3+S_4+S_5)$.

$S_5=S_B-S_1-S_2-S_3-S_4$, so $C(S_5)\cap C(S_1)=\varnothing$, $C(S_5)\cap C(S_2)=\varnothing$, $C(S_5)\cap C(S_3)=\varnothing$, $C(S_5)\cap C(S_4)=\varnothing$. $S_4=S_E-S_2-S_3$, so , . By Lemma 1, the components in $C(S_1)$ is down when mission is over. By Lemma 2,3,4, the components in the components in $C(S_2)$ or $C(S_3)$ or $C(S_4)$ is up when mission is over. So $C(S_1)\cap C(S_2)=\varnothing$, $C(S_1)\cap C(S_3)=\varnothing$, $C(S_1)\cap C(S_4)=\varnothing$. By Lemma 2 and Lemma 3, $C(S_2)\cap C(S_3)=\varnothing$. Hence, $C(S_1),\ C(S_2),\ C(S_3),\ C(S_4),\ C(S_5)$ are disjoint.

The components in the set of $C(S_1)$ failed and have not been replaced by any spares in the phase by Lemma 1. The state transition probability of these components P_1 is

$$P_1=\prod_{i\in H_1}\left(1-e^{-\lambda_i T^{Work}}\right)^{|S_1|_{Y_i}} \tag{8}$$

The components in the set of $C(S_2)$ did not fail in the phase by Lemma 2. The state transition probability of these components P_2 is

$$P_2=\prod_{i\in H_2}e^{-|S_2|_{Y_i}\lambda_i T^{Work}} \tag{9}$$

When $|S_3|>0$ and $|S_5|>0$, the components in $C(S_3)$ should be replaced after its failure after all components in $C(S_5)$ fail by lemma 3. Let $\varphi(t)$ is the density function of when all components in $C(S_5)$ fail. It is calculated by

$$\varphi(t)=\left(\prod_{i\in H_5}|S_5|_{Y_i}\lambda_i e^{-\lambda_i t}\left(1-e^{-\lambda_i t}\right)^{|S_5|_{Y_i}-1}\right)\cdot\left(\prod_{j\in H_3}e^{-|S_3|_{Y_j}\lambda_j t}\right) \tag{10}$$

In the remain time of $T^{Work}-t$, the components in $C(S_3)$ should be replaced after failure and the number of spares is consumed to be X . Hence, the state transition probability $P_{3,5}(\bar{X})$ of the components in $C(S_3)$ and $C(S_5)$ is calculated by

$$P_{3,5}(\bar{X})=\prod_{i\in H_3}\int_0^{T^{Work}}\varphi(t)\cdot\frac{1}{x_i\,!}\left(|S_3|_{Y_i}\lambda_i\left(T^{Work}-t\right)\right)^{x_i}e^{-|S_3|_{Y_i}\lambda_i(T^{Work}-t)}dt \tag{11}$$

When $|S_5|=0$ and $|S_3|>0$, the components in $C(S_3)$ should be replaced after its failure directly by lemma 3. So, $P_{3,5}(\bar{X})$ is calculated by

$$P_{3,5}(\bar{X})=\prod_{i\in H_3}\frac{1}{x_i\,!}\left(\left(|S_3|_{Y_i}\right)\lambda_i T^{Work}\right)^{x_i}e^{-|S_3|_{Y_i}\lambda_i T^{Work}} \tag{12}$$

When $|S_3|=0$ and $|S_5|>0$, the components in $C(S_5)$ fail in the phase without spare replacement. Hence, the state transition probability $P_3(\bar{X})$ of the components in $C(S_3)$ and $C(S_5)$ is calculated as shown below

$$P_{3,5}(\bar{X})=\begin{cases}\prod_{i\in H_3}\int_0^{T^{Work}}\varphi(t)\cdot\frac{1}{x_i\,!}\left(|S_3|_{Y_i}\lambda_i\left(T^{Work}-t\right)\right)^{x_i}e^{-|S_3|_{Y_i}\lambda_i(T^{Work}-t)}dt, & |S_3|>0\ and\ |S_5|>0\\ \prod_{i\in H_3}\frac{1}{x_i\,!}\left(\left(|S_3|_{Y_i}\right)\lambda_i T^{Work}\right)^{x_i}e^{-|S_3|_{Y_i}\lambda_i T^{Work}}, & |S_3|>0\ and\ |S_5|=0\\ \prod_{i\in H_5}\left(1-e^{-|S_5|_{Y_i}\lambda_i T^{Work}}\right), & |S_3|=0\ and\ |S_5|>0\\ 1, & |S_3|=0\ and\ |S_5|=0\end{cases} \tag{13}$$

When $|S_4|>0$, the components in $C(S_4)$ do not need to be replaced in the phase and they are up when the mission is over by Lemma 4. So we know these components did not fail in the phase. Hence, the state transition probability P_4 of the components in $C(S_4)$ is calculated by

$$P_4=\prod_{i\in H_4}e^{-|S_4|_{Y_i}\lambda_i T^{Work}} \tag{14}$$

By Lemma 6, $C(S_1),\ C(S_2),\ C(S_3)+C(S_5),C(S_4)$ are disjoint. $P\left(S_B,\ S_E,\ \bar{X},\ F,T^{Work},\ T^{Max}\right)$ is calculated by the product of the state transition probabilities of these three parts as shown below

$$P\left(S_B,\ S_E,\ \bar{X},\ F,T^{Work},\ T^{Max}\right)=\begin{cases}P_1P_2P_{3,5}(\bar{X})P_4, & \bar{X}T^R\le T^{Max}-T^{Work}\\ 0, & \bar{X}T^R>T^{Max}-T^{Work}\end{cases} \tag{15}$$

5. An example of military exercise

Based on the example of the surface-to-air missile system which is mentioned in Section 1, this example will take into account the electronic convertor. The electronic convertor has two components of this type in parallel. It should be working when the weapon system is in any tracking&shooting phase. Three components ($C_1,\ C_2,\ C_3$) of types X_1 and two components ($C_4,\ C_5$) of type X_2 are taken into account in this example. The failure rates are $\lambda_1=0.0007$ and $\lambda_2=0.0005$. The vector of the replacement time is $T^R=(2,\ 3)$. Now a surface-to-air missile system will execute an exercise mission with four phases whose phase fault trees are shown in Fig.3. The fourth phase is the same with the first phase.

We can get the minimal path sets and the system success logic functions of four phases. $F_1 = F_4 = C_1 + C_2$, $F_2 = C_1C_4 + C_2C_4 + C_3C_4 + C_1C_5 + C_2C_5 + C_3C_5$ and $F_3 = C_1C_3C_4 + C_2C_3C_4 + C_1C_3C_5 + C_2C_3C_5$. In the beginning of the whole mission, all components are in up states. So the vector of the initial system state is $S_0 = S_B^{(1)} = (1,\ 1,\ 1,\ 1,\ 1)$ .. The work times are $T_1^{Work} = T_4^{Work} = 45$, $T_2^{Work} = 160$ and $T_3^{Work} = 400$. The maximal duration times are $T_1^{Max} = T_4^{Max} = 60$, $T_2^{Max} = 165$ and $T_3^{Max} = 420$.

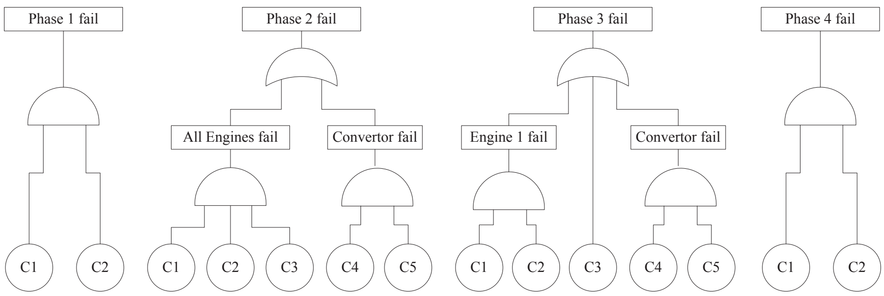

Fig.3. Phase fault trees of the example

We can get $L_m(F)$ of each phase easily form the system success logic functions of three phases. The sets are as shown in table 1.

Based MSRP and perfect maintenance policy, we can get the system state after spare replacement $S_D(S,\ F_i)$ as shown in table 2. We calculated the mission success probability using the algorithm as below.

Experimental results of this example under different initial spares scenario are reported in Table 3 and Fig. 4.

From the exprimental results of this example, we can find easily the minimal initial spares scenario [3,1] if the mission success probability should be more than 0.95 under MSRP.

Table 1. Set of the vectors in minimal path sets of each phase.

Number of phase	$L_m(F)$
1, 4	(0, 1), (1, 0)
2	(0, 0, 1, 0, 1), (0, 1, 0, 0, 1), (1, 0, 0, 0, 1) (0, 0, 1, 1, 0), (0, 1, 0, 1, 0), (1, 0, 0, 1, 0)
3	(0, 1, 1, 0, 1), (1, 0, 1, 0, 1), (0, 1, 1, 1, 0), (1, 0, 1, 1, 0)

Table 2. System state after spare replacement of each phase

Number of phase	S	$S_D(S,\ F_i)$ using MSRP	$S_D(S,\ F_i)$ using perfect policy
1, 4	(0, 0, 0/1, 0/1, 0/1)	(1, 0, 0/1, 0/1, 0/1)	(1,1,1,1,1)
2	(0, 0, 0, 0, 0)	(0, 0, 1, 1, 0)	
	(0, 0, 0, 0, 0), (0, 0, 1, 0, 0), (0, 0, 0, 1, 0)	(0, 0, 1, 1, 0)	
	(0, 0, 0, 0, 1)	(0, 0, 1, 0, 1)	
	(0, 1, 0, 0, 0)	(0, 1, 0, 1, 0)	
	(0, 0, 0, 1, 1)	(0, 0, 1, 1, 1)	
	(1, 0, 0, 0, 0)	(1, 0, 0, 1, 0)	
	(1, 1, 0, 0, 0)	(1, 1, 0, 1, 0)	
	(0, 1, 1, 0, 0)	(0, 1, 1, 1, 0)	
	(1, 0, 1, 0, 0)	(1, 0, 1, 1, 0)	
	(1, 1, 1, 0, 0)	(1, 1, 1, 1, 0)	
3	(1, 0, 0, 1, 0), (0, 0, 0, 1, 0), (0, 0, 1, 1, 0), (1, 0, 1, 0, 0), (0, 0, 1, 0, 0), (1, 0, 0, 0, 0), (0, 0, 0, 0, 0)	(1, 0, 1, 1, 0)	
	(1, 0, 0, 0, 1), (0, 0, 0, 0, 1), (0, 0, 1, 0, 1)	(1, 0, 1, 0, 1)	
	(0, 0, 1, 1, 1), (1, 0, 0, 1, 1), (0, 0, 0, 1, 1)	(1, 0, 1, 1, 1)	
	(0, 1, 1, 0, 0), (0, 1, 0, 1, 0), (0, 1, 0, 0, 0)	(0, 1, 1, 1, 0)	
	(0, 1, 0, 0, 1)	(0, 1, 1, 0, 1)	
	(0, 1, 0, 1, 1)	(0, 1, 1, 1, 1)	
	(1, 1, 1, 0, 0), (1, 1, 0, 1, 0), (1, 1, 0, 0, 0)	(1, 1, 1, 1, 0)	
	(1, 1, 0, 0, 1)	(1, 1, 1, 0, 1)	
	(1, 1, 0, 1, 1)	(1, 1, 1, 1, 1)	

Calculation_of_mission_success_probability (X)
for phase_num from 1 to n
scenarios_of_system_state (phase_num) = Get_states_of_path_set(phase_num);
end
scenarios_of_spares_usage =Get_feasible_scenarios_of_spares_usage(X);
feasible_scenarios = Cartesian(scenarios_of_system_state, scenarios_of_spares_usage);
for each feasible_scenario(i) in feasible_scenarios
if (it satisfies the condition in equation (5)) then
for p from 1 to n
$P_{phase}(p)$ *= Calculation_of_state_transition_probability(feasible_scenario(i));*
// equation (15)
end

$$P_{mission}(i) = \prod_{p=1}^{n} P_{phase}(p);$$

end
end

$$P_{mission} = \sum_{i} P_{mission}(i); \qquad \text{// equation (6)}$$

end

Table 3. Mission success probabilities under different amount of initial spares using MSRP

number of X_1 spares \ number of X_2 spares	0	1	2	3
0	0.528606	0.563374	0.566820	0.567062
1	0.808845	0.862045	0.867317	0.867688
2	0.880945	0.938887	0.944629	0.945034
3	0.894152	0.952962	0.958791	0.959201

Table 4. Mission success probabilities under different amount of initial spares using perfect maintenance policy

number of X_1 spares \ number of X_2 spares	0	1	2	3
0	0.153131	0.253415	0.276997	0.279930
1	0.364261	0.602812	0.658908	0.665884
2	0.477438	0.790094	0.863609	0.872749
3	0.511017	0.845644	0.924317	0.934097

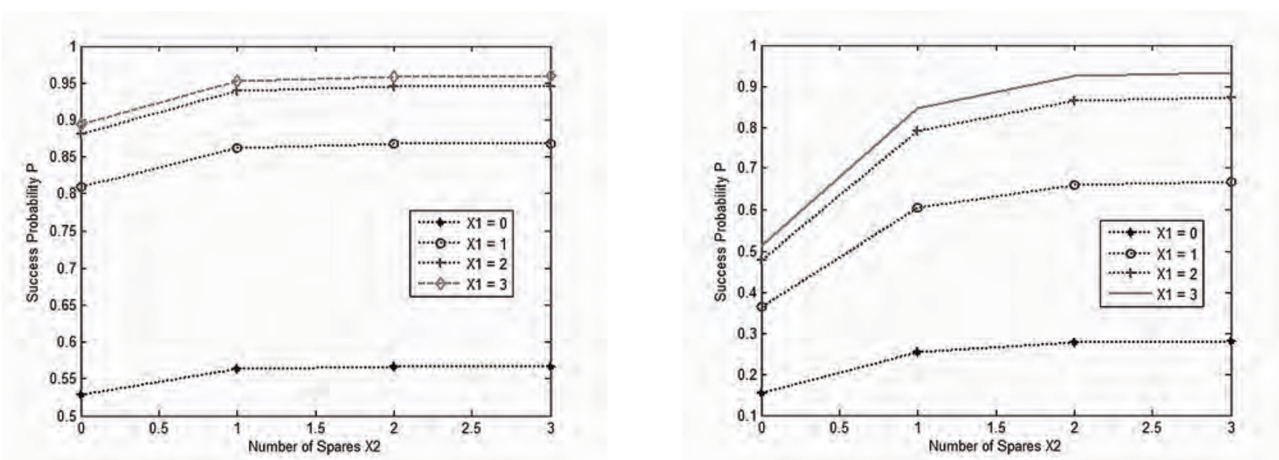

Fig. 4. Mission success probability curves under different initial spares scenario

6. Summary

This paper presents a success probability model of the phased missions under given limited spares. The spare replacement policy considered in this paper is MSRP and the spare replacement time is not neglected. In the interval of two phases, any maintenance policy can be considered by using different functions of $\bar{X}_D(S, F)$ and $S_D(S, F)$. The model advanced in this paper also can be used in the reliability analysis of PMS with cold standby components considering the switch time or not. In the practice application of this model, the system may be divided into several parts with independent models to reduce the size of the system state space, and the success probability of whole mission can be calculated by the combination of the probabilities of all parts.

Acknowledgements

This study was done whilst Dr. Tao Zhang was visiting in the University of Nottingham. His research and visiting were supported by the National Science Foundation of China, under Grant No. 70971132. The authors gratefully acknowledge Prof. John Andrews who is the Royal Academy of Engineering and Network Rail Professor of Infrastructure Asset Management. He is also the Director of The Lloyd's Register Educational Trust Centre for Risk and Reliability Engineering at the University of Nottingham. Thank him for many helpful and constructive comments.

References

1. Mo Yu-chang, Siewiorek Daniel and Yang Xiao-zong. Mission reliability analysis of fault-tolerant multiple-phased systems. Reliability Engineering and System Safety, 2008; (93): 1036–1046.
2. Ma Y. and Trivedi K.S. An algorithm for reliability analysis of phased-mission systems. Reliability Engineering and System Safety, 1999; (66): 157–170.
3. Vaurio J.K. Fault tree analysis of phased mission systems with repairable and non-repairable components. Reliability Engineering and System Safety, 2001; (74): 169-180.
4. Vaurio J.K. Making systems with mutually exclusive events analyzable by standard fault tree analysis tools. Reliability Engineering and System Safety, 2001; (74): 75-80.
5. Andrews J.D. Birnbaum and criticality measures of component contribution to the failure of phased missions. Reliability Engineering and System Safety, 2008; (93): 1861-1866.
6. Mura I., Bondavalli A., Zang X. and Trivedi K.S. Dependability modeling and evaluation of phased mission systems: a DSPN approach. In: Proceedings of Dependable Computing for Critical Applications (DCCA), 1999, (7): 299-318.
7. Chew S.P., Dunnett S.J. and Andrews J.D. Phased mission modelling of systems with maintenance-free operating periods using simulated Petri nets. Reliability Engineering and System Safety, 2008; (93): 980–994.
8. Zang X., Sun H. and Trivedi K. S. A BDD-based algorithm for reliability analysis of phased-mission systems. IEEE Trans. Reliability, 1999; 48(1): 50-60.
9. Tang Z. and Dugan J. B. BDD-based reliability analysis of phasedmission systems with multimode failures. IEEE Trans. Reliability, 2006; 55(2): 350-360.
10. Zhang Tao, Guo Bo, Guo Ji-zhou and Zhang Jian-jun. A New BDD-Based Algorithm for Reliability Analysis of Phased-Mission Systems. ICRMS'2004, Xi'an, China, 2004; (8): 11-15.
11. Wang D., Trivedi K. S. Reliability Analysis of Phased-Mission System With Independent Component Repairs, IEEE TRANSACTIONS ON RELIABILITY, 2007; 56(3): 540-551.
12. Zhang Tao, Gao Da-hua, Guo Bo, Wu Xiao-yue and Tan Yue-jin. Spare availability model for phased mission systems(in Chinese). Journal of Systems Engineering, 2006; 21(1): 86-91.
13. Guo Bo, Zhang Tao, Zhang Quan and Tan Yue-jin. Phased-Mission availability assessment model for system given limited spares(in Chinese). Systems Engineering–Theory & Practice, 2005; 2: 94-100.

Tao ZHANG, Ph.D.
Guanghan BAI, Ph.D. student
Prof. Bo GUO, Ph.D.

College of Information System and Management
National University of Defense Technology
47 Yanwachi Street, Changsha, 410073, China
E-mail: zhangtao@nudt.edu.cn , boguo@nudt.edu.cn

Article citation info:
VALIŠ D, KOUCKY M, ZAK L. On approaches for non-direct determination of system deterioration. Eksploatacja i Niezawodnosc – Maintenance and Reliability 2012; 14 (1): 33–41.

David VALIŠ
Miroslav KOUCKY
Libor ZAK

ON APPROACHES FOR NON-DIRECT DETERMINATION OF SYSTEM DETERIORATION

METODY POŚREDNIEGO BADANIA STARZENIA SIĘ SYSTEMU

Nowadays the system requirements are set up and evaluated in various manners. We have plenty of excellent options available taking about an item technical state. We can also consider other states by many diagnostic options. The paper deals with the mathematical processing, monitoring and analysis of the oil field data got as a result from the laser spectrography in frame of the tribodiagnostic oil tests. The mathematical methods based on time series and their analysis and calculation processed by suitable method are used in the paper for oil data analysis. Due to the fact that the data sample is classified as fuzzy and uncertain from many reasons the FIS (Fuzzy Inference System) is used.

Keywords: *oil diagnostics, health and condition monitoring, non-destructive diagnostics and prognostics.*

Obecnie wymagania systemu mogą być ustalane i oceniane w różny sposób. Mamy do dyspozycji wiele doskonałych opcji oceny stanu technicznego obiektów. Istnieje również wiele możliwości diagnozowania innych stanów. W artykule przedstawiono proces matematycznego przetwarzania, monitorowania i analizy danych eksploatacyjnych dotyczących oleju uzyskanych na podstawie spektrografii laserowej przeprowadzonej w ramach diagnostyki tribologicznej. Do analizy danych wykorzystano metody matematyczne oparte na szeregach czasowych oraz odpowiednie metody analizy i obliczania szeregów czasowych. Ponieważ dostępne dane sklasyfikowano jako rozmyte i niepewne, zastosowano System Wnioskowania Rozmytego FIS.

Słowa kluczowe: *diagnostyka oleju, monitorowanie stanu technicznego oleju, prognozowanie i ocena stanu technicznego metodami nieniszczącymi.*

1. Introduction

The growing dependability and operation safety requirements of modern equipment together with the increasing complexity and continuous reduction of economic costs of operation and maintenance might be satisfied among others by the consistent use of modern diagnostic systems. At present such systems can be equipped with signal processors related to board computers and with intelligent sensors which are the source of primary information on a technical state in real time. The main task of object technical state diagnostics is not only to find out incurred failures but also to prevent from occurrence the failures with the help of sensible detection and changes localization in the object structure and in its behaviour changes.

A tribotechnical system, friction in it, wear and lubrication is the main subject of this paper. Regarding the tribotechnical system, the basic information on tribological process, operating and loss variables are provided. Tribology is the science and technology of interacting surfaces in relative motion. The function of a tribotechnical system (TTS) is to use the system structure to convert input variables (e.g., input torque, input speed, input type of motion, and sequence of motions) into technically utilizable output variables (e.g., output torque, output speed, output motion) (Fig. 1).

Tribological loads in a TTS are generated by input and disturbance variables' action on the system structure. They chiefly include contact, kinematic, and thermal processes [2]. According to [2], the tribological load represents "the loading of the surface of a solid caused by the contact and relative motion of a solid, liquid or gaseous counterbody." It is introduced via the real contact areas. Plastic deformation and wear can cause the real contact areas to change during TTS operation. When mechanical energy is converted by friction, energy dissipates, which makes itself noticeable by changing the thermal situation. Since the thermal behaviour also continuously adapts to the new conditions as a result of wear, changes to the contact geometry, and resulting changes in the friction, dynamic rather than static influencing variables determine the tribological loading in a real contact. The contact geometry, the processes occurring in the contact, and the thermal behavior of a TTS are influenced by, among other things, the load, the motion conditions, the element properties, and the friction state. While the apparent contact area alone is decisive in fluid lubrication, according to [2], in mixed lubrication, i. e., when the dimensionless film parameter

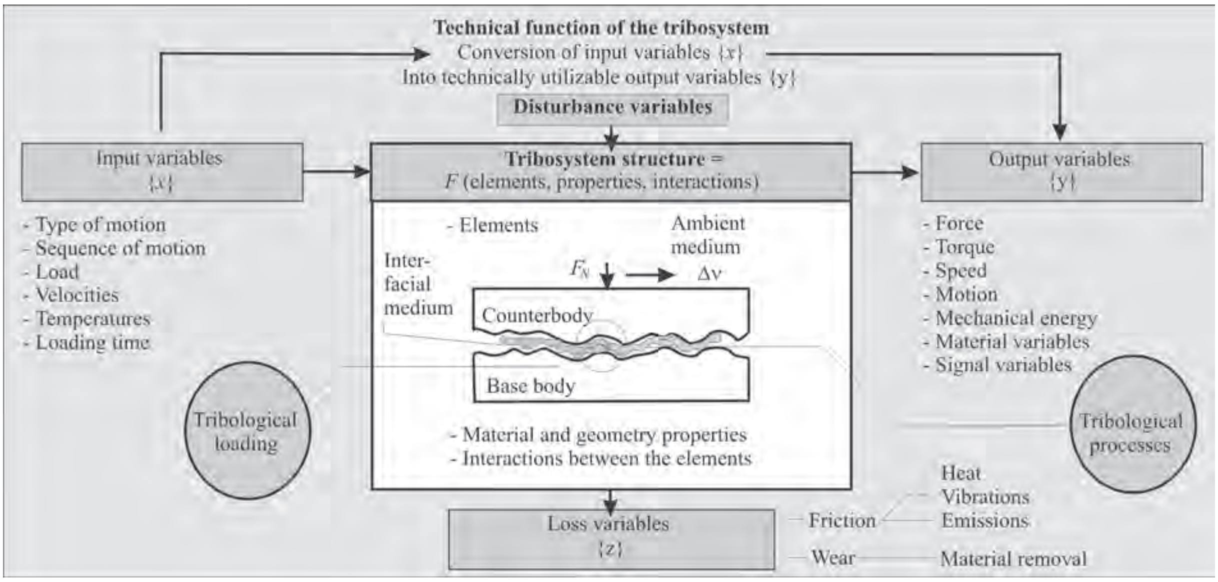

Fig. 1. Expanded representation of a tribotechnical system (TTS) according to [2]

$$\Lambda = \frac{h_{\min}}{(R_{q1}^2 + R_{q2}^2)^{1/2}} \qquad (1)$$

with the minimum lubrication film thickness h_{min} and the root-mean-square (rms) surface roughnesses R_{q1} and R_{q2} of the base body and counterbody is in the range $\Lambda<3$, in boundary lubrication with $\Lambda<1$ and for dry friction both the apparent contact area and the real contact areas must be allowed for (Fig. 1). When there are contacts between the friction bodies, *interactions* occur in the real contact areas and in the near-surface zones. *Atomic/molecular* interactions occur on the one hand and *mechanical* interactions on the other. Whereas the former cause adhesion on solid–solid boundary layers are extremely important technically in the form of physisorption and chemisorptions on solid–fluid boundary layers, the latter lead to elastic and plastic contact deformations and to the development of the real contact areas.

The type of interaction that primarily occurs depends greatly on the friction state. Thus, when a lubricant is present the atomic/molecular interaction can be disregarded more often than the mechanical. Friction and wear in a given TTS ultimately depend on the interactions between the elements. The friction state, the effective mechanisms of friction and wear, and the contact state can be used to describe the interactions. The tribological loads occurring in the real contact areas produce *tribological processes*. These subsume the dynamic physical and chemical mechanisms of friction and wear and boundary-layer processes that can be attributed to friction and wear.

The type of interaction that primarily occurs depends greatly on the friction state. Thus, when a lubricant is present the atomic/molecular interaction can be disregarded more often than the mechanical. Friction and wear in a given TTS ultimately depend on the interactions between the elements. The friction state, the effective mechanisms of friction and wear, and the contact state can be used to describe the interactions. The tribological loads occurring in the real contact areas produce tribological processes. These subsume the dynamic physical and chemical mechanisms of friction and wear and boundary-layer processes that can be attributed to friction and wear.

2. Objects on diagnostics and diagnostics methods

The assumed objects of diagnostics, i.e. the tank engines T-72M4CZ, TATRA 810 and PANDUR II have not been ready yet in terms of design to use the ON-LINE system, though in practice similar possibilities for other applications have already existed. It results from the information stated above that we are still supposed to use OFF-LINE engine diagnostics system when sampling lubrication fluid at certain intervals, and using known and optimised special tribodiagnostic methods [4-9].

Recognition of a technical state is a basic assumption for making a diagnosis used for determining either operability or non-operability, or for the detection, recognition, distinction, and localization of system parts faults. Although the data on the object condition obtained from a lubrication fluid is available, little importance is attached to it when changing the oil. If the condition of a lubrication fluid affected not only evaluation of the object condition but also modification and optimisation of exchange dates, it would be notably positive in terms of economic optimisation.

When evaluating data, the information is transformed many times and provides only estimated reality which might be different from reality itself. That is why the pattern recognition is an important and very complex area of technical diagnostics. Generally the recognition is divided into two groups depending on which methods are used - syntactic or signature.

Parsing/Syntactic Method – is based on recognizing a qualitative way. A word or a symbol string represents the pattern reflecting an object, an event or a process.

Signature Method – is based on recognizing objects, events, or processes with the help of an arranged set of numbers which describe the object characteristics.

Technical state patterns are given by n-dimensional vectors of numerical values of diagnostic quantities recorded in different parts of a diagnosed object at the same time. In matrix form the technical state pattern might be defined by a column vector [7]:

$$x = [x_1, x_2, \ldots, x_n]^T \tag{2}$$

where numbers $x_1, x_2, \ldots, x_n$ are diagnostic characteristics magnitudes, or calculated characteristics determining vector coordinates in n-dimensional space.

Single process recognition classes correspond with single diagnoses of technical states of a diagnosed object. The diagnoses set *D*:

$$D = \{D_1, D_2, \ldots D_R\} \tag{3}$$

is explicitly classified as belonging to a diagnoses indicators set D.

Then the decision rule $D_i = s(x)$ matches each specific signature vector with a corresponding diagnose – state indicator. In practice the diagnose indicator is transformed into a formulation or a corresponding diagnose – state code.

In practice, when applying a signature recognition method, it is necessary to:

- select an optimal number of diagnostic characteristics so that the necessary resolution capability of a classifier could be obtained using minimum number of quantities and measured data;
- set an algorithm, i.e. the rules used when classifying into single diagnoses.

In diagnostics in many cases there is no exact line between an up state and fault, i.e. there is no mutually explicit representation among points spaces and points classes spaces and corresponding technical states – diagnoses. The failure classes intersect which means that the same magnitudes of measured characteristics might correspond with different diagnoses. If the vagueness in classes distribution is not given by a stochastic character of measured characteristics but by the fact that the exact line among states classes does not exists, it will be good to use fuzzy set theory and adequate multi-criteria fuzzy logic.

Note:

The obtaining of functional – process diagnostic parameters which will be explicitly matched with an appropriate technical state in real time is the basic problem of modern tools, e.g. formal logic, expert systems, neural networks, fuzzy logic, and many other methods available nowadays. It is about the parameters which form the line among good, acceptable, limit, and disrepair state, or between an up state and fault in binary logic. It results from the example of an engine diagnostics that the usage of multi-criteria fuzzy logic can be appropriate in decision process when analyzing diagnostic information, e.g. applying the analysis of lubrication oil which contains relatively complex, more dimensional information on states, events, and a course of wearing. Moreover, the oil can be found in complex mechanical closed systems such as an engine, a gear box, a hydraulic system, etc. Regarding complex usage of lubrication oil it will be necessary to monitor and assess other parameters while analyzing machine wear. One of the most important information sources might be the results of ferographical analysis (a type, a size, material composition, distribution, morphology, speed of generation, etc.) and particles wear in real time, or lubrication oil degradation got by the methods FTIR (Furier Transform Infrared Spectroscopy), etc. However, it has not been possible to get this information in real time yet.

3. Oil field data assessment and system health determination

Having enough field data obtained from a statistically important set of diagnosed objects is a basic assumption for solving this problem successfully (e.g. the engines themselves, etc.). We have assumed so far that the signatures belonging to a certain diagnosis – state are known, or that it is possible to suggest and set up a classifier which classifies a pattern into a right diagnosis. In practical applications the signatures are of the nature of deterministic variables with a stochastic part. As a result of this a signature vector changes and single diagnoses are not disjunctive in a signature space. When using deterministic classification methods it is not possible to decide explicitly into which diagnosis a signature vector should be classified. In such cases statistical methods are used.

Technical state diagnostics and engine monitoring includes system approach which deals with sampling, analysis and information utilisation which is important in relation to a mechanical or thermodynamic engine state. Generally it is about monitoring and assessing wearing particles and pollution in life fluids (e.g. hydraulic and engine oils), or metal wearing particles monitoring, non-metal polluting particles monitoring, products of burning process by high or low temperatures, soft pollutants of organic origin which form oil resin, so called cold sediments, oil and fuels oxidation products, hard-solid pollutants of inorganic origin, dust particles of silicon origin, etc. The monitoring covers a life fluid sample collection and its off-line analysis using easy, standard or special – instrumental methods. The increased forming of metal magnetic wearing particles is usually monitored too, using magnetic detectors with recording and signalization. Using the on-line diagnostics based on a laser particles analyser appears to be a very progressive method. This method enables us to find wearing particles according to a corresponding wearing mechanism (fatigue), adhesion, abrasion, cavitations, corrosion, vibration, combination of the situations mentioned above together with expressing the state, prognosis, trends calculations, etc., supported by intelligent software in the future in real time.

3.1 Utilisation of regression model

For the sake of the analysis there were used engine oil samples where, depending on cumulative operation time, it was possible to monitor the concentration of wearing specific particles. It was about soot particles as a burning process product as well as abrasive metal particles as fatigue process products, cutting abrasive processes, and sliding abrasive processes. In the Tables below there is a list of these particles.

a) Soot particles data

We start from the presumption, which is not always consistent with reality, that local minima correspond to oil change. We intended to straighten courses between oil changes by the help of regression. It might be expected that tangents will be constant or they will show a small growth which can be interpreted by return as increasing wearing. As an experiment it could be possible to set tangents or intervals and the corresponding oil change intervals. The real state would be diagnosed by field data on the basis of which (using statistical hypothesis testing) the intervals between oil changes would be modified (increasing tangent – shortening intervals).

Table 1. Input data of soot particles

Sample	Soot (%)	Sample	Soot (%)	Sample	Soot (%)	Sample	Soot (%)
1	0.031771816	16	0.185519338	31	0.131379321	46	0.298258215
2	0.103316583	17	0.235333502	32	0.164228171	47	0.314934731
3	0.125431612	18	0.250645906	33	0.198963374	48	0.125000909
4	0.1473445	19	0.263931781	34	0.214886084	49	0.109051809
5	0.168435231	20	0.282059491	35	0.249506742	50	0.116552792
6	0.13423948	21	0.32115677	36	0.274932355	51	0.129438415
7	0.137344524	22	0.322607964	37	0.301216871	52	0.035240542
8	0.138561517	23	0.357020229	38	0.203418538	53	0.040360887
9	0.182563171	24	0.399251908	39	0.097838856	54	0.054815382
10	0.240091324	25	0.367105871	40	0.15223287	55	0.087472059
11	0.234781966	26	0.36917761	41	0.187827662	56	0.128711835
12	0.256827921	27	0.377272516	42	0.220623925	57	0.141270027
13	0.107033946	28	0.399431527	43	0.23116672		
14	0.166212305	29	0.035686743	44	0.242863998		
15	0.193901226	30	0.119831741	45	0.264045507		

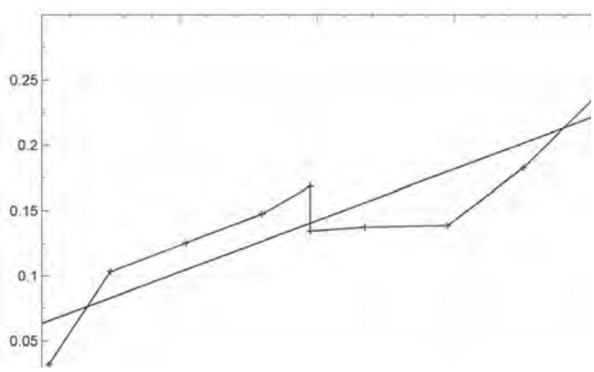

Fig. 2. Soot concentration to the first change

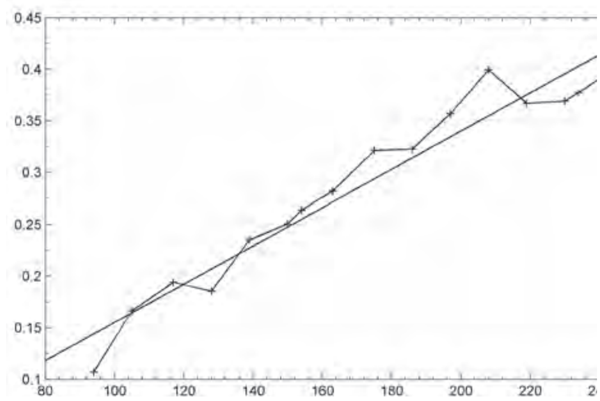

Fig. 3. Soot concentration to the second change: regression by the line y = 0.018x + 0.0296, determination coefficient R = 0.97

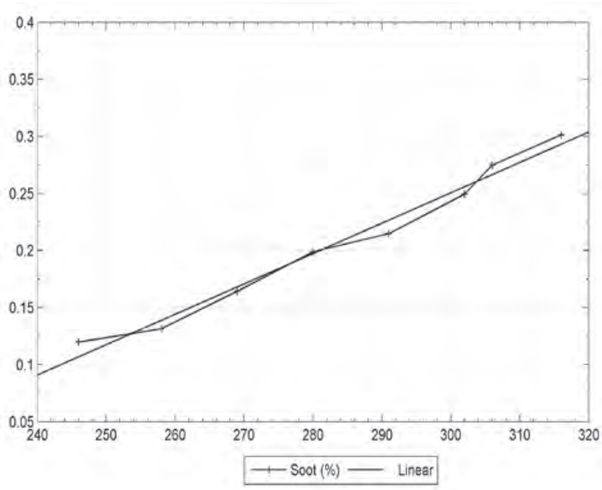

Fig. 4. Soot concentration to the third change: regression by the line y = 0.0027x + 0.5474, determination coefficient R = 0.99

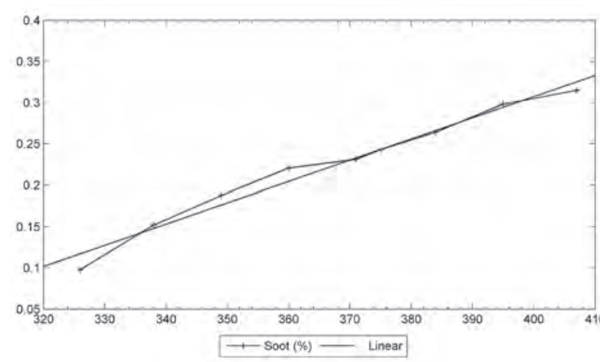

Fig. 5. Soot concentration to the fourth change: regression by the line y = 0.0026x + 0.72, determination coefficient R = 0.99.Regression by the line y = 0.0026x + 0.72, determination coefficient R=0.99

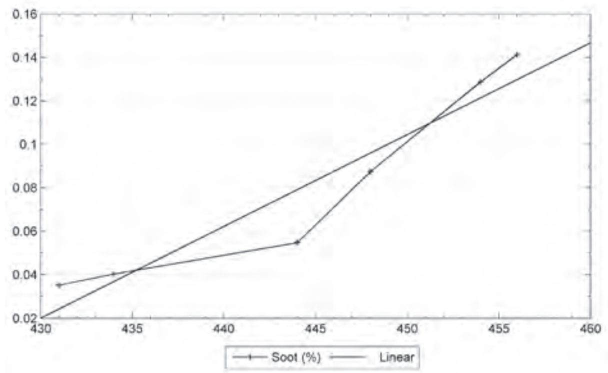

Fig. 6. Soot concentration to the fifth change, regression by the line $y = 0.0042x – 1.79$, determination coefficient $R = 0.95$

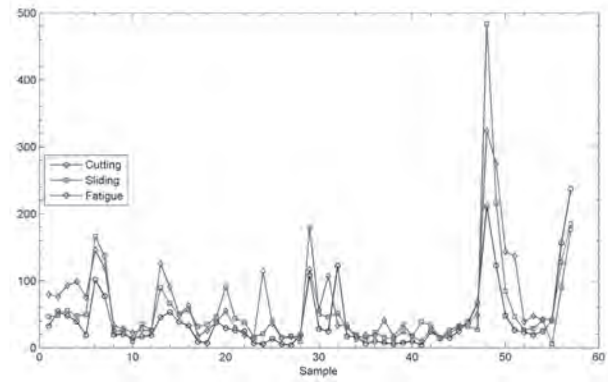

Fig. 7. Total course of cutting, sliding and fatigue particles

Table 2. Input data of cutting, sliding, fatigue particles

Sample	Cutting	Sliding	Fatigue	Sample	Cutting	Sliding	Fatigue
1	32.3381511	46.19006729	79.69317579	30	28.51932859	49.71670866	56.26627159
2	54.43107224	48.15056419	76.42622399	31	24.65869081	45.84933078	107.1173915
3	47.7745769	55.48026347	92.84393597	32	122.2669096	51.72775424	33.3818934
4	39.31019068	47.45829821	98.55917168	33	17.08991575	29.84530449	33.77119803
5	18.86055315	49.26862264	75.44025481	34	16.55065846	19.24586105	13.0867945
6	101.8758668	166.3172793	145.8493638	35	5.773758411	12.7022686	18.86094451
7	77.18351507	136.9976914	120.0213284	36	9.638239861	22.74575508	17.73239851
8	19.23974991	24.62658668	33.09119701	37	7.700790524	15.40158081	40.81693268
9	20.3872683	25.77249193	28.08072448	38	5.771924973	13.46782494	16.54559851
10	14.22187865	9.49721241	22.54989433	39	7.695899963	24.24149847	34.24646163
11	16.94164109	34.65355778	26.95227838	40	9.622930765	17.32127523	16.93596685
12	18.48091865	26.56723869	24.64204156	41	3.850395441	38.12156081	9.625988245
13	45.42258263	89.30431986	125.4877148	42	23.86369467	33.48662567	27.71286666
14	53.08758593	66.16782999	90.39810944	43	15.40647697	13.48066711	14.63811278
15	38.88133812	48.88801241	48.50426865	44	15.01138079	26.17358899	20.78513956
16	32.70757484	56.56398487	62.71806693	45	24.65330708	32.73876286	30.81295347
17	9.248981953	31.60101461	17.34331131	46	38.52843809	31.59361362	38.14325213
18	7.315261722	34.65355682	25.79618037	47	67.08244026	26.98707104	48.96461153
19	38.93652487	45.87753093	38.16693771	48	211.2935009	483.2885046	323.3624358
20	29.67515659	90.95250392	54.72660637	49	122.9303293	216.4200897	273.7473412
21	25.81434846	43.92251658	29.66719174	50	47.77693057	84.38728714	143.7644463
22	24.65829825	37.7580657	18.87903285	51	26.56841278	46.20474243	136.6924605
23	6.927727699	16.16534972	13.47210288	52	23.10237217	26.95276642	38.88703585
24	5.775592804	21.17717361	114.2053576	53	19.23974991	28.85962486	47.32773209
25	13.48066711	39.67050409	35.8188839	54	24.65134203	41.21526575	41.60434842
26	5.386788368	15.38691235	14.23700106	55	40.39064407	5.77009201	43.0862869
27	3.847949982	17.31577492	16.54559851	56	156.7627567	90.79354894	127.6534103
28	19.24586177	9.23762238	16.55065835	57	236.9066696	175.971869	184.4765167
29	107.8546431	179.933398	116.3448297				

b) Data – cutting, sliding, fatigue

The obtained field data show smoothly increasing tangent – see figures 2 – 6. Regression to the first change by the line $y = 0.002x + 0.0635$, determination coefficient $R = 0.93$, regression to the second change. The total course of observed particles (cutting, sliding and fatigue) is further presented in figure 7.

3.2 Utilization of FIS (Fuzzy Inference System)

A Fuzzy Inference System (FIS) is based on the terms *fuzzy set* and *fuzzy relation* which were introduced by Lotfi A. Zadeh in 1965 following the [14]. The fuzzy set is one of the possible generalizations of the term set. The fuzzy set is a pair ($\mathbf{U}$, μ_A) where $\mathbf{U}$ is universe and μ_A: $\mathbf{U} \rightarrow \langle 0,1 \rangle$ is a function describing that U elements belong to A fuzzy set. The membership is marked with $\mu_A(x)$. The fuzzy set is the generalization of a "typical" set because the following formula applies for a "typical" set A membership

μ_A: $\mathbf{U} \rightarrow \{0, 1\}$ and $x \in \mathbf{A} \Leftrightarrow \mu_A(x) = 1$ and $x \notin \mathbf{A} \Leftrightarrow \mu_A(x) = 0$.

Let $\mathbf{U}i$, $i = 1, 2, ..., n$ be universes. Then the fuzzy relation R over the universe $\mathbf{U}$ is regarded as the fuzzy relation $\mathbf{U} = \mathbf{U}_1 \times \mathbf{U}_2 \times ... \times \mathbf{U}_n$.

Nowadays one of the most widely used applications is a *Fuzzy Inference System* – FIS (once used as a term "fuzzy regulator"). The FIS is considered to be a fuzzy relation which gives resultant values when put together with input values. There are several types of the FIS. In this paper we applied the type P: $u = R(e)$ where an output quantity value depends only on the magnitude of an input quantity.

Let $\boldsymbol{E_i} = (E_i, \boldsymbol{T}(E_i), \mathrm{E}_i, \mathrm{G}, \mathrm{M})$, $i = 1, ..., n$ be input language variables, and $\boldsymbol{U} = (U, \boldsymbol{T}(U), \mathrm{U}, \mathrm{G}, \mathrm{M})$ be an output language variable. E_i, U are the names of variables, $\boldsymbol{T}(E_i)$, $\boldsymbol{T}(U)$ is a set of language values, E_i, U are relevant universes, G is grammar, M represents the meaning of language values. The FIS is considered to be:

$\mathbf{R} = \mathbf{R}_1$ otherwise $\mathbf{R}_2$ otherwise, ... , otherwise $\mathbf{R}_p$,where $\mathbf{R}_k$, $k = 1, …, p$ is as follows:

$\mathbf{R}_k$ **= if** E_1 **is** $X_{E1,k}$ **and** E_2 **is** $X_{E2,k}$ **and ..... and** E_n **is** $X_{En,k}$**, then** U **is** $Y_{U,k}$ $X_{Ei,k} \in \boldsymbol{T}(Ei)$, $Y_{U,k} \in \boldsymbol{T}(U)$ for each $i = 1, ..., n$, for each $k = 1, ..., p$.

The meaning of the statements $\mathbf{R}$ is expressed by $\mathrm{M}(\mathbf{R}_k) = \boldsymbol{R}$, and $\mathrm{M}(\mathbf{R})$ is a fuzzy relation above E1×E2×...×En×U which

$$R = M(\mathrm{R}) = \bigcup_{k=1}^{p} M(\mathrm{R_k}) \tag{4}$$

is defined as follows:

Regarding other rules $\mathbf{R}$ is considered as unification, and $\mathrm{M}(\mathbf{R}_k)$ is defined $\mathrm{M}(\mathbf{R}_k) = A_{E1,k} \times A_{E2,k} \times ... \times A_{En,k} \times A_{U,k}$, $A_{Ei,k} = \mathrm{M}(X_{Ei,k})$ which is a fuzzy set above the universe E_i, $i = 1, …, n$ and = M() is a fuzzy set over the universe U, $k = 1, …, p$. $\mathrm{M}(\mathbf{R}_k)$ is a fuzzy relation over the universe $\mathrm{E}_1 \times \mathrm{E}_2 \times ... \times \mathrm{E}n \times \mathrm{U}$.

When entering into the FIS, any fuzzy set will be above E_i (a_{Ei}). Then the magnitude of an actuating quantity a_U is determined by the formula $a_U = (a_{E1} \times a_{E2} \times ... \times a_{En})^\circ\boldsymbol{R}$. A_U consists of the fuzzy relation ($a_{E1} \times a_{E2} \times ... \times a_{En}$) above the universe $\mathrm{E}_1 \times \mathrm{E}_2 \times ... \times \mathrm{E}_n$, and the relation $\boldsymbol{R}$ defined above the universe $\mathrm{E}_1 \times ... \times \mathrm{E}_n \times \mathrm{U}$. The fuzzy set above the universe U is the result of this composition.

In many cases the fuzzy set is not required to be an output from the FIS, but a specific value $u_0 \in U$, i.e. we want to carry out *defuzzification*. The centroid method is the most widely used defuzzification method. The FIS specified this way is called *Mamdani* FIS [6].

If we do not know how the process works (i.e. FIS rules cannot be set), but the sufficient amount of input and output data is available, we can use the modification of Mamdani-FIS Sugeno (Takani-Sugeno FIS) [6] and [11]. This FIS is described by suitable parameters during tuning performed on well-known data. Sugeno FIS input language values are similar to Mamdani-type FIS, but the output quantity value is expressed by a different formula:

$\mathbf{R}_k$ **= if** E_1 **is** $X_{E1,k}$ **and** E_2 **is** $X_{E2,k}$ **and ... and** E_n **is** $X_{En,k}$, then $U = F_k$,

where F_k describes the value in the universe U for k-th rule.

This value depends on the magnitude of inputs (a_{E1}, a_{E2},..., a_{En}) into FIS: $F_k \equiv F_k(a_{E1}, a_{E2},..., a_{En})$. If $\mathrm{E}_1, \mathrm{E}_2, ..., \mathrm{E}_n$, are the subsets of the universe U of real numbers, it can be stated that $u_k = f_k(\mathrm{defuzz}(a_{E1}), \mathrm{defuzz}(a_{E2}), …, \mathrm{defuzz}(a_{En}))$.

The function f_k is mostly considered to be a function in a constant form and it is expressed by the following way:

$f_k(\mathrm{defuzz}(a_{E1}), \mathrm{defuzz}(a_{E2}), …, \mathrm{defuzz}(a_{En})) = \alpha_k$,

or a linear form expressed as follows:

$f_k(\mathrm{defuzz}(a_{E1}), \mathrm{defuzz}(a_{E2}), …, \mathrm{defuzz}(a_{En})) =$
$= \alpha_k + \beta_{1,k}\ \mathrm{defuzz}(a_{E1}) + \beta_{2,k}\ \mathrm{defuzz}(a_{E2}) + … + \beta_{n,k}\ \mathrm{defuzz}(a_{En})$,

where α_k, $\beta_{i,k}$, $i = 1, 2, …, n$, $k = 1, 2, …, p$ are suitable invariables. The magnitude of these invariables is set during FIS tuning. In most cases the fuzzy sets are not considered as an input into Sugeno FIS, but only the values from $\mathrm{E}_1, \mathrm{E}_2, ..., \mathrm{E}_n$.

Let us take into account the input denoted by $(x_1, ..., x_n) \in \mathbf{R}^n$. Then

$f_k(x_1, … x_n) = \alpha_k$,
$f_k(x_1, … x_n) = \alpha_k + \beta_{1,k}\, x_1 + \beta_{2,k}\, x_2 + … + \beta_{n,k}\, x_n$.

The rules are put in the following equation:

$\mathbf{R}_k \equiv$ **if** x_1 **is** $X_{E1,k}$ **and** x_2 **is** $X_{E2,k}$ **and … and** x_n is $X_{En,k}$, then $u_k = f_k(x_1,… x_n)$.

This means that if the input $(x_1, ..., x_n)$ belongs to the area specified by the language values $X_{E1,k}$ up to $X_{En,k}$, then the output is found by the function f_k. The weighted value u_k of the input z_k is determined the same way as the FIS of Mamdani-type using the level of conformance between the inputs $(x_1, ..., x_n)$ and the fuzzy sets $A_{E1,k}$ up to $A_{En,k}$. When applying the rules $\mathbf{R}_1$ up to $\mathbf{R}_p$ we get for the input $(x_1, ..., x_n)$ the values u_1, up to u_p, and using weighted values w_1 up to w_p and a weighted average we obtain a resultant output value u.

3.3 Searching for a proper FIS form used for the prediction of a time series

In order to predict successfully a time series by the FIS of Sugeno-type, it is necessary to select appropriately the n-number of FIS input variables and the p-number of language values for each input variable. The time series is divided into *tuning data* and *checking data*. Regarding the tuning data we stabilized the FIS for a different number of input variables and a different number of input variable values. The number of input variables n specifies how many members of a time series enters into the FIS before predicted values, and therefore affects the prediction. We gradually selected different n-s. Using the time series we matched the following member as an output quantity to the input set of n elements, thereby getting the time series into $n + 1$ dimensional space. Applying a cluster analysis we found clusters. Relevant language values and one FIS rule of Sugeno-type were made for each cluster. This rule was selected in a linear form $Z_k = \alpha_j + \beta_{1,k}$ defuzz(a_{E1})+$\beta_{2,k}$ defuzz(a_{E2}) + … + $\beta_{n,k}$ defuzz(a_{En}). By means of optimization over tuning data we found invariables α_j, $\beta_{i,j}$ i= 1, 2, …, n, k = 1, 2, …, p (where n is the number of language variables, and p is the number of language values).

Using the FIS designed and stabilized this way we predicted other members of the time series. Comparing the predicted data to the checking data we determined the quality of the prediction. This comparison was made applying mainly two criteria – MAPE – an average error, and MAX – a maximum error. Let (R_1, R_2, …, R_k) be the real members of the time series, and (P_1, P_2, …, P_k) be the time series predicted members, where k is the number of members under examination. Then

$$MAPE = \frac{1}{k}\sum_{i=1}^{k}\frac{|P_i - R_i|}{R_i} \tag{5}$$

$$MAX = \max_{i=1,\ldots,k}\frac{|P_i - R_i|}{R_i} \tag{6}$$

The design and stabilization of the FIS Sugeno along with the comparison was performed in Matlab 5.3 – FuzzyToolbox program.

The FIS can be viewed as a device which for the n members of a time series determines next time series members. However, this device is not a “black box” as it is for neural networks for example. If we generate all possible inputs into the FIS and calculate output values from the FIS for them, the FIS activity can be shown as a FIS area. If we have n inputs (n members of a time series), and m outputs (we predict m members of a time series), the FIS area can be displayed in $n + m$ dimensional space. It is convenient to display the area in the form which shows the dependency of output quantities on input ones. The shape of the FIS area helps us to assess which input (a time series member) affects a selected output most. In *Fig. 1* and *2* there is a FIS with three inputs and one output. We obtain a four-dimensional space which can be displayed in three pictures showing the dependency of an input value on the combination of two input values. The FIS was designed so that it could predict only one following member of a time series. If we want to predict more steps, we repeat the calculation m-times using the FIS, whereas the predicted value is considered to be real and will be applied as an input into the FIS to calculate another value. In order to predict a time series correctly it is necessary to choose the appropriate number of inputs into the FIS (n), and the number of values for each input (when dealing with the FIS of Sugeno-type the number of values at all levels is the same (p) and equals the number of the FIS rules). The prediction depends on the number of inputs (n) and the number of values (p) which is noticeable especially in the series showing a trend and periodic unit. These series usually occur right in the area of mechanical systems´ operation. If there are too many FIS rules, the FIS is too sensitive to small changes. If there are few of them, the FIS is not able to describe changes. Some dependencies are introduced in Figure 8 below.

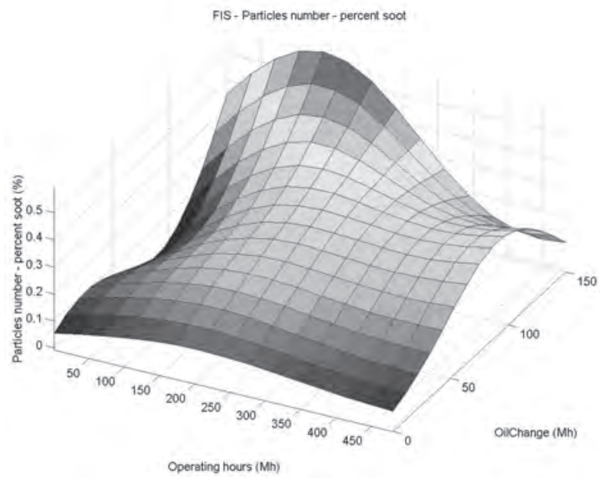

Fig.8. Course and correlation of soot particles onto operating hours

4. Proposals for system health condition calculation based on the results from tribodiagnostics

In case of taking single oil samples it is about a time line which might be possibly not stationary, and before making next calculation it needs to become stationary (non-constant mean value and dispersion); standard transformations do not provide satisfactory results.

Cumulative series of the quantities mentioned above show a linear course (determination coefficient higher than 0,97), so by analogy the linearization could be used for soot particles as an indicator for interval length modification between oil changes.

However, the analysis results detected from the oil provide a potential space for the modification of oil exchangeable date considering the number of particles present in the oil before the actual change. The situation is interesting especially with regard to the velocity of their occurrence. A recognized number of particles before the actual change would not necessarily mean a critical number which could threat reliable engine function or cause an accident. However, the exchange date is determined by an oil producer, and the time period in which the exchange is performed might be significantly affected by other characteristics. The presence and the number of particles which occurred in a lubricating system by mechanical processes should be viewed in the future as one of the most important factors in the process of lubrication fluid state assessment.

However, regarding the dependence courses of single particles occurrence between individual performed changes it is possible to observe slow increase in the particles number with a cumulative number of operational units. When using [5] we can apply the formula expressing velocity of wearing particles occurrence m.

$$m = m_o + at \tag{7}$$

Where $a = \frac{d_m}{d_t}$ is a coefficient of increase trend – second derivation of regression curve

m_o is a velocity of wearing products occurrence (oil degradation) – first derivation of the regression curve while crossing the applicable state limit [mg.Mh-1]. The limits and criteria used for determining an up state are usually based on a statistical analysis, and some possible forms of it are to be found in [5] and [8].

Since the number of oil particles is fuzzy itself we have to create a rule of unacceptable increase of that number. This fact is presented by the acceleration factor of oil particles creation. Variation of that number alongside with the possible failure consequences comes to modifications of total risk number.

Fuzzy logic seems to be one of the good tools for determining the importance of the acceleration factor magnitude. Following approaches represented in figure 8 are to be adapted according to the degradation processes and limit states got by the observation. The outcome and suitable variation of the fuzzy number represents our strategy in maintenance or mission planning. These facts overcome only such possibilities since we have strict cuts of all expenses spent not only on the armed forces. Economical and costs optimization plays significant role in the life cycle costing and many other decisions made during complex system in service operation.

Outcomes from FIS calculation present oil quality development.

These results can be used for:

the setting of an observed item – engine condition;

the identification of a risk source – the occurrence of a possible dangerous event – failure.

Some dependencies are introduced in Figures 9 below:

The output of the FIS method application:

Procedure: **hours=soot_enginehours([0.1 0.2 0.5 0.55 0.9 1.1], soot_FIS)**

Input: [0.1 0.2 0.5 0.55 0.9 1.1]

Output: 0 3.6905 35.2711 45.1254 .91.3312 . 97.6548
5.6635 8.8995 45.4304 51.7286 107.8874 161.2406

Example based onto the graph: The soot content input e.g. 0,5 indicates number of operating hours between 35.27 and 45.43. We understand one operating hour as approximately 15 kilometres of drive for tracked vehicles.

Practically it means that the higher number of particles in oil represented by increasing acceleration factor the more significant decrease of the system performance may occur and in fact it may represent higher risk of system failure. Such failure might have more outcomes and consequences some of which

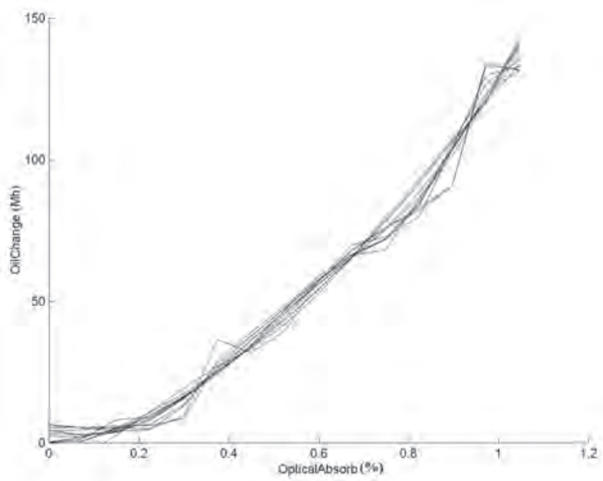

Fig. 9. Course of soot contents relation upon number of operation hours.

are not welcome in system operation especially in the area of military systems like battle vehicles for instance [12].

Possible expressions of acceleration factor increase based on magnitude of particles number is represented in Figure 10 bellow.

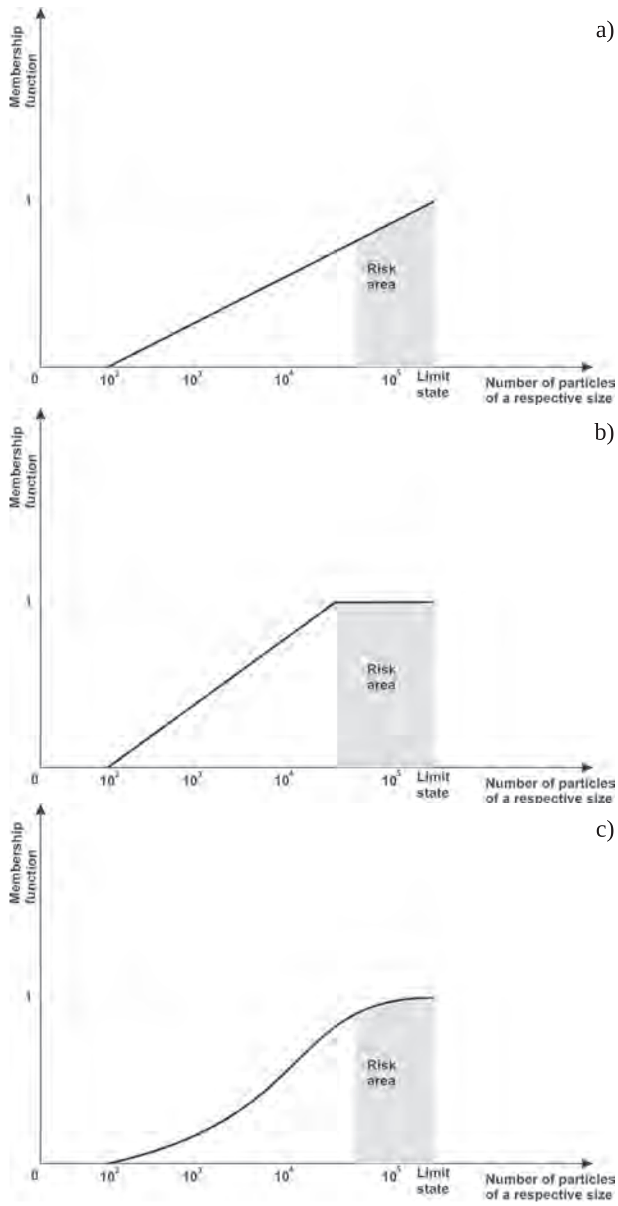

Fig. 10. Possible expressions of acceleration factor increase based on magnitude of particles number. a) Triangular shape of fuzzy number, b) Trapezoidal shape of fuzzy number, c) Progressive shape of fuzzy number

5. Conclusion

The aim of the paper contents is to shed light on the area of tribodiagnostics including the methods which are applicable and suitable for oil analysis. Results of the analysis can be used in a much better way and the impact they made on operation characteristics of a technical object might be perceived much strongly. The data regarding lubrication fluid which is available due to performed analyses is a good source of information when considering the cost savings in case the oil is changed systematically [8-9]. It would be also good to see the results of the analysis in a broader context as an interesting reflection of an actual state of a technical object from where the oil was taken. When taking into account the results of the tribological analysis, the cost savings might be manifested as extension of time of oil changes and relating maintenance costs and downtime resulting from object unavailability by extraneous causes [14]. Since there is a wide spectrum of suitable methods while analysing an immediate state and prognosis (PHM – Prognostics and Health Monitoring), and because the area falls very deeply into interdisciplinary studies, the specification of relevant dependencies of the analysis results on a real technical state is not at all an easy task to do.

Having this tool we are capable to understand of mechanisms of failures better. Such procedures enable to be prepared for coming failures and progression to faults. The diagnostics is cheaper than on-line assets and failure mechanisms are determinable in advance. Some specific classifications of failures are also used in relation to risk sources which are recognised due to oil diagnostics [13].

Acknowledgement*: This paper has been prepared with great support of the Ministry of Education, Youth and Sports of the Czech Republic, project No. 1M06047 "Centre for Quality and Reliability of Production" and with project for institutional development of K-202 University of Defence, Brno.*

4. References

1. Czichos H, Habig K H. Tribologie-Handbuch; Reibung und Verschleiß, Weisbaden: Vieweg, 2003.
2. Koucky M, Valis D. Suitable approach for non-traditional determination of system health and prognostics. Zeszyty naukowe Wyszej Szkoły Oficerskej Wojsk Lądowych im. Gen. T. Kościuszki 2011; 1(159): 123-134.
3. Koucky M, Valis D. Deterioration Dependability Diagnostics. Revised by J. Čáp, V. Píštěk, F. Pešlová. Brno: handsdesign, 2010. Section II., Diagnostics – on approaches for non-destructive diagnostics: p.77-86.
4. Lippay J. Tribological diagnostics of heavy of road lorries Tatra 815 engines which operate with OA-M6 ADS II oil. Inauguration Thesis, Brno: Military Academy, 1991.
5. Mamdani E H. Applications of fuzzy logic to approximate reasoning using linguistic synthesis. IEEE Transactions on Computers 1977; 26(12): 1182-1191.
6. Stodola J. Combustion Engines Wear and Degradation Processes Modeling. EAEC – European Automotive Congress. Beograd 2005: 26-34.
7. Stodola J. Model of Lubricating Oil Filling-up, Modification, and Degradation in the Combustion Engines. Tribology. Eslingen, 2004.
8. Stodola J. Machines Wear and Degradation Processes Modeling. International Conference Transport Means. Kaunas: Lituenia, 2004: 27-30.
9. Stodola J. Wear Particles Identification and Modelling Degradation Processes of the Combustion Engines Possibilities. Symposium "The Control and Reduction of Wear in Military Platforms". AVT-109. Williamsburg, Virginia, USA 2004. Paper Reference MP-AVT-109-11, www.rta.nato.int/Reports.as.
10. Sugeno M. Industrial applications of fuzzy control. Elsevier Science Pub. Co. 1985.
11. Valis D, Mlynczak M, Nowakowski T. How to manage risk? An approach based on standards. Problemy Eksploatacji – Maintenance problems 2011; 1(80): 137-148.
12. Valis D, Bartlett L. The Failure Phenomenon: A Critique. International Journal of Performability Engineering 2010; 6(2): 181-190.
13. Zadeh L A. Fuzzy sets. Information and Control 1965; 8: 338-353.
14. Zajac M, Valis D. Fundamental risk assessment in example of transhipment system. Reliability & Risk Analysis: Theory & Applications 2010; 1(1): 56-64.

Assoc. Prof. David Vališ, Ph.D.
Department of Combat and Special Vehicles
Faculty of Military Technologies
University of Defence
Kounicova 65, 662 10 Brno, Czech Republic
E-mail: david.valis@unob.cz
Assoc. Prof. Miroslav Koucky, Ph.D.
Department of Applied Mathematics
Faculty of Natural Sciences, Humanities and Art
Technical University of Liberec
Studnetská 2, 461 17 Liberec, Czech Republic
E-mail: miroslav.koucky@tul.cz
Dr. Libor Zak
Department of Applied Mathematics
Faculty of Mechanical Engineering
Brno University of Technology
Technicka 2896/2, 616 69 Brno, Czech Republic
E-mail: zak.l@fme.vutbr.cz

Article citation info:
KNEFEL T. Technical assessment of Common Rail injectors on the ground of overflow bench tests. Eksploatacja i Niezawodnosc – Maintenance and Reliability 2012; 14 (1): 42–53.

Tomasz KNEFEL

TECHNICAL ASSESSMENT OF COMMON RAIL INJECTORS ON THE GROUND OF OVERFLOW BENCH TESTS

OCENA TECHNICZNA WTRYSKIWACZY COMMON RAIL NA PODSTAWIE DOŚWIADCZALNYCH BADAŃ PRZELEWÓW*

The majority of actually produced Diesel engines operated as power units in passenger cars are equipped with injection systems of Common Rail type. Injectors with solenoid valve are implemented to a large extent of these engines. In the paper is discussed an assessment of differences in fuel dosing accomplished by injectors of various generations and are estimated quantities of fuel needed to actuate operation of the injectors. It has been specified a share of overflow volume in dose of injected fuel. One introduced also an index of efficiency, as a quantity to evaluate amount of decompressed fuel. Elementary overflows and differences in the elementary overflows are presented, both in case of efficient and inefficient injectors. There are evaluated leaks for elements from the 1st generation. It has been proposed a methodology of proceeding to assess technical conditions of the injectors after some time of operation.

Keywords: *Diesel engine, Common Rail injection system, solenoid-valve injector, diagnostics and technical assessment of injectors.*

Większość aktualnie produkowanych silników o zapłonie samoczynnym do napędu samochodów osobowych jest wyposażona w układy zasilania typu Common Rail. W dużej liczbie stosowane są wtryskiwacze z elektromagnetycznym zaworem. W artykule przedstawiono ocenę różnic w dawkowaniu realizowanym przez wtryskiwacze różnych generacji oraz oszacowano ilości paliwa niezbędne do uruchomienia wtryskiwaczy. Określono udział przelewu w dawce wtryskiwanego paliwa. Wprowadzono pojęcie wskaźnika sprawności, jako wielkości umożliwiającej ocenę ilości rozprężanego paliwa. Przedstawiono jednostkowe przelewy i różnice w jednostkowych przelewach zarówno dla sprawnych wtryskiwaczy, jak i niesprawnego. Wyznaczono przecieki dla elementów I generacji. Zaproponowano metodykę postępowania przy ocenie stanu technicznego wtryskiwaczy po pewnym okresie eksploatacji.

Słowa kluczowe: *silnik o zapłonie samoczynnym, układ wtryskowy Common Rail, elektromagnetyczny wtryskiwacz, diagnostyka ocena techniczna wtryskiwaczy.*

1. Introduction

Modern Diesel engines used in passenger cars, in majority of cases are equipped with hydraulic accumulator type injection systems. Such situation is caused by unquestionable advantages, from which the best seems to be a possibility of shaping of injection rate, and the same, pressure in combustion chamber of the engine. This process can be accomplished in relatively easy way with use of injectors operating in Common Rail system, through change of fuel discharge intensity from the injectors. Also, in the injectors used in hydraulic accumulator type injection systems occurs a process of batching of fuel dose supplied to the cylinder, which in the next step is reduced in size by atomizer and when mixed with air becomes air-fuel mixture initially prepared to ignition. Thus, the injectors as working elements of injection systems play very important role in obtainment of pre-assumed parameters of combustion engine operation [1]. However, due to operational conditions, the injectors remain the most sensitive for damage components of the system [3]. To detect a malfunctions in the accumulator type injection systems are used various methods of diagnostics, inclusive of methods based on model of the system [2]. It is worth, however, to consider a development of relatively simple, standardized rules of assessment of already used injectors, and in such way, after introduction of such rules, assure operation of correctly functioning elements.

Nowadays, in passenger car's engines are used two types of the injectors: the first ones, introduced to production earlier, are actuated by solenoid valve; and the second ones, which operate owing to stack of quartz plates and implementation of piezoelectric effect [7, 10]. Anyhow, in prevailing number of Common Rail systems are actually still implemented injectors actuated by solenoid valve. From beginning of their implementation to vehicles in 1997, such injectors were perfected and still developed mainly in order to enable high pressure fuel injection, to assure possibly short time of reaction on preset electric excitation and change of fuel discharge intensity from the atomizer [5, 6, 8, 11].

(*) Tekst artykułu w polskiej wersji językowej dostępny w elektronicznym wydaniu kwartalnika na stronie ***www.ein.org.pl***

2. Objective of the tests

Process of needle lift control in the injectors with solenoid valve occurs with use of quick-shift valve, incorporated into upper part of the injector (Fig. 1). Fuel flowing in under high pressure is divided into two streams, the first stream flowing in through opening „D”, to control chamber „K” located under valve stem, causes opening of the needle. It means that this portion of fuel becomes decompressed and through opening „W”, together with leaks arisen on mating surfaces of precision pairs, is directed, via overflow tubes, back to fuel tank. For needs of the present paper, this portion is called shortly as: „overflow”.

Fuel quantity, injected by the injector to engine’s combustion chamber is the second stream of the fuel.

To the analyzes which are described below were also introduced a notions of „injectors of the 1st and the 2nd generation”. As the 1st generation injectors are called such injectors, which were used in the first, after launch of accumulator type injection systems, series of mass production engines. Together with development of feeding systems, one commenced assembly of more new injectors, which enable accomplishment of smaller dwell times between partial doses. Such injectors are called as the 2nd generation. Issue of possibility of division into parts does not belong to subject-matter of the present considerations, for which two objectives are assumed. The first objective, cognitive one, is assessment of differences in dosing of Common Rail injection system, operating at beginning with the 1st generation, and next with the 2nd generation injectors, as well as estimation of fuel quantity necessary to activate the injectors.

It have been evaluated differences in overflow value between correctly functioning injectors in various areas of injection system operation. There were also taken into consideration consequences of control signal generated by inefficient injector. Simultaneously, attempt was taken to evaluate volume of fuel leaks with respect to injected fuel quantity. The second objective, utilitarian one, is development of a proposal of diagnostic criterion for injectors actuated with use of solenoid valve.

3. Objects of the tests and test bed

Injectors, both of the 1st and the 2nd generation were the objects of the tests. The first type injectors are used in turbocharged engine of 1700ccm class and are equipped with 6 holes with diameter of 0,15 mm. In turn, injectors of the 2nd generation serve to feeding of turbocharged engine of 1300ccm class, and are equipped with 5 holes having diameter of 0,13 mm [4].

All the injectors were controlled with use of the same, KSSiP-2 type laboratory controller of Common Rail system, developed and produced by the Technical University of Bielsko-Biała. Operating parameters were input from level of PC class computer. Moreover, the test bed has comprised:

- Star-8 test bed, totally modernized for needs of testing of Common Rail injection systems, equipped with wavy motion electric motor and fuel tank with heating, cooling and temperature control systems, among others,
- high pressure pump with three pistons, and throttling type of pressure control,
- hydraulic rail having 20ccm capacity, used in the engine having 1700ccm swept capacity,
- AVL pressure measuring line (SDL-31 extensometric transducer, A09 amplifier) connected to computer and oscilloscope, enabling measurements of pressure in the rail.

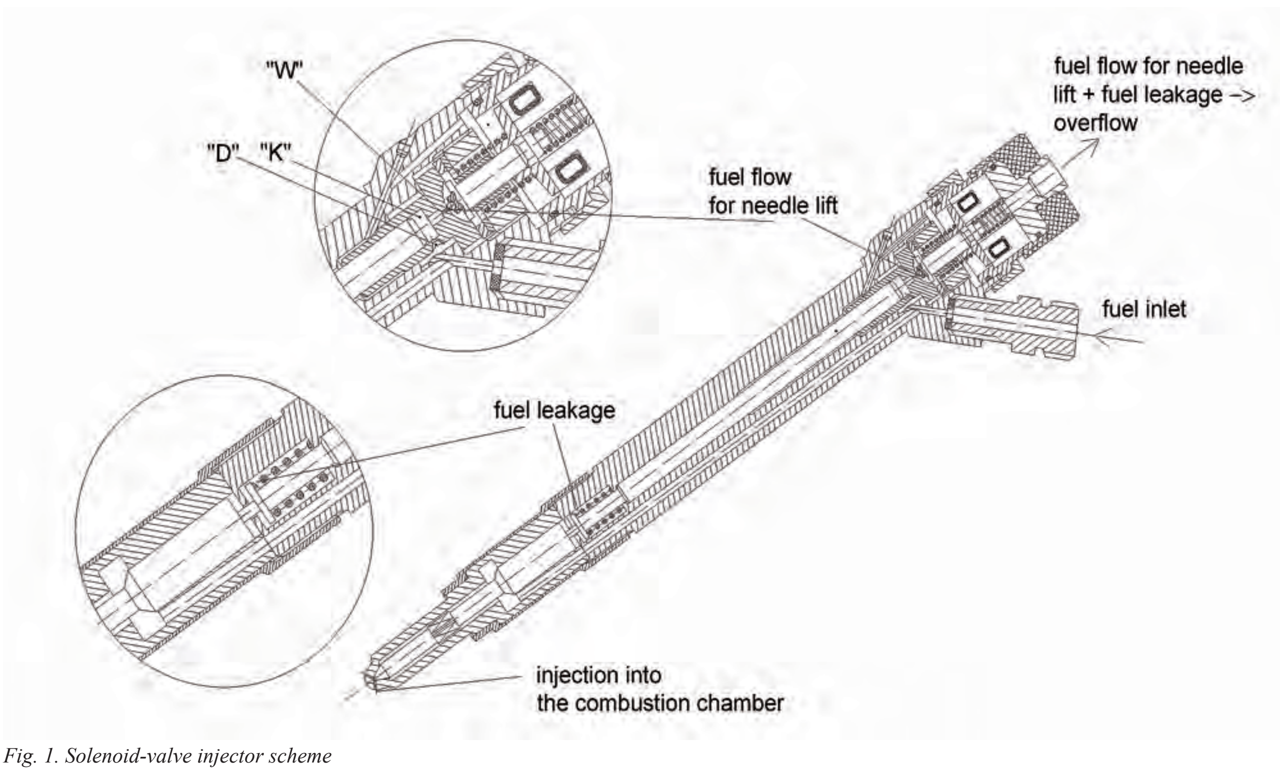

Fig. 1. Solenoid-valve injector scheme

In course of the stand tests, the injection system had operated without pressure stabilization and dosage correction systems.

During the measurements one measured both mass of fuel supplied by individual injectors, as well as masses flowing out through overflow pipes. Graduated cylinders were weighted on electronic scales of the WPE type, produced by Zakład Mechaniki Precyzyjnej RAD-WAG in Radom. Both elementary dose of injected fuel and elementary mass of the overflow were calculated as average value from 250 working cycles of the injectors. Temperature of the fuel was maintained on constant level within range of 40±2°C.

4. Characteristics of dosage and overflow of the injectors

In the first succession, for each one from the injectors of the 1st generation, one measured injected fuel quantities of fuels and (to a separate graduated cylinders) overflows flowing out from overflow pipes. Each time, commencing and termination of the measurement occurred automatically after calculation of preset number of working cycles. There were supplied single injected fuel quantity injections. Results of measurements of the injected fuel quantities, as well as overflows, depending on a preset time of injection and with respect to a single cycle, are presented in the Fig. 2. Making analysis of the presented runs, it can be noticed that elementary dose of the fuel is practically in linear dependence from opening time of control valve of the injector, and grows together with its increase. Such shapes of the characteristics cause, that tested injectors perfectly suit to operation in electronically controlled power units, where control of injected fuel quantity is accomplished through change of opening time of control valve of the injectors and change of injection pressure. Applied values of opening times for the 1st generation injectors effected in fact, that presented fragments of the characteristics result from operation of the needle in non ballistic range of travel, and hence, after reaching maximal lift [1].

Different runs were obtained for the inefficient injector marked as No. 4. Linear characteristics are obtained at the pressure of 990 bar, but after slight growth of the pressure in the rail (up to 1000 bar) one obtains nonlinear characteristics, with significantly changed values.

Values of elementary overflows are growing as well; both together with growth of the opening time and pressure inside the rail, but attained increments of the values are smaller than in case of the injected fuel quantities. In majority of cases, the changes occur in nonlinear way.

Measured values of the overflows in the injector No. 4 (for considered levels of the pressure) are distinctly higher than in case of other injectors. Significant changes are seen even at small changes of the pressure. It is visible especially for the highest pressure, where the differences reach nearly 100 %.

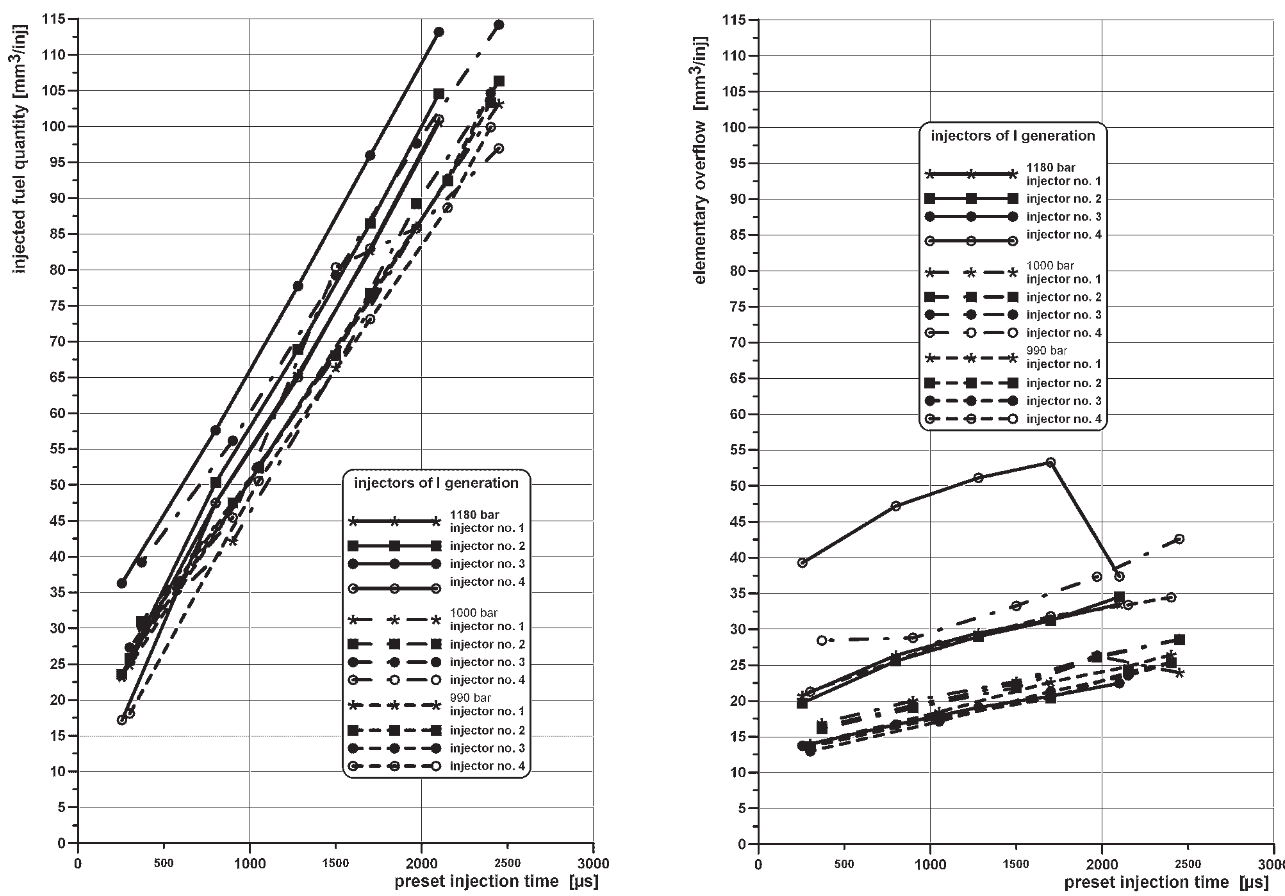

Fig. 2. Injected fuel quantities and overflows of the 1st generation injectors at different injection pressures

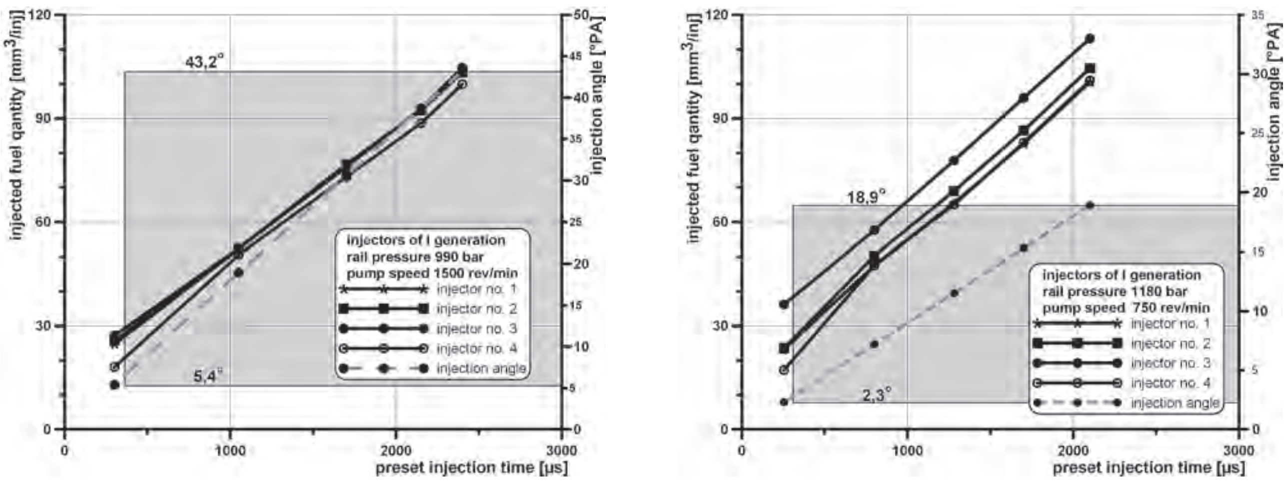

Fig. 3. Injected fuel quantities and injection angles versus preset injection time for a different injectors of the 1st generation

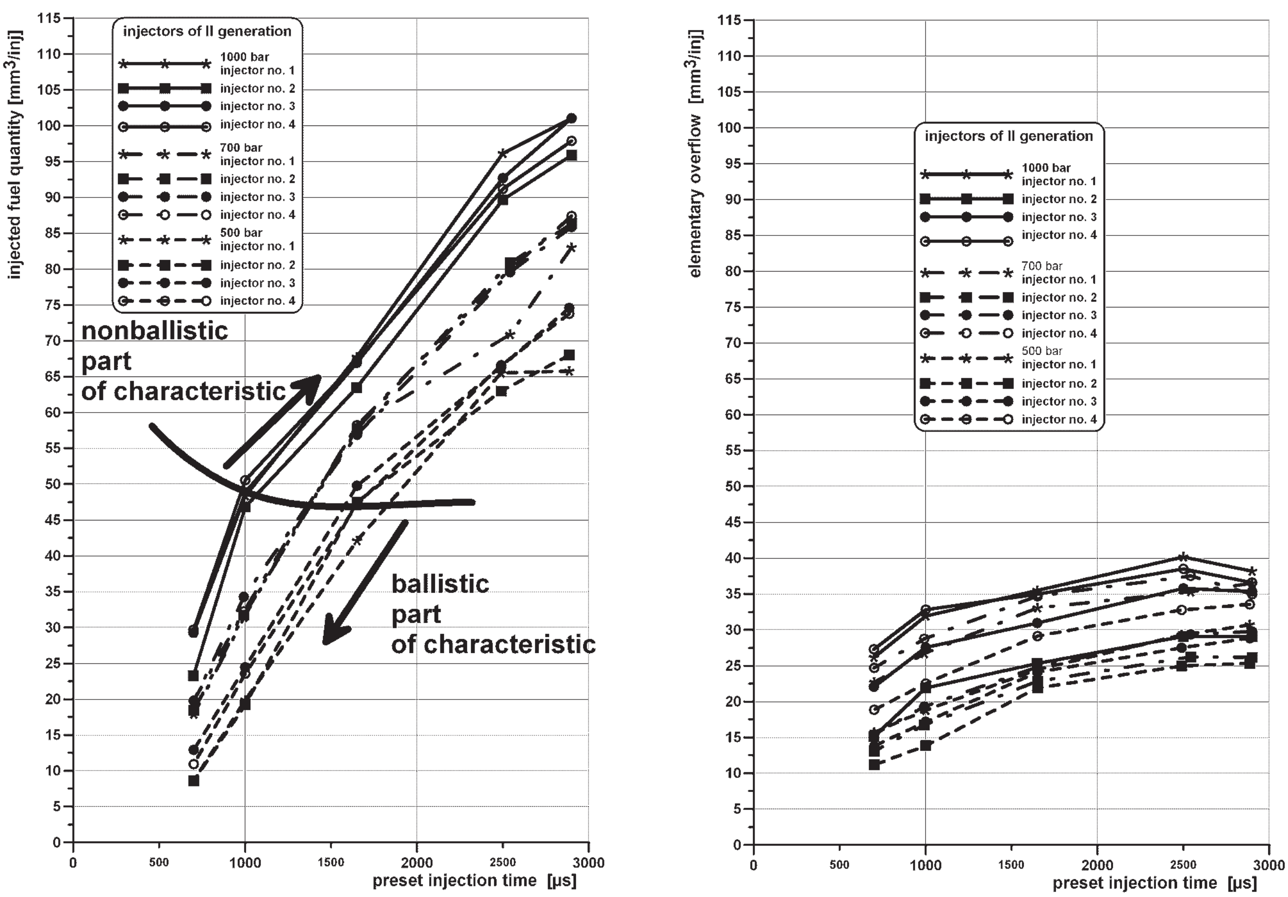

Fig. 4. Injected fuel quantities and overflows versus total preset injection time for different injectors of the 2nd generation

As mentioned earlier, one from advantages of accumulator type injection system is possibility of shaping of engine operation parameters through change of injection parameters. Exemplary characteristics of the 1st generation injectors, drawn for various fuel pressure in the rail (990 and 1180 bar) and for two rotating speeds of high pressure pump (1500 and 750 rpm) are presented in the Fig. 3. In the diagrams are additionally plotted, with dotted lines and grey color rectangles, the ranges of variability of injection angle. The angles were recalculated into crankshaft rotation degrees of a hypothetical engine. The measurements were performed in such way to have similar sizes of fuel dose at different operational parameters of the system. It is seen that is possible to supply the same size of the dose at different parameters of injection. It is possible, at relatively small injection angle (2,3 ÷ 18,9°; Fig. 3, RH side part), to set a higher pressure of the injection to obtain a better atomization, i.e. supply to cylinder in short time a bigger quantity of energy. Hence, it is possible to use also a lower pressures of the injection, but the angles attained shall be bigger (5,4 ÷ 43,2°; Fig. 3, LH side part), however, in such case fuel supply shall be distributed for more degree of crankshaft rotations angle. Fact if high values of the injection angle shall be utilized by engine designers remains the open issue.

There were also performed measurements of dosing for the 2nd generation injectors. Similarly like earlier, the measurements were made for not split injection dose, and results are presented in the Fig. 4. It can be seen, that change of supplied fuel dose in function of time occurs with various intensity. Total area of the characteristics can be divided into three areas. The first area denotes the most often used at partial engine loads area of ballistic range of injectors operation, up to maximal lift of the needle. This area includes interval from 1000 up to about 1700 µs. The second area, non-ballistic area, when the needle supports on bumper, is characteristic of the times up to 2500 µs and can be used to feeding of engines at high loads or during start-up. The third part characterizes area with opening times longer than 2500 µs. In spite of high values of preset time, there wasn't observed any excessive growth of injector's temperature, the injectors functioned correctly, but as seen from analyses of technical data from service stations, the times from this area are not used in practice.

Boundaries of the areas of the characteristics depend substantially on pressure of the fuel. Transition from ballistic to non-ballistic area of engine operation occurs earlier in case of pressure growth. In the presented example, at the pressure of 1000 bar the needle reaches the bumper as early as for 1000 µs, at lower pressure (500 bar) - for 1650 µs. To have more precise determination of the boundaries, one should perform measurements of dosing for more points.

Group of injectors discussed here is characteristic of lower rate of dose's value growth in function of the opening time than in case of the 1st generation injectors. For the same pressures a smaller values are obtained. It results from fact of smaller cross-section areas of outflow active surfaces in used atomizers.

Similarly like in case of the first group of the injectors, values of elementary overflows are growing together with growth of the opening times, and with growth of pressure within rail. Rates of the growth values are smaller than in case of doses, and are comparable to the overflows of the first generation injectors. Division of the characteristics into parts, with similar values of the boundaries like in case of the doses, can be seen. Measured values of the overflows are bigger than values obtained for the first generation injectors.

5. Comparison of doses and overflows

To make direct comparison and quantitative assessment of fuel doses and overflows (expressed in mm^3/injection) for the both groups of the injectors, in the Figs. 5 and 6 are shown the both quantities. There were selected only such operating points, in which the injectors operated with rail pressure of 1000 bar. There were set various values of injection duration.

Values of the overflow of the 1st generation injectors (injectors No.1, 2, 3) grow together with growth of injected dose and all are included within range of 16,1 mm^3/injection in case of the shortest time, to 28,6 mm^3/injection in case of the longest time. In the analyzed range of injectors operation, the overflows

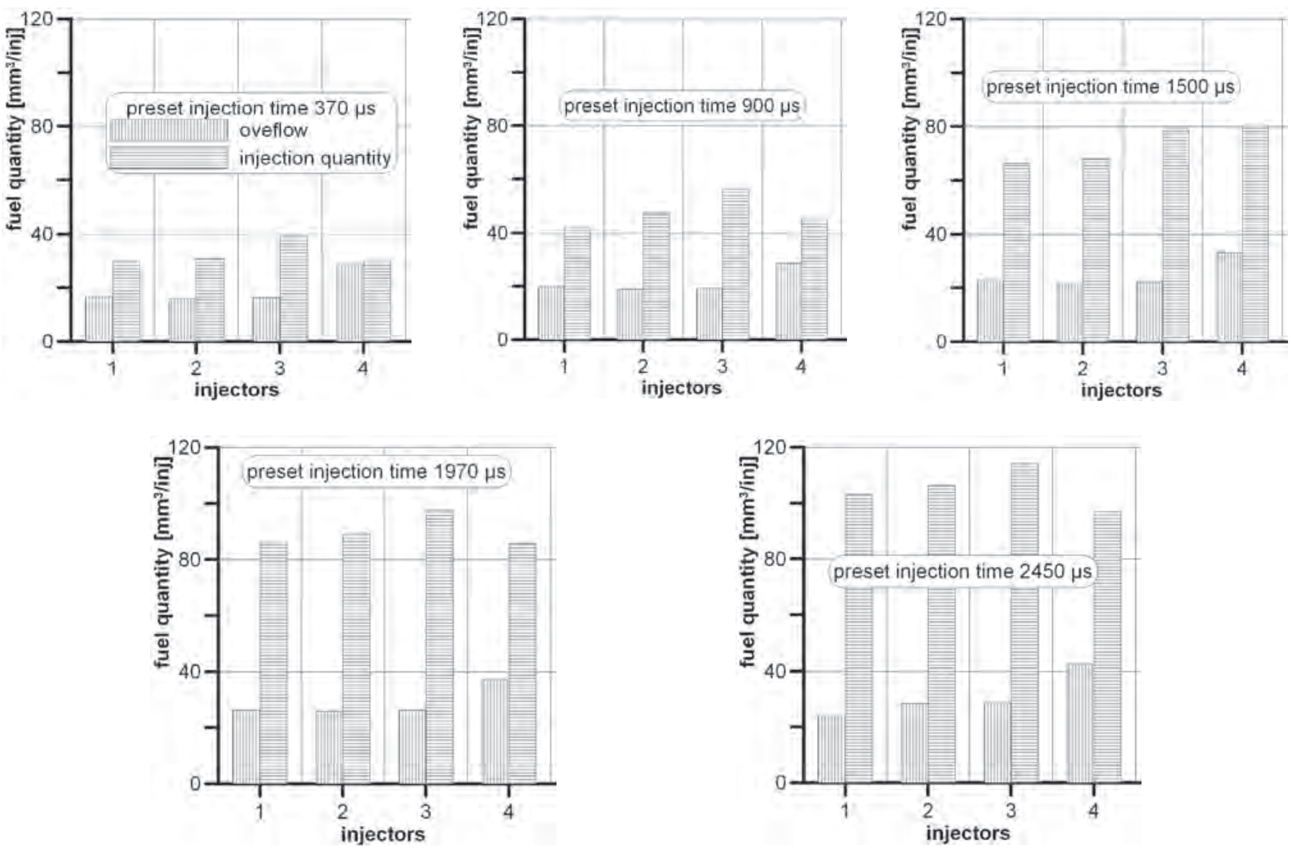

Fig. 5. Comparison of injected fuel quantities and overflows for injectors of the 1st generation

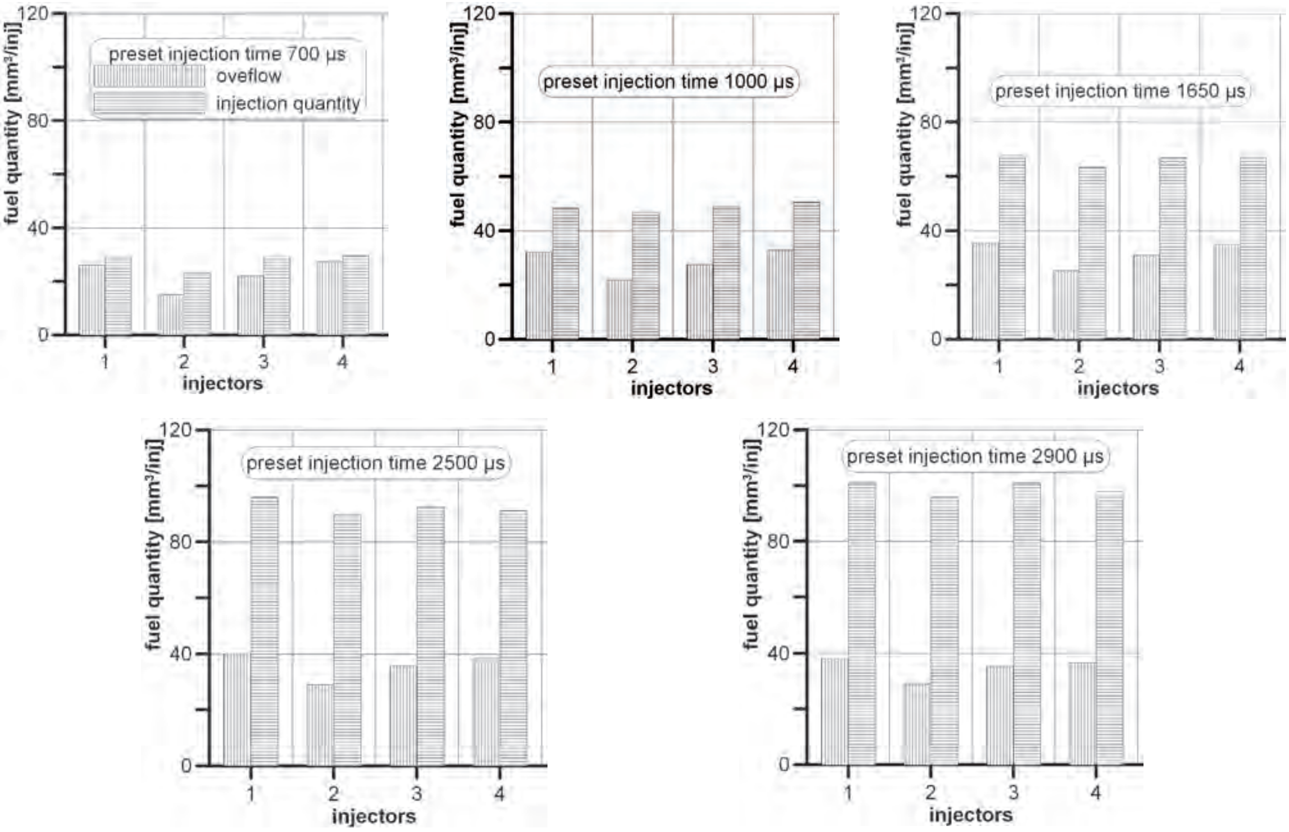

Fig. 6. Comparison of injected fuel quantities and overflows versus for injectors of the 2nd generation

increase with about 77 %. Very good compatibility of values for these three injectors attracts our attention here – their runs practically coincide. Anyhow, for inefficient injector No. 4 they are maintained on a higher level (28,4÷42,6 mm^3/injection, growth with 50 %).

The overflows in the 2nd generation injectors reach values from 11,1÷40,4 mm^3/injection (growth with 260%). Big divergences in the values are present, reaching even up to 30 %. At similar level of dosing, injectors of the 2nd generation are characteristic of bigger values of the overflow.

This short analysis enables to ascertain, that for short opening times, especially for injectors of the 2nd generation, volumes of the overflow are comparable with volumes of supplied doses. It proves about relatively big amount of energy which needs to be used in such case to accomplish injection of the fuel. Increase of the overflow values occurs more slowly than increase of the doses, and therefore share of energy needed to injectors' operation decreases together with growth of injection time.

The above considerations caused, that for the both groups of the injectors, based on the same measurement points, one performed analysis of percentage share of the overflow in the

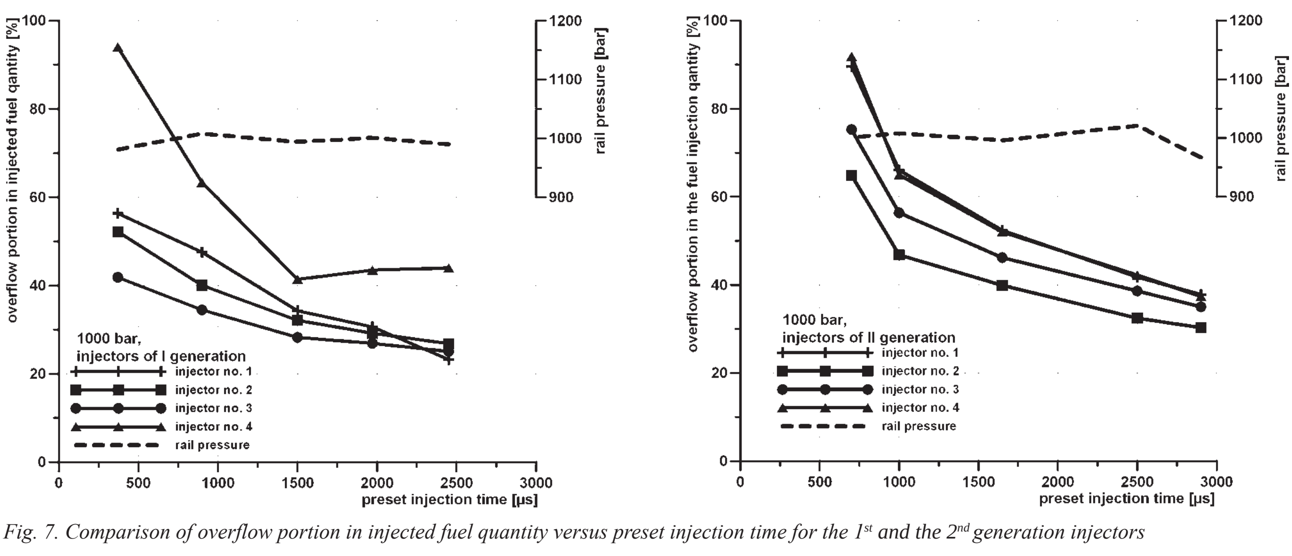

Fig. 7. Comparison of overflow portion in injected fuel quantity versus preset injection time for the 1st and the 2nd generation injectors

dose. The share was evaluated in each point as a quotient of the overflow and supplied dose of fuel. Results, in function of the opening time, are presented in the Fig. 7. Additionally, in the diagrams are shown values of fuel pressure in the rail, prevailing during the injection.

For the first three injectors of the 1st generation, share of the overflow in the dose decreases together with growth of their opening time, while for the forth injector the share initially decreases from 94% at 370 µs to 42% at 1500 µs, and next grows to 44% at 2450 µs. Among three other injectors, the biggest decrease occurs successively: for the first one (with 33%) from 56% to 23%, for the second one (with 25%) from 52% at 370 µs to 27% at 2450 µs and the smallest decrease for the third injector which amounted to 16% (from 41% at 370 µs to 25% at 2450 µs). It has been acknowledged, that pressure change in the rail didn't have any important effect on results of the analysis.

In turn, for injectors of the 2nd generation, two curves showing values of share of the overflow for the injectors No. 1 and No. 4 slightly differ from each other. At the beginning (for 700 µs) their values amount to: 90% for the injector No. 1 and 92% for the injector No. 4, while for the longest opening times (2900 µs) value of the share for the both injectors amounts to 37%. For these injectors, change of overflow's share in the dose for complete analyzed range of changes of opening time amounts to 51% and 53% respectively. Other two curves differ from each other with values in each point of the opening time, from 10% at 700 µs to 6% at 2900 µs, whereas changes of overflow's share in the dose occurs from 75% to 36% for the third injector, and from 65% to 30% for the injector No. 2. Effect of pressure changes seems to be not significant.

In complete range of analyzed opening times, share of the overflow in the dose of the 2nd generation injectors is bigger than for the 1st generation injectors, obviously except inefficient injector No.4. For small dosages, it reaches even 90 %. Intensity of the changes for the 2nd generation is meaningful, especially in case of injectors No, 1 and 4 (from 90 % to 36 %). Values presented here can prove about striving of design engineers after obtainment of short actuation times in the 2nd generation injectors, through induction of a bigger fuel stream (comparing with the 1st generation), resulting in lifting of the needle. At the same pressure, quantity of fuel needed to lift the needle is approximately constant, and hence, strongly reducing share of the overflow when the dose is growing.

It is interesting to compare runs of overflow shares for the 2nd generation injectors with run plotted for inefficient, forth injector of the 1st generation. Values and intensity of changes are similar. Hence reservation, that it should be taken a special care during possible usage of the above mentioned runs to assessment of technical conditions of the injectors. To make the assessment, it is necessary to know reference runs, performed for a given type of correctly functioning injectors.

6. The efficiency index of injectors and differences in elementary overflows

Considerable share of the overflows in the dose was the reason for which the author has introduced conventional concept of injector's efficiency index. The matter here is to assess what is a share of fuel injected to the cylinder in total amount of the fuel supplied to the injector, and what is a share of decompressed fuel which is directed back to fuel tank. The index was defined as quotient of elementary dose of fuel and sum of elementary overflow and dose. Results are summarized in the Fig. 8. For the both groups of the injectors, values of the index are growing together with growth of the opening time, i.e. – for the sake of constant pressure – together with growth of the dose. Three efficient injectors of the 1st generation, in relation to the 2nd generation injectors, in complete analyzed range of their operation reach higher values of the index. The highest ones were recorded for the injector No. 3, for which the index changed from 70 to 80 %. The fourth injector, i.e. inefficient one, reaches values from 52 % for a shorter, to 72 % for a longer opening time. These are values comparable to or even little bit higher than in the injectors of the 2nd generation, for which, especially at short opening times, one obtains values from 52 to 60 % only.

The runs presented here confirm previous observations about bigger fuel streams used to actuate the 2nd generation injectors. It is seen, that in situation of short opening times, in some cases even half of fuel supplied to injectors under high

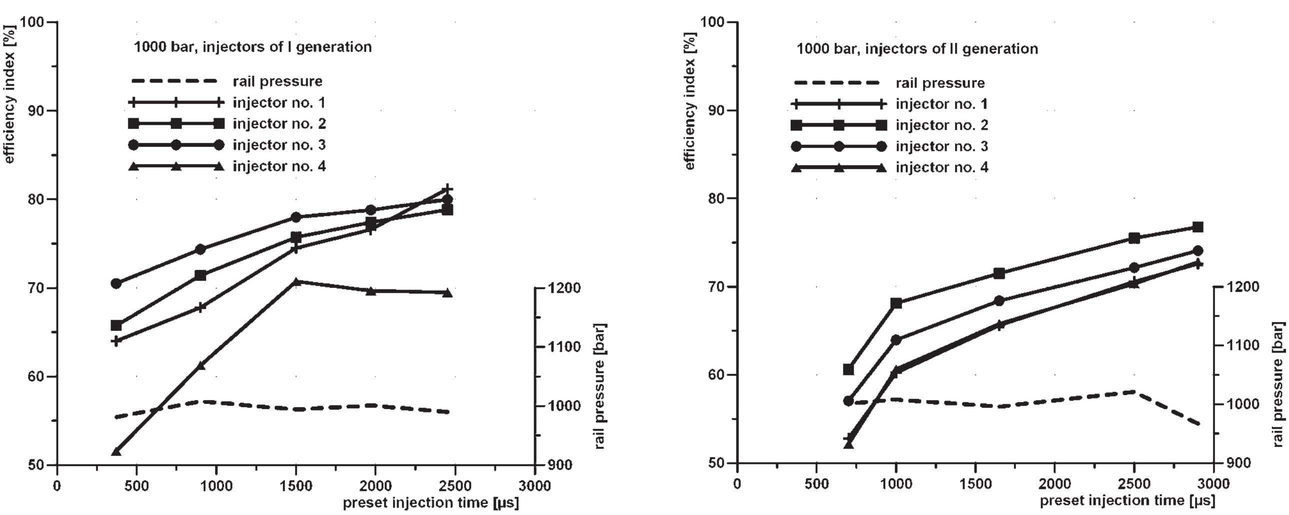

Fig. 8. Comparison of efficiency index versus preset injection time for the 1st and the 2nd generation injectors

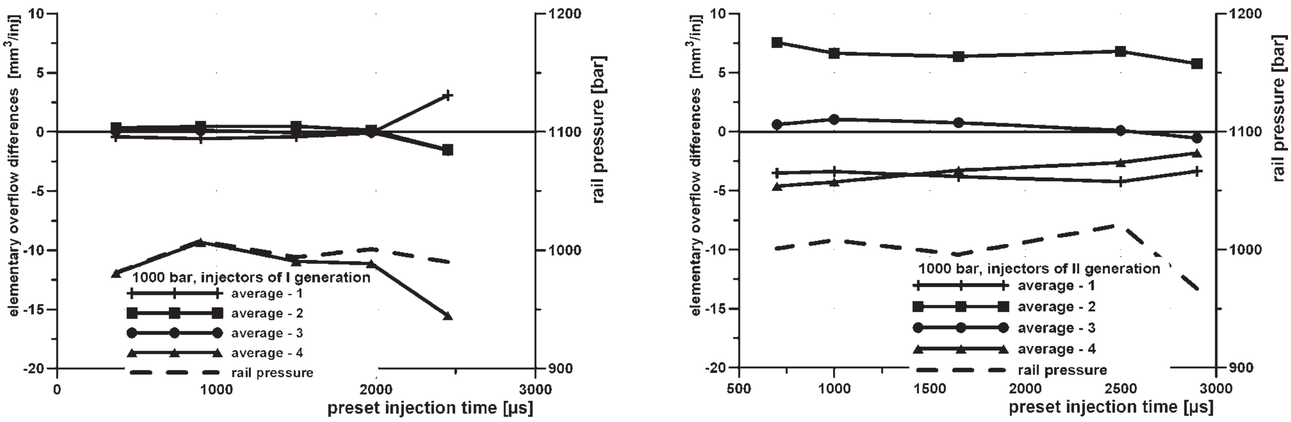

Fig. 9. Comparison of elementary overflow differences versus preset injection time for the 1st and the 2nd generation injectors

pressure is returned to fuel tank. In consequence, part of energy supplied to the fuel in order to increase pressure becomes lost, what obviously reduces efficiency of the injection system.

In course of further analysis, for the both generations, and depending on the opening time of the injectors, one evaluated absolute differences (Fig. 9) and percentage differences (Fig. 10) of elementary overflows. As a benchmark values, separately for each group of the injectors, one assumed average values of the overflows calculated for each from opening times of the injector. Only correctly functioning injectors were taken into consideration. Hence, individual solid lines illustrate (for a given time) differences between average value of the overflow of a given injector (Fig. 9) and (in percent) quotients of the differences mentioned above and the average value (Fig.10). In the Figures these values are denominated as „average – 1", average – 2", etc. With dotted lines are drawn pressure runs in the hydraulic rail.

zero value, and simply overlap each other. It proves about very similar parameters of their control streams. Absolute differences do not exceed 1 mm^3/injection, with exception of measurement points with the highest value of preset opening times of the injectors, where they reach value of 3 mm^3/injection. Percentage differences (Fig. 10) do not exceed 3 %, only for the longest time they take values from interval of 5,6 ÷ 11,4 %.

Results for the 2nd generation injectors are slightly different. Immediately is noticeable a bigger scatter of the results, although all are practically linear. For two injectors the differences are bigger; for two others are smaller than the average. Injector No. 2 differs most from the others. Its overflows are the smallest, and therefore the biggest departures from the average occur, amounting to about 6 mm^3/injection. Relative percentage differences take higher values: injectors No. 2 and 3, with smaller values of the overflows, differing from the average from 1,5 to 33 %, while the two others, with higher overflows from 2 to 15 %.

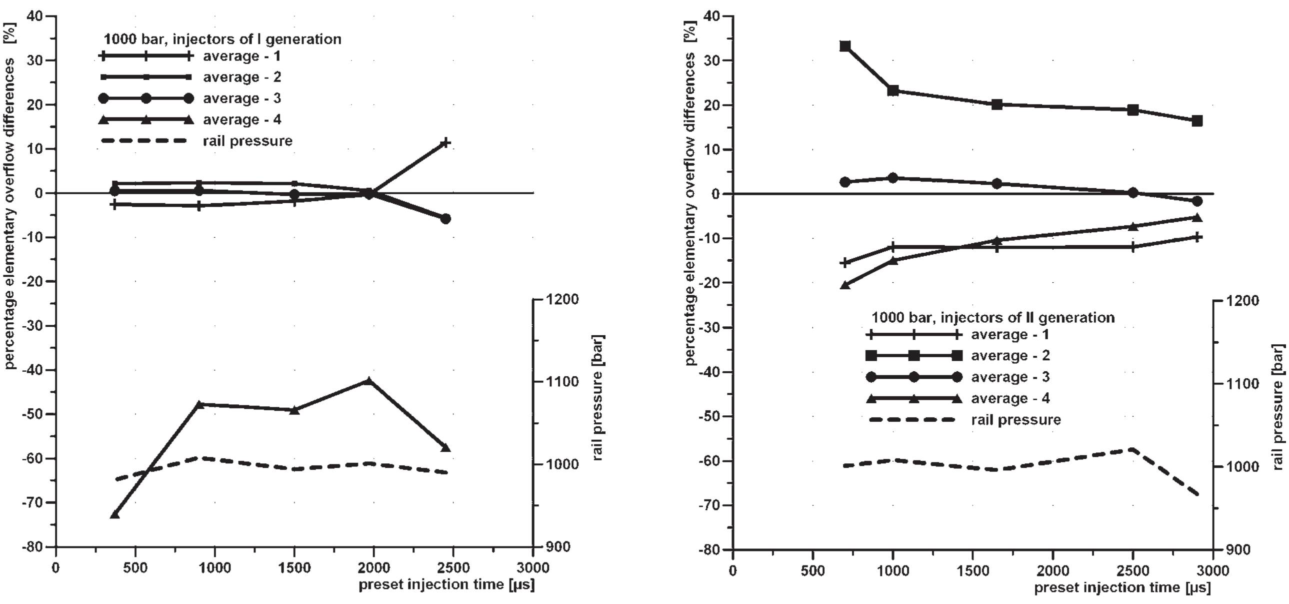

Fig. 10. Comparison of percentage elementary overflow differences versus preset injection time for the 1st and the 2nd generation injectors

Making analysis of results obtained for the 1st generation injectors is possible to be noticed (Fig. 9) that runs of three correctly functioning injectors are similar, and oscillate around

On base of the presented analyses it is possible to ascertain, that the most suitable is assessment and comparison of the overflows based on relative percentage differences. Quantitative ap-

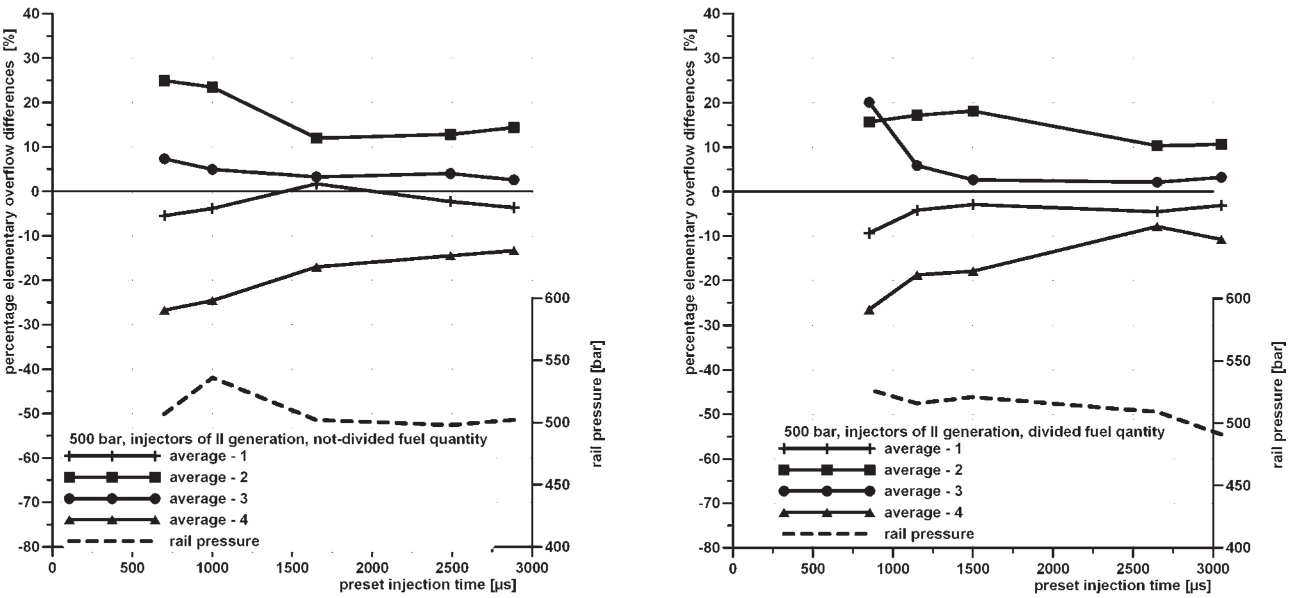

Fig. 11. Comparison of percentage elementary overflow differences versus total preset injection time for not-divided and divided injected fuel quantity (2nd generation injectors)

proach only, as well as approach based on simple differences is not sufficient. It is the best seen on example of the 2nd generation injectors, where evaluation of relative differences revealed comparatively big discrepancies of the analyzed values.

Using the runs presented in the Fig. 11, one endeavored to assess an effect of fuel supply method on size of differences in the elementary overflows. To do it, in the first succession one made measurements of not divided dose, result of such measurements are presented in the LH side of the Fig. 11. Next, previously preset injection times were divided into two equal parts, separated with dwell of 150 µs. Results of these measurements are shown on the RH side of the Fig. 11. During this stage injectors of the 2nd generation were used. Values observed in the both diagrams slightly change with respect to each other. Such small differences can result from adoption of relatively small value of the dwell, what resulted in situation in which the needle was permanently lifted. Due to it, significant change of the overflow value was not possible. It seems that changes of the pressure do not have any effect on runs of the differences.

In both groups of the measurements is possible to notice a bigger values of differences for smaller values of the times, and smaller for bigger time. Probably, it results from more stable, at long opening times of the injector, behavior of the needle during injection.

In the face of confirmed significant differences in overflow values of the injector No. 4, comparing with the injectors of the 1st generation, it has been decided to take attempt to evaluate a reasons of their presence. The overflows, except fuel used to actuation of the injectors, consist also of leaks, and therefore, such leaks needed to be evaluated for the analyzed group of the injectors. For the conventional injectors, evaluation of the leaks between pressure faces is the most commonly performed with use of pressure drop in time method. In case of the injectors from Common Rail system, more accurate and more convenient seems to be the method of direct measurement, implemented in the present work and performed with use of complete injection system incorporated in the test stand. Prior start of measurement of the leaks, one disconnected electric cables supplying control signal to solenoid valve of the injectors. Owing to it, control valve remained closed and fuel flow across control chamber was not possible; and the fuel flowing out through overflow pipes came from leaks only. The leaks were collected into graduated cylinder. Simultaneously, one measured number of potential cycles of injection system operation. Size of measured leaks is presented in the same way as in case of the doses and the overflows, in reference to a single operational cycle.

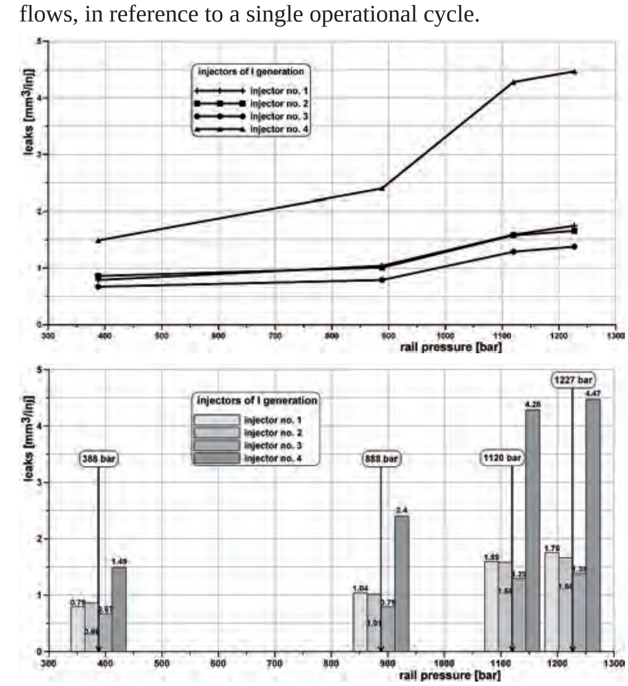

Fig. 12. The 1st generation injectors leakages versus rail pressure

In rail were maintained pressures possibly the most similar to the pressures used in the measuring points selected earlier. It had created some problems, because pressure in the rail after disconnection of the injectors was very unstable, and its stabilization and maintenance during measurements on the assumed level had required many attempts. Various values of the pressure were obtained via change of rotational speed and output capacity of high pressure pump.

In the Fig. 12, in function of pressure inside the rail, are presented leaks in tested injectors of the 1st generation. In the linear diagram is distinctly seen, that the values for injectors No. 1 and 2 are very similar, and are changing from 0,8 mm^3/injection to1,8 mm^3/injection. Injector No. 3, in complete range of pressure change, is typical of smaller leaks, which amount from 0,7 mm^3/injection at 388 bar to 1,4 mm^3/injection for 1227 bar. Whereas, for the injector No. 4, values of the overflow are changing from 1,5 mm^3 to less than 4,5 mm^3, and thus the increments and generated values are much more bigger than for the other injectors. To visualize differences in the leaks, the same values are presented in form of bar diagram. It can be seen that as the pressure is growing, size of the leak from injector No. 1, with respect to the injector No.2, is also growing, anyhow the difference between them remains relatively small. Values of the leaks from the fourth injector are three times higher than leaks from the third injector.

It could be seen, that increased leaks from the fourth injector can explain reasons of significant discrepancies in presented earlier runs concerning injectors of the 1st generation. For sure, growth of the leaks resulted in reduction of supplied dose, although it is difficult to ascertain to which extent. However, differences between efficient and inefficient injectors are too big to be explained by the leaks only. A source of the discrepancies could be also not proper operation of control valve of the fourth injector, caused, for instance, by wrong assembly or smaller active flow area of the atomizer.

As already mentioned earlier, development of a proposed diagnostic criterion for the injectors used in hydraulic accumulator systems became one from the main objectives of the present work. Although overflows of the injectors were evaluated earlier, there was also a need to assess what would be an effect of high pressure pump's rotational speed on this quantity. The problem is to find answer to question if tests of the injectors can be performed for any rotational speed of high pressure pump, or not. Obviously, leaks from the injectors, but not from the high pressure pump, are significant in course of these considerations.

Suitable measurements of elementary overflows were performed for injectors of the 1st generation. In the Fig. 13 are shown results of the measurements, being difference between average value for three correctly functioning injectors, and value of the overflow for a given injector. Because it was suspected that rotational speed can have an effect on leaks of the injectors, a special attention was paid on results obtained for the injector No. 4. It was demonstrated earlier, that just in this case the biggest volume of fuel flowed though clearances between flow areas.

In the first succession one performed measurements in conditions conducive to high values of the leaks, i.e. high pressure of fuel and low rotational speed of the pump. Speed of 750 rpm was taken, and for such speed one applied pressure higher than for other speeds, which amounted to 1180 bar (dotted line). There were obtained in such way results, being some kind of re-

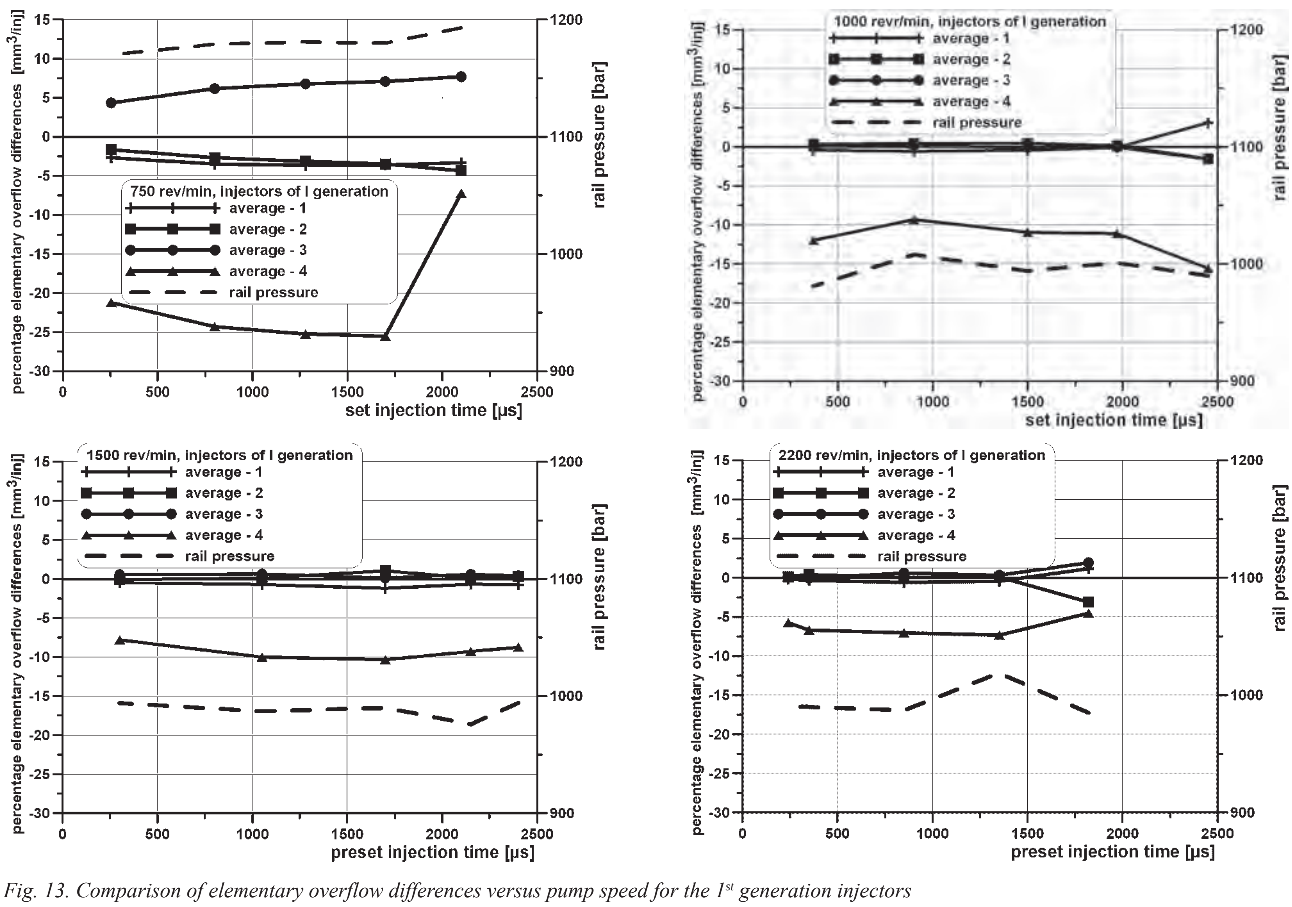

Fig. 13. Comparison of elementary overflow differences versus pump speed for the 1st generation injectors

ference values for the leaks, which can be obtained in the tested injection system. They did not constitute, however, a subject-matter of detailed considerations. Further measurements were carried out for the same values of 1000 bar in the rail (dotted lines), and for more and more high rotational speeds equal to 1000, 1500 and 2200 rpm.

Growth of the rotational speed resulted in reduction in differences of the elementary overflows. When the changes in case of correctly functioning injectors are small, and it can be assumed that they lay within limits of measurement error, while for the injector No. 4 are significant. For this injector, the leaks between pressure faces of precise pairs decrease together with growth of the rotational speed, even with 50 %. Because measurements of the analyzed cases were performed at practically constant and equal pressures of fuel, reasons of this phenomenon should be seen in increased, together with increase of the rotational speed, frequency of injectors operation. The frequency causes that share of time, when movement of the needle occurs and when dynamic caulking of the precise pair is possible, is bigger. From the above is evident, that is not without a meaning, at which rotational speed verification tests should be carried out. Assumption of too high speeds could result in wrong image of injectors condition.

7. Summary

Performed comparative analysis of the injectors of two generations enables their assessment from possibility of usage in Diesel engine point of view. In the Table 1, for the both groups of the injectors, are listed maximal and minimal values of analyzed quantities. Limit values in parentheses, written in grey color fields, concern damaged injector of the 1st generation.

Based on the performed comparative analysis and list of values of individual quantities one has formulated the final remarks. Boundaries of injectors' characteristics area depend on fuel pressure. Transition from ballistic to non ballistic area of the operation occurs earlier when a higher pressure prevails in the rail.

Taking into consideration analyzed range of the 1st generation injectors operation, it is seen, that for this group of the injectors dependence of injection dose for preset time of the opening becomes linear, practically in whole analyzed range. It enables precise batching of fuel doses, what is important when multipoint injection is used. Also it is possible to use compensation algorithms for small doses, necessary due to wear of the system during its operation [5].

Run of the analyzed characteristics of the 2nd generation injectors are partially linear, what can prove about not-complete opening of the needle on initial fragments of the characteristics. Values of elementary overflows increase both with growth of the opening time and growth of pressure in the rail. Intensity of overflow's growth is smaller in case of the doses. Measured values of the overflows are different for the both generations. The bigger ones were measured for injectors of the 2nd generation. For this group of the injectors, they grow more rapidly together with increase of opening time of the injector.

Together with growth of the dose, share of the overflow in the dose decreases. Share of the overflow in doses of the 2nd generation injectors is bigger than for injectors of the 1st generation. For small doses it reaches even 90 %. Rate of change of the shares for the 2nd generation is also considerable. Higher values of the overflow can prove about pursuit after shorter times of the needle lifting for the injectors of the 2nd generation.

At the same constant pressure, quantity of fuel necessary to lift the needle is approximately constant, and hence, strongly decreasing share of the overflow when the dose increases. Based on the mentioned above runs, one can make assessment of technical conditions of the injectors, while it is very important to know the reference runs, made at least for a few dozens of correctly functioning injectors of the same type. It can happen however, that measurement results for efficient and inefficient components are similar, like already happened in case of injectors of the 2nd generation and injector No. 4 from the 1st generation.

For the both groups, when pressure values are constant, the efficiency index increases together with growth of the opening time. In complete analyzed range, injectors of the 1st generation feature higher values of the efficiency index than injectors from the second group. It results from smaller volumes of fuel used to activation of the injectors.

When the opening times are shorter, nearly half of fuel supplied to the injectors at high pressure is used to activation of the injectors. Maximal value of the efficiency index reached level of 80 %.

Table 1. Summary of compared parameters for both groups of the injectors

quantitative confrontation compared parameters	**1st generation injectors**		**2nd generation injectors**	
	minimal value	**maximal value**	**minimal value**	**maximal value**
overflow [mm^3/inj]	**16,1**	**28,6 (42,6)**	**11,1**	**40,4**
overflow portion in injected fuel quantity [%]	**23,2**	**56,3 (94)**	**30,3**	**91,9**
injectors efficiency index [%]	**64**	**81.2 (70,7)**	**52,1**	**76,8**
elementary overflow differences [mm^3/inj]	**-1,6**	**3,1 (-9,3)**	**-4,6**	**7,5**
percentage elementary overflow differences [%]	**-5,6 (-72,6)**	**11,4**	**-20,5**	**33,3**

Differences between elementary overflows referred to average value can result from manufacturing tolerances of solenoid valves which control operation of the injectors, and hence, different reaction times of the solenoid valves on control pulse.

For injectors of the 1st generation, together with growth of rotational speed of high pressure pump, differences in volumes of the overflows decrease, especially for inefficient injector. It was caused by reducing share of leak in the overflow, which size was similar for all injectors.

None significant effect of division of injection dose on differences in the elementary overflows, referenced to the average value, has been confirmed. It could be result of implemented short time of the dwell.

Fuel leaks, measured for correctly functioning injectors of the 1st generation are changing from 0,67 mm^3/injection at pressure 388 bar to 1,75 mm^3/injection at 1227 bar. In case of inefficient fourth injector, the leaks amounted to: from 1,49 to 4,47 mm^3/injection respectively, and hence they are from 120 to 150 % bigger. Their values depend on pressure of fuel in the rail and rotational speed of high pressure pump. Increase of the rotational speed effects in growth of frequency of injectors operation, what increases share of time when dynamic caulking of this precise pair is possible.

Low values of the leaks (like e.g. in the injector No. 3) result in reduction of the overflows, and the same, improve the efficiency index.

Therefore, in case of any doubts concerning technical conditions of the injectors from Common Rail system, one should perform measurements both of the overflows and the leaks.

On base of the test results and performed analyses, one proposes to adopt the following methodology of proceeding during evaluation of criteria values and assessment of new injectors from Common Rail systems, which are actuated by solenoid valve:

1. Accomplishment of measurements for not divided dose of the injection.
2. Determination of two points for measurement of overflow and leaks – the first point corresponding to engine parameters on idle speed [3], and the second point corresponding to the lowest rotational speed of maximal torque.
3. Evaluation of criteria values of leaks and overflows for a given type of injectors, based on measurement results of representative group of at least 20 injectors.

In practice, based on evaluated criteria values, to perform assessment of injectors already being in use, one proposes the following order of the activities:

1. Accomplishment of measurements for not divided dose of injection.
2. Measurements of the overflow in measuring points; obtained values referred to criteria values should not differ more than 10%.
3. In case of ambiguous measurement results, measurement of the leaks in evaluated operational points.

Bibliography

1. Bosch Robert GmbH. Diesel-Engine Management. Chichester: John Wiley & Sons, 2005.
2. Clever S, Isermann R. Signal- and Process Model-Based Fault Detection and Diagnosis of a Common Rail Injection System. FISITA 2008 World Automotive Congress, VDI/FVT, München, 2008-06-143.
3. Günther H. Common Rail workshop practice: construction, verification, diagnostics. Warszawa: WKiŁ, 2010.
4. Imarisio R, Giardina Papa P, Siracusa M. The New 1.3 L 90 PS Diesel Engine. Combustion Engines 2005; 3: 22-31.
5. Jorach R, Bercher I, Meissonnier G, Milovanovic N. Common-Rail-System von Delphi mit magnetventilen und Einkolben-Hochdruckpumpe. MTZ 2011; 3: 186-191.
6. Leonard R, Parche M, Alvares-Avila C, Krauß J, Rosenau B. Drucübersetztes Common-Rail-System für Nutzfahrzeuge. MTZ 2009; 5: 368-375.
7. Leonhard R, Warga J: Common-Rail-System von Bosch mit 2000 bar Einspritzdruck für Pkw. MTZ 2008; 10: 834-840.
8. Leonhard R, Warga J, Pauer T, Rückle M, Schnell M. Magnetventil-Common-Rail-Injektor mit 1800 bar. MTZ 2010; 2: 86-91.
9. Maier R, Projahn U, Krieger K. Anforderungen an Einspritzsysteme fűr Nutzfahrzeug-Dieselmotoren. Teil 1 MTZ 2002; 9: 658-673, Teil 2 MTZ 2002; 10: 856-860.

Tomasz Knefel, DSc, Eng.,
Department of Internal Combustion Engines and Vehicles
Technical University of Bielsko-Biała
2 Willowa str., 43-309 Bielsko-Biała, Poland
phone 33 / 82 79 332, fax. 33 / 82 79 351
e-mail: knefel@ath.bielsko.pl

Article citation info:
RUSIŃSKI E, CZMOCHOWSKI J, PIETRUSIAK D. Problems of steel construction modal models identification. Eksploatacja i Niezawodnosc – Maintenance and Reliability 2012; 14 (1): 54–61.

Eugeniusz RUSIŃSKI
Jerzy CZMOCHOWSKI
Damian PIETRUSIAK

PROBLEMS OF STEEL CONSTRUCTION MODAL MODELS IDENTIFICATION

PROBLEMY IDENTYFIKACJI MODELI MODALNYCH STALOWYCH USTROJÓW NOŚNYCH*

Complex identification of steel construction modal models requires simultaneous numerical and experimental analysis of the object. Such an approach allows to obtain more accurate results while the methods complement each other. Results presented, concern stacker feeding bridge which operates in open pit mine. Operational modal analysis was made. Application of this method enables to assess influence of working condition on the modal characteristic. Experimental results were validated with use of numerical method.

Keywords: *modal analysis, steel construction, finite element method.*

Kompleksowa identyfikacja modeli modalnych stalowych ustrojów nośnych, wymaga ujęcia zarówno eksperymentalnego jak i numerycznego. Obie metody stanowią wzajemne uzupełnienie i umożliwiają dokładniejszą identyfikację. Przedstawione wyniki badań dotyczą mostu podającego zwałowarki działającej w kopalni węgla brunatnego. Przeprowadzono eksploatacyjną analizę modalną. Zastosowanie tej właśnie metody badawczej, uwzględnia wpływ warunków działania i obciążenia obiektu. Wyniki uzyskane w ten sposób zestawiono z eksperymentem numerycznym.

Słowa kluczowe: *analiza modalna, konstrukcje stalowe, metoda elementów skończonych.*

1. Introduction

Modal models identification, especially of large size objects, is a many stage, complex process. Numerical solution of eigenproblem clearly defines frequencies and deflection shapes of the system. However, taken simplifications of the numerical model can influence on the results and shift frequencies from the real one. Serious problem is the proper representation of operational conditions. On the other hand, modal model identification with experimental method only, may lead to fault mode shape recognition. Application of both methods simultaneously allows to get complex knowledge about the object [1].

Fig. 1. View of the stacker feeding bridge

(*) Tekst artykułu w polskiej wersji językowej dostępny w elektronicznym wydaniu kwartalnika na stronie ***www.ein.org.pl***

Correctly identified dynamic characteristics give significant information for the proper operation. It is especially important in case of load carrying structures of large size machinery. Dimensions of bucket wheel excavators and stackers operating in open pit mines, excess dimensions of common machines. Main source of vibrations are high level and amplitude alternating excavation forces. Additional excitation occurs in drives [18] and conveyors [8] when material moves hitting pulleys and in places of duping of the material to the next conveyors. Technological movements as travel, turning or luffing the boom are also significant vibration sources. Dynamic load of stackers, in comparison to bucket wheel excavators, is not so high, but the structure is more slender and susceptible. As a result, high vibrations amplitudes are likely to occur in presence of not so high forces and its alternations.

Good knowledge of dynamic characteristics is necessary to reduce vibrations of the object. Indirect result of its decrease will be increased durability of the structure while the fatigue will be reduced [2, 12].

Lower vibration amplitudes decrease also the probability of stability loss of the object or its substructures. There are known cases of such a high vibration amplitudes that in the result some parts of the structure were in collision [5]. Thanks to the proper identification of modal model, modification of the construction was possible in purpose to eliminate the unfavorable effect.

Moreover, mechanical vibrations have negative influence on human being. Permissible acceleration values states in the standards [10, 11]. It is possible that, in some extreme cases, certain human organs can be in the resonance [3].

Results of experimental modal analysis and numerical modal analysis of the ZGOT 12500 stacker feeding bridge (fig. 1) are presented.

Total mass of the bridge with the conveyor equals around 310 Mg. Important fact is the possibility to move the lower support. Thanks to it, the extent can change from 69.2 m to 75.8 m.

2. Modal analysis

2.1. Experimental and operational modal analysis

The classic method of dynamic characteristics identification is experimental modal analysis. To perform such a test there is a need to excite the object with impulse of known force or a harmonic signal of known force and frequency. To apply required input, modal hammers or modal shakers are in common use [17]. This approach allow to determine impulse transient

$$h(t) = \sum_{r=1}^{N} (Q_r \Psi_r \Psi_r^T e^{\lambda_r t} + Q_r^* \Psi_r^* \Psi_r^T e^{\lambda_r^* t}) \quad (1)$$

function (1) where Qr a scale factor, Ψr is a modal vector, λ is a pole of the system, *t* is time.

Most popular methods of modal parameters estimation in time domain, is solving of the eigenproblem with use of numerical methods (Eigensystem Realization Algorithm) and method using exponential decaying harmonic functions (Least Square Complex Exponential) [17].

Implementation of experimental modal analysis for large object investigation can be problematic. Proper excitation of a bucket wheel excavator or a stacker would require use of a shaker of very big power. Till now, the excitation was performed with force impulse generated by sudden release of a mass hanged-up on a bucket wheel boom [5]. The method is quite troublesome. For the duration of preparation and performing the experiment the machine must be stopped. It is especially unfavorable because of constant need for coal in the power plant. To make field testing, adequate big mass and releasing device must be prepared. The mass must be released in moment when force acting on the bucket wheel boom achieve required level.

The application of operational modal analysis [6, 16], in comparison to experimental modal analysis is much more easier. Thanks to this method it is possible to estimate modal parameters on the basis of output data only. As a result, field testing is limited to the accelerometers location and data acquisition. Stop of the machine is not required. Since the excitation is not known, the input must be substituted by correlation function (2), where *x* and *y* signals measured in different points.

$$R_{xy}(\tau) = \int_{-\infty}^{+\infty} x(t) y^*(t-\tau) dt \quad (2)$$

For the modal parameters estimation, already mentioned Least Square Complex Exponential algorithm, Balanced Realization algorithm (method formulated in the stochastic space and, basis on the equation of state) or Canonical Variate Analysis algorithm (method very similar to the Balanced Realization) [16, 17] are used.

Data acquired in this way cover also the real operational and load condition. The dynamic characteristics of bucket wheel excavator can change with the changing position of bucket wheel boom or load carrying structure. Operational modal analysis allows to determine modal parameters of the machine in different configurations.

2.2. Numerical modal analysis

In numerical modal analysis, eigenproblem stated with equation (3) where „K" is stiffness matrix and „M" is inertia matrix, is solved.

$$(K - \lambda M)\psi = 0 \quad (3)$$

Solution of equation (3) is possible with use of algorithms i.e: Rayleih-Ritz reduction, subspace integration or reverse integration. However, most commonly used is Lanczos algorithm [13, 7]. Its widespread application is due to the fact that it enables to solve large tasks in relatively short time. The complexity of the problem do not influence significantly on the steps number required to solve the task.

3. Determination of modes

3.1. Operational modal analysis

Location of the measuring sensors and directions in which accelerations will be measured is very important.

Sensors were placed in 9 points on the stacker feeding bridge structure. Acquisition were made simultaneously on the 12 channels. Points and directions were selected in such a way to enable proper interpretation of maximum number of modal deflection shapes [5, 9, 4, 14, 15]. Location of points do

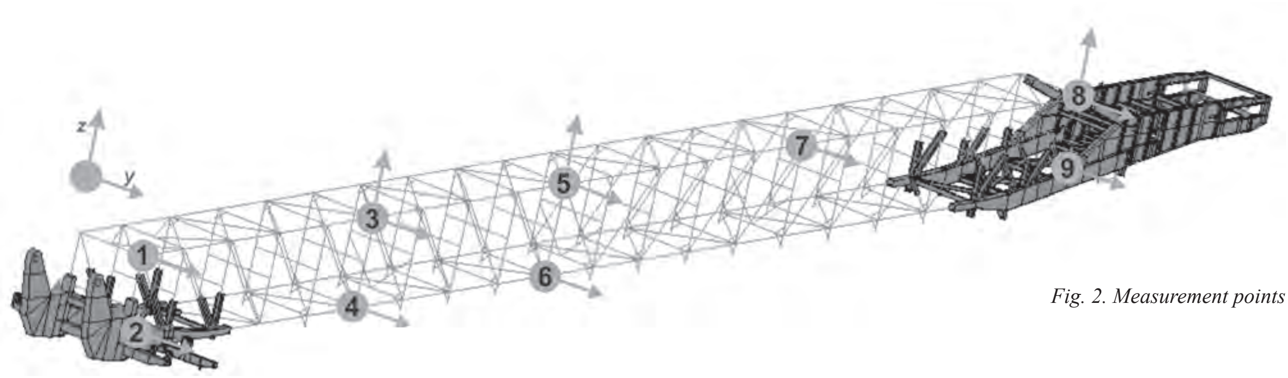

Fig. 2. Measurement points

Table 1. Measurement points description

Channel	Measurement point	Vertical member	Direction
1	1	1/21	y
2	2		y
3	3	6/21	y
4			z
5	4		y
6	5	10/21	y
7			z
8	6		y
9	7	15/21	y
10	8	21/21	y
11			z
12	9		y

not corresponds exactly to the ½ and ¼ bridge length in which mode nodes are possible to observe. Precise description of measurement points is stated in table 1. Vertical members of the bridge, in figure 2, are numbered from left to the right. The "z" direction coincides with the normal vector of the plane created by the bridge structure. The "y" direction is transverse to the bridge structure. Data were acquired during simultaneous travel of the stacker and adjustable support to keep the bridge extent constant.

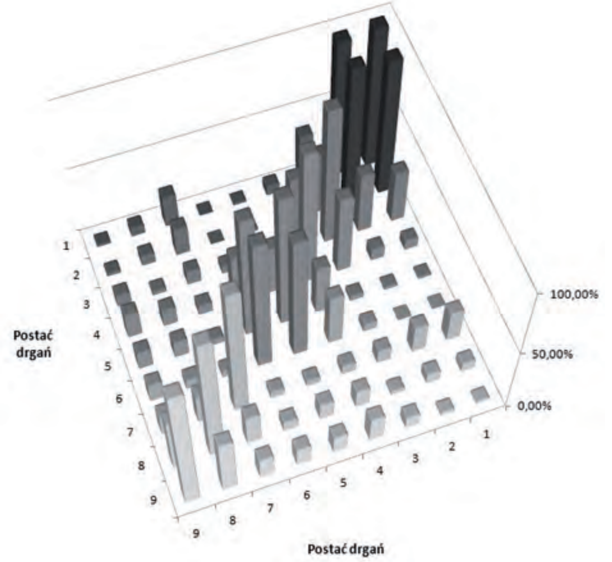

Fig. 3. Auto MAC matrix of modes determined in field testing

Preliminary results analysis allows to distinguish 9 different modal modes. The auto MAC (Modal Assurance Criterion) factor [17] points out a strong correlation between 1st and 2nd and between 5th and 6th mode. Those modes describes the same pole and their presence could be i.e. the method error. Graphical representation of auto MAC factor is presented in figure 3. Red and orange color corresponds adequately to the 1st, 2nd and 5th, 6th correlated modes. In all modes, except 4th, high phase scatter is observable. This leads to the conclusion that the excitation vibrations strongly affects on the presented modal deflection shapes. Particular modes defined with operational modal analysis method are presented in the table 2.

3.2. Numerical modal analysis

Numerical modal analysis [14] was performed on the beam-shell model. Application of beam elements reduces size of the model and in consequence the computation time. General stiffness of the frame members is well represented by the beam type elements, but the local stiffness of, for example gusset plates, is neglected. In the table 3, modes determined in the numerical modal analysis are shown.

3.3. Results comparison and analysis

Numerical analysis allows clear and direct determination of natural frequencies and deflection shapes. Model created in this way do not covers the influence of all external environmental and operational factors. This may influence on the results of the analysis.

Interpretation of experimental data is much more complex. Modes frequencies are often smeared over the whole bandwidth. In such case it is difficult to correctly determine particular mode. To define complex normal modes deflection shapes, more sensors is required, but this highly increase costs. In operational method, external factors, that might be omitted in the numerical model, are included. That is the main advantage of this approach. Additionally the whole preparation and measurement process can be done during operation of the machine. Excavation loads can have significant influence on the dynamic characteristic.

Rough data analysis indicates big divergence between numerical and experimental results. The corresponding modes were distinguished after detailed investigation of frequencies and deflection shapes. Certainly, first modes determined in

Table 2. Normal modes determined with operational modal analysis

Mode	Deflection shape
Modes 1 i 2, frequency ~ 0.90Hz	
Mode 3, frequency ~ 1.1Hz	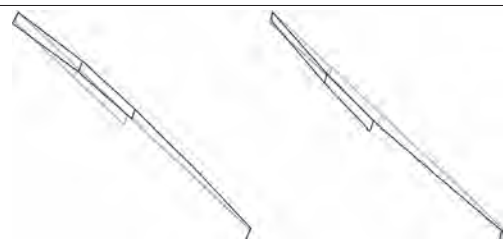
Mode 4, frequency ~ 1.24Hz	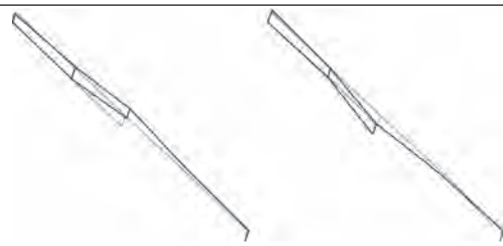
Modes 5 i 6, frequency ~ 1.69Hz	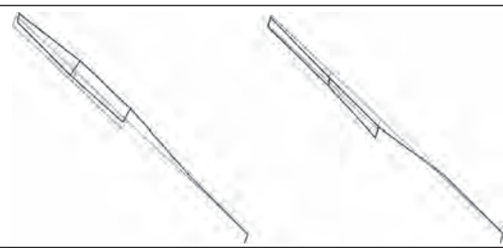
Mode 7, frequency ~ 4.12Hz	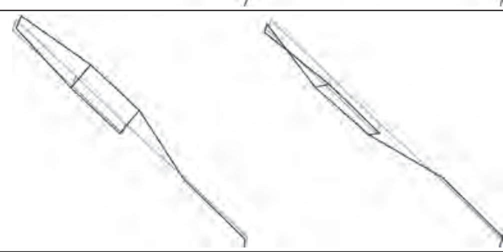
Mode 8, frequency ~ 6.33Hz	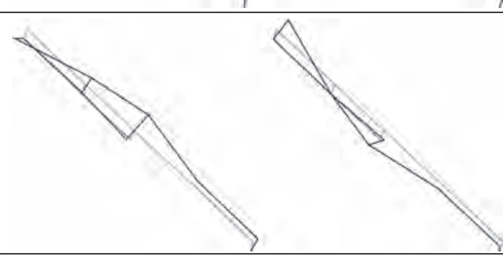
Mode 9, frequency ~ 8.83Hz	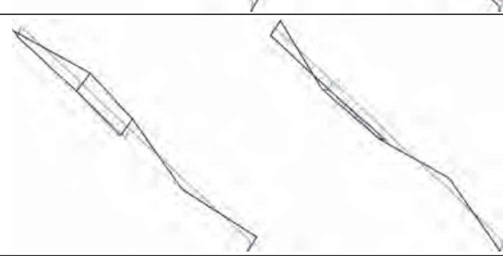

Table 3. Normal modes determined with operational modal analysis

Mode	Deflection shape
Mode 1, frequency – 0.90Hz	
Mode 2, frequency – 1.17Hz	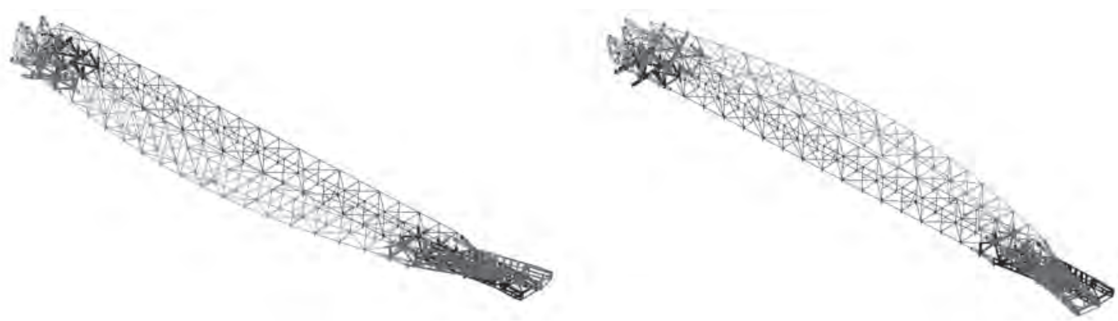
Mode 3, frequency – 1.52Hz	
Mode 4, frequency – 1.60Hz	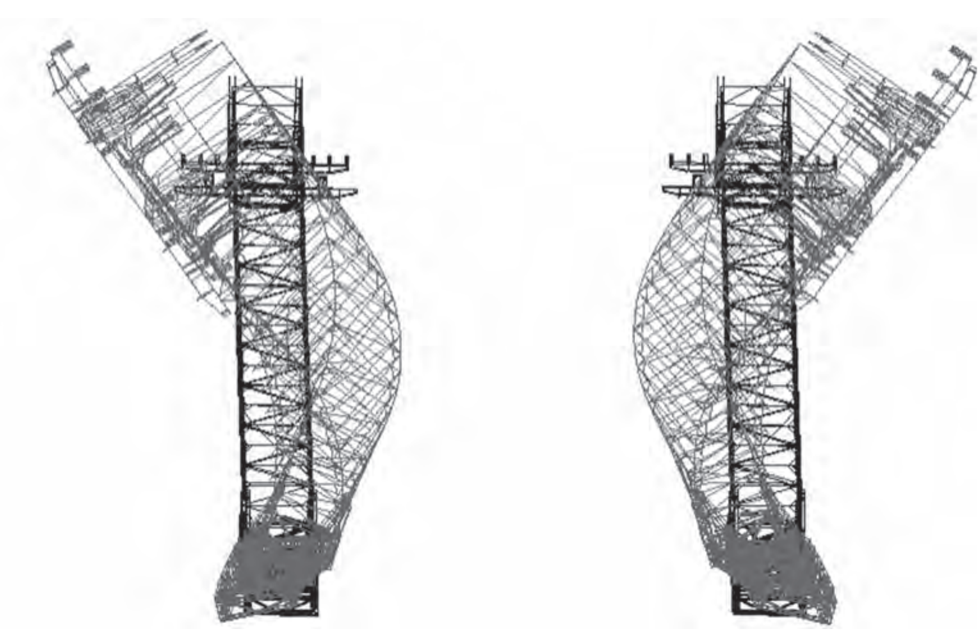

Mode 5, frequency – 3.12Hz	 
Mode 6, frequency – 3.85Hz	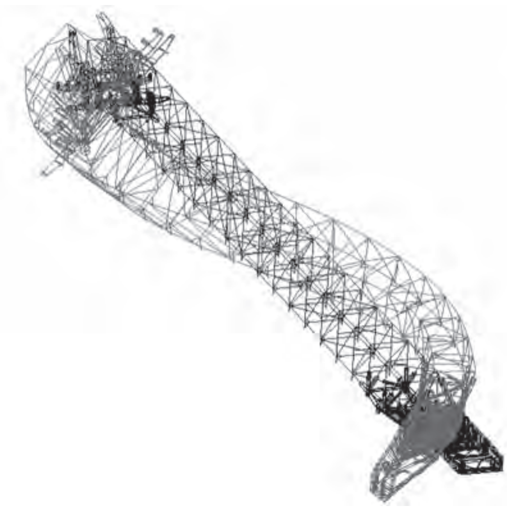 
Mode 7, frequency – 4.29Hz	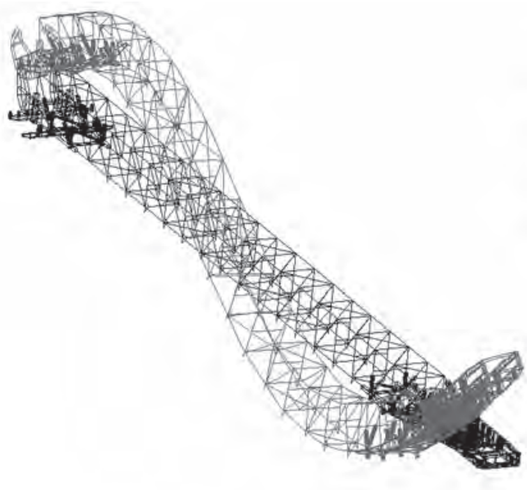 

Mode 8, frequency – 4.56Hz	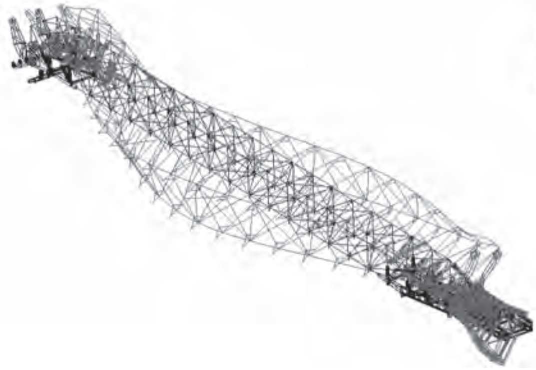 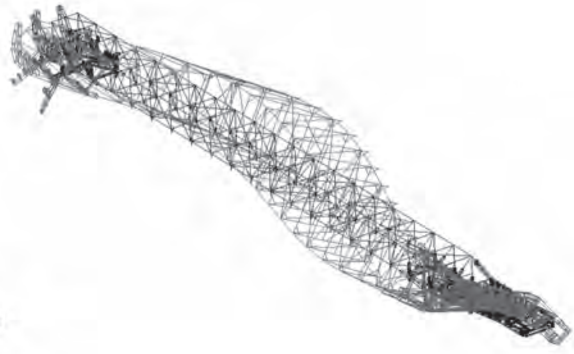
Mode 9, frequency – 5.79Hz	 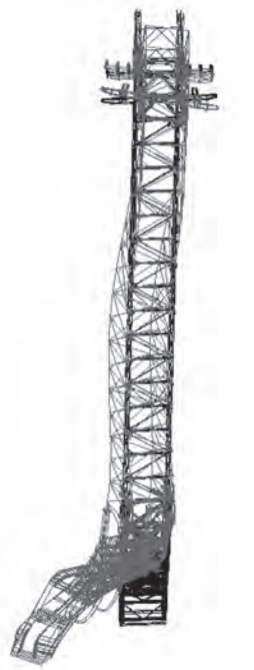

both methods are related. The frequency in field testing and numerical testing is around 0.90 Hz. The deflection shape is bending the structure in transverse direction. Following related modes are 4th field testing mode and 2nd numerical simulation mode. Moreover, 3rd operational mode should be taken under consideration. The frequency of this mode equals to 1.24 Hz and do not extend much form the two already mentioned. Additionally, the deflection shape is also bending in vertical plane. We can suppose that 3rd and 4th operational mode is the same mode but strongly smeared. With this assumption the approximate frequency of the mode will equal around 1.17 Hz. Next related modes are mode 4th of numerical analysis and 5th and 6th mode determined with operational modal analysis method. The deflection shape is bending in the vertical plane and horizontal displacement of one end of the supplying bridge (but only in numerical model). Field testing show only vertical displacement. However there was no measurement point in the horizontal direction. Because of that fact there is no enough data to unequivocally define those modes as correlated. The average frequency for those modes equals around 1.65 Hz.

For the rest of results it is difficult to find related modes. The complexity is much higher and most of the frequencies are different. Eigenvectors of higher modes are not clearly defined. In some cases it is possible to observe some relations i.e.: 4th numerically determined mode and 7th mode determined with operational modal analysis. However, ambiguity of experimental results would cause wrong modes identification.

4. Summary and conclusions

Simultaneous application of numerical and experimental methods is very good approach for identification of modal models of steel constructions. Results obtained in this way complement each other and enable more accurate model identification. Numerical model gives clear information what modal deflection shape can occur. Unfortunately, simplified geometry and assumption made during modeling can have strong influence on the vibration frequencies. For precisely frequency determination the field testing must be performed. Unfortunately, because of the insufficient amount of measurement points, interpretation of mode shapes can be difficult mostly. Numerical model support is very helpful during experimental data interpretation.

This approach in the case of stacker supplying bridge enabled to identify main normal mode frequencies and mode shapes. Nevertheless, significant divergences between numerical and experimental model are observable. With experimental method, clear determination of mode shapes of higher order was not possible. The cause of that is mainly probably location and number of measurement points. This influenced especially on the torsional mode shapes identification. Lack of the torsional modes lead to the conclusion that the travel of the machine do not excite this modes well. To conclude, the most significant modes of the stacker supplying bridge are the basic bending modes. The rest of modes are so unlikely to excite that do not make any danger to the structure.

Acknowledgements: Research co-financed by the European Union within the European Social Fund.

Literature

1. Bosnjak S, Zrnic N, Oguamanam D. On the dynamic modeling of bucket wheel excavators. FME Transaction 2006; 34: 221-226.
2. Bosnjak S, Zrnic N, Simonovic A, Momcilovic D. Failure analysis of the end eye connection of the bucket wheel excavator portal tie-rod support. Engineering Failure Analysis 2009; 16: 740-750.
3. Cempel C. Wibroakustyka stosowana. Warszawa: PWN, 1989.
4. Czmochowski J, Moczko P. Numerical-Experimental Analysis of Bucket Wheel Excavator Body Vibrations. 22nd Danubia-Adria Symposium of Experimental Methods in Solid Mechanics. Extended Abstracts 2005: 294-295.
5. Czmochowski J. Identyfikacja modeli modalnych maszyn urabiających w górnictwie węgla brunatnego. Wrocław: Oficyna Wydawnicza Politechniki Wrocławskiej, 2008.
6. Hermans L, Van der Auweraer H. Modal Testing and Analysis of Structures Under Operational Conditions: Industrial Applications. Mechanical Systems and Signal Processing 1999; 13(2): 193-216.
7. Hughes T. The Finite Element Method. New York: Dover Publications, 2000.
8. Jonak J, Gajewski J. Operating diagnostics and monitoring issues of selected mining belt conveyers. Eksploatacja i Niezadownosc – Maintenance and Reliability 2006; 4: 74-78.
9. Pietrusiak D, Czmochowski J, Kowalczyk M, Lagwa Ł. Określenie właściwości dynamicznych koparki KWK1500 metodą eksploatacyjnej analizy modalnej. Górnictwo Odkrywkowe 2010; 4: 45-50.
10. Eurokod 7. Projektowanie geotechniczne. Część 1. Zasady ogólne. PN-EN 1997-1:2008.
11. Metody pomiarów i oceny drgań maszyn pod względem bezpieczeństwa i higieny pracy. PN-N-01357:1990.
12. Rusinski E, Czmochowski J, Iluk A, Kowalczyk M. An analysis of the causes of a BWE counterweight boom support fracture. Engineering Failure Analysis 2010; 17(1): 179-191.
13. Rusinski E, Czmochowski J, Smolnicki T. Zawansowana Metoda Elementów Skończonych. Wrocław: Oficyna Wydawnicza Politechniki Wrocławskiej, 2000.
14. Rusinski E, Czmochowski J. Die Modalanalyse des Oberbaus eines Baggers vom Typ SchRs-800. Surface Mining, Braunkohle & Other Minerals 2001; 53(3): 319-324.
15. Smolnicki T, Rusinski E, Przybyłek G. Wybrane aspekty dostrajania modeli dyskretnych koparki wielonaczyniowej kołowej. Górnictwo Odkrywkowe 2006;7/8: 146-148.
16. Uhl T, Lisowski W, Kurowski P. In-operational Modal Analysis and Its Applications. Kraków: Wydawnictwo Katedry Dynamiki Maszyn i Robotyki AGH, 2001.
17. Uhl T. Komputerowo wspomagana identyfikacja modeli konstrukcji mechanicznych. Warszawa: WNT, 1997.
18. Wilk A, Madej H, Figlus T. Analysis of the possibility to reduce vibroactivity of the gearbox housing. Eksploatacja i Niezadownosc – Maintenance and Reliability 2011; 13 (2): 42-49.

prof. dr hab. inż. Eugeniusz RUSIŃSKI
e-mail:eugeniusz.rusinski@pwr.wroc.pl

dr hab. inż. Jerzy CZMOCHOWSKI, prof. PWr
e-mail:jerzy.czmochowski@pwr.wroc.pl

mgr inż. Damian PIETRUSIAK
e-mail:damian.pietrusiak@pwr.wroc.pl

Institute of Machine Design And Operation
Wrocław University of Technology
Łukasiewicza 7/9, 50-371 Wrocław

Article citation info:
Sun R, Peng WW, Huang HZ, Ling D, Yang J. Improved reliability data curve fitting method by considering samples distinction. Eksploatacja i Niezawodnosc – Maintenance and Reliability 2012; 14 (1): 62–71.

Rui SUN
Wei-Wen PENG
Hong-Zhong HUANG
Dan LING
Jianping YANG

IMPROVED RELIABILITY DATA CURVE FITTING METHOD BY CONSIDERING SAMPLES DISTINCTION

UDOSKONALONA METODA DOPASOWYWANIA KRZYWYCH DO DANYCH NIEZAWODNOŚCIOWYCH UWZGLĘDNIAJĄCA RÓŻNICE MIĘDZY PRÓBKAMI

In engineering practice, we face a problem of using some collected data to evaluate a kind of machine or equipment. Curve fitting is a common method to solve this problem. Least square method is wildly applied in this procedure. If the source data of curve fitting can be grouped in samples and the distinction of samples obviously express some character in source data collecting which cannot be ignored. Conventional curve fitting method cannot handle these source data. To deal with this disadvantage, we introduce an improved curve fitting method. Through source data analysis, we can find out the relationship between sample location and weight factor in curve fitting, and use these weight factors for curve fitting. To approach the true curve, we introduce an iterative procedure to modify the weight factors. An engineering example is given to illustrate this proposed method.

Keywords: *curve fitting, sample distinction, weigh assignment, iterative process.*

W praktyce inżynieryjnej stykamy się z problemem wykorzystania zgromadzonych danych do oceny maszyn lub sprzętu. Dopasowywanie krzywych to metoda powszechnie używana do rozwiązywania tego typu problemów. W procedurze tej szeroko stosuje się metodę najmniejszych kwadratów. Jeżeli dane wejściowe dopasowywane krzywą można pogrupować tak by tworzyły oddzielne próbki, a różnice między próbkami w sposób oczywisty odzwierciedlają pewną właściwość dotyczącą gromadzenia danych, której nie można pominąć, to konwencjonalna metoda dopasowywania krzywych nie pozwala na analizę takich danych wejściowych. Aby przezwyciężyć to ograniczenie, przedstawiamy udoskonaloną metodę dopasowywania krzywych. Poprzez analizę danych wejściowych, możemy określić związek pomiędzy położeniem próbki a czynnikiem ważonym w dopasowaniu krzywej oraz wykorzystać czynniki ważone przy dopasowywaniu krzywej. Aby osiągnąć jak najdokładniejsze przybliżenie do krzywej rzeczywistej wprowadziliśmu procedurę iteratywną modyfikującą czynniki ważone. Zastosowanie zaproponowanej metody zilustrowano na przykładzie danych z badań niezawodnościowych.

Słowa kluczowe: *dopasowywanie krzywych, różnice między próbkami, ważenie danych, proces iteratywny.*

1. Introduction

In reliability engineering, data are collected through reliability experiment or real time data collection for reliability analysis. The main methods to handle these data are classic statistical analysis method and linear estimate method. The results of reliability analysis is used for conduct state evaluating, residual life estimating, maintain planning, replacement policy evaluation, warranty cost prediction, and so on.

Regression analysis and curve fitting is a method to obtain the approximate analytic expression of discrete data. In reliability engineering, linear and non-linear regression methods are widely used depending on the characters of collected data [1, 6, 12-14]. In linear regression method, the least squares method is the most used method [4].

If collected data is a suitable data serial, in other words, the collected data have been grouped in one data set, current regression and curve fitting methods can be used easily. In other situations, however, collected data could be grouped in some data sets, which are significantly different from each other. Because the difference can not be ignored, all collected data can not be regrouped and arranged in one serial. To address this problem, weight factors are introduced in curve fitting methods, such as weighted least square (WLS) method [9].

If we can get some prior curve information, curve fitting procedure could be more efficient and is expected to be more precise. If we do not have the premise condition, make the best of source sample data become the only way to solve this problem. WLS gives a valid way to dig source data information and is used for curve fitting, the idea of WLS can be referenced in our method.

In Section 2, we introduce curve fitting method with the least square method, and analyze the advantages and disadvantages of the conventional least square method. Section 3 introduces an improved least square method to solve the samples distinction problem, analyze sample data distributions, finds out relationship between sample data and true curve, uses iterative process to achieve true curve. In this method, polynomial function has been chosen as the primary function, and an engineering example is given. Section 4 gives the conclusion.

2. Curve fitting with least square method

2.1. Theory of least square method

Least square method is a common curve fitting method, and it's used in many subject domains. The primary concept of least square method is given as below [4] .

For example, we get sample:

$$\{x_1, x_2, \cdots, x_n\},\ \{y_1, y_2, \cdots, y_n\},$$

And we know the curve function form is

$$y = \varphi(x) = c_1\varphi_1(x) + c_2\varphi_2(x) + \cdots + c_m\varphi_m(x)\ (m<n)$$

The curve fitting problem is translated to find the vector C and the constraint is shown as:

$$\min R = \sum_{i=1}^{n}(\varphi(x_i - y_i))^2 = \sum_{i=1}^{n}(c_1\varphi_1(x) + c_2\varphi_2(x) + \cdots + c_m\varphi_m(x) - y_i)^2 \quad (1)$$

Primary function selection is a key point in the least square method. The primary function is formed according to the basic sample characters. More specifically, the primary function's selection is based on the basic sample data distributions. Exponential distribution functions, two-parameter Weibull distribution functions, three-parameter Weibull distribution functions, and polynomial distribution functions are commonly used as primary functions, especially under situation of no other data information. In this paper, we use the polynomial as the primary function.

Current research can be concluded in two categories. Some researchers focused on the function selection, trying to get more data information, such as the object property, sample data collection method, data distribution, and trying to get more reasonable and valid function from the prior information [5, 16, 17]. Other researchers focus on the parameter identification [2, 3, 11, 15, 18].

2.2. Disadvantages of the least square method

Given the conventional least square method for curve fitting, if we can get enough samples, and all samples have been formulated in the same type, the fitting result is rational. However, if the source sample data have been group in some sample sequences, the conventional least square method can not handle this sample form. This brought the weight least square method. We can give different weight factors to different sample items according to the importance. The conventional least square method can be rewritten as follow, which is called the weighted least square method [7, 19].

$$\min R = \sum_{i=1}^{n} r_i(\varphi(x_i) - y_i)^2 = \sum_{i=1}^{n} r_i(c_1\varphi_1(x) + c_2\varphi_2(x) + \cdots + c_m\varphi_m(x) - y_i)^2 \quad (2)$$

Because we want to minimize R, $\bar{r} = \{r_1, r_2, \cdots, r_n\}$, which can be called as penalty factor. If sample item $\{x_i, y_i\}$ is located close to the mean of distribution than other sample items, r_i should be bigger than any other factor to prevent the fitting result departing from the true situation.

This produces another critical problem on the definition of the factor vector $\bar{r}$. The general method is to assign according to some prior information, such as the source data collection method evaluation, experts' experience, etc. If the equipment is brand new, we can not get enough prior information for factor assignment, sample analysis becomes the only way to factor assignment.

In the next section, we assume the collected data follow some kind of distribution. The closer the sample departs from the true curve, the higher is the distribution density. We can deduce the weight factor with the sample distribution density, and modify the weight factors in iterative procedure. This idea partly comes from the research work of Jiang and Jing [8, 10].

In the improved curve fitting method based on the least square method, the weight factors are used to form the fitting source point sequences, but not the penalty function.

3. Improved curve fitting method base on least square method

3.1. Samples analysis

The first key point of this improved curve fitting method is how to get the initial weight factors and how to modify them in the iterative procedure. To get the weight factor of each sample item, we should analyze the sample first. Fig.1 shows the sample distribution and the true curve. In Fig.1, the black curve is the true curve, collected samples distribute around the curve. Points compose four sample items. We know each sample provides information for curve fitting more or less. If a sample is closer to the true curve, it should include more information than other samples and should play more important role in the curve

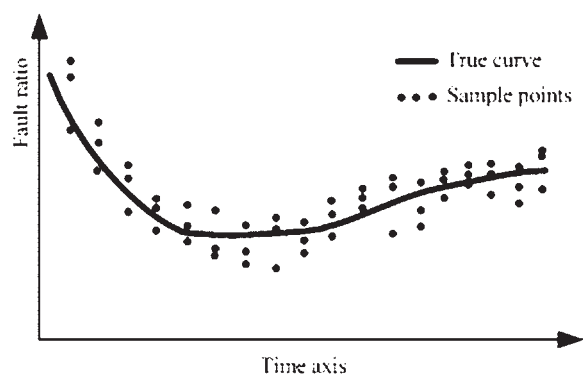

Fig. 1. True curve and sample distribution

fitting. That is to say this sample should have more weight than others.

3.2. Initial weight factor identification and initial curve generation

Through sample analysis, we know the sample that is the closest to the true curve should have the biggest weight factor in curve fitting. The new problem has been brought. Since we do not know the true curve, we do not know the exact distance between the true curve and each sample, and we can not get weight factors easily.

Though small sample means the existence of randomness in sample collection, these samples must match certain distribution. If through well pretreatment, source samples are unbiased and noises has been well suppressed. This source samples distribution has an obvious character that the more the samples gather, the more it is close to the true curve. That is to say, the higher the sample points gather density, the closer it is to the true value.

According to this character, we can deduce the weight factor from the distance between the sample and the true curve. Furthermore, we can use the distance between one sample and all other samples to represent the distance between the sample and the true curve.

We can assume curve fitting with n samples, each sample has m sample points, which are described as $\overline{S} = \{s_1, s_2, \cdots, s_n\}$, $s_n = \{p_{n,1}, p_{n,2}, \cdots, p_{n,m}\}$.

Thus, we can calculate the distances as follow:

$$L_{i,j} = \sqrt{\sum_{\substack{k=1 \\ k \neq i}}^{n} (p_{i,j} - p_{k,j})^2} \tag{3}$$

As the analysis before, the more the distance between one sample item and all other sample items, the less importance it take in curve fitting procedure. So we can assign initial weight factor as follows:

$$w_{i,j,0} = \frac{\frac{1}{L_{i,j}}}{\sum_{k=1}^{n} \frac{1}{L_{i,j}}} \tag{4}$$

The subscript 0 means this weight factor is the initial weight factor. The weight factor assignment considers the relationships among all sample items only. The precision of this assignment method is not considered. The fitting result precision is based on the iterative procedure, but not on the initial weight factor assignment.

Using the weight factor, we can get the first curve fitting source points as follows:

$$p_{j,0} = \sum_{i=1}^{n} w_{i,j,0} p_{i,j} \tag{5}$$

Using the first curve fitting source points, we can get the initial curve with the least square method.

3.3. Primary function determination

The primary function selection makes great influence to the fitting precise and computing efficiency, and become a key point in curve fitting.

Many researchers prefer to determine the primary function according to the source data. In mechanical and electronic engineering practice, standard 2-parameter, 3-parameter Weibull distribution and exponential distribution are the conventional choices, which should be chosen according to the underlying failure time.

Some researchers get progress in primary function determination or primary distribution identification, and provide or deduce some effective primary function and fitting method. These primary functions or distribution identification methods are mostly based on some prior information or familiar information of the collected data.

These primary functions have been proved in some basic theoretical research or engineering practices. They have one similar characteristic that the source data distributions have been known, and only the parameters need to be identified, or source data distribution can be estimated from similar system, similar product or from experience.

If these preconditions cannot be satisfied, primary distributions or primary functions selection method are not suitable. In this situation, general primary function should be used for curve fitting procedure. Polynomial is a common general primary function.

$$y = f(x) = a_0 + a_1 x^1 + \cdots + a_n x^n$$

Parameter n should be determined in fitting procedure.

3.4. Iterative process

With the initial weight factors $W_0 = \{w_{i,j,0} \mid i = 1, 2, \cdots, n, j = 1, 2, \cdots, m\}$, we can get the curve fitting result $C_0 = f_0(x)$. The subscript "0" means it is the first curve fitting result. Consequently, we can define the initial weight factors as $W_1 = \{w_{11}, w_{12}, \cdots, w_{1n}\}$.

The next step is an iterative procedure, in which we take the last step fitting result $C_0 = f_0(x)$ as the true curve to calculate weight factors. The weight factor of each sample can be changed in each step. The weight factor is assigned according to the dis-

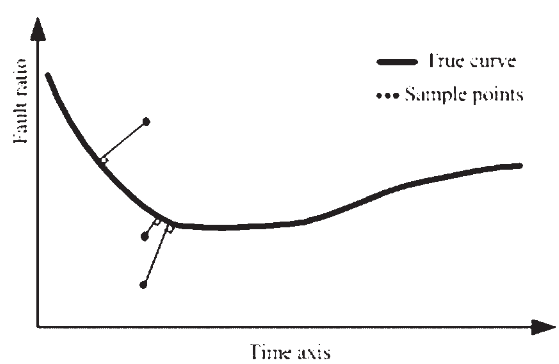

Fig. 2. Distance from sample points to fitted curve.

tance, since we get $C_0 = f_0(x)$ as fitting result. We use the distance between sample and curve, but not among samples.

Because the weight factor assignment is according to the distance, we calculate the distance firstly. The distance is between sample points and fitting curve, which means the shortest distance from the point to the curve. In other word, it means the vertical distance.

Fig.2 shows the vertical distance with three sample points at the same time point. The distance calculation method is an optimization search method.

$$L_{i,j,k} = \min\{\sqrt{(x_{i,j}-x)^2+[y_{i,j}-f(x)]^2} \mid x \in (0, x_n)\} \tag{6}$$

The sample points in one sample can be treated as a discrete time series. As points are not independent among each other, the value of each point is related to the points before and has impact on the points subsequently. Weight factor assignment should not be considered as single point's distribution, but a sample series. So in the iterative procedure, we assign points in the same sample the same weight factor. Weight factor can be obtained according to the sample average distance $L_{i,k}$.

$$L_{i,k} = \frac{1}{m}\sum_{j=1}^{m} L_{i,j,k} \tag{7}$$

Sample weight factor $w_{i,k}$, namely sample points weight factor $w_{i,j,k}$, is defined as

$$w_{i,k} = w_{i,j,k} = \frac{\frac{1}{L_{i,k}}}{\sum_{i=1}^{n}\frac{1}{L_{i,k}}} \tag{8}$$

Using this weight factor, we can get the fitting points in this curve fitting step:

$$p_{j,k} = \sum_{i=1}^{n} w_{i,j,k}\, p_{i,j} \tag{9}$$

With this fitting source points, we can get fitting result curve $C_k = f_k(x)$. This stage is an iterative procedure. Here we get the fitting result curve with this curve, and we can calculate the distance between the sample point and the fitting curve. By reassigning weight factor according to these distances, the fitting source points with new assign weight factor can be calculated, and the new fitting curve with these source points can be obtained.

3.5. Terminal condition

The iterative procedure is an approach proceeding to the true curve. When the iterative precision is enough, we can take the fitting result as the true curve, and the iterative procedure should be stopped. When to end the iterative procedure is called the terminal condition. In the iterative procedure, the terminal condition can be defined as two forms as follow:

Form 1:

Use the curve distance to evaluate iterative effect. Define C_k as the fitting result curve of step k in the iterative procedure, minimum value $\varepsilon > 0$, and $\overline{D_{k,k-1}}$ as the distance between C_k and C_{k-1} . If $\overline{D_{k,k-1}} < \varepsilon$, the iterative procedure should be stopped.

Form 2:

Use the weight factors' changes to evaluate iterative effect. Define $W_{k,k-1}$ as the average weight factor change of step k and step $k-1$ in iterative procedure.

$$W_{k,k-1} = \sqrt{\frac{\sum_{j=1}^{m}\sum_{i=1}^{n}(w_{i,j,k}-w_{i,j,k-1})^2}{n \times m}} \tag{10}$$

Define minimum value $\varepsilon > 0$. If $W_{k,k-1} < \varepsilon$, we think the subsequent iterative procedure can not bring obvious improvement, and the iterative procedure should be stopped.

These two forms represent the progress of iterative procedure. In practice, we can choose one of them according to the practical situation. In this paper, we use Form 2 terminal condition when considering the computing complexity.

3.6. Flowchart of this improved least square method

The flowchart of this curve fitting method is shown in Fig.3.

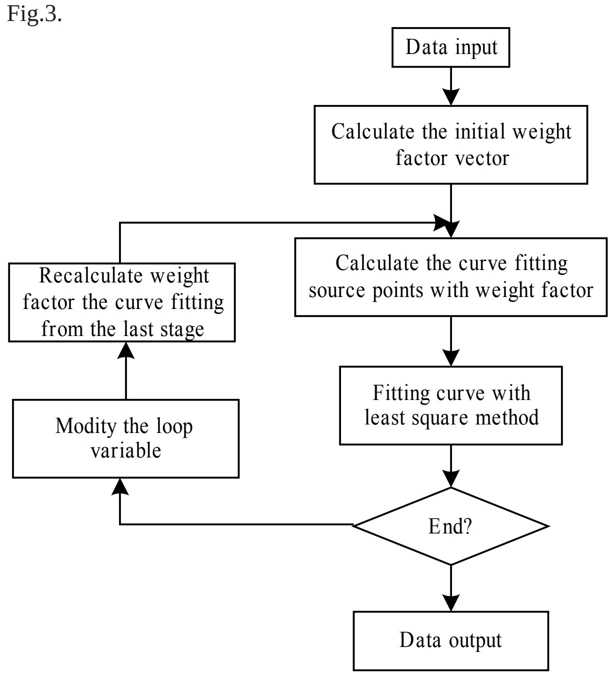

Fig. 3. Flowchart of this curve fitting method

3.6. Engineering example

In this section, we use this improved curve fitting method to handle a new type diesel engine life failure data.

For a new type diesel engine's maintenance plan and service guarantee plan, we must get the lift failure rules. Failure record is shown in Table 1. From this table, we can find that

Table 1. Failure record of some type of diesel

Unit number	Used district	Unit serial	Unit type	Failure mileage
D0303552563	Si Chuan	D0303	YC4108ZQ	110
D0303551997	Yun Nan	D0303	YC4108ZQ	398
D0303551110	Yun Nan	D0303	YC4108ZQ	1309
D0303551777	Guang Xi	D0303	YC4108ZQ	2182
…	…	…	…	…

Table 2. Four districts failure records

Mileage (10^3km)	0-1	1-2	2-3	3-4	4-5	5-6	6-7	7-8	8-9	9-10
*S*1	66	100	125	82	83	58	72	57	48	43
*S*2	40	60	42	18	18	12	17	12	15	14
*S*3	16	17	28	15	22	17	9	7	15	8
*S*4	14	10	6	2	2	0	3	2	3	2
Mileage (10^3km)	10-11	11-12	12-13	13-14	14-15	15-16	16-17	17-18	18-19	19-20
*S*1	46	43	27	17	14	12	10	7	3	10
*S*2	15	9	8	4	6	10	2	5	7	3
*S*3	6	3	5	3	5	3	3	1	2	3
*S*4	3	2	2	1	0	0	1	3	2	1

Table 3. Failure records in all districts

Mileage (10^3km)	0-1	1-2	2-3	3-4	4-5	5-6	6-7	7-8	8-9	9-10
S	136	187	201	117	125	87	101	78	81	67
Mileage (10^3km)	10-11	11-12	12-13	13-14	14-15	15-16	16-17	17-18	18-19	19-20
S	69	56	40	24	26	28	17	14	13	16

they are mainly used in four districts. We can divide collected data to form four samples, and use these four samples to curve fitting.

All failure records in four districts are collected. The mileage ranges from 0 to 6×10^4 . We use the data mileage ranging from 1 to 2×10^4 , and divide the mileage axis to 20 intervals, and collect the failures as Table 2.

On the contrary, if we ignore the districts distinctions, the failure mileages collected in 20 intervals have been shown in Table 3.

From the failure records, we can get the failure frequency in all intervals, and list them in Table 4.

From Table 4, we can observe that the sample *S*4 looks different from the other three samples. The main reason is the sample size. Because the sample size of *S*4 is about 1/17 of *S*1, the existence of randomness makes obvious impact to the *S*4 statistical values which can be noticed in Fig.4. The cerulean points represent sample *S*4. Fig.5 is the conventional method source points scatter diagram. We ignore the districts difference, and get characteristics from all samples collected. Obviously,

Table 4. Four sample failure frequency

Mileage (10^3km)	0-1	1-2	2-3	3-4	4-5	5-6	6-7	7-8	8-9	9-10
*S*1	0.0698	0.1058	0.1323	0.0868	0.0878	0.0614	0.0762	0.0603	0.0508	0.0455
*S*2	0.119	0.1786	0.125	0.0536	0.0536	0.0357	0.0506	0.0357	0.0446	0.0417
*S*3	0.0812	0.0863	0.1421	0.0761	0.1117	0.0863	0.0457	0.0355	0.0761	0.0406
*S*4	0.2188	0.1563	0.0938	0.0313	0.0313	0	0.0469	0.0313	0.0469	0.0313
Mileage (10^3km)	10-11	11-12	12-13	13-14	14-15	15-16	16-17	17-18	18-19	19-20
*S*1	0.0487	0.0455	0.0286	0.018	0.0148	0.0127	0.0106	0.0074	0.0032	0.0106
*S*2	0.0446	0.0268	0.0238	0.0119	0.0179	0.0298	0.006	0.0149	0.0208	0.0089
*S*3	0.0305	0.0152	0.0254	0.0152	0.0254	0.0152	0.0152	0.0051	0.0102	0.0102
*S*4	0.0313	0.0156	0	0	0.0156	0.0469	0.0313	0.0156	0.0156	0

Table 5. Fitting result coefficients with conventional and improved method

	x^5	x^4	x^3	x^2	x^1	x^0
Equal weight fitting result	0.1735	-0.9514	2.005	-2.219	1.703	0.04554
Improved method fitting result	0.1882	-1.015	2.084	-2.244	1.7359	.0.02376

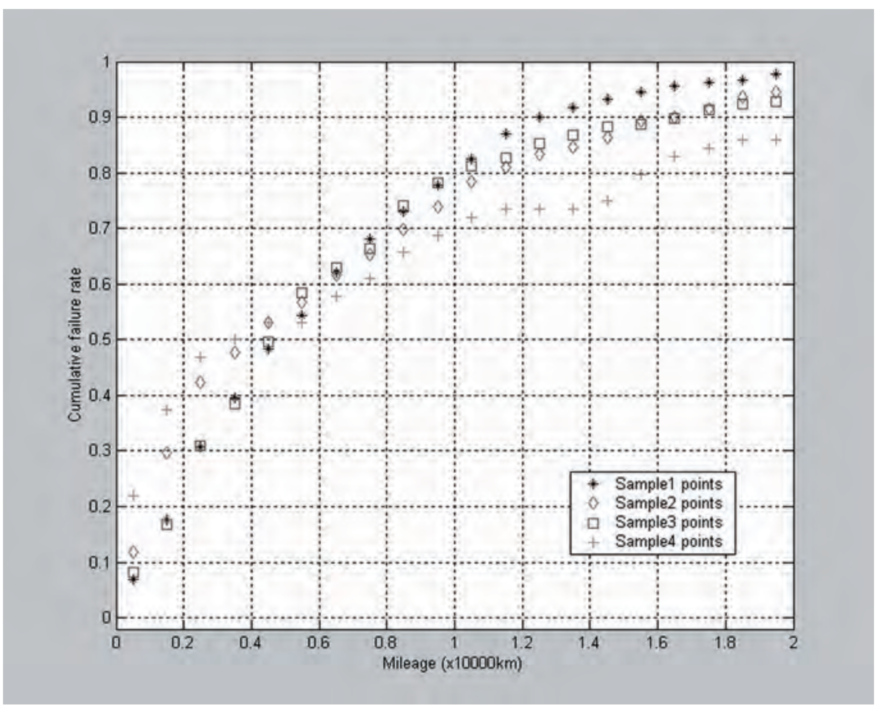

Fig. 4. Four districts sample scatter diagram

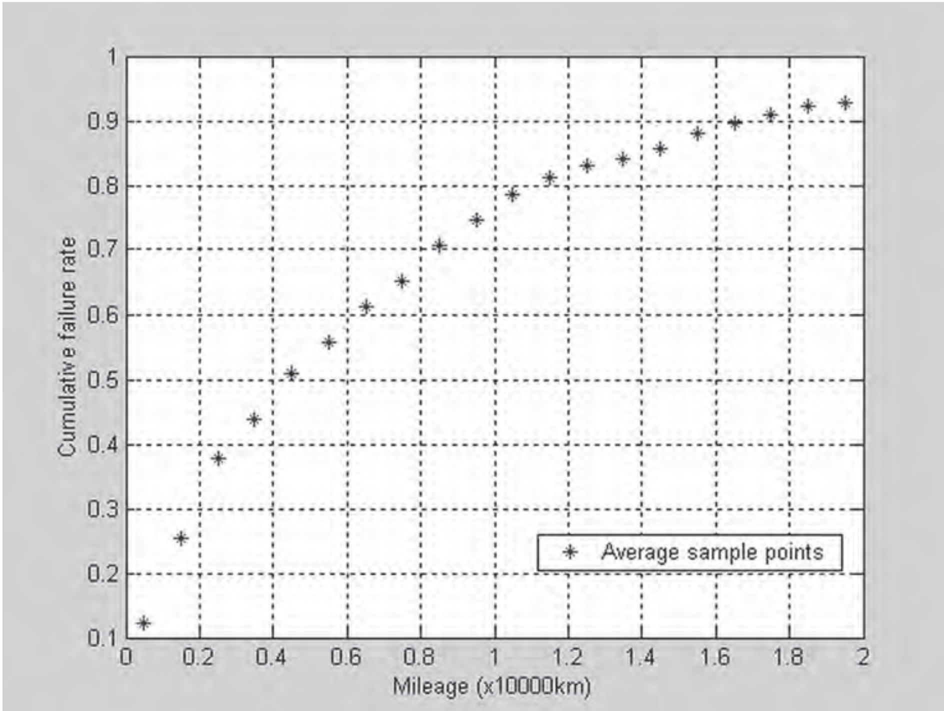

Fig. 5. All districts sample scatter diagram

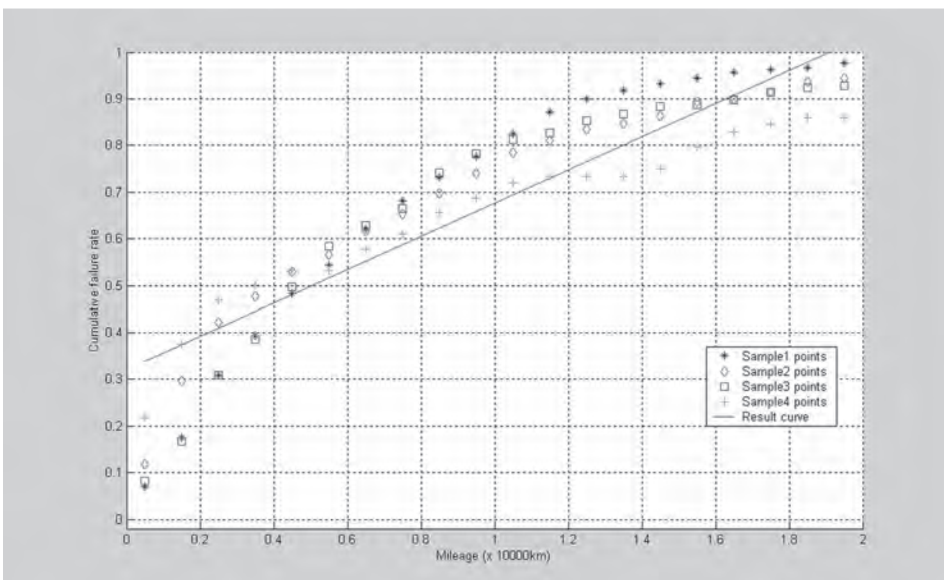

Fig. 6. Fitting with 1-order polynomial

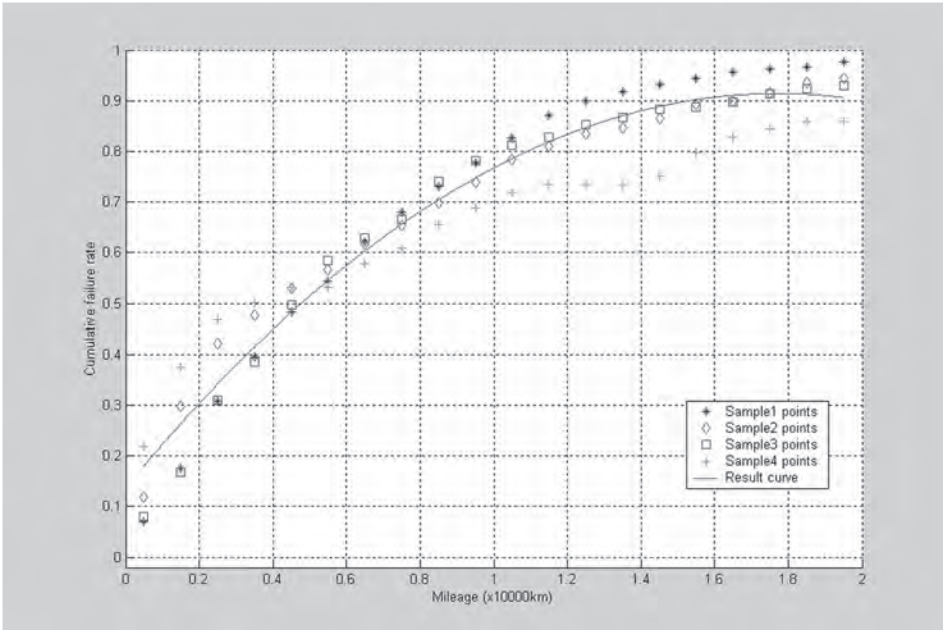

Fig. 7. Fitting with 2-order polynomial

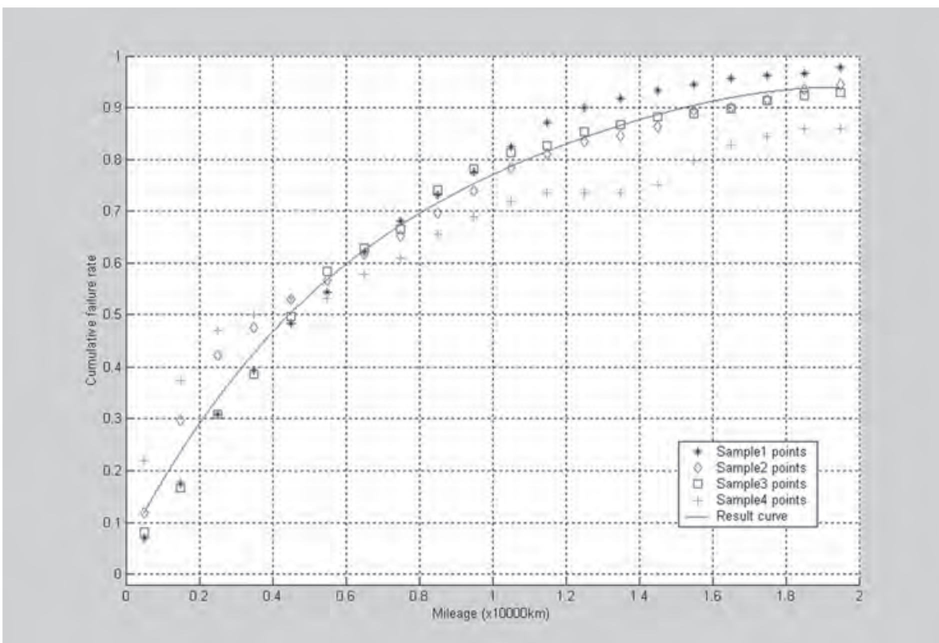

Fig. 8. Fitting with 4-order polynomial

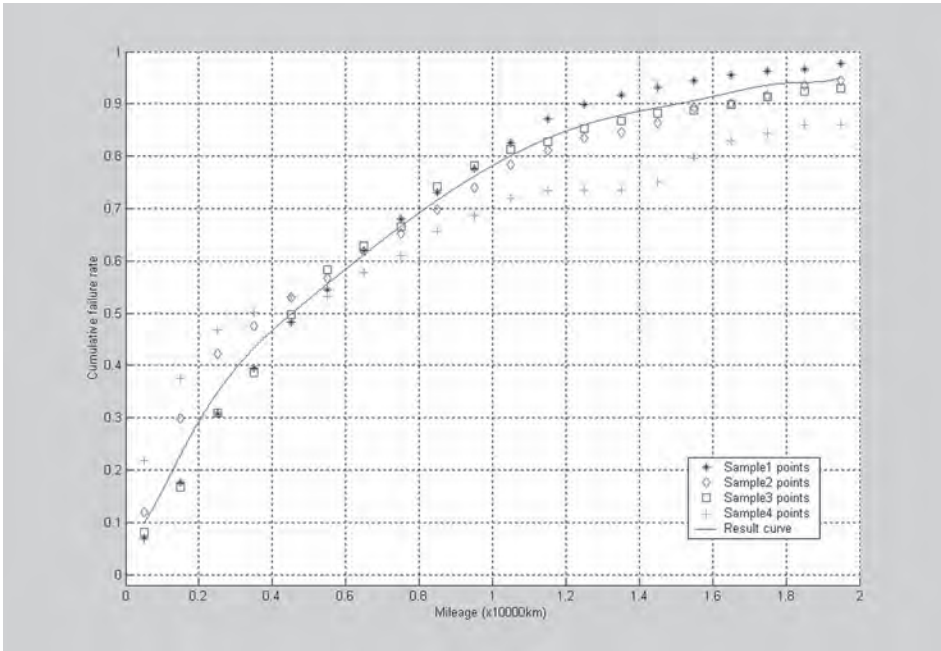

Fig. 9. Fitting with 10-order polynomial

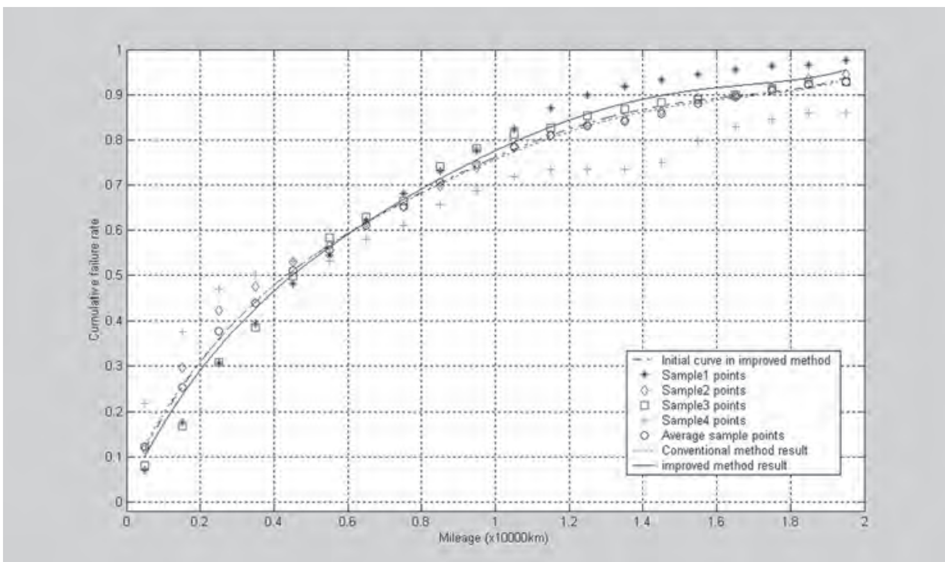

Fig. 10. Fitting result with conventional and improved method

this method loses the impact of districts to diesel. However, the samples like Table 4 can be handled in the improved method.

Polynomial fitting experiments had been done with polynomial order from 1 to 10, and the fitting result has been show as Fig.6 to Fig. 9. Higher order polynomial fitting attempts to use more computing resource and expects to get obvious influence. From Fig. 6 to Fig. 9, we can find the fitting result does not have obvious improvement with the increase of polynomial order if the polynomial order is bigger than 2. Here we use the polynomial fitting method with an order of 5 to handle source data.

Fig.10 shows the fitting result with the conventional and the improved method introduced in this paper. In Fig.10, four different shape group points denote four samples. Dotted line curve denotes the fitting result with the conventional polynomial fitting method, the dot dash one is the initial fitting curve using the improved method, and the iterative result has been shown as the solid one. From Fig.10, we can find in the area where sample points dense gather, the fitting results of these two methods are similar with each other. However, it should be noted in the interval of $(1.0 \sim 1.8) \bullet 10^3$, the improved method fitting result is more close to the area where sample dense gather, and this result is more convincing. In other words, in this interval, one of these four samples is apart from others. The improved method is more flexible to handle this abnormal data situation, and this ability mostly comes from the iterative procedure.

The fitting result coefficients with conventional and improved method do not have enough obvious difference. But from the curve figure, we can find the improved method has obvious advantage in this curve fitting situation.

4. Conclusion

From the engineering example and fitting result analysis, we can find when the samples dense gather, improved polynomial fitting method can get similar fitting result as the conventional method. However, if one or more samples are apart from the others, the improved polynomial fitting method can get more convincing result than the conventional method.

Acknowledgements

This research was partially supported by the National Natural Science Foundation under the contract number 51075061.

5. References

1. Cuyt A. Wuytack L. Nonlinear Methods in Numerical Analysis. Elsevier, Amsterdam, 1987.
2. Ling Dan, Huang Hong-Zhong, Liu Yu. A method for parameter estimation of mixed Weibull distribution. Proceedings of the 55th Annual Reliability & Maintainability Symposium. Fort Worth, TX, USA, 2009.
3. Ling Dan, Huang Hong-Zhong, Miao Qiang, Yang Bo. Parameter estimation for Weibull distribution using support vector regression. Proceedings of 2007 ASME International Design Engineering Technical Conference & Computers and Information in Engineering Conference, Las Vegas, NV, USA, 2007.
4. De Levie Robert. Curve fitting with least squares. Critical Reviews in Analytical Chemistry 2000, 30(1): 59-74.
5. Dhillon B S. A hazard rate model. IEEE Transactions on Reliability 1978; 28(2): 150.
6. Huang H Z, Guan L W, Wu H F. A study on linear regression model with fuzzy weight and its application to S-N Curve in its regression analysis. Machine Design 2000; 17: 11-12.
7. Ji F, Yao W. Weighted least square method for S-N curve fitting. Transaction of Nanjing University of Aeronautics & Astronautics 2004; 21: 53-57.
8. Jiang S R, Kececioglu D. Maximum likelihood estimates, from censored data, for mixed-Weibull distributions. IEEE Transactions on Reliability 1992; 41: 248-255.
9. Ji F, Yao W. Weighted least square method for S-N curve fitting. Transaction of Nanjing University of Aeronautics & Astronautics 2004; 21(1): 53-57.
10. Jing L, Jwo P. A maximum likelihood method for estimating P-S-N curves. International Journal of Fatigue 1997; 19: 415-419.
11. Jiang R Y, Murthy D N P.. Modeling Failure-Data by mixture of 2 Weibull Distribution: A Graphical Approach. IEEE Trans. Reliability 1995; 44: 477-488.
12. Karr C L, Weck B. Least median squares curve fitting using a genetic algorithm. Engineering Applications of Artificial Intelligence 1995; 8: 177-189.
13. Vasanth Kumar K, Porkodi K, Rocha F. Isotherms and thermodynamics by linear and non-linear regression analysis for the sorption of methylene blue onto activated carbon: Comparison of various error functions. Journal of Hazardous Materials 2008; 794-804.
14. Vasanth Kumer K, Sivanesan S. Pseudo second order kinetic models for safranin onto rice husk: Comparison of linear and non-linear regression analysis. Process Biochemistry 2006; 41: 1198-1202.
15. Michael P, Maureen S. Curve-fitting with piecewise parametric cubics. Computer Graphics 1983; 17: 229-239.
16. Murthy D N P, Xie M, Jiang R Y. Weibull Models, New York, Wiley, 2003.
17. Nelson W. Applied Life Data Analysis, New York, Wiley, 1982.
18. Silverman B W. Some aspects of the spline smoothing approach to non-parametric regression curve fitting. Royal Statistical Society 1985; 47: 1-52.
19. Xu M J, Yoram E. Use of weighted least-squares method in evaluation of the relationship between dispersivity and field scale. Ground Water 1995; 33: 905-908.

Rui SUN, Ph.D. candidate
Wei-Wen PENG, Master Student
Prof. Hong-Zhong HUANG, Ph.D.
Associate Professor Dan LING, Ph.D.
Jianping YANG, Ph.D. candidate
School of Mechatronics Engineering
University of Electronic Science and Technology of China
Chengdu, Sichuan, 611731, China
E-mail: hzhuang@uestc.edu.cn; rispper@uestc.edu.cn

Article citation info:
RUSIN A, WOJACZEK A. Optimization of power machines maintenance intervals taking the risk into consideration. Eksploatacja i Niezawodnosc – Maintenance and Reliability 2012; 14 (1): 72–76.

Andrzej RUSIN
Adam WOJACZEK

OPTIMIZATION OF POWER MACHINES MAINTENANCE INTERVALS TAKING THE RISK INTO CONSIDERATION

OPTYMALIZACJA OKRESÓW MIĘDZYREMONTOWYCH MASZYN ENERGETYCZNYCH Z UWZGLĘDNIENIEM RYZYKA*

The goal of preventive as well as corrective maintenances is to keep or to restore acceptable level of efficiency and safety of operation of given object. Optimization of maintenance processes allows obtaining these effects at possibly lowest costs. Mathematic model of optimization of maintenance intervals having regard to the risk are presented in the paper. Precise calculations were made for steam turbines that operate in power units.

Keywords: *optimization, maintenance intervals, power machines, risk.*

Celem obsług prewencyjnych jak i korekcyjnych jest zachowanie lub przywrócenie akceptowalnego poziomu efektywności i bezpieczeństwa eksploatacji danego obiektu. Optymalizacja działań remontowych pozwala na uzyskanie tych efektów przy możliwie niskich kosztach. W artykule przedstawiono model matematyczny optymalizacji okresów międzyremontowych z uwzględnieniem ryzyka. Szczegółowe obliczenia przeprowadzono dla turbin pracujących w blokach energetycznych dużej mocy.

Słowa kluczowe: *optymalizacja, okres międzyremontowy, maszyny energetyczne, ryzyko.*

1. Introduction

Maintenance activities, both preventive and corrective ones after a failure occurs, are to keep or restore acceptable level of operation of given object. The goal of these operations is to improve reliability and safety of operation, at as low as possible costs. Development of new techniques and methods of maintenances within the recent years is connected with formal regulations and expectations to improve operation safety of every technical object. These requirements are especially significant for large systems that provide correct functioning of many branches of economy. Power system as well as its basic subsystems of generation and transmission belong, among other, to these systems. Reliability of generation subsystem depends on reliability of power units as well as its main components, i.e. turbines, boilers and generators. The proper and safe operation of these machines and devices provide the safety of electric energy generation in its various forms, i.e. electric energy as well as heat. On the other hand, the market and competition of electric power manufactures at this market requires reducing any possible costs, including maintenance activities that have significant contribution to the final price of energy.

The method to determine the maintenance intervals presented in further sections of the paper is based on operation costs minimization or maximization of profit on operation. Both objective functions forms take into account the risk level. Precise considerations were made for steam turbines components that operate in large power units.

2. Maintenance intervals optimization model

As it was mentioned before, the basic purpose of preventive maintenances is to cancel of negative effects of various wear processes that deteriorate technical condition of objects and to restore it to such a level that object could operate safely until the next renovation not being submitted to a failure within this period. Frequently the industrial usage accomplishes these activities within regular periods of time on the basis of operational experience. More and more frequently, the knowledge gained from diagnostic tests and operation monitoring system of given device is used as well. An approach suggested beneath assumes taking into consideration both the costs of maintenances and operation safety level. Technical risk level connected with operation of given object may be the measure of this safety. Technical risk is understood as the product of probability of an adverse event occurrence as well as it consequences [1, 2, 8, 9, 10]. Denoting the risk as R we note:

$$R = \sum_{i=1}^{n} P_i C_i \qquad (1)$$

where: P_i – probability of event "i" occurrence,
C_i – consequences of event "i" occurrence,
n – number of dangerous events that relate to given object.

The risk so defined may constitute the basis to formulate optimization criteria of periods and scopes [3, 11] of preventive

(*) Tekst artykułu w polskiej wersji językowej dostępny w elektronicznym wydaniu kwartalnika na stronie ***www.ein.org.pl***

maintenance. To do so the concept of admissible risk level is to be used. The basis to perform calculations of probability of disadvantageous events are data on object operation, including, the first of all, data about failures and damage of components. Knowledge on wear processes is indispensable, which, i.e. processes may lead to damage of components. The second of factor, that decides of risk level, i.e. failure and damages consequences are most frequently expressed in terms of monetary units. The appropriate establishing them requires profound knowledge on operation conditions, repairs as well as economy issues of given enterprise.

If consequences shall be expressed in monetary units, so the risk described with relationship (1) has this measure. It becomes an economic category and can be taken into consideration in economic calculation. Using this fact, we may present the planning procedure of maintenance as a procedure of total costs optimization K_c. Risk shall be taken into account in these costs as well. Thus, we obtain:

$$K_c = K_r + R \tag{2}$$

The first term in the above sum K_r denotes total costs incurred to maintenance a given object, i.e.:

$$K_r = \sum_i K_{ri} \tag{3}$$

whereas the second term of the dependence (2) denotes the total risk that given object creates:

$$R = \sum_j R_j \tag{4}$$

Referring the costs in the term (2) to operation time t we obtain a relative cost per unit of time:

$$\overline{K}_c = \frac{K_r + R}{t} = \overline{K}_r + \overline{R} \tag{5}$$

where $\overline{K}_c, \overline{K}_r, \overline{R}$ are the values referred to the time unit. The optimum value of period between overhauls shall be obtained via objective function minimization V, which is – in our case – the total cost $\overline{K}_c$, i.e:

$$V = \overline{K}_c \tag{6}$$

$$V \rightarrow min \quad \Rightarrow \quad t = t_o \tag{7}$$

that is presented on graph in Fig. 1.

If, during optimization process we shall take into consideration the profit Z obtained on object operation, thus objective function could be a difference between profit Z and total costs K_c that take the risk into consideration as well. Thus, we may note:

$$V = \Delta \overline{K} = \overline{Z} - \overline{K}_c = \overline{Z} - (\overline{K}_r + \overline{R}) \tag{8}$$

The goal of optimization for such formulated objective function form is its maximization, i.e.:

$$V \rightarrow max \Rightarrow t = t_o \tag{9}$$

Every value in the above mentioned formulae are related to the unit of time. If we assume that profit is a linear function of operation time thus unit profit as referred to time unit shall be constant and optimum determined from relationship (9) shall be the identity with the optimum obtained from relationship (7).

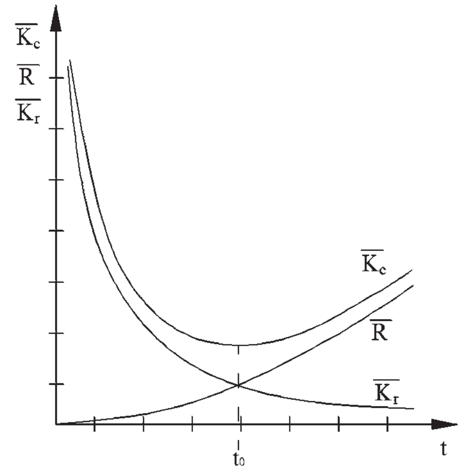

Fig. 1. Concept of selection of optimum maintenance intervals

However, as time elapses, object efficiency drop occurs then the profit in consecutive periods is lesser and lesser that denotes that value $\overline{Z}$ is a decreasing function of time.

In case of machines and power devices, their efficiency η is defined as ratio of energy generated (for instance electric energy) E_w to energy supplied (for instance chemical energy of fuel) E_d:

$$\eta = \frac{E_w}{E_d} \tag{10}$$

Thus, generated energy is a function of efficiency that depends on time:

$$E_w(t) = \eta(t) E_d \tag{11}$$

Assuming that profit Z of operation is proportional to energy volume generated, we may note:

$$Z = pE_w = p\eta(t) E_d \tag{12}$$

where: p is a constant that describes share of profit in total incomes obtained from generated energy E_w.

Thus we may assume that at constant energy volume supplied the profit drop in given period is proportional to devices efficiency drop.

In such a case, optimum obtained from optimization of objective function expressed by relationship (9) may differ from objective function optimum described with equation (7), Fig. 2.

The goal of preventive maintenances is to improve the object operation properties. Taking into consideration the scope of restoration of object output condition, we may distinguish [7]:

- perfect maintenance that restores entirely the initial usable object properties – an object may be considered as a new one,
- minimum maintenance that does not change usable properties of object; its failure intensity does not change,
- imperfect maintenance, as a result of which, object usable properties are improved but not to the level as a new object had.

According to the above classification, minimum and perfect maintenances are boundary state of imperfect maintenance. There are many methods of imperfect maintenance described in

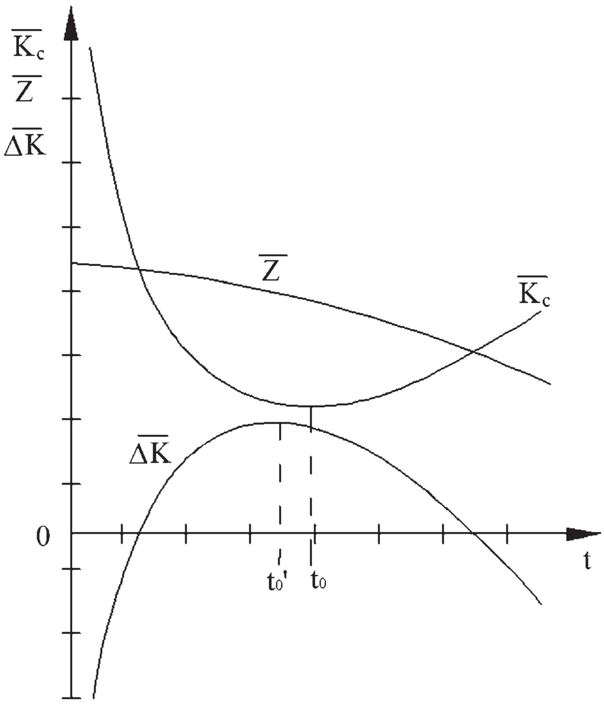

Fig. 2. Concept of selection of optimum maintenance intervals taking the profit into consideration

references [5, 7]. One of them is so called a method of virtual object age [5, 7]. According to this method, if object virtual age after (n-1) of preventive maintenances was (t^*_{n-1}), then, after the next maintenance has the value:

$$t^*_n = t^*_{n-1} + (1 - a)\Delta t \tag{13}$$

where: Δt is a time interval between n-1 and n-th preventive maintenance.
a is so called age reduction coefficient that assumes value from interval <0;1>. Value of this coefficient depends on scope and results of maintenance.

If maintenance activities cancel significantly negative results of operation and wear processes then value of coefficient a assumes values close to one. In an opposite case, when object condition, after maintenance did not change in practice, coefficient a assumes the value zero. Undoubtedly, effects of maintenance expressed with coefficient a depend on investments paid to execute it.

Further part of the paper describes an example of optimization of preventive maintenance intervals of power machines using the optimization model set forth above.

3. Optimization of preventive maintenance intervals of rotor assemblies of turbines

Turbine rotor assembly that includes, among other, the shaft, rotor blades, discs, bearings, clutches and sealing compose the main turbine component of basic meaning for its reliability and availability. Failure frequency statistics and data on turbine operation indicate that basic failure of rotor assembly are as follows [2, 4, 6, 9]:

- damage of blades caused by vibrations as well as corrosion and erosion processes,
- bearings damage that result from design errors, improper lubrication or turbine operation errors,
- excessive relative elongations of rotor and casing caused, among other, with operation errors of boiler or turbine, design errors,
- leak of oil system caused by cracks of its elements,
- excessive vibrations of turbine shaft, caused by thermal shocks,

Moreover, other failures are also possible, including tear of rotor, but probability of its occurrence is very small at initial stage of operation; it becomes significant after long operation periods.

Finally, four scenarios were assumed for precise analyses of most frequent failures of rotor assembly. These are:

1. Failure of turbine bearings causing secondary damage of flow system,
2. Failure of turbine bearings without damage of other elements,
3. Failure of blade in turbine flow system,
4. Failure of labyrinth sealing of rotor.

The first two scenarios mentioned above relate to turbine bearings; how to distinguish them is advised with the scope and consequences of its damage. If damage of bearings causes damage of flow system of rotor, financial consequences connected with repair as well as necessary standstill of machine and thus losses in energy generation are many times greater. Damage areas described with the above scenarios are marked on turbine diagram in Fig. 3.

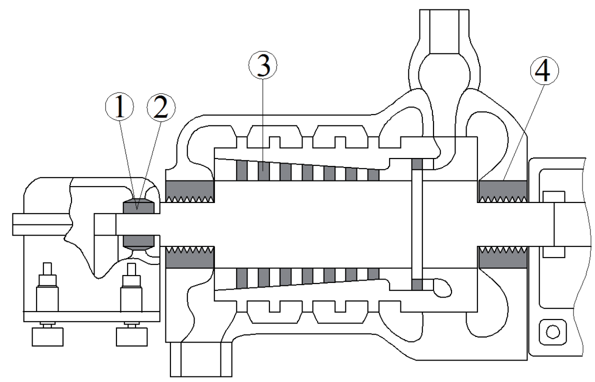

Fig.3. Turbine diagram

On the basis of operation data it was found that operation time up to a failure according to all contemplated scenarios could be described with Weibull cumulative distribution functions:

$$F(t) = 1 - exp\left[-\left(\frac{t}{\alpha}\right)^{\beta}\right] \tag{14}$$

where, α, β are Weibull distribution parameters. Values of these parameters for separate events are shown in Table 1.

Table 1

Scenario No	Weibull distribution parameters		Relative failure costs
	α	β	
1	296	2,9	1,00
2	148	3,4	0,33
3	444	2,7	0,33
4	80	2,9	0,04

On the basis of cost analysis connected with occurrence of the above mentioned failures, relative values were established that were referred to the costs of most serious failure described with scenario No 1. These costs, indicated also in Table 1, cover direct repair costs, replacement parts, losses caused by lost production as well as other additional costs incurred in connection with occurrence of failure. Assessment of occurrence probability of a given sort of failure as well as its costs makes possible to calculate the risk. Time functions of risks connected with four scenarios mentioned as well as total risk of rotor assembly were shown in Fig. 4. Risk value is expressed in terms of monetary relative units according to Table 1.

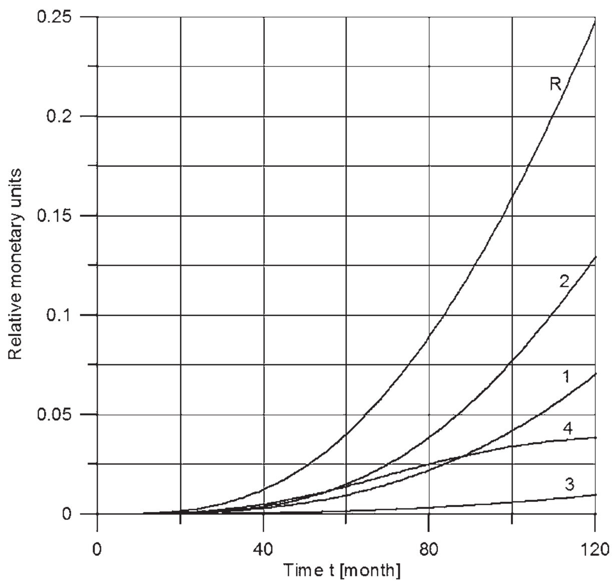

Fig. 4. Risks connected with operation of rotor assembly

Knowledge on investment outlay connected with repairs related to rotor assembly, whose purpose is to avoid the above mentioned damages allows – according to relationship (7) – determining the optimum time to execute maintenance. In calculations, the relative cost of preventive maintenances was assumed equal 0,1 of failure cost described with scenario No 1. Result of such optimization is given in Fig. 5. For data assumed, the optimum time to execute maintenance is 67 months.

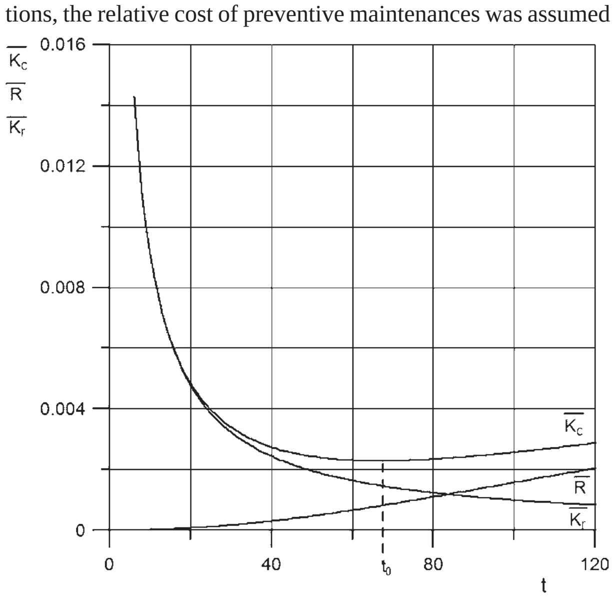

Fig. 5. Optimum maintenance time of the turbine rotor assembly according to criterion (7)

Optimisation results according to criterion (9) are shown in Fig. 6. Maximum profit per time unit was assumed equal to 0.01 of failure cost according to scenario 1. Power unit efficiency within 60 months varies from 34% up to 32%. Optimum time to execute maintenance t_o' = 52 months.

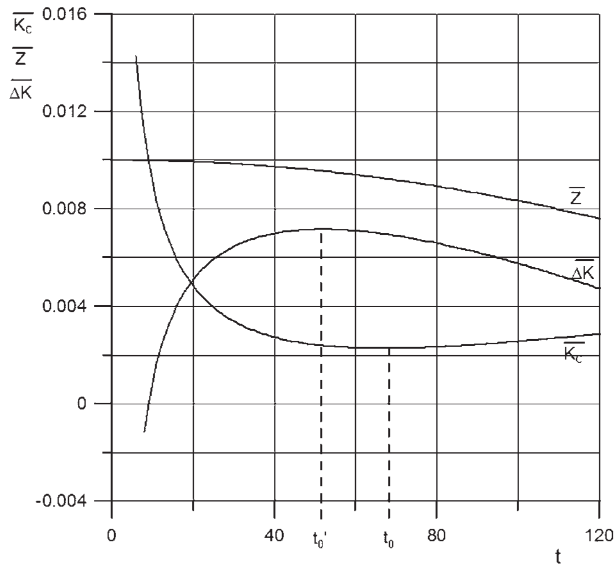

Fig. 6. Comparison of optimum maintenance times of turbine rotor assembly according to criterion (7) and (9)

Assuming that repair actions performed restore the initial condition of rotor assembly component and operation conditions do not change, consecutive maintenances should take place within the same period of time. However it is known in practice that it is not possible to restore entirely the initial condition of elements and renovation process itself should be considered as an imperfect maintenance. Accepting such assumption and assuming that renovation effect could be described by so called virtual object age in accordance with relationship (13), then consecutive periods between maintenances shall depend on value of coefficient of age reduction *a*. Examples of periods optimization between maintenances for two different coefficients *a* are shown in Fig. 7 and 8. Fig. 7 specifies optimum maintenance periods under assumption that reduction coefficient value is 0.95, whereas Fig. 8 gives optimum solution for coefficient *a* = 0.85. In both cases, optimization was accomplished for objective function described with relationship (9).

It results from specific relationships, that consecutive time between maintenances subject to slight reduction. For assumed data the recent times between maintenances are shorter by 2 up to 3 months than the initial ones.

4. Summary

The mathematical model of selection of time between maintenances set forth in the paper takes into account both economy effects and risk level connected with operation of given object. This model has been used to estimate the time between overhauls of steam turbines that constitute one of main component of power unit. On the basis of real data on failure frequency of turbines of domestic power units the probability was calculated

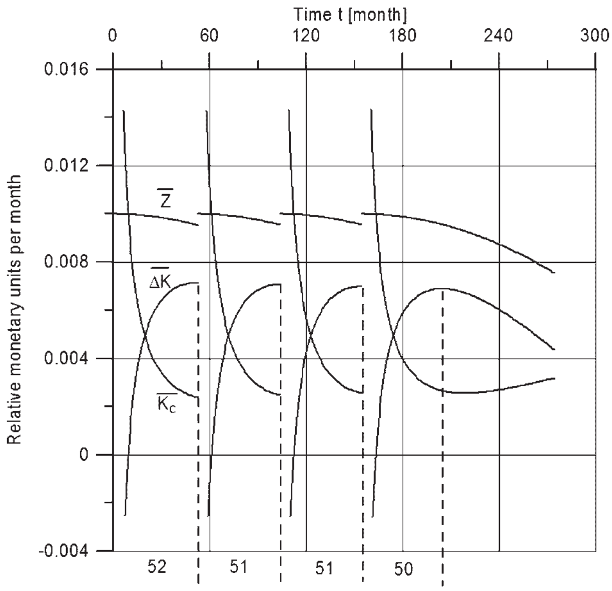

Fig. 7. Optimum times of preventive maintenances for a = 0.95

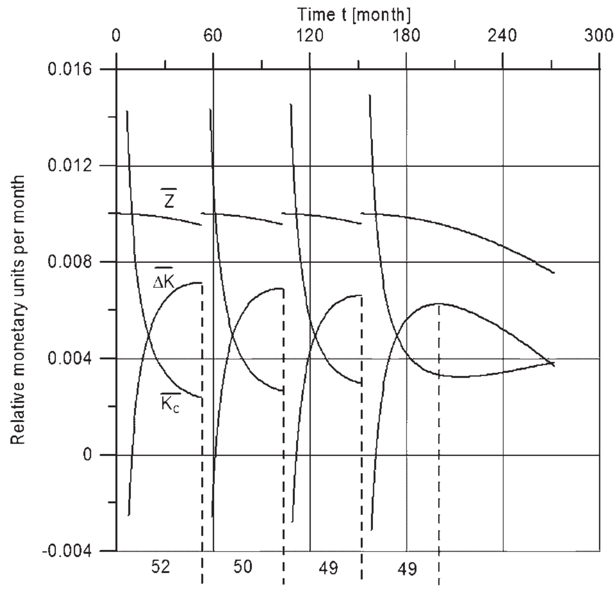

Fig. 8. Optimum times of preventive maintenances for a = 0.85

of occurrence of four main failure scenarios. Relative values of consequences of these events were estimated as well as risk level. As a result of solutions of optimization tasks for various formulation of objective function the optimum periods to execute the first and consecutive maintenances of turbine were obtained. Duration of these times between maintenances depends on quality of performed overhaul.

The results presented in this paper were obtained from research work co-financed by the National Centre of Research and Development in the framework of Contract SP/E/1/67484/10 – Strategic Research Programme – Advanced technologies for obtaining energy: Development of a technology for highly efficient zero-emission coal-fired power units integrated with CO_2 capture.

5. References

1. Apeland S, Aven T. Risk based maintenance optimization: foundational issues. Reliability Engineering and System Safety 2000; 67: 285-292.
2. Bareiβ J, Roos E, Jovanovic A, Perunicic M, Balos D. Risk-based maintenance concept-European development and experience in implementation on high-temperature steam tubes and pipes. VGB Power Tech 2006; 1/2: 77-82.
3. Carazas F G, Souza G F M. Risk-based decision making method for maintenance policy selection of thermal power plant equipment. Energy 2010; 35: 964-975.
4. Jovanovic A. Risk-based component life management in fossil power plants. OMMI 2002; 1: 1-6.
5. Kallen M J, Noortwijk J M. Optimal maintenance decisions under imperfect inspection. Reliability Engineering and System Safety 2005; 90: 177-185.
6. Krishnasamy L, Khan F, Haddara M. Development of a risk-based maintenance (RBM) strategy for a power-generating plant. Journal of Loss Prevention in the Process Industries 2005; 18: 69-81.
7. Pham H, Wang H. Imperfect maintenance. European Journal of Operational Research 1996; 94: 425-438.
8. Rusin A. Assessment of operational risk of steam turbine valves. Int. J. of Pressure Vessels and Piping 2004; 4: 373-379.
9. Rusin A. Awaryjność, niezawodność i ryzyko techniczne w energetyce cieplnej. Gliwice: Wydawnictwo Politechniki Śląskiej, 2008.
10. Rusin A. Technical risk involved in long-term operation of steam turbines. Reliability Engineering and System Safety 2007; 92: 1242-1249.
11. Rusin A, Wojaczek A. Selection of maintenance range for power machines and equipment in consideration of risk. Eksploatacja i Niezawodnosc - Maintenance and Reliability 2007; 3(35): 40-43.

Prof. dr hab. inż. Andrzej Rusin
Mgr inż. Adam Wojaczek
Institute of Power Engineering and Turbomachinery
Silesian University of Technology
ul. Konarskiego 18, 44-100 Gliwice, Poland
andrzej.rusin@polsl.pl
adam.wojaczek@polsl.pl

Article citation info:
SAHARKHIZ E, BAGHERPOUR M, REZA FEYLIZADEH M R, AFSARI A. Software performance evaluation of a computerized maintenance management system: A statisticalbased comparison. Eksploatacja i Niezawodnosc – Maintenance and Reliability 2012; 14 (1): 77–83.

Eshagh SAHARKHIZ
Morteza BAGHERPOUR
Mohammad Reza FEYLIZADEH
Ahmad AFSARI

SOFTWARE PERFORMANCE EVALUATION OF A COMPUTERIZED MAINTENANCE MANAGEMENT SYSTEM: A STATISTICAL BASED COMPARISON

OCENA DZIAŁANIA OPROGRAMOWANIA KOMPUTEROWEGO SYSTEMU ZARZĄDZANIA UTRZYMANIEM RUCHU. BADANIA STATYSTYCZNO-PORÓWNAWCZE

In today highly competitive markets, application of maintenance management systems is un-avoidable. However, in refinery environments due to huge investment amount of operating systems, applying advanced maintenance management systems (Such as Computerized Maintenance Management System which is called CMMS) is increasingly seems to be a crucial task. In order to implement high performance CMMS software, the existing ones should be analyzed. In this paper, performance of two CMMS related software entitled IFS™ and MAINTA™, are introduced, analyzed and compared using significant statistical analysis with a case study in a refinery. The results of both hypothesis testing and economical study finally proposed the MAINTA™ software.

Keywords: *CMMS, statistical analysis, economic study, maintenance management.*

Na dzisiejszych, niezwykle konkurencyjnych rynkach, zastosowanie systemów zarządzania utrzymaniem ruchu jest niezbędne. Przykładem są zakłady rafinerii, w których, ze względu na wysokie sumy inwestowane w systemy operacyjne, zastosowanie zaawansowanych systemów utrzymania ruchu (takich jak Komputerowy System Zarządzania Utrzymaniem Ruchu CMMS) wydaje się coraz bardziej istotnym zadaniem. Aby jednak wdrożyć wysokiej klasy oprogramowanie CMMS, należy najpierw przeanalizować istniejące programy. W niniejszym artykule, przedstawiono, przeanalizowano i porównano za pomocą analizy statystycznej działanie dwóch programów typu CMMS o nazwach IFS™ oraz MAINTA™. Analizy oparto na studium przypadku przeprowadzonym w rafinerii. Wyniki testowania hipotez oraz analizy ekonomicznej wyłoniły oprogramowanie MAINTA™ .

Słowa kluczowe: *CMMS, analiza statystyczna, analiza ekonomiczna, zarządzanie utrzymaniem ruchu.*

1.Introduction

CMMS are using increasingly in control and maintenance management for equipments in servicing and producing in several industries. The principals of CMMS used for the first time in hospital maintenance system due to importance of medical equipments health, and also according to the fact that bad results in hospital maintenance could lead many people to dead. Currently, private companies realized the importance of maintenance management systems as a tool for enhancing the performance of maintenance and repairing systems. Emerging small and private computers in past years caused to popularity of these systems among companies. As the computer skills of maintenance and equipment personnel became grater, the respect to such systems as an attractive option is now greater than before. Thus, investment on CMMS by different advanced organizations increasingly grows. Typically, these systems are designed in a manner that provide significant support the requirements of documentations control through ISO 9001:2008 and as a part of philosophy of productivity maintenance can be also applied. Many of the existing CMMS have the same efficiency, and common components which had been provided by the most of CMMS software including several main modules (figure 1) that cover the basic activities of maintenance and repairing systems.

Krouzek [6] presented a case study of the development and implementation of the Czechoslovak UNDP/UNIDO project "Application of Modern Computerized Maintenance System". He highlighted the economies achieved in terms of both tangible benefits and costs incurred. Also he claimed that the general maintenance functions were outlined and their incorporation into the project activities was described. He expressed the evaluation of multiple aspects of the CMMS is provided with particular attention given to system modularity and integrity,

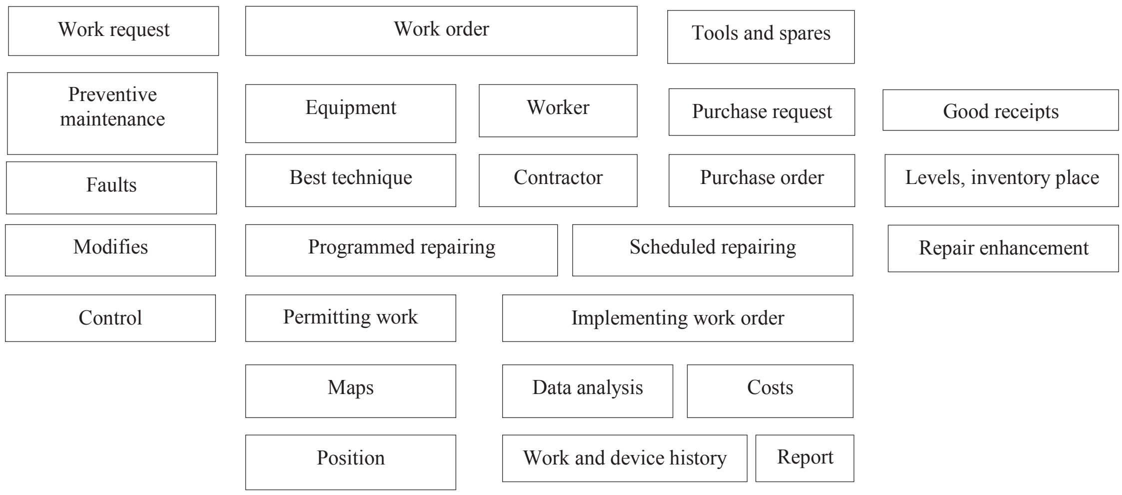

Figure 1. Major components of CMMS

stepwise development and implementation, and hardware and software support.

Jones and Collis [4] obtained an overview of the use of computers in maintenance management to inform the maintenance management systems could be beneficial according to principal application of re-engineering. Fernandez *et al* [2] discussed the role of CMMSs as a powerful tool necessary for obtaining information from raw data and support the decision-making process. Furthermore, a CMMS has been designed, developed, customized and implemented for a disc brake pad manufacturing based company in England. In addition, a maintenance maturity grid has been proposed to support the CMMS implementation. The implemented CMMS aimed to reduce total downtime and frequency of failures of the machines by improving the efficiency and effectiveness of the maintenance force. Swanson applied Galbraith's (Organization Design, Addison-Wesley, and Reading, MA) information-processing model to study how the maintenance function applies different strategies to cope with the environmental complexity. Also he expressed, based on data from a survey of plant managers, the analysis shows that maintenance responds to the complexity of its environment with the use of CMMS, preventive and predictive maintenance systems, coordination and increased workforce size (Swartone [13]). Gabbar *et al* [3] presented the detailed system design and mechanism of improved RCM (reliability-centered maintenance) process where integrated with CMMS. The proposed approach was integrated with design and operational systems and consolidates some successful maintainability approaches to formulate an efficient solution for optimized plant maintenance system. The major components of the enhanced RCM process are identified and a prototype system is implemented as integrated with the various modules of the adopted CMMS (MAXIMO). They also run a case study to show the effectiveness of the proposed RCM-based CMMS solution in optimizing plant maintenance over the traditional approaches (Gabbar *et al* [3]). O'Donoghue and Prendergast [11] examined the basis of various maintenance management strategies used to date through an international manufacturing environment. These strategies assist the maintenance function and enable the maintenance process to be optimized. Also, they expressed special focus was given to CMMSs, indicating how this particular strategy was successfully implemented in a medium sized Irish textile manufacturing company. Labib [8] proposed to implement the holonic concept in maintenance systems. The main features of the holonic concept were set using fixed rules and flexible strategies. In this paper, the author attempted to put these concepts into the maintenance systems through manufacturing environment. He then discussed holonic concepts with emphasis on applications in maintenance of manufacturing systems. Braglia et al [1] provided a structured methodology to permit an optimal selection of the best (CMMS) software within process industries. They proposed a robust approach, structured and useful in practice, for the selection of CMMS software, which takes into account multiple criteria and overcomes the limitations of subjective decisions. Rusin and Wojaczek [12] worked on analysis of maintenance options for power machines and equipment. The assumed criterion for the selection of the range of repair works was the level of technical risk posed by a given facility below the accepted allowable level. For the assumed maintenance periods minimal sets of equipment were determined. Kundler [7] discussed the maintenance parameter based on the statistical analysis, and results for further operational were used in his paper. The statistical analysis was used for planning process of the product management. The analysis of different incident types and their characteristics based on the collected statistical maintenance data over operational period from 2001 to 2006 was performed. Kans [5] developed a conceptual model for identifying maintenance management including IT requirements, with its practical application in a process for the IT requirements for maintenance management. Moreover, he promoted the use of a structured procedure for the identification of IT requirements for maintenance management.

Generally, main objective of applying a CMMS is managing advanced maintenance system, including and precise investigating, precise implementing of repairing in an operating system, estimating the repairing costs and finally reducing the costs and relevant idle times. In this respect, different companies including IBM®, SAP®, IFS®, Apave® came to this field and all of them following a unique objective, assuring the buyer in order to cost and time saving. Manbachi *et al* [9] presented a new comprehensive solution for maintenance scheduling of power generating units in deregulated environments by applying an annual independent market. The solution was obtained by using a Genetic Algorithm (GA) and a Monte-Carlo Simulation (MCS). In a deregulated environment, each Generation Company (GENCO) desired to optimize its payoffs, whereas an Independent System Operator (ISO) had its reliability solicitudes. Michele and Daniela [10] identified the challenges for maintenance, repair and renewal planning faced by asset owners and managers. Integration with existing systems such as CMMS, Geographic Information Systems, is seen as the largest challenge for developing and using decision-support tools in the area of asset management. Wenyuan and Wenbin [14] presented a modeling study of optimizing the preventive maintenance (PM) interval of a production plant within the context of a case study. They obtained an estimated mean number of the defects identified at the PM epoch by the plant maintenance technicians. Once the parameters of the model were known, a PM model was proposed to optimize the expected downtime per unit time with respect to the PM interval.

2. Two challenging CMMS software:

2.1. MAINTA ™

The MAINTA software initially developed by APAVE which is a French based company . This software has some helpful features for planning and controlling the maintenance operations, and also for creating necessary facilities and equipments in logistic and supporting services, stores control and creating necessary feedbacks for providing manager reports. Additionally, some other important features of this software are:

- Implementing and structural properties
- Repairing capabilities and properties
- Logistic and goods capabilities and properties

The MAINTA™ system was designed throughout three structures: data base and server program (which can be installed on a central server), and a user that by an installed program on a PC can connect to the server. The server program can be installed on different servers and even on multiple servers if the number of users has a growth. The network managers and users need to special training terms before making any change in system. Also the store management (reserve, purchase, reception and etc), the work order management (the planned preventive maintenance work order, defective work order, annual work order, the service work order), reporting system (graph and issue results to Excel files), all represents advantages of Mainta ™.

2.2. IFS

The IFS ™ (Industrial and Financial System) can be installed in an operating system. The IFS Navigator opens the following items:

- Equipment: In this part you can see codes, information, properties and spare pieces related to apparatus and machinery.
- Work order management: In this part, it can trace the faults reports and work orders.
- Documentation: In this part, you can see all information about site including: onshore information, offshore information, repairing information and methods, repairing reports, evidence and information of HSE (Health Safety Environment).
- Creating the fault report: In IFS you can see work orders and preventive maintenance easily and you can realize that currently a work order is in which stage and status. The reports and costs are including those that can be investigated easily and viewing the documents and maps can be done easily.

3. IFS™ and MAINTA ™ Comparison using statistical analysis

In this section, we addressed the IFS™ and MAINTA™ features by evaluating form that are completed using expert judgments and analyzed by SPSS ™ as statistical analysis software.

3.1. Descriptive Statistical analysis

In this section, initially descriptive statistical analysis of the case under consideration in this paper is given in Table 3.

Based on the above table, it can be concluded that almost about 36% of participants in this research selected IFS™ and about 64% selected MAINTA™.

Table 2 also addressed the useful descriptive statistician data which are related to basic information in questions.

Based on the above table it can be concluded that the mean scores (participants views) obtained in basic information for MAINTA™ software is a little greater than for IFS software. Also the scores of standard deviation for MAINTA software is 4.28 and for IFS software is 5.08, and in other hand, the mini-

Table 1. Frequency distribution of participants based on maintenance and repairing software

Software	Frequency	Percent	Valid percent	Cumulative percent
IFS ™	10	35.7	35.7	35.7
Mainta™	18	64.3	64.3	64.3
Total	28	100	100	-

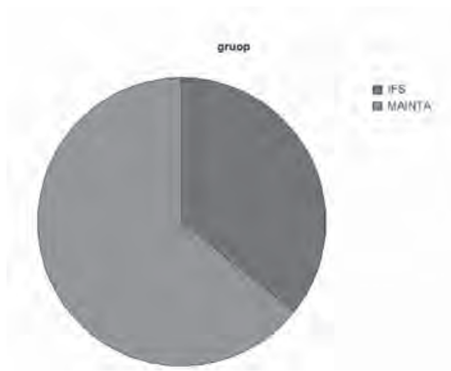

Fig. 2. The frequency percent distribution of participants, base on using the maintenance and repairing software

Table 2. Summary of statistical results related to basic information section

Software	Mean	Median	Standard deviation	Maximum	Minimum	Variance
IFS™	11.4	9.5	5.08	19	5	25.82
Mainta™	11.67	12.5	4.28	18	6	18.35

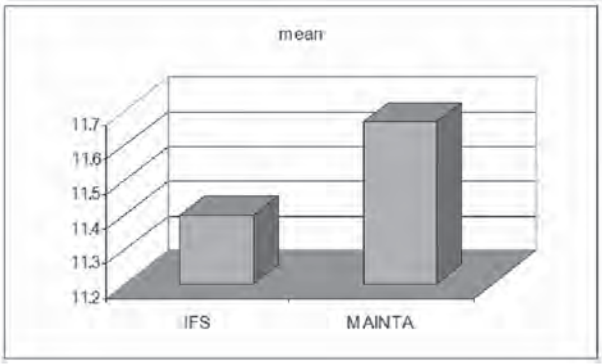

Fig. 3. The mean scores of participants in basic information section

mum and maximum scores are belong to IFS software that are 5 and 19 from 20, respectively.

Table 3 addressed the useful descriptive statistician data that are related to basic information in questions.

It can be concluded based on the above table that the mean scores obtained for MAINTA software is equal to 10.72 and for IFS software is equal to 13.1 in planning section. Also the standard deviation for MAINTA software is 5.72 and for IFS is 3.67 and in other word the variances for MAINTA and IFS are 32.68 and 13.43, respectively.

Table 3. Summary of statistical results related to planning section.

Software	Mean	Median	Standard deviation	Maximum	Minimum	Variance
IFS™	13.1	12.5	3.67	19	8	13.43
Mainta™	10.72	11.5	5.72	18	0	32.68

It can be concluded based on the above table the mean scores obtained for MAINTA software is equal to 10.89 while for IFS software is equal to 13.6. Also the standard deviation for MAINTA software is 4.66 and for IFS is 3.27 and in other word the variances for MAINTA and IFS are 72.21 and 10.71, respectively.

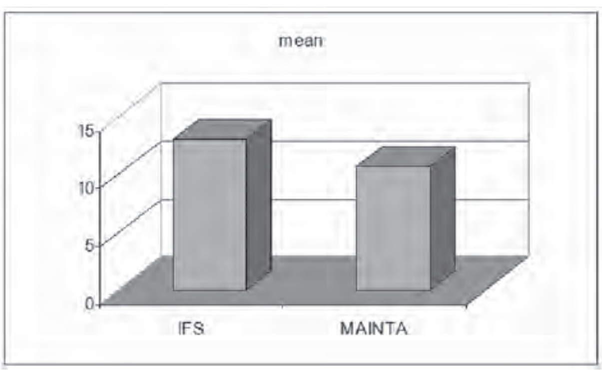

Fig. 4. The mean scores of planning section

Table 5. Summary of statistical results related to reports sections

Software	Mean	Median	Standard deviation	Maximum	Minimum	Variance
IFS	13.6	12.5	3.27	19	10	1071
Mainta	10.89	12	4.66	17	0	21.75

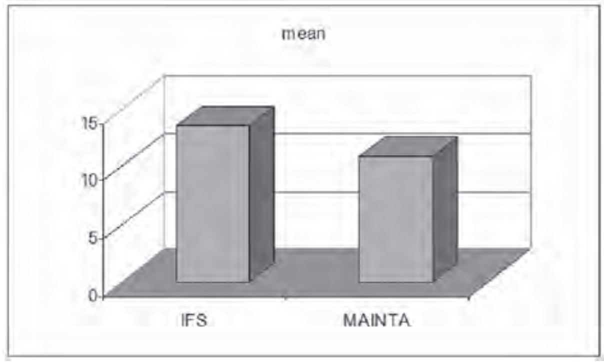

Fig. 5. The mean scores of reports section

It can be summarized based on the above table that the mean scores obtained for MAINTA software is equal to 12.3 and for IFS software is equal to 14.56 in other requirements section. Also the standard deviation for MAINTA software is 3.76 and for IFS is 4.32 and in other word the variances for MAINTA and IFS are 14.14 and 18.68, respectively.

Table 6. Summary of statistical results related to other requirements.

Software	Mean	Median	Standard deviation	Maximum	Minimum	Variance
IFS	14.56	11.5	4.32	20	6	18.68
Mainta	12.3	15.5	3.76	20	6	14.14

3.2. Comparison based on hypothesis Testing:

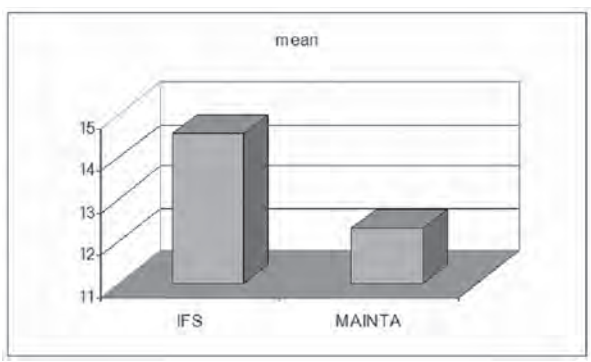

Fig. 6. The mean scores of other requirements section

3.2.1. The first hypothesis:

Assumption H0: There is not a significant difference between viewpoint of MAINTA and IFS users in basic information section.

Assumption H1: There is a significant difference between viewpoint of MAINTA and IFS users in basic information section.

H_0: $\rho = 0$

H_1: $\rho \neq 0$

For proofing the above assumption, it can use the independent parametric T-test. Table 7 addressed the first assumption of research.

Table 7. Evaluation of the first assumption

Statistical amount (t)	Degree of freedom (Df)	Punctual value (p-value)	The 95% Confidence level		Result
			Upper limit	Lower limit	
-0.148	26	0.884	3.44	-3.97	Assumption rejected

Considering the above mentioned punctual level (0.884) which is higher than 0.05, thus we conclude that there is not a significant difference between viewpoint of MAINTA and IFS users in basic information section. Thus, the first assumption of research is rejected and the H0 therefore is proved. However, respect to pervious tables that the mean scores for MAINTA software a little is bigger than the IFS score, thus it can be concluded that the MAINTA is seldom better than IFS software in Basic Information section, but there is not any significant difference between these two softwares from statistical point of view.

Table 8. Evaluation of the second assumption

Statistical amount (t)	Degree of freedom (Df)	Punctual value (p-value)	The 95% Confidence level		Result
			Upper limit	Lower limit	
1.182	26	0.248	6.51	-1.75	Assumption reject

3.2.2. The second assumption of research:

Assumption H0: There is not a significant difference between viewpoint of MAINTA and IFS users in planning section.
Assumption H1: There is a significant difference between viewpoint of MAINTA and IFS users in planning section.
H_0: $\rho = 0$
H_1: $\rho \neq 0$

For proofing the above assumption, it can use the independent parametric T-test. Table 8 addressed the second assumption of research.

Considering the above mentioned punctual level (0.244) which is higher than 0.05, thus we conclude that there is not a significant difference between viewpoint of MAINTA and IFS users in planning section. Thus the second assumption of research is rejected and the H0 assumption is then proved. But respect to pervious tables that shows the mean scores for IFS software is higher than the MAINTA, thus it can say that the IFS is much better than MAINTA software in planning section, but there is not any significant difference between these two software.

3.2.3. The third assumption:

Assumption H0: There is not a significant difference between viewpoint of MAINTA and IFS users in reporting section.
Assumption H1: There is a significant difference between viewpoint of MAINTA and IFS users in reporting section.
H_0: $\rho = 0$
H_1: $\rho \neq 0$

For proofing the above assumption, it can use the independent parametric T-test. Table 3.8 addressed the third assumption of research.

Considering the above mentioned punctual level (0.117) which is higher than 0.05, thus we conclude that there is not a significant difference between viewpoint of MAINTA and IFS users in reporting section. Thus the third assumption of research is rejected and the H0 assumption is proved. But respect to pervious tables that shown the mean scores for IFS software is higher than the MAINTA, thus it can say that the IFS is much better than MAINTA software in reporting section, but there is not any significant difference between these two software.

Table 9. Evaluation of the third assumption

Statistical amount (t)	Degree of freedom (Df)	Punctual value (p-value)	The 95% Confidence level		Result
			Upper limit	Lower limit	
1.62	26	0.177	6.14	-0.72	Assumption reject

3.2.4. The fourth assumption of research:

Assumption H0: There is not a significant difference between viewpoint of MAINTA and IFS users in other requirements section.
Assumption H1: There is a significant difference between viewpoint of MAINTA and IFS users in other requirements section.
H_0:$\rho = 0$
H_1:$\rho \neq 0$

For proofing the above assumption, it can use the independent parametric T-test. Table 10 addressed the second assumption of research.

Considering the above mentioned punctual level (0.161) which is higher than 0.05, thus we conclude that there is not a significant difference between viewpoint of MAINTA and IFS users in other requirements section. Thus the fourth assumption of research is rejected and the H0 assumption is proved But respect to pervious tables that shown the mean scores for IFS software is higher than for MAINTA, thus it can say that the IFS is much better than MAINTA software in other requirements section, but there is not any significant difference between these two software.

Table 10. Evaluation of the fourth assumption

Statistical amount (t)	Degree of freedom (Df)	Punctual value (p-value)	The 95% Confidence level		Result
			Upper limit	Lower limit	
-1.44	26	0.161	0.95	-5.46	Assumption reject

3.2.5. The fifth assumption of research:

Assumption H0: There is not a significant difference between viewpoint of MAINTA and IFS users totally.
Assumption H1: There is a significant difference between viewpoint of MAINTA and IFS users totally.
H_0:$\rho = 0$
H_1:$\rho \neq 0$

For proofing the above assumption, it can use the independent parametric T-test. Table 11 addressed the fifth assumption descriptive statisticians of research.

Table 11. Descriptive report for research assumption

Groups	Mean	Standard deviation	Standard devition error
IFS	50.4	14.73	4.66
MAINTA	47.83	1389	3.27

Table 12. Evaluation the fifth assumption proof of research

Statistical amount (t)	Degree of freedom (Df)	Punctual value (p-value)	The 95% Confidence level		Result
			Upper limit	Lower limit	
0.459	26	0.650	14.07	-8.93	Assumption reject

Based on above table it can conclude that the mean scores that respondents assigned to IFS software is higher than MAINTA.

Considering the above mentioned punctual level (0.650) which is higher than 0.05, thus we conclude that there is not a significant difference between viewpoint of MAINTA and IFS users totally. Thus the fifth assumption of research is rejected and the H0 assumption is proved. But respect to table 11 that shown the mean scores for IFS software is higher than for MAINTA, thus it can say that the IFS totally is much better than MAINTA software, but there is not any significant difference between these two software. Of course there is a significant difference between them in financial viewpoint.

In one of tenders it was seen that the final cost related to IFS software is much higher than MAINTA which detail information is provided in Table 13.

4. Conclusion and further recommendation

Based on an investigation conducted in 2000 and 2004, the consistency of software is the most important reason for companies through software selection process. However, costs of implementation, maintenance and updating (typically between 17 to 22 percent of total cost for purchasing the license) are belonging to costs that a buyer should pay since the CMMS softwares lost their efficiency if they don't update periodically. On the other hand, most of software developers don't allow users to change the software settings and this only allowed with paying an additional cost. Respect to importance of installation and implementation of CMMS software and similarity of most softwares in efficiency viewpoint, for each case, the software should be evaluated both technically and financially through a significant statistical analysis. Finally the overall score should be considered for making the final decision. It normally varies from a company / project to the others due to attribute required for implementation. The results of this study indicates the two software were the same from technically point of view which confirmed by hypothesis testing. Therefore the cheaper one was selected. Further research can be conducted for the other cases in various companies since the results of this research was adapted on a field study and this does not necessarily means the obtained results of this study can be applied through all cases. Therefore, for different cases, fields study using statistical analysis to be separately implemented.

Table 13. The costs related to the two software

Item	IFS proposal	APAVE proposal
Onshore (45 users)+ offshore (30 users)	CMMS and EDMS (Euros)	CMMS and EDMS (Euros) + CERDO (Euros)
Software license	Higher price	-
Implementation (installation, configuration, initial customization)	Higher price	-
Training	Higher price	-
Annual maintenance (hot-line+ new version)	Higher price	-
Total	Higher price	-

4. References

1. Braglia M, Carmignani G, Frosolini M, Grassi A. AHP-based evaluation of CMMS software. Journal of Manufacturing Technology Management 2006; 17(5): 585-602.
2. Fernandez O, Labib A W. A decision support maintenance management system Development and implementation. International Journal of Quality & Reliability Management 2003; 20(8): 965-979.
3. Gabbar H A, Yamashita H, Suzuki K, Shimada Y. Computer-aided RCM-based plant maintenance management system. Robotics and Computer Integrated Manufacturing, 2003; 19: 449–458.
4. Jones K, Collis S. Computerized maintenance management systems. Property Management 1996; 14(4): 33–37.
5. Kans M. An approach for determining the requirements of computerized maintenance management systems. Computers in Industry 2008; 59: 32–40.
6. Krouzek J V. Economies of computerized maintenance management systems. Engineering Costs and Production Economics 1987; 12(1-4): 335-342.
7. Kundler J. Long-term maintenance of aeronautical information system on the base of statistical methods. Eksploatacja i Niezawodnosc – Maintenance and Reliability 2007; 36: 49-54.
8. Labib A W. A decision analysis model for maintenance policy selection using a CMMS. Journal of Quality in Maintenance Engineering 2004; 10(3): 191–202.

9. Manbachi M, Mahdloo F, Haghifam M R, Ataei A, Changkyoo Yoo. A New Approach for Maintenance Scheduling of Power Systems, Using a Genetic Algorithm and Monte-Carlo Simulation. Eksploatacja i Niezawodnosc – Maintenance and Reliability 2010; 48: 82-90.
10. Michele D S, Daniela L. Decision-support tools for municipal infrastructure maintenance management. Procedia Computer Science 2011; 3: 36–41.
11. O'Donoghue C D, Prendergast J G. Implementation and benefits of introducing a computerised maintenance management system into a textile manufacturing company. Journal of Materials Processing Technology 2004; 153-154: 226–232.
12. Rusin A, Wojaczek A. Selection of maintenance range for power machines and equipment in consideration of risk. Eksploatacja i Niezawodnosc – Maintenance and Reliability 2007; 35: 40-43.
13. Swanson L. An information-processing model of maintenance management. Int. J. Production Economics 2003; 83: 45–64.
14. Wenyuan LV, Wenbin W. Modelling Preventive maintenance based on the delay time concept in the context of a case study. Eksploatacja i Niezawodnosc – Maintenance and Reliability, 2011; 51: 5 -11.

Eshagh Saharkhiz , MSc (Eng)
Department of Mechanical Engineering, Shiraz Branch
Islamic Azad University
Shiraz, Iran
E-mail: saharkhiz_eshagh@yahoo.com

Dr Morteza BagherPour, Ass. Prof.
Department of Industrial Engineering
Iran University of Science and Technology
Tehran, Iran
E-mail: bagherpour@iust.ac.ir

Dr Mohammad Reza Feylizadeh, Ass. Prof.
Department of Industrial Engineering, Shiraz Branch
Islamic Azad University
Shiraz, Iran
E-mail: feylizadeh_mr@yahoo.com

Dr Ahmad Afsari, Ass. Prof.
Department of Mechanical Engineering, Shiraz branch
Islamic Azad University
Shiraz, Iran
E-mail: Dr_A_Afsari@yahoo.com

Article citation info:
RADKOWSKI S, SZCZUROWSKI K. Use of vibroacoustic signals for diagnosis of prestressed structures. Eksploatacja i Niezawodnosc. Maintenance and Reliability 2012; 14 (1): 84–91.

Stanisław RADKOWSKI
Krzysztof SZCZUROWSKI

USE OF VIBROACOUSTIC SIGNALS FOR DIAGNOSIS OF PRE-STRESSED STRUCTURES

WYKORZYSTANIE SYGNAŁU WIBROAKUSTYCZNEGO W DIAGNOSTYCE STRUKTUR SPRĘŻONYCH*

The paper presents the issue of assessment of the technical condition of a prestressed structure while particularly underscoring the possibilities offered by amplitude modulation effects which are found in the observed vibroacoustic signal. The basis for such an approach is the thesis that change of distribution of stress in the cross-section of a prestressed structure is accompanied by a measurable change of the parameters of a vibroacoustic signal.The thesis stems from the assumption that the condition of prestressing of a structure, as it is being bent, is accompanied by the phenomenon of dispersion and hence of the change of wave propagation parameters, especially the occurrence of a measurable difference between the values of phase and group velocities.Analysis of the relations between the state of stress and the values of phase and group velocities creates the possibilities of developing the reverse diagnostic models and determining the quantitative changes of such parameters of technical condition as compressive forces, Young's modul or the stress in the structure. The paper has been developed on the basis of the author's Ph.D. thesis.

Keywords: *technical diagnosis, amplitude modulation, group velocity, phase velocity, prestressed structures.*

W pracy przedstawiono zagadnienie oceny stanu technicznego struktury sprężonej ze szczególnym uwypukleniem możliwości wykorzystania efektów modulacji amplitudowej występujących w obserwowanym sygnale wibroakustycznym. Podstawą takiego podejścia jest teza że zmianie rozkładu naprężeń w przekroju poprzecznym struktury sprężonej towarzyszy mierzalna zmiana parametrów sygnału wibroakustycznego.Wynika ona z założenia, że wraz z wywołaniem stanu sprężenia wstępnego w zginanej konstrukcji zachodzi zjawisko dyspersji, a tym samym zmiana parametrów propagacji fali, w szczególności występowanie mierzalnej różnicy wartości prędkości fazowej i grupowej.Analiza relacji między stanem naprężeń a wartościami prędkości fazowej i grupowej stwarza możliwość budowania diagnostycznych modeli odwrotnych i wyznaczania ilościowych zmian takich parametrów stanu technicznego, jak siły sprężające, moduł Younga czy naprężenia panujące w konstrukcji.Praca powstała na podstawie rozprawy doktorskiej autora.

Słowa kluczowe: *diagnostyka techniczna, modulacja amplitudowa, prędkość grupowa, prędkość fazowa, konstrukcje sprężone.*

1. Introduction

At the turn of 20th century the communities associated with use of prestressed concrete structures started extensive work related to gaining in-depth knowledge on the conditions which would assure durability of existing structures and extend their useful life to as long as 80 years (the structures were designed for 50 years), minimize the cost of repairs and monitoring as well as improve safety in the long run [8]. Unfortunately in many cases tens of years have passed since construction of such structures and even the originally planned operating life of the structures has ended. Thus a problem has emerged of how to evaluate the condition of the structures from the point of view of safety requirements. Consequently attention started to be paid to the methods of detecting the degree of such structures' degradation, their faults, cracks and other types of defects, of which some could prove critical and cause catastrophic defects of the entire structure.

One of the major directions of work was to find the new methods of evaluating the condition of prestressed structures. The paper provides information on the work related to application of vibration and acoustic methods while making the assumption that the early phases of development of micro-defects in a prestressed structure will be accompanied by change of distribution of stress in the cross-section. Thus an attempt was made to develop a non-invasive method of detection of changes in distribution of stress while relying on the information contained in the vibroacoustic signal generated by a dynamically excited prestressed structure.

Ultrasonic methods can be divided into two groups. The first one involves measurement of the velocity of ultrasonic

(*) Tekst artykułu w polskiej wersji językowej dostępny w elektronicznym wydaniu kwartalnika na stronie ***www.ein.org.pl***

wave propagation across a reinforced concrete structure while the other one involves analysis of changes of the parameters of a wave propagating in the material.

Measurement of propagation velocity takes place while using two surfaces of the examined element and it is intended to measure the distance travelled by a propagating wave. Examination of the velocity of an ultrasonic pulse in a material involves introduction of an ultrasonic wave to the material and measurement of the time it takes for the head of this wave to travel from the transmitting processor to the receiving processor. Knowing the time it takes the pulse to travel and the length of the path one can determine the velocity at which the wave passes [11].

The second group of ultrasonic methods includes Impact-echo [12], Pulse-echo [7] and surface method [11].

These methods exploit the effect related to the disturbance which affects ultrasonic waves as they pass through a material and bounce of the boundary of an element or another discontinuity of a material. After relevant analyses of a signal (e.g. FFT) it is possible to infer about the path that a wave traveled.

These methods enable quick determination of the thickness of elements to which access is possible only from one side, such as platform slabs, road surfaces, and they enable location of all types of internal defects of reinforced concrete structures, such as inclusions of other materials (e.g. wood), deficiencies (e.g. void pockets of air), cracks or corrosion.

The Pulsed Eddy Current (PEC) method is a relatively new non-destructive method. It is used for inspecting and identifying hidden corrosion in the layer of structures containing ferromagnetic elements [9]. Its main advantage is the possibility of covering a wide range of frequencies excited by a strong pulsation of the electromagnetic field. The method is also quite simple while the equipment required to use it is relatively cheap.

The Acoustic Emission method is a passive monitoring method which involves detection of disturbance caused by the stressing wave emitted as a crack develops or when a fiber breaks. In contrast with this, the classic ultrasonic methods of defect detection are of active type, which means that they involve sending a stressing wave into the examined object in order to identify the existing defect.

Effectiveness of the Acoustic Emission method was verified in several studies. It turned out that a stressing wave was generated as a result of existence of corrosion and micro-cracks and that this wave could be detected with the use of acoustic emission sensors [4].

The method can be used for constant monitoring without any limitations. Unfortunately it is a passive method and it can be only used for registration of signals generated as a result of cracks or other changes inside the material, however it does not offer the possibility of direct assessment of severity of defects as they emerge.

Magnetic methods were often used in examination of concrete structures to locate the elements of reinforcement. They were also used for routine inspections of fibers and overhead lines. Burdekin et al. [1] presented a project realized in the 1970's and 1980's at Southwest Research Institute. The project was devoted to detection of corrosion and fractures of steel stressing elements in pre-tensioned prestressed concrete and post-tensioned prestressed concrete beams.

Nonlinear Vibroacoustic Methods were developed in the 1980's at the Institute of Applied Physics of the Russian Academy of Sciences for the purpose of controlling the quality of thermoinsulating screens used in Russian space shuttles. Dimitri M. Donskoy and Alexander Sutin [13], who were developing these methods, presented a method based on the analysis of a non-linear vibroacoustic signal The traditional linear acoustic methods use the effects of reflection, dispersion and absorption of acoustic energy. These methods enable detection of defects on the basis of momentary changes of a signal's phase and/or amplitude. Thanks to the non-linear relations it is possible to detect these changes in other frequency bands than the emitted signal's bands. It all depends on the type of non-linear transformation of acoustic energy by a defect. The method mentioned here assumes that the materials with cracks cause change of the signal and generate its much bigger non-linearity.

The advantage of non-linear methods is the possibility of their application in highly non-homogenous structures such as composites and concrete. When a sinusoid acoustic wave encounters a defect, it changes at the contact surface (growth of compression, reduction of stress). It is a phenomenon which to some degree is analogous to closing of a crack during compression and its opening during stressing. It leads to generation of further harmonic frequencies of the generated signal.

While referring to the current state of knowledge, it is worth noting that the research of prestressed structures mainly focuses on detection of faults and defects of materials. It is also from this point of view that the dynamic responses of structures are analyzed.

2. Assessment of existing methods

All the methods mentioned here have the purpose of detecting cracks, inclusions, corrosion or other defects in prestressed concrete structures and they are directed at finding the places of their occurrence, that is places affected by corrosion in reinforcing strings or bars, corrosion of concrete, cracks in tendons or concrete, inclusions or other defects of the material. It is only on the basis of the obtained information that it becomes possible to determine whether a given defect is critical for a whole structure. Acoustic emission could be an example as it enables detection of emerging cracks without determining their influence on the entire structure or the magnetic methods which are used for observing changes of the magnetic field around the damaged stressing strings. In addition, determination of the state of the entire structure with the use of the above mentioned methods requires substantial time since each test can only cover part of a structure.

3. A proposal of a new approach

The proposed new approach of assessing the condition of prestressed elements, such as prestressed concrete elements, involves observation of dynamic changes of the characteristics of entire elements as they take place under the influence of changes in the structure of stress [2].

In the existing practice, the dynamic response of a structure is used for detecting, locating and defining the degree of defect development in non-destructive research. By defining a structural defect as a kind of a deviation of the geometric and material-related properties from the norm, we can expect changes to occur in the dynamic response of a system to a defined load.

A phenomenon which is important in prestressed structures is the qualitative change in the structure of stress in the cross-section. Compressive stress is applied across the whole cross-section during the construction stage. During operation the degradation processes lead to changes in the designed distribution of stresses in the cross-section. The possibility of detecting the changes in the distribution of stresses creates an opportunity for determining the condition of the prestressed structures and for forecasting the residual time of their use.

The phenomenon of modulation of a vibroacoustic signal's parameters, trigerred by changes in the conditions of wave propagation across material as a result of changes in distribution of stress in the cross-section of a prestressed structure, is used overcome the aforementioned difficulties in the proposed method of diagnosis.

3.1. Examination of frequency changes in a prestressed structure

Impact of pre-stressing on the frequency structure of vibration signal in prestressed structures is analyzed in the literature devoted to the dynamics of continuous systems while using various models. For example Graff [5], while analyzing vibration in a beam subjected to stretching, adopted the starting Bernoullie-Euler model to which he additionally applied stretching forces (Fig. 1).

The vibration equation takes the following form:

$$EI\frac{\partial^4 y}{\partial x^4} - T\frac{\partial^2 y}{\partial x^2} + \rho A\frac{\partial^2 y}{\partial t^2} = 0 \qquad (1)$$

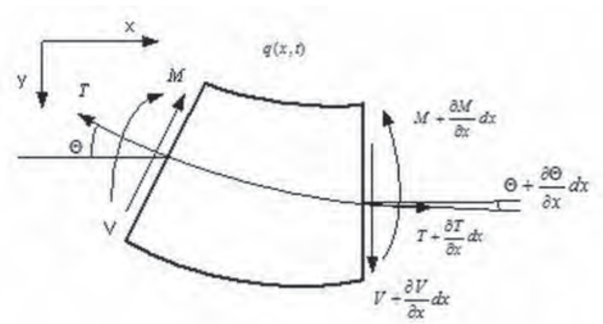

Fig. 1. Element of a model of a Bernoullie-Euler beam [5]

In the case of occurrence of compressive forces, the orientation of force T has to be changed to the opposite one in equation (1). By solving equation (1) we will obtain an expression defining the value of the frequency of n-th form of vibration depending on the value of the compressive force:

$$f_n = \frac{n^2\pi^2}{l^2}\left(\frac{EI}{\rho A}\right)^{\frac{1}{2}}\left(1-\frac{Tl^2}{n^2\pi^2 EI}\right)^{\frac{1}{2}} \qquad (2)$$

Equation (2) demonstrates that application of tensile forces leads to growth of frequency of a beam's natural vibration, while application of compressive forces leads to the reduction of frequency. When the distribution of stress in the beam's cross-section changes, the effect of wave propagation at various speeds will occur, which could become an additional important factor having influence on the process of generation of a wave's group velocity and the associated phenomena of modulation of a vibroacoustic signal's parameters.

Based on the model of a Bernoullie-Euler's beam, as presented in Fig. 1 and described by the following relation (1)

$$\frac{\partial^4 y}{\partial x^4} - \frac{T}{EI}\frac{\partial^2 y}{\partial x^2} + \frac{1}{c^2}\frac{\partial^2 y}{\partial t^2} = 0 \qquad (3)$$

where, $c^2 = \frac{EI}{\rho A}$ we can determine the wave number.

Occurrence in the equations of a factor which depends on the tensioning force points to the phenomenon of dispersion and the necessity of determining the dependence of phase velocity on the value or ratio of the forces. Hence the relationship which defines the phase velocity can be presented in the following form:

$$c_f = k\cdot c = c\sqrt{\frac{T}{2EI}+\left(\frac{T^2}{4E^2I^2}+k^4\right)^{\frac{1}{2}}} \qquad (4)$$

while the relation between the group velocity and phase velocity can be presented as:

$$c_g = c_f - ck^4\left(\frac{T}{2EI}+\left(\frac{T^2}{4E^2I^2}+k^4\right)^{\frac{1}{2}}\right)^{-\frac{1}{2}}\cdot\left(\frac{T^2}{4E^2I^2}+k^4\right)^{-\frac{1}{2}} \qquad (5)$$

Relationship (5) points to dependence of the group velocity on the value of compresive forces and the wave number k.

While using the relationship between the speed of wave propagation and length of a wave:

$$f = \frac{k\cdot c_f}{2\pi} \qquad (6)$$

where $k = \left(\frac{\omega}{c}\right)^{\frac{1}{2}}$, it becomes possible to determine the dispersion curve, presented in Fig. 2, which describes the frequency of proper vibration of the examined beam in the function of wave velocity.

As can be easily noted, typical harmonics cannot be expected in materials having dispersion properties since the frequencies of subsequent forms of vibration are a multiple of the fundamental frequency [3].

Changes which phase velocity undergoes also affect group velocity. In accordance with the adopted assumption, changes of group velocity, accompanying growth of transverse force, should be visible in the form of changes of modulating frequency around the carrier frequency which changes along with the changes of phase velocity.

The above mentioned effect could have been observed in the spectra of the dynamic response of prestressed beams examined at the test-bed in Kielce University of Technology. Fig. 3 presents an example of this phenomenon.

In addition occurrence, in the equations, of an element which is dependent on the tensile force, points to the existence

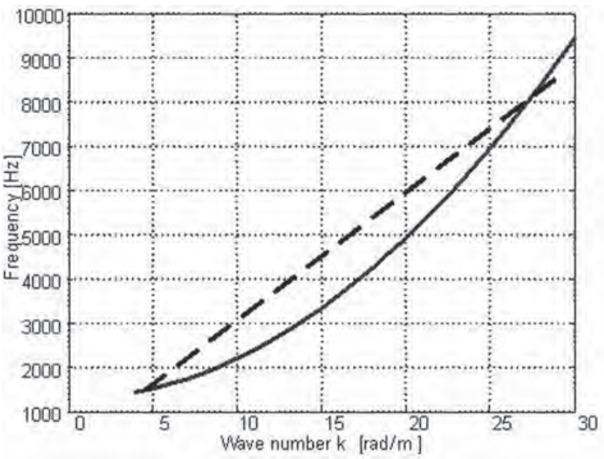

Fig. 2. Change of frequency based on relation (5) [3]

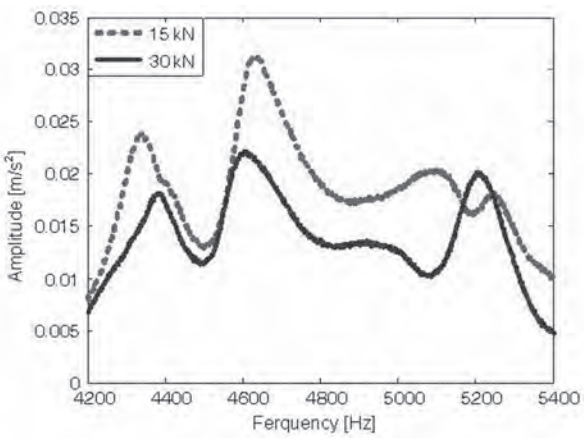

Fig. 3. Changes of amplitude modulation accompanying changes of the load in a selected band [3]

of dispersion and the necessity of determining the dependence of phase velocity on the value of the forces [3; 10].

While using the aforementioned model, vibration frequency is obtained as a function of tensile forces and the wave number:

$$\omega = kc\left(k^2 + \frac{T}{EI}\right)^{\frac{1}{2}} \tag{7}$$

By presenting the compressive force equal to zero (T = 0), we obtain the generally known relation between the frequencies, wave number and wave propagation velocity. It is worth noting that under such an assumption it is still possible to adopt the same wave number as in the case of lack of dispersion since the boundary conditions do not change. Finally, while accounting for the relations $c_f = k\,c$ and $\omega = k\,cf$, we can obtain:

$$c_f^2 = \omega \cdot c = kc^2\left(k^2 + \frac{T}{EI}\right)^{\frac{1}{2}} \tag{8}$$

where the dependence of wave propagation on both, the wave number and the stressing force is visible. As the tensile force increases, so will the wave propagation velocity, while in the case of growth of compressive force – wave propagation velocity will decrease.

The relation obtained on the basis of equation (1), which defines the group velocity in a prestressed structure, has been confirmed in terms of quality during an experiment while quantitative estimates would be burdened with too big an error.

The next item which was analyzed was the model of longitudinal vibration of a beam.

3.2. Equation of longitudinal vibration of a beam

Let us consider free longitudinal vibration of a beam so as to then take into account the effect of compression under a transverse load. In accordance with the model presented in Fig. 4, the relevant equation will take the following form:

$$c_0^2\frac{\partial^2 y}{\partial x^2} = \frac{\partial^2 y}{\partial t^2} \tag{9}$$

where $c_0 = \sqrt{\frac{E}{\rho}}$ is the velocity of propagation of displacement or stress in a beam.

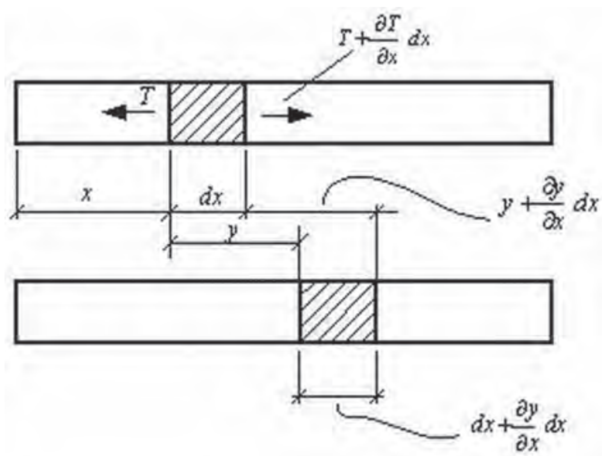

Fig. 4. Model of propagation of longitudinal vibration

Once the stressing forces are taken into account, equation (9) can be expressed in the following form:

$$\frac{\partial^2 y}{\partial x^2} - \frac{p}{T}y = \frac{1}{c_0^2}\frac{\partial^2 y}{\partial t^2} \tag{10}$$

As a result we will obtain relationships defining the phase velocity

$$c_f = c_0\left(1 + \frac{p}{Tk^2}\right)^{\frac{1}{2}} \tag{11}$$

and the group velocity

$$c_g = c_f - c_0\frac{\frac{p}{T}}{k^2\left(1 + \frac{p}{Tk^2}\right)^{\frac{1}{2}}} \tag{12}$$

This way we have demonstrated that two velocities of wave propagation can occur in this case: the phase velocity and the group velocity, which is the requirement for occurrence of amplitude modulation. Fig. 5 illustrates the obtained relation .

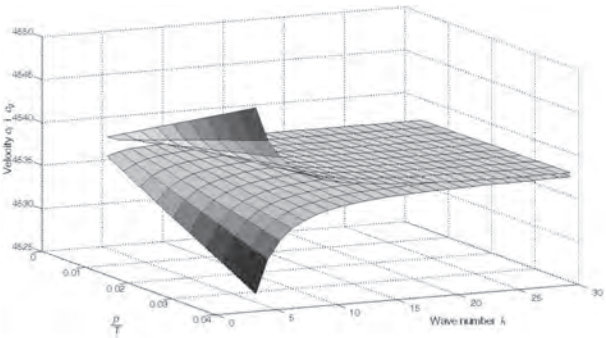

Fig. 5. Changes of group velocity depending on the relation between longitudinal and transverse forces (p/T) in a situation of change of k wave number and change of the direction of stress

To explain the issue of occurrence of amplitude modulation even further, let us quote, after Ignacy Malecki, the model of propagation of two harmonic waves whose ω_1 and ω_2, differ slightly:

$$c_g = c_f - c_0 \frac{\frac{p}{T}}{k^2\left(1+\frac{p}{Tk^2}\right)^{\frac{1}{2}}} \tag{13}$$

While continuing the analysis of the terms of occurrence of amplitude modulation, relation (13) can be presented in the form of a product:

$$y = 2A\cos\left(\frac{1}{2}(k_2-k_1)x - \frac{1}{2}(\omega_2-\omega_1)t\right)\times$$
$$\times\cos\left(\frac{1}{2}(k_2+k_1)x - \frac{1}{2}(\omega_2+\omega_1)t\right)$$

While accounting for further transformation:

$$y = A\cos(k_1x-\omega_1t) + A\cos(k_2x-\omega_2t) \tag{15}$$

where $\frac{d\omega}{dk} = c_g$, $\frac{\omega}{k} = c_f$ (14)

The obtained relation demonstrates connection between amplitude modulation and the necessity of existence of two different wave velocities: phase velocity (c_f) and group velocity (c_g).

4. Description of the object of research

As part of the research several types of prestressed beams were prepared out of which the first type was selected for preliminary research, namely the beams made of B20 class concrete with the dimensions of 1510×102×200mm, reinforced by four bars with diameter of Ø10 made of reinforcing steel which have been installed along the centerline of the beam. The bars have been run at the distance of ca. 25 mm from the sides, with prestressing between 17 and 20 MPa which has been realized by two tendons strings with seven wires. The second set of bars included prestressed concrete beams with dimensions of 110×140×1300 mm which were made of C 40/50 concrete. Prestressing was achieved under the influence of 4 prestressing bars (with ø 6.8 mm), spaced symmetrically. The prestressing force in the beams changes from 0 kN to 100 kN. The beams did not have any additional reinforcement.

All the beams were subjected to three-point bending, from zero until full fracture of a beam. The diagram is presented in Fig. 6. With a defined load, the structure was forced with a modal hammer which enables force measurement. The dynamic response was registered with the use of accelerometers in the preselected points.

5. Experiments and experimental verification of models

In the case of the first type of beams, while analyzing the dynamic responses it could be noted that a distinct qualitative change of the observed diagnostic parameters occurred when the load of ca. 35 kN was applied. One should note that the analytical calculations, which include the assumed values of initial stress, point to the possibility of occurrence of tensile stress for the preset value of the shearing force. Analyses of dynamic phenomena, especially the frequency-related analysis of the registered signals, were conducted to confirm the occurrence of the observed boundary between the occurring phenomena.

5.1. Examination of the frequency of the beam's natural vibration

Beams of the first type (B20) concrete were used in the research, however the beams marked as 118 and 125 were the good beams while defects, having the form of local moisture development (119) and damage to the part of the cross-section of the string (122) were simulated in the remaining ones.

Figures 7 and 8 present the changes that the selected frequencies undergo as the load on the beams increases. Particular attention should be paid to two characteristic frequencies, 1500 Hz and 7000 Hz. These are the frequencies which are distinctive among the vibration frequencies for all the beams, even in spite of the fact that in the case of the beam affected by moisture, the first of the two frequencies has much more bigger value.

To enable easier comparison of the changes, the scale has been changed in two ways. The first one involved dividing all the frequencies by the maximum frequency (Fig. 7), the other involved deduction of the maximum frequency from all the frequencies (Fig. 8).

In addition the approximated waveforms of the changes was presented with the use of the curves of the second order. In the case of non-defective beams the description relying on a curve of the second order seems to be sufficient. In the case of the beams to which defects were introduced, the description seems not to be very precise and thus higher order curves are necessary to use. Unfortunately examination of the changes of vibration frequency calls for applying substantial loads to the beams, which could lead to their destruction, thus rendering

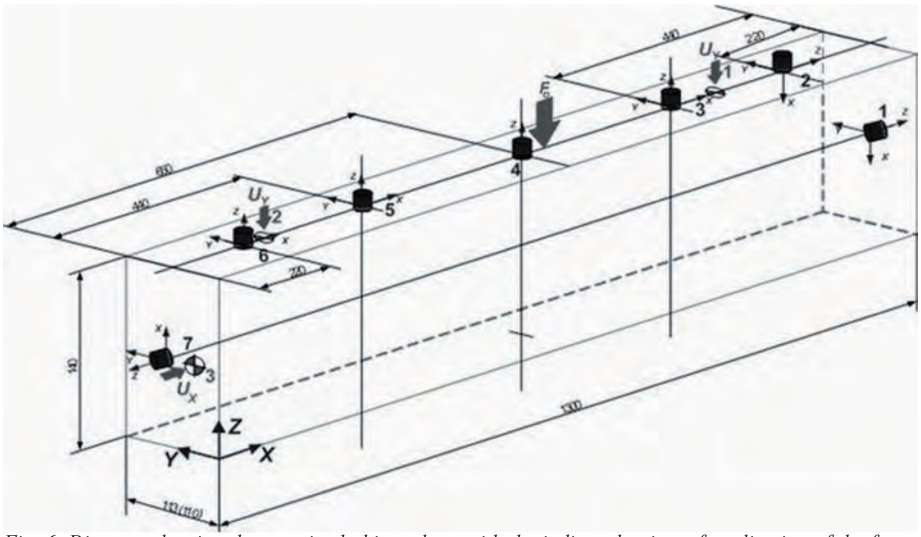

Fig. 6. Diagram showing the examined object along with the indicated points of application of the force, measurement points and places of excitation

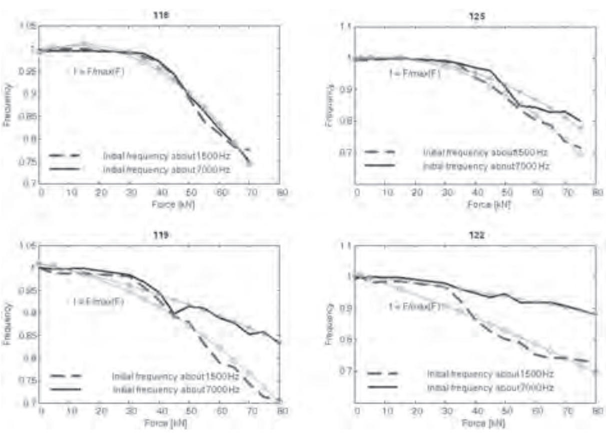

Fig. 7. Changes of selected frequencies depending on the load, with the scale changed in the following form f = fi/fmax

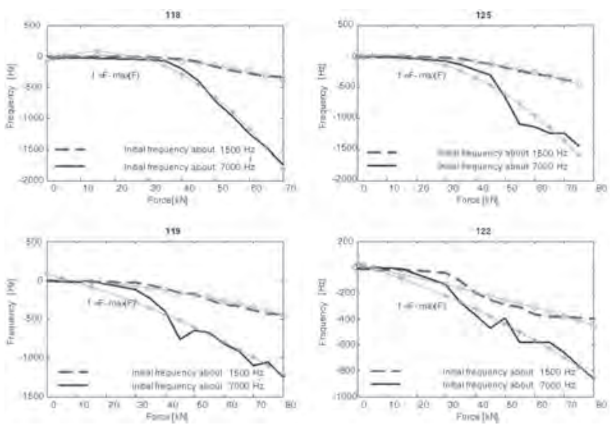

Fig. 8. Changes of selected frequencies depending on the load in a situation of change of scale. f = Fi - Fmax

the procedure useless from the point of view of non-destructive techniques.

5.2. Examination of the phenomenon of dispersion

Relevant combination of loads (ratio of transverse forces to longitudinal forces) contributes to the occurrence of the effect of dispersion, differentiation of group velocity and causing the accompanying effect of amplitude modulation, as presented in Fig. 9. Change of the modulating frequencies, as presented in Fig. 10, was caused by the changes of distribution of stess in the cross-section of the beams and could be used for evaluating the ratio of transverse to longitudinal forces (Fig. 11).

The phenomenon of dispersion was observed this way and in addition the changes of the impact of the load on a structure's dynamic response were analyzed.

6. Conclusions

Relevant combination of loads (applying a transverse load) has contributed to the occurrence of the dispersion effect, diversification of the group velocity and generation fo the accompanying effect of amplitude modulation. At the same time, change of modulating frequencies has been caused by changes of the distribution of stress in the cross-section of the beams and it could used for evaluating the ratio of transverse forces to longitudinal forces, as presented in Fig. 10. This observation enables construction of models on the basis of which one can determine the compressive forces in structures which can be then used to determine whether the assumption regarding non-occurrence of tensile stress is still valid. Thus obtained information will enable determination whether the examined structure could continue to be operated and in what conditions (e.g.reduction of the permitted load for a bridge). The propsed method could be also used for new structures in which it is necessary to determine whether stressing was done correctly, as discussed more extensively by the authors in [6].

The article has been written on the basis of a successful Ph.D. dissertation which was realized as part of COST Action 534 EU Program which was carried in the Technical Diagnosis and Risk Analysis Team.

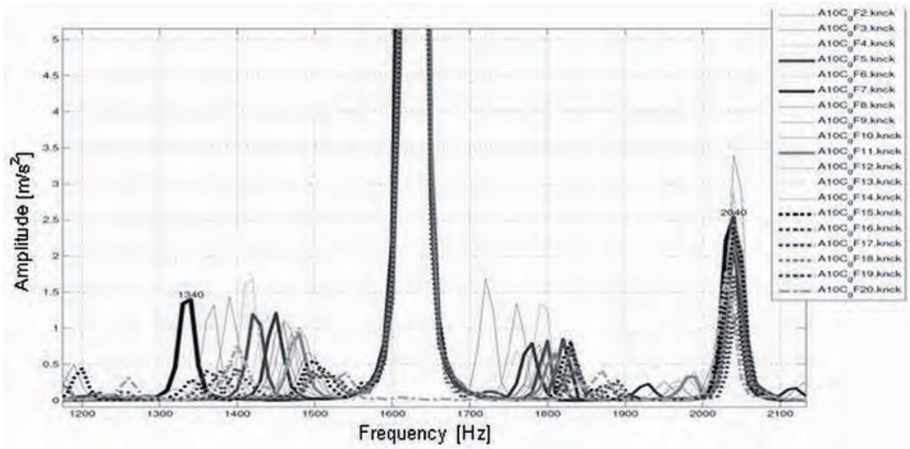

Fig. 9. Fragment of the signal's spectrum for a sample to which load was applied in the form of a transverse force with a frequency of around 1630 Hz, with the effect of dispersion

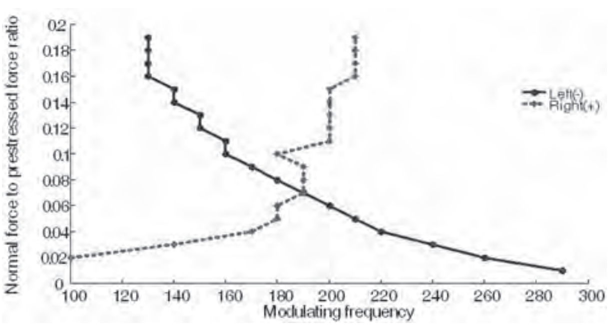

Fig. 10. Changes of modulating frequencies depending on the change of the ratio of transverse forces to longitudinal forces

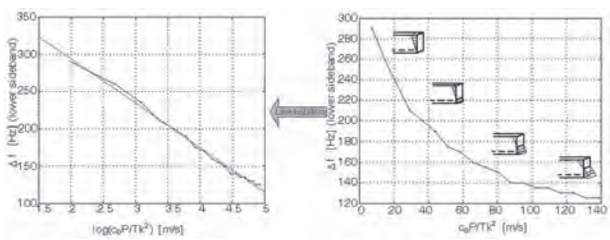

Fig. 11. Linearization of the frequencies of modulating functions depending o the change of the ratio of transverse and longitudinal forces

7. References

1. Burdekin F M, John D G, Payne P A , Locke C, Smith T A, Simm K and Dawson J L. Non-destructive methods for field inspection of embedded or encased high strength steel rods and cables - Phase I NCHRP Project 10 - 30(1), University of Manchester. 1986.
2. Gałęzia A, Mączak J, Radkowski S, Szczurowski K. A method of stress distribution assessment in prestressed structures, 7th International Seminar on Technical System Degradation Problems, Liptovský Mikuláš 200; 39-40
3. Gałęzia A, Mączak J, Radkowski S, Szczurowski K. – co-authors of Chapter 3.5.5: Amplitude modulation for diagnosis of the stste of prestressed structures w Rob POLDER et al.: COST ACTION 534. New materials, Systems, Methods and Concepts for Prestressed Conrete Structures. Final report COST Office, Brussels, 2009; 194÷202,
4. Gołaski L, Świt G. Acoustic non-destructive techniques as a new method for evaluation of damages in prestressed concrete structures: failure of concrete structures. Second Workshop of COST on NTD assessment and new systems in prestressed concrete structures, COST Action 534 New materials and systems for prestressed concrete structures. Kielce, 2005; 151 - 159.
5. Graff K F Wave motion in elastic solids. New York: Dover Publications. Inc. 1991.
6. Jurkiewicz A, Micek P, Apostoł M, Grzybek D. O potrzebie monitorowania procesu sprężenia konstrukcji mostowych (Of the need of monitoring the process of prestressing of bridge structures). Eksploatacja i Niezawodnosc – Maintenance and Reliability 2008;1: 17-22.
7. Krause M, Wiggenhauser H. Ultrasonic pulse echo technique for concrete elements using synthetic aperture. UTonline Application Workshop, NDTnet - May 1997, Vol.2 No.05.
8. Memorandum of understanding for the implementation of a European Concerted Research Action designated as COST Action 534: „New materials and systems for prestressed concrete structures" COST Office, Brussels, 2002.
9. Moulder J C, Kubovich M W, Uzal E, and James H R. Pulsed Eddy-Current Measurements of Corrosion-Induced Metal Loss: Theory and Experiment. Review of Progress in Quantitative Nondestructive Evaluation. 1995; 14: 2065 - 2072.
10. Radkowski S., Szczurowski K. Hilbert transform of vibroacoustic signal of prestressed structure as the basis of damage detection technique Dubrovnik: Proceedings of the Conference on Bridges. 2006; 1075 - 1082.

11. Runkiewicz L. Badania Konstrukcji Żelbetowych (Research of Reinforced Concrete Structures). Warszawa, Biuro Gamma. 2002.
12. Sansalone M.J., Streett W.B. The Impact-Echo Method. The Online Journal of Nondestructive Testing & Ultrasonics, NDTnet 1998 February, Vol.3 No.2.
13. Suzin, A.M., and Donskoy, D.M. Nonlinear Vibro-Acoustic Nondestructive Testing Technique. NDT & E International Volume 34, Issue 4, 1 June 2001, 231-238.

Prof. dr hab. inż. Stanisław Radkowski
Dr inż. Krzysztof Szczurowski
Institute of Vehicles
Warsaw University of Technology
Ul. Narbutta nr 84, 02-524 Warszawa, Polska
E-mail: kszczur@simr.pw.edu.pl